



*Official Journal of the  
Malaysian Medical Association*

# *MJM Case Reports Journal*

**Volume: 5**

**Issue No: 1**

**April 2026**

ISSN 2948-3859

# MJM Case Reports



*Official Journal of the  
Malaysian Medical Association*

*Volume 5 Number 1 April 2026*

## EDITORIAL BOARD

*International Advisory Board*

**Laureate Professor Dr Nicholas Talley**  
**Assoc Prof Dr Mahesh Choolani**

*Advisor*

**Prof Datuk Dr Lekhraj Rampal**

*Editor in Chief*

**Prof Victor Hoe Chee Wai**

*Handling Editor*

**Dr Ravindran Vashu**

*Editors*

**Prof Dato' Dr NKS Tharmaseelan**

**Prof Dr Shatriah Ismail**

**Prof Dr Irfan Mohamad**

**Dr Liew Boon Seng**

**Prof Dr Chew Keng Sheng**

**Dr Navin Kumar Devaraj**

**Prof Dr Andee Dzulkarnaen**

**Assoc Prof Dr Sanjiv Rampal**  
**Lekhraj Rampal**

*Editorial Manager*

**Ms Mahaletchumy Alagappan**

ISSN 2948-3859

The MJM Case Reports Journal is published three times a year.

**All articles which are published  
represent the opinion of the authors and are not necessarily those of the  
Malaysian Medical Association unless otherwise expressed.**

*Copyright reserved © 2026*  
Malaysian Medical Association

**Advertisement Rates:**

Enquiries to be directed to the Secretariat.

**Secretariat Address:**

Malaysian Medical Association  
4th Floor, MMA House, 124, Jalan Pahang, 53000 Kuala Lumpur.  
Tel: (03) 4042 0617, 4041 8972, 4041 1375 Fax: (03) 4041 8187  
E-mail: [info@mma.org.my](mailto:info@mma.org.my) / [mjm@mma.org.my](mailto:mjm@mma.org.my)  
Website: [www.mma.org.my](http://www.mma.org.my)

# MJM Case Reports

## INSTRUCTION TO AUTHORS

### Requirements

All submission must be in English. All authors are encouraged to follow the MJM format and ICMJE and COPE guidelines. The case reports (maximum five patients/cases) must follow these requirements:

- Case reports, excluding abstract and references, should not exceed 2,000 words
- A maximum of two (2) tables; three (3) photographs; and up to ten (10) references.
- It shall adhere to the stipulated *MJM Case Reports* format
- There should be no more than seven (7) authors. All authors must have made an individual contribution to the writing of the article and not just involved in the patient's care.
- Patient's details are anonymised as much as possible and appropriate consent/permission obtained
- The case has never been published or has currently been submitted elsewhere for publication

Manuscript text should be submitted as Microsoft Word documents. Tables and flow-charts should be submitted as Microsoft Word documents. Images should be submitted as separate JPEG files (minimum resolution of 300 dpi).

Submissions must conform to the International Committee of Medical Journal Editors Recommendations for the Conduct, Reporting, Editing, and Publication of Scholarly Work in Medical Journals. The Editorial Board reserves the right to reject manuscripts that do not conform to this and policies of *MJM Case Reports*. Neither the Editorial Board nor the Publishers accept responsibility for the views and statements of authors expressed in their contributions.

Authors are advised to adhere closely to the Instructions to Authors. Manuscripts not meeting all the requirements will not be considered for publication and be returned to the authors for correction. Manuscripts should be submitted online through *MJM Case Reports Editorial Manager*.

All submissions must be accompanied by a completed Author Declaration Form, Copyright Transfer Form and Conflict of Interest Form duly signed by all authors. (Forms can be download here).

### Article Processing Charge

The *MJM Case Reports* Article Processing Charge (APC) is a non-refundable administrative fee. The current rate takes into account the administrative process required for each submission, and this is a new journal. Hence, the fee will be reviewed from time to time. Payment of the APC does not guarantee acceptance of the manuscript. Submitted manuscripts will only be sent for reviews once the APC has been successful completed.

MMA Member - RM 400.00

Non-Member/ Overseas - RM 500.00

### Preparing your manuscript

Manuscripts should be divided into individual section headings and contain the following information. It should not exceed 2000 words (excluding title page, abstract and references).

#### Title page:

The title page should clearly state the title of the case report without the use of any abbreviations, include full name(s) of the author(s), degrees (limited to one degree or diploma), and affiliations. All the authors' affiliations shall be provided after the authors' names. Indicate the affiliations with a superscript number at the end of the author's degrees and at the start of the name of the affiliation. If the author is affiliated to more than one (1) institution, a comma should be used to separate the number for the said affiliation.

Do provide preferred abbreviated author names for indexing purpose, e.g.L Rampal (for Lekhraj Rampal), BS Liew (for Liew Boon Seng), B Abdullah (for Baharudin Abdullah), Hoe VC (for Victor Hoe Chee Wai).

Please indicate the corresponding author and provide the affiliation, full postal address and email.

#### Summary:

The abstract should provide a background to the case, summarise its key points, highlight its novelty, learning outcome and implication for clinical practice. It should not be longer than 250 words.

#### Keywords:

Keywords allows appropriate indexing of the published article to aid future searching. Three to five keywords related to the case report should be provided.

#### Introduction:

The introduction provides a background and overview of the problem that will be highlighted in the case report. It also aims to summarise the relevant literature pertaining to the topic. It ends with an introduction to the patient/clinical condition that will be discussed in the following section.

#### Case presentation:

This section provides details of the case. The following is a suggested order of the case presentation.

- Case history – demographic details and medical history
- Physical examination results
- Results of relevant tests or investigations
- Treatment plan
- Outcome of the treatment plan

#### Discussion:

This section expands on the background written in the introduction. It will focus on the importance of the case and its novelty. Relevant literature should be cited to put this case in the context of the wider published papers.

#### Conclusion:

The case report ends with a summary of the key points and how it adds to our understanding of specific disease or condition.

#### Acknowledgements:

This section acknowledges the contribution of others who assisted in the production of the case report manuscript but do not fulfil authorship criteria.

#### Declarations:

A statement confirming ethical approval and patient (or carer/guardian) consent for publication must be provided. Any funding information should be provided here. Any competing interests by the authors with the manuscript must be declared in this section.

#### Abbreviations:

If abbreviations are used in the manuscript, they should be defined in the text at first use in the abstract and main text sections, unless they are standard unit of measurements. No abbreviations should be used in the title in the Title Page. Abbreviations should be kept to a minimum.

#### Formatting of text:

Numbers one to ten in the text are written out in words unless they are used as a unit of measurement, except in figures and tables. Use single hard-returns to separate paragraphs. Do not use tabs or indents to start a paragraph. Do not use the automated formatting of your software, such as hyphenation, endnotes, headers, or footers (especially for references). Submit the manuscript in plain text only and removed all 'field codes' before submission.

Do not include line numbers. Include only page numbers.

**References:**

*MJM Case Reports*, follows the Vancouver numbered referencing style. Citations to someone else's work in the text, should be indicated by the use of a number. In citing more than one article in the same sentence, you will need to include the citation number for each article. A hyphen should be used to link numbers which are inclusive, and a comma used where numbers are not consecutive. The following is an example where works 1,3,4, and 5 have been cited in the same place in the text.

- Several effective drugs are available at fairly low cost for treating patients with hypertension and reducing the risk of its sequelae.<sup>1,3-5</sup>

The list of all of the references that are cited in the article should be presented in a list labelled as 'References'. This reference list appears at the end of the paper. Authors are responsible for the accuracy of cited references and these should be verified by the author(s) against the original documents before the manuscript is submitted. It is important that the author should never place in the list of references a document that he or she has not seen. The journals' names should be abbreviated according to the style used in the Index Medicus. All authors when six or less should be listed; when seven or more list only the first six and add et al.

If you are citing the author's name in your text, you must insert the citation number as well.

- Jewell BL<sup>8</sup> underlined that as focus in the SARS-CoV-2 pandemic shifts to the emergence of new variants of concern (VOC), characterising the differences between new variants and non-VOC lineages will become increasingly important for surveillance and maintaining the effectiveness of both public health and vaccination programme.

If you are citing more than one author's name in your text and you want to cite author names in your text, use 'et al.' after the first author.

- Example: Rampal et al.<sup>9</sup> highlighted that the disregard of the manuscript guidelines and instruction to authors of the journal you submit, is one of the common reasons for 'Rejection' of the article.

**Example of references:**

Rampal L, Liew BS, Choolani M, Ganasegeran K, Pramanick A, Vallibhakara SA, et al. Battling COVID-19 pandemic waves in six South-East Asian countries: A real-time consensus review. *Med J Malaysia* 2020; 75(6): 613-25.

NCD Risk Factor Collaboration (NCD-RisC). Worldwide trends in hypertension prevalence and progress in treatment and control from 1990 to 2019: a pooled analysis of 1201 population-representative studies with 104 million participants. *Lancet* 2021; 11; 398(10304): 957-80.

**Tables:**

All tables and figures should have a concise title explaining its content and should not occupy more than one printed page. They should be numbered consecutively with Arabic numerals (e.g. Table 1), and placed after the sections of the manuscript which they reflect, particularly the results which they describe on separate pages. Cite tables in the text in consecutive order. Indicate table footnotes with lower-case letters in superscript font. Place the information for the footnote beneath the body of the table.

**Photographs:**

Clinical Photographs should conceal the subject's identity. Images should be submitted as separate JPEG files (minimum resolution of 300 dpi). Proof of permission and/or consent from the patient or legal guardian must be submitted with the manuscript. A statement on this must be included as a footnote to the relevant photograph.

**Colour reproduction:**

Illustrations and diagrams are normally reproduced in black and white only. Colour reproductions can be included if so required and upon request by the authors. However, a nominal charge must be paid by the authors for this additional service; the charges to be determined as and when on a per article basis.

**Editorial policy**

The journal follows ICMJE and COPE guidelines with regards to concerning its editorial policies on publication ethics, scientific misconduct, consent and peer review criteria. Authors are encouraged to follow the CARE guidelines (for CAsE REports).

## Case Reports

- From hyperactivity to harmony: A primary care case report on screen-limiting success 1  
*Azwanis Abdul Hadi, Siti Aisyah Yahaya*
- Clagett open-window thoracostomy revisited in empyema necessitans secondary to pulmonary tuberculosis – A case report 4  
*Muhamad Azri Muhamad Marican, Anas Sjahroeddin Ressang Aminuddin*
- Primary breast angiosarcoma: A case report 8  
*Mogen Raj Dhava, Liew Vin Sem, Che Jamal Abdillah Che Aman, Azmi Hassan*
- A silent impostor: Neurosyphilis mimicking incomplete oculomotor nerve palsy 13  
*Wan Mohd Redzuan Wan Hassan, Julieana Muhammed, Hor Jyh Yung, Wong Chee Keong, Abdul Salim Ismail, Kow Wen Jin, Syed Anwar Syed Hussain*
- Continuous renal replacement therapy in a post-bentall procedure patient complicated by sepsis and acute kidney injury: A case report 17  
*Budiana Rismawan, Ani Haryani*
- Inherited malignant brain tumour: A case of constitutional mismatch repair deficiency 21  
*Sugan Selvanathan, Teh Kok Hoi, Teh Chair Ying, Subasri Armon*
- Shadows of a triad: Exploring the gaps in miller fisher syndrome 25  
*Wan Mohd Redzuan Wan Hassan, Julieana Muhammed, Hor Jyh Yung, Wong Chee Keong, Abdul Salim Ismail, Nurul Najihah Khalid Alwalid Dziauddin3 Mohammad Syafiq Idris*
- A rare presentation of paracentral acute middle maculopathy during early gestation 28  
*Siti Hajar Darussalam, Amirah Mohammad Razali, Teck Chee Cheng, Jemaima Che Hamzah, Mohammad Mohd Isa*
- Huge tubo-ovarian abscess with elevated CA-125 pre-operative diagnosis dilemma: A case report 32  
*Su Chok Kim, Yew Tze Wei, Tze Cheng Yew, Harris Roland Demong*
- Case report of hyperemesis gravidarum: Hormonal change due to pregnancy and hypothyroidism 35  
*Nieke Andina Wijaya, Shod Abdurrachman Dzulkarnain, Soedarsono Hadipranata*
- Miller fisher syndrome mimicking cavernous sinus thrombosis and thyroid eye disease: A diagnostic dilemma in a hyperthyroid patient 41  
*Nur Azureen Mohd Ali, Julieana Muhammed, Farhana Ibrahim*
- Placental-site trophoblastic tumor with deep myometrial invasion - a rare entity: The Malaysian experience 44  
*Pei Yoke Wang, Mohd Faizal Ahmad, Mohamad Faiz Mohamed Jamli, Marliza Hadzar, Eng Ngen Chong, Chee Meng Yong*
- A case report: Co-existence of uterine arteriovenous malformation with persistent trophoblastic disease – The diagnostic and management dilemmas 50  
*Rajkumar Chelladurai, Kalavathy Subramaniam*
- Optimizing care in caesarean scar pregnancy: Lesson from five cases with different management modalities 53  
*Siti Sarah Ahmad, Sharifa Azlin Hamid, Bavanandam Naidu, Ismail Aliyas*
- Isolated portal vein thrombosis as a rare complication of minimal change disease in nephrotic syndrome 58  
*Aini Izzati Abdullah, Hoong Heng Loh, Yik Shen Lim, Siti Salwani Othman, Anim Md Shah*

## CONTENTS

## Page

- 
- Transmastoid repair of delayed traumatic cerebrospinal fluid (CSF) leak in a paediatric patient with skull base fracture 62  
*Yuanzhi Cheah, Asfa Najmi Mohamad Yusof, Noor Dina Hashim, Ing Ping Tang*
  - Rouleaux formation in acute myeloid leukemia: A morphological clue to COVID-19 co-infection 65  
*Kaveta Balasubramaniam, Zainina Seman, Sabariah Md Noor*
  - <sup>99m</sup>Tc-Sestamibi scintigraphy to differentiate benign and malignant renal masses: A case report 68  
*Muhammad Azizul Daud, Khadijah Abdul Hamid, Othman Puteh, Khin Thuzar Pyone, Wan Fatimah Wan Sohaimi*
  - When ulcers do not heal: Recognising behçet’s disease from recurrent oral ulcers in primary care 71  
*Syed Mohd Taufiq Wan Obeng, Muhammad Naqib Ibrahim, Aznida Firzah Abdul Aziz*
  - Tuberculosis and Bartonella co-infection in people living with human immunodeficiency virus (HIV) 75  
*Juwie Chuah, Gan Wee Fu*
  - Priapism in chronic myeloid leukemia: A rare case report 79  
*Ni Putu Merlynda Pusvita Dewi, Adiba Hasna Hanifah*
  - The silent “Cheeky” mystery: A case of indolent yet invasive dermatofibrosarcoma protuberans 84  
*Ingrid Ting Pao Lin, Azam Hilmi Mohd Zain, Koh Siang Chai, Min Moon Tang*
  - Primary nasal tuberculosis complicated by mrsa co-colonization and septal perforation: A rare case report 88  
*Sonny Soebjanto, Shod Abdurrachman Dzulkarnain*
  - Unravelling the Frozen Gaze: A rare occurrence of superior orbital fissure syndrome (SOFS) post craniofacial trauma 92  
*Hui Wen Tay, Sherrie Mei Yee Chong, Juliana binti Khairi, Szu Ching Khoo, Marzuki bin Zainal Abidin*

# From hyperactivity to harmony: A primary care case report on screen-limiting success

Azwanis Abdul Hadi, MMed, Siti Aisyah Yahaya, MBBS

Department of Family Medicine, Kulliyyah of Medicine, International Islamic University Malaysia, Kuantan, Pahang, Malaysia

## SUMMARY

**Excessive screen use in children may be linked to inattention, hyperactivity, and emotional dysregulation, mimicking neurodevelopmental disorders. Early recognition and differentiation from neurobiological causes in primary care are essential for appropriate management. An 8-year-old boy presented with hyperactivity and inattention, using screens five hours daily on weekdays and twelve hours on weekends. Assessment showed high screen dependency score (48/60). The Vanderbilt ADHD scores were markedly elevated, with ten positive responses across both the inattentive and hyperactive symptom domains, and clear impairment in the performance domain, particularly in relationships with parents and siblings. These findings fulfil the DSM-5 criteria for a possible diagnosis of ADHD, despite normal developmental milestones and preserved speech and sensory functions. A three-month, parent-led intervention was subsequently introduced, incorporating Google Family Link and structured routine modifications. This method successfully reduced screen time to under two hours on weekends and eliminated it entirely on weekdays. Following the intervention, the screen dependency score fell markedly to 17/60. The Vanderbilt scores also normalised, with no positive responses to the previously affected domains. Performance ratings improved reflecting better behavioural regulation and attention. This case underscores the importance of assessing screen use and implementing parent-led strategies as effective interventions within the primary care setting.**

## INTRODUCTION

In the digital age, screen media use has become an integral part of children's daily lives, with exposure often starting in early childhood. Excessive screen time, defined as use exceeding established health guidelines, has been linked to inattention, hyperactivity, emotional dysregulation, and impaired social interaction.<sup>1,2</sup> In primary care, early recognition of screen-related behavioural changes is vital to avoid misdiagnosis, prevent unnecessary pharmacological treatment, and implement timely lifestyle interventions. Herein, we present a case of a child with behavioural changes secondary to excessive screen exposure, detected early and managed through a structured, parent-led, non-pharmacological approach. This report underscores the need for systematic assessment of children's screen time in primary care during behavioural evaluations, acknowledging that high screen exposure may influence behaviour and resemble signs seen in other conditions. It demonstrates how

structured, parent-led strategies can be applied in a primary care setting and encourages clinicians to assess daily screen habits as part of routine practice to support early identification and targeted management of modifiable lifestyle factors.

## CASE PRESENTATION

An 8-year-old Malay boy, currently a student, was brought to the clinic by his mother. The primary concern was his hyperactive behaviour and difficulty with attention, particularly in academic settings. The mother described that he frequently fidgeted, left his seat when he was expected to remain seated, and struggled to engage in quiet play. While he did not exhibit excessive talking, arguing, or temper loss, his teacher noted that although he sometimes had trouble sitting still and maintaining focus during class, he did not disrupt his classmates or leave the classroom.

The child's academic challenges extended to homework, where he often made careless mistakes and showed reluctance to initiate tasks that required sustained effort. Notably, despite these issues, he interacted well with his peers and siblings, maintained appropriate facial expressions, made good eye contact, and responded adequately to social cues. The mother also revealed that he spent a significant amount of time watching television and playing games on a smartphone, which raised the concern of excessive screen exposure playing a role in his behavioural presentation. The child was first exposed to screen devices at the age of two years old. On weekdays, he spent more than five hours per day on screens, increasing to over twelve hours during weekends. The most frequently used devices were smartphones and televisions, primarily used for watching fast-paced action cartoons on YouTube or broadcast television and smartphone online games. The mother was not consistently aware of the content her son watched, and no screen-time boundaries were in place. Screen use often occurred during mealtimes, at bedtime, and within the bedroom. The mother operated an online business that required her to engage with her smartphone for nearly 24 hours a day. Importantly, there was no significant family history of autism or ADHD, and his antenatal, postnatal, and overall developmental milestones were uneventful.

On clinical examination, the boy was observed to be active with no dysmorphic features. His sensory functions were intact, as confirmed by a normal hearing assessment by an audiologist and a speech evaluation by a speech therapist.

*This article was accepted: 05 January 2026*

*Corresponding Author: Siti Aisyah Yahaya*

*Email: aisayahahaya89@gmail.com*

Prior to intervention, initial screening revealed a notably high score on the screen dependency scale for media addiction (48/60), and Vanderbilt Assessment results met DSM-5 criteria for a possible ADHD diagnosis. The child scored 2 or 3 on five of the nine inattention items (questions 1–9), and similarly on five of the nine behaviour (hyperactivity/impulsivity) items (questions 10–18). In the performance domain, he received a score of 4 on two of the eight items, indicating impaired relationships with both parents and siblings. These findings supported the view that excessive screen time might have been a contributing factor to his hyperactivity and attentional difficulties.

The mother was enrolled in a screen addiction programme organised by our clinic. During the programme, she was introduced to the Google Family Link app as a tool to monitor and manage her child's screen time. The intervention strategy focused on limiting the boy's exposure to screens, including television and smartphones, to improve his behavioural concerns. This non-pharmacological approach was structured over a three-month period, with parental assistance to adjust his daily routine.

At his follow-up review after three months of intervention, the mother reported significant improvements. Following the intervention, screen time had been substantially reduced. On weekdays, the child no longer used television or smartphone games. During weekends, screen exposure was limited to less than two hours of approved television viewing, subject to parental permission. Instead, he spent most of his time playing or engaging in activities with his siblings. His ability to remain seated and attentive had improved, as he was able to engage for hours in focused activities such as building Lego sets. Additionally, a consistent daily schedule had been implemented, notably including an earlier bedtime. Post-intervention assessments showed marked improvement, with the screen dependency score on the media addiction scale dropped dramatically from 48 to 17. Vanderbilt Assessment results resolved, with all symptom domains scoring 0, indicating that the previous concerns regarding inattention and hyperactivity were no longer present. Additionally, in the performance domain, the child scored 3 (moderately good) consistently across all items, reflecting restored and healthy relationships with parents and siblings.

## DISCUSSION

Excessive screen time, defined as media exposure that exceeds internationally recommended guidelines, has become a significant public health concern in recent years. The American Academy of Paediatrics (AAP) advises that children under two years of age should have no screen exposure, and those aged two to five years should be limited to a maximum of one hour per day.<sup>3</sup> However, these recommendations are frequently exceeded, with children often engaging in prolonged, unsupervised screen use. This is particularly concerning, as evidence has consistently shown that excessive screen exposure can have far-reaching implications on cognitive, behavioural, and socio-emotional development.

High screen time has been associated with reduced IQ scores, deficits in metacognition and inhibition, and poorer self-regulation abilities.<sup>4,5</sup> These neurocognitive changes are

frequently accompanied by heightened emotional reactivity and lower effortful control. Consequently, children with high daily screen exposure may present with increased externalising behaviours, such as hyperactivity, impulsivity, and restlessness.<sup>2,4</sup> This case illustrates such an association, as the patient demonstrated elevated scores on both the Screen Dependency Scale (SDS)<sup>6</sup> and Vanderbilt ADHD assessment, highlighting the potential overlap between screen-related behavioural symptoms and those seen in neurodevelopmental disorders.

Although the child's presentation could have been interpreted as indicative of attention-deficit/hyperactivity disorder (ADHD), careful evaluation suggested that his symptoms were likely influenced by lifestyle factors. The distinction between true neurobiological disorders and screen-related behavioural concerns is critical in primary care. ADHD is characterised by persistent, context-independent symptoms of inattention, impulsivity, and hyperactivity, which occur across multiple settings, including home, school, and social environments, and typically do not improve substantially with lifestyle modification alone.<sup>7</sup> Accurate diagnosis requires a thorough clinical history, the use of validated rating scales, and corroborative input from multiple informants such as parents and teachers.

In contrast, screen-related behavioural changes are often context-specific, emerge or worsen in parallel with increased screen exposure, and may resolve or significantly improve with structured reduction in screen use.<sup>8</sup> Importantly, these cases rarely necessitate long-term pharmacological therapy; instead, they respond well to behavioural strategies, environmental restructuring, and parental education about healthy media use.<sup>8,9</sup> The use of structured assessment tools, such as the SDS, alongside a detailed screen time history, can greatly aid in differentiating between these conditions in a primary care setting.<sup>10</sup>

The ability to make this distinction has important implications. Misdiagnosing screen-related behavioural problems as ADHD may lead to premature labelling, unnecessary pharmacological treatment, and avoidable specialist referrals. Primary care physicians, who are often the first point of contact for concerned parents, are in a unique position to identify modifiable lifestyle factors contributing to behavioural symptoms. A thorough assessment should include exploration of the child's daily routines, sleep habits, family dynamics, and the nature and duration of screen exposure.

In this case, the mother was enrolled in a screen addiction programme organised by our clinic. During the session, she was introduced to the Google Family Link app, a parental control tool that enables monitoring, setting time limits, and restricting inappropriate content. The intervention plan focused on gradually reducing the child's screen time, including television and smartphone use, and re-establishing a structured daily routine. Over a three-month period, the parents were supported to implement consistent limits and introduce alternative activities such as sibling play and interactive family engagement.

This approach aligns well with the core principles of family medicine, including prevention, health promotion, and active family involvement. Parent-led, non-pharmacological

strategies are supported by the literature as effective, accessible, and cost-efficient options that can be integrated into routine primary care. By addressing underlying factors early and within the child's environment, such strategies may also lessen reliance on specialist referrals and medical treatment.

The success observed in this case shown by the marked reduction in daily screen time was reflected in improvements in both SDS and Vanderbilt scores, with better attention, reduced hyperactivity, more consistent routines, and earlier bedtimes. These outcomes suggest that screen-related behavioural issues can be identified and may improve with early intervention, especially when parents are equipped with the right knowledge and tools to support lasting change. Involving the mother directly in the management plan and providing educational resources and practical digital tools strengthened her ability to set and enforce healthy limits, underscoring the value of parental empowerment in achieving positive outcomes.

From a systems perspective, it demonstrates how primary care can address common behavioural concerns, potentially lowering the need for specialist referral. This not only reduces healthcare costs and waiting times but also fosters continuity of care and strengthens the therapeutic relationship between the physician and family. Incorporating screen time assessment into standard paediatric behavioural evaluations is therefore recommended. Simple, structured questions during consultations can uncover excessive screen use, allowing for early counselling and the introduction of preventive measures. The lessons from this case align with the growing body of evidence supporting a proactive, holistic approach to addressing child behavioural concerns in primary care.

## CONCLUSION

This case suggests that excessive screen time in children may be associated with behaviours resembling neurodevelopmental disorders, and that a structured, parent-led, non-pharmacological intervention coincided with notable improvements in attention, behaviour, daily routines, and overall functioning. While promising, causality cannot be established from a single case, and further research with comparison groups and extended follow-up is needed to confirm these observations.

In primary care, systematic assessment of screen exposure can identify modifiable lifestyle factors, guide targeted support, and reduce the risk of misdiagnosis. Differentiating screen-related behaviours from underlying neurobiological

conditions requires thorough history taking and validated measurement tools. The positive outcomes in this case underscore the importance of parental engagement and practical strategies in supporting sustainable change. By showing how tailored lifestyle modification can align with improved outcomes, this report highlights the value of careful behavioural evaluation and supports non-pharmacological approaches within routine primary care.

## REFERENCES

1. Bal M, Kara Aydemir AG, Tepetaş Cengiz GŞ, Altındağ A. Examining the relationship between language development, executive function, and screen time: A systematic review. *PloS one*. 2024; 19(12): e0314540.
2. Likhitweerawong N, Boonchooduang N, Khorana J, Phinyo P, Patumanond J, Louthrenoo O. Executive dysfunction as a possible mediator for the association between excessive screen time and problematic behaviors in preschoolers. *Plos one*. 2024; 19(4): e0298189.
3. McArthur BA, Volkova V, Tomopoulos S, Madigan S. Global prevalence of meeting screen time guidelines among children 5 years and younger: a systematic review and meta-analysis. *JAMA pediatrics*. 2022; 176(4): 373-83.
4. Vohr BR, McGowan EC, Bann C, Das A, Higgins R, Hintz S, et al. Association of high screen-time use with school-age cognitive, executive function, and behavior outcomes in extremely preterm children. *JAMA pediatrics*. 2021; 175(10): 1025-34.
5. Fitzpatrick C, Harvey E, Cristini E, Laurent A, Lemelin JP, Garon-Carrier G. Is the association between early childhood screen media use and effortful control bidirectional? A prospective study during the COVID-19 pandemic. *Frontiers in psychology*. 2022; 13: 918834.
6. Abdul Hadi A, Roslan SR, Mohammad Aidid E, Abdullah N, Musa R. Development and validation of a new gadget addiction scale (Screen dependency scale) among pre-school children in Malaysia. *International journal of environmental research and public health*. 2022; 19(24): 16916.
7. French WP. Assessment and treatment of attention-deficit/hyperactivity disorder: part 1. *Pediatr Ann*. 2015; 44(3): 114-20.
8. Nagata JM, Al-Shoaibi AA, Leong AW, Zamora G, Testa A, Ganson KT, Baker FC. Screen time and mental health: a prospective analysis of the Adolescent Brain Cognitive Development (ABCD) Study. *BMC Public Health*. 2024; 24(1): 2686.
9. Song K, Zhang JL, Zhou N, Fu Y, Zou B, Xu LX, et al. Youth screen media activity patterns and associations with behavioral developmental measures and resting-state brain functional connectivity. *Journal of the American Academy of Child & Adolescent Psychiatry*. 2023; 62(9): 1051-63.
10. Hadi AA, Abd Latip NA, Aidid EM. Screen media dependency and its associated factors among preschool children in Kuala Lumpur. *Malaysian Journal of Medicine and Health Sciences*. 2023; 19(3): 204-14.

# Clagett open-window thoracostomy revisited in empyema necessitans secondary to pulmonary tuberculosis – A case report

Muhamad Azri Muhamad Marican, MBChB, Anas Sjahroeddin Ressang Aminuddin, MBBS

Department of Surgery, Hospital Sultan Zainal Abidin, Kuala Terengganu, Malaysia

### SUMMARY

This report details the case of a 47-year-old male who developed empyema necessitans, a rare complication where a pleural infection extends into the chest wall, secondary to chronic pulmonary tuberculosis. The patient initially presented in 2020 and was managed with anti-tuberculous therapy but declined surgical intervention. Two years later, he returned with recurrent empyema thoracis and a trapped lung. Despite chest tube drainage and targeted antibiotics for a superimposed *Pseudomonas aeruginosa* infection, his condition did not resolve. Consequently, he underwent a Clagett open-window thoracostomy. This surgical procedure, which involves creating an opening into the chest cavity for drainage and packing, revealed extensive pleural fibrosis that prevented lung re-expansion. The Clagett window facilitated effective infection control and promoted the growth of healthy granulation tissue, leading to a favorable outcome. This case underscores the enduring relevance of the Clagett thoracostomy as a vital surgical option for complex and refractory chronic empyema, especially in the context of extensive tuberculous fibrosis.

### INTRODUCTION

Empyema necessitans is an uncommon but serious complication of pleural infection, in which purulent material dissects through the parietal pleura into the chest wall and surrounding soft tissues.<sup>1</sup> It has been described for centuries but remains most frequently associated with tuberculosis, particularly in regions where the disease is endemic. Chronic tuberculous empyema presents a formidable therapeutic challenge because of the dense fibrous peel that encases the lung and prevents re-expansion, leaving a persistent cavity that sustains infection despite antibiotics or drainage.<sup>1,3</sup>

Surgical intervention is often required when medical treatment fails. Among the available approaches, the open window thoracostomy first described by Clagett and Geraci in 1963 has stood the test of time.<sup>2</sup> The procedure involves removal of rib segments and creation of a marsupialized opening into the pleural cavity to allow continuous drainage, reduce the bacterial burden, and encourage the gradual filling of the space with granulation tissue.

Over the decades, several series have confirmed the value of this technique for chronic empyema, especially in cases where the lung is destroyed or irreversibly trapped.<sup>4,5,6</sup> More

recently, the use of vacuum assisted closure therapy has been introduced as an adjunct, accelerating granulation and shortening the time to closure.<sup>7,8</sup> Even in the modern era of minimally invasive surgery and intrapleural fibrinolytics, open window thoracostomy continues to provide dependable outcomes in selected patients with advanced disease.<sup>9,10</sup>

The present case report describes a patient with tuberculous empyema complicated by empyema necessitans, successfully managed with a Clagett open window thoracostomy. This case highlights the ongoing importance of a procedure that, although introduced more than half a century ago, remains highly relevant in contemporary thoracic surgery.

### CASE PRESENTATION

A 47-year-old male was first diagnosed with right-sided empyema thoracis secondary to pulmonary tuberculosis in September 2020. At that time, a chest tube was inserted, and surgical decortication was recommended. However, the patient declined the operation and opted for medical management. He completed a one-year course of anti-tuberculous therapy (ATT) in August 2021 but was subsequently lost to follow-up.

In July 2023, he presented to the emergency department with a two-week history of dyspnoea, productive cough, and haemoptysis. A chest X-ray revealed a massive right-sided pleural effusion. A chest tube was inserted, and the drained pus grew *Pseudomonas aeruginosa* on culture. The patient was started on intravenous antibiotics based on sensitivity testing and referred to the cardiothoracic surgery service for further management.

### Investigations

The admission chest X-ray showed a large, opacified right hemithorax with a contralateral tracheal shift, consistent with a massive pleural effusion and no underlying lung aeration (Figure 1-A). A contrast-enhanced computed tomography (CECT) scan of the thorax confirmed a large, right-sided fluid collection with markedly thickened parietal pleura. The scan also revealed a direct extension of the collection into the subcutaneous tissue between the 9th and 10th ribs posteriorly, establishing the diagnosis of empyema necessitans (Figure 2-A). The axial view clearly demonstrated the chronic trapped right lung, encapsulated by a thick visceral peel (Figure 2-B).

This article was accepted: 20 November 2025

Corresponding Author: Muhamad Azri Muhamad Marican

Email: azrimarican88@gmail.com

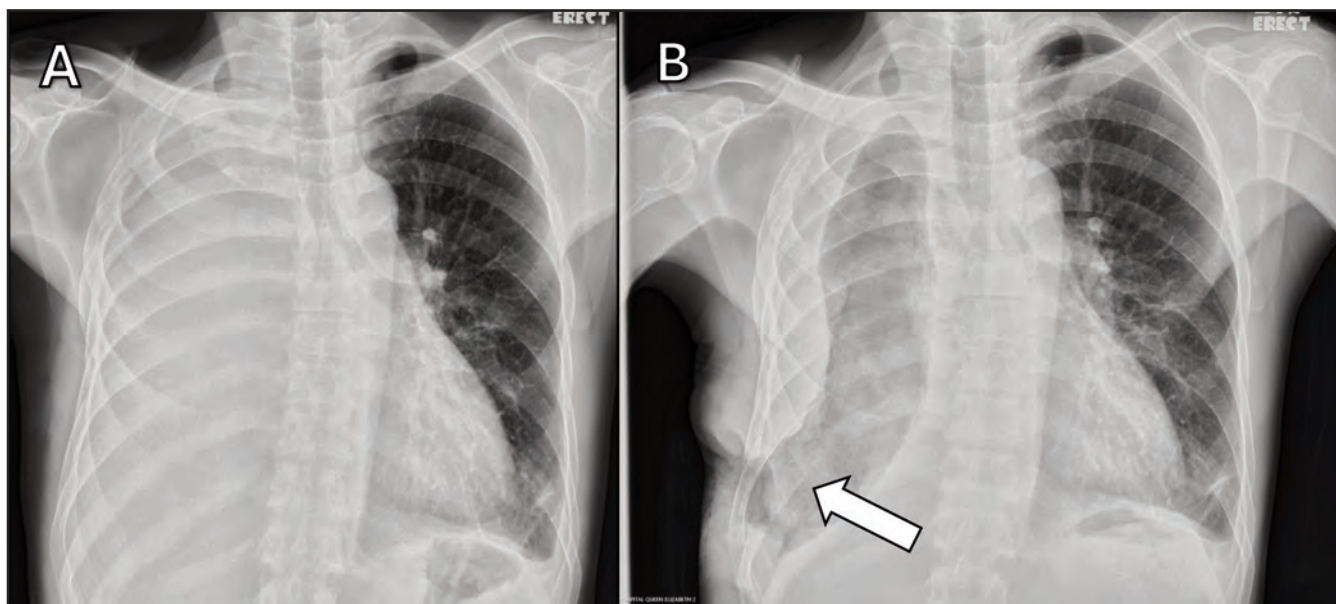


**Fig. 1:** A. Chest x-ray showed total opacity of right lung with no lung aeration before operation. B. Chest x-ray showed no more effusion over right lung cavity after right Clagett open-window thoracostomy and arrow showed the rib resected during operation

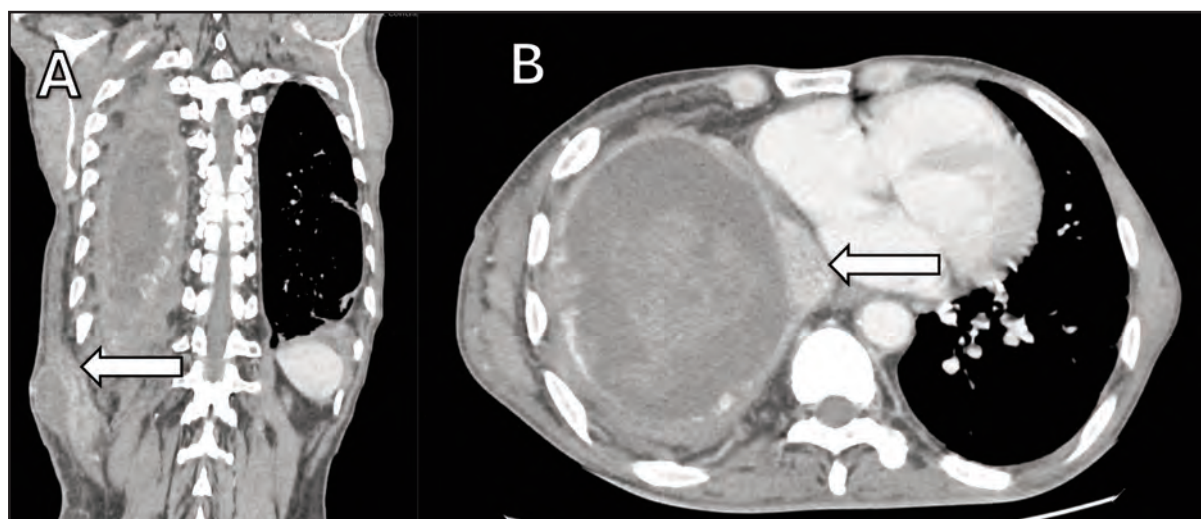


**Fig. 2:** A. Contrast-enhanced CT (coronal view) showed right empyema thoracis with thick parietal cortex and extension to the subcutaneous tissue between 9th and 10th ribs (arrow). B. Contrast-enhanced CT (axial view) showed right empyema thoracis with chronic trapped lung (arrow)

### Management

The initial surgical intervention consisted of an incision and drainage of the chest wall abscess at its most fluctuant point. A cruciate incision was made over the right posterior 9th and 10th intercostal spaces, releasing approximately 2500 mL of frank pus. Cultures again grew *Pseudomonas aeruginosa*, and the patient was treated with a six-week course of intravenous antibiotics.

Following this, daily dressings were performed through the incision site to the pleural cavity, but the opening began to narrow, compromising adequate drainage. A decision was therefore made to perform formal right-sided Clagett open window thoracostomy.

Intraoperatively, a preliminary video-assisted thoracoscopic surgery (VATS) was performed to assess the pleural space. This revealed a cavity almost entirely lined by a thick, fibrous cortex, with no identifiable viable lung tissue. Multiple sites of slow, oozing haemorrhage were noted from the raw surfaces. To create the window, an incision was made at the most dependent part of the right thoracic cavity, and segments of two lower ribs were resected. The skin edges were then sutured down to the parietal pleura with a non-absorbable monofilament suture, creating a marsupialized opening and covering the sharp, cut rib edges. The cavity was thoroughly irrigated with antiseptic solution.

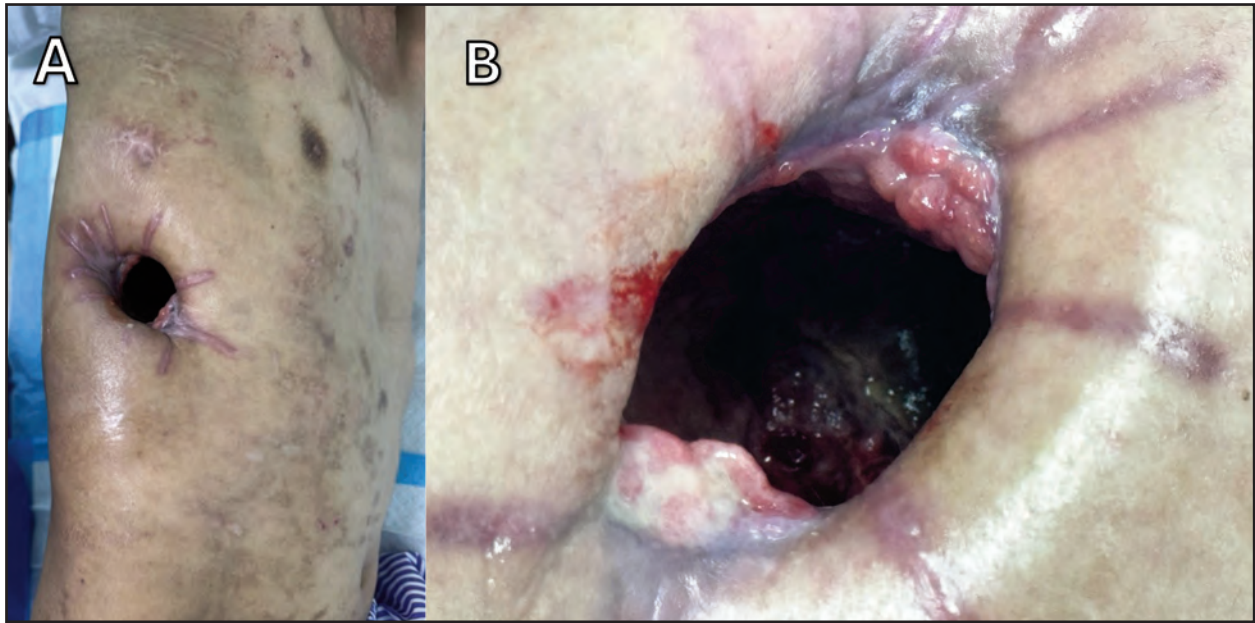


**Fig. 3:** A. Right Claggett open-window thoracostomy after the edges healed and covered with skin. B. Close-up picture of the right Claggett open-window thoracostomy wound

Postoperatively, the patient underwent daily dressing changes of the Claggett window. He was continued on oral antibiotics to suppress the infection. Over time, healthy granulation tissue progressively filled the pleural cavity (Figure 3). A follow-up chest X-ray demonstrated the resolution of the fluid-filled cavity, which was being replaced by newly formed tissue (Figure 1-B).

## DISCUSSION

Empyema necessitans remains a striking reminder of how chronic pleural infections can evolve if not adequately treated. Although rare in the modern antibiotic era, it is still encountered in tuberculosis-endemic regions, where chronic empyema with a trapped lung poses significant management challenges.<sup>1,3</sup> In these patients, the lung is encased by a rigid fibrous peel that prevents re-expansion, leaving a chronically infected cavity that is resistant to standard measures such as antibiotics and intercostal drainage.

The Claggett open window thoracostomy, first described in 1963, was originally conceived for post-pneumonectomy empyema but has since proved to be a versatile tool for managing chronic, refractory pleural infections of various causes.<sup>2</sup> The enduring value of the procedure lies not in restoring lung function but in reliably controlling sepsis. By providing a marsupialized opening into the pleural cavity, it ensures continuous drainage, prevents accumulation of infected fluid, and allows meticulous wound care. Over time, this facilitates the gradual replacement of the cavity by granulation tissue, effectively transforming a hostile space into one capable of healing.<sup>4,5</sup>

The technical principle of placing the window at the most dependent part of the cavity is central to its success. Gravity aids drainage and reduces the risk of residual loculations that

could sustain infection.<sup>4,6</sup> Long-term studies have confirmed that, when performed correctly, open window thoracostomy offers durable infection control with acceptable morbidity<sup>5,6</sup>. Failure is more likely when the stoma is inadequate in size, when a persistent bronchopleural fistula remains, or when the patient's nutritional status is poor.<sup>6</sup>

The evolution of adjunctive technologies has further refined the management of chronic empyema. Negative pressure wound therapy, commonly applied through vacuum assisted closure (VAC) systems, has been shown to accelerate granulation, reduce bacterial burden, and shrink the cavity more quickly than traditional dressings.<sup>7,8</sup> Although VAC was not available in the present case, its growing use in specialized centers represents a valuable adaptation of the original Claggett principles. Importantly, this case demonstrates that even without such adjuncts, the fundamental technique remains highly effective.

In contemporary thoracic practice, the place of open window thoracostomy must be considered in the broader context of minimally invasive surgery, intrapleural fibrinolytics, and advanced antimicrobial therapy. While these modalities can be effective in early or less complex empyema, refractory case particularly those with a trapped lung continue to demand surgical drainage. Recent outcome studies affirm that open window thoracostomy continues to provide reliable results in such patients.<sup>9</sup> Moreover, once infection is controlled and granulation tissue is established, reconstructive techniques can be employed to restore chest wall integrity and quality of life.<sup>10</sup>

This case illustrates how the principles described by Claggett more than half a century ago remain relevant today. In a patient with long-standing tuberculosis, secondary bacterial infection, and a chronically entrapped lung, the Claggett window offered definitive sepsis control and allowed

progressive healing. For surgeons working in tuberculosis-endemic settings, it is a reminder that time-tested procedures, when applied thoughtfully, continue to have a vital role alongside modern innovations.

#### CONCLUSION

The Clagett open window thoracostomy remains an indispensable surgical tool for the management of complex, refractory empyema necessitans, especially in cases secondary to pulmonary tuberculosis with extensive fibrosis and a trapped lung. The procedure offers a reliable method for achieving definitive infection control and promoting gradual healing through granulation tissue formation. This case demonstrates that even without modern adjuncts, the fundamental principles of the Clagett window provide a robust and effective solution, affirming its relevance in contemporary thoracic surgical practice.

#### CONFLICT OF INTEREST

The authors declare no conflict of interest.

#### PATIENT CONSENT

Written informed consent was obtained from the patient for the publication of this case report and any accompanying images.

#### REFERENCES

1. Ahmed AE, Yacoub TE. Empyema thoracis. *Clin Med Insights Circ Respir Pulm Med.* 2010; 4: 1-8.
2. Clagett OT, Geraci JE. A procedure for the management of postpneumonectomy empyema. *J Thorac Cardiovasc Surg.* 1963; 45: 141-5.
3. Ali SM, Siddiqui AA, McLaughlin JS. Open drainage of massive tuberculous empyema with progressive reexpansion of the lung: an old concept revisited. *Ann Thorac Surg.* 1996; 62(1): 218-24.
4. Smolle-Jüttner F, Beuster W, Pinter H, et al. Open window thoracostomy in pleural empyema. *Eur J Cardiothorac Surg.* 1992; 6(12): 635-8.
5. Maruyama R, Ondo K, Mikami K, Ueda H, Motohiro A. Clinical course and management of patients undergoing open window thoracostomy for thoracic empyema. *Respiration.* 2001; 68(6): 606-10.6.
6. Okumura Y, Takeda S, Asada H, Inoue M, Sawabata N, Shiono H, et al. Surgical results of open window thoracostomy for chronic empyema: the long-term outcome and risk factors for failure. *Surg Today.* 2005; 35(1): 22-6.
7. Palmén M, van Breugel HN, Geskes GG. Open window thoracostomy treatment of empyema is accelerated by vacuum-assisted closure. *Ann Thorac Surg.* 2009; 88(4): 1131-6.
8. Sziklavari Z, Grosser C, Neu R, Schemm R, Kortner A, Szöke T, et al. Minimally invasive vacuum-assisted closure therapy in the management of complex pleural empyema. *Interact Cardiovasc Thorac Surg.* 2013; 17(3): 437-41.
9. Cain CJ, Margolis M, Lazar JF, Henderson H, Hamm M, Malouf S, et al. Short and long-term outcomes of surgical intervention for empyema in the post-fibrinolytic era. *J Cardiothorac Surg.* 2021; 16(1): 187.
10. Kleeven A, Daemen JHT, de Loos ER, van der Hulst RRWJ, Qiu SS. Chest wall reconstruction after the Clagett procedure and other types of open-window thoracostomy: a narrative review. *J Thorac Dis.* 2023; 15(12): 7063-76.

# Primary breast angiosarcoma: A case report

**Mogen Raj Dhava, MD, Liew Vin Sern, MSurg, Che Jamal Abdillah Che Aman, Dr Gen Surg, Azmi Hassan, MMed**

Department of General Surgery, Hospital Sultan Haji Ahmad Shah, Temerloh Pahang, Malaysia

### SUMMARY

**Breast angiosarcoma is a rare and aggressive malignancy arising from vascular endothelial cells. It is categorized into primary and secondary types, with primary breast angiosarcoma (PBA) occurring de novo and accounting for less than 0.04% of all breast malignancies. The condition often mimics other breast cancers clinically and radiologically, leading to diagnostic difficulty. Imaging lacks specificity, and diagnosis depends mainly on histopathological and immunohistochemical findings. Mastectomy remains the mainstay treatment to achieve negative margins, while the role of adjuvant radiotherapy or chemotherapy remains uncertain. Due to its rarity and aggressive course, further studies are required to improve management strategies and survival outcomes.**

### INTRODUCTION

Breast angiosarcoma (BA) is a rare form of malignancy, accounting for less than 1% of all breast cancers. It originates from vascular endothelial cells and may occur spontaneously as primary breast angiosarcoma (PBA) or as a secondary malignancy following radiotherapy.<sup>2,5</sup> Primary BA arises de novo in non-irradiated breast tissue and has a reported incidence of less than 0.04% of all breast malignancies.<sup>3,5,6</sup> Secondary BA, in contrast, occurs predominantly in elderly women after breast-conserving surgery with adjuvant radiotherapy, typically within the irradiated field.<sup>4,5,7</sup> Both subtypes are aggressive, with poor prognosis and high recurrence potential.<sup>1,3</sup>

### CASE PRESENTATION

A 49 years old, postmenopausal Malay woman, previously not known to have medical illness, presented with left breast swelling for the past 7 years. Initially, the mass was smaller in size, however, rapidly increasing in size for the past 6 months. Besides, the patient was also complaining about retraction of left nipple and intermittent serous left nipple discharge. Patient had a history of taking oral contraceptive pills/ Otherwise, no complaints over the right breast, no constitutional symptoms, no history of exposure to radiation/radiotherapy, no history of cancer among first degree relatives and the patient was not on any hormone replacement therapy.

Physical examination revealed palpable fungating mass measuring 15cm x15cm occupying the entire left breast with necrotic patches (Figure 1). The left nipple was found to be

inverted. On palpation the mass was hard, non-tender and fixed to the overlying skin. The anterior group of left axillary lymph nodes were palpable. Otherwise, the assessment over the right breast and axilla were insignificant.

Subsequently, mammography(MMG) and Ultrasonography (USG) of bilateral breasts and axilla were done as part of the triple assessment. Mammography (Figure 2) of the left breast is reported as a large irregular lobulated high density lesion seen occupying all quadrants of the left breast. There is associated mild architectural distortion, nipple retraction and overlying skin thickening. Otherwise, no suspicious cluster of microcalcification and left axillary lymph nodes seen.

USG of the left breast (Figure 3) showed a large lobulated heterogeneously hypoechoic mass with posterior shadowing occupying the central part of the breast measuring 4.1x9.0x7.6cm at the subcutaneous region of skin and nipples.

Primary radiological assessment concluded as suspicious left breast lesion with subcutaneous skin involvement, and it highly suggestive of malignancy.-(Breast Imaging Reporting and Data System) BI-RADS Category 5.

Consequently, the patient had undergone Tru-cut biopsy, which revealed malignant tumour consisting of solid growth of spindle and epithelioid cells. Apart from necrosis and blood lakes are seen, tumour cells display marked nuclear atypia. Immunohistochemical markers of the tumor cells are positive for CD 31, and negative for CK7, LCA, CK AE1 AE3 and S100. Hence, the biopsy results further concluded as primary breast angiosarcoma.

Subsequently, a contrast enhanced computed tomography (CECT) of Thorax (Figure 4) done prior to surgery. Revealed large fungating, irregular, lobulated, heterogeneously enhanced mass is seen occupying the entire left breast, measuring approximately 9.5x9.0x9.7cm. Anteriorly,it infiltrates the left nipple and the overlying skin, causing skin thickening. Posteriorly, there is infiltration to the underlying left pectoralis major muscle. Surrounding subcutaneous fat streakiness around the mass.

Our patient had undergone radical mastectomy of the left breast. In view of larger chest wall defects (Figure 5), primary closure was unfeasible. Hence, reverse abdominoplasty technique was done for the closure of extensive post-mastectomy chest wall defect (Figure 6). Post-operative



Fig. 1: (Preoperative appearance):Fungating mass measuring about 15cm x15 cm occupying the entire left breast with necrotic patches

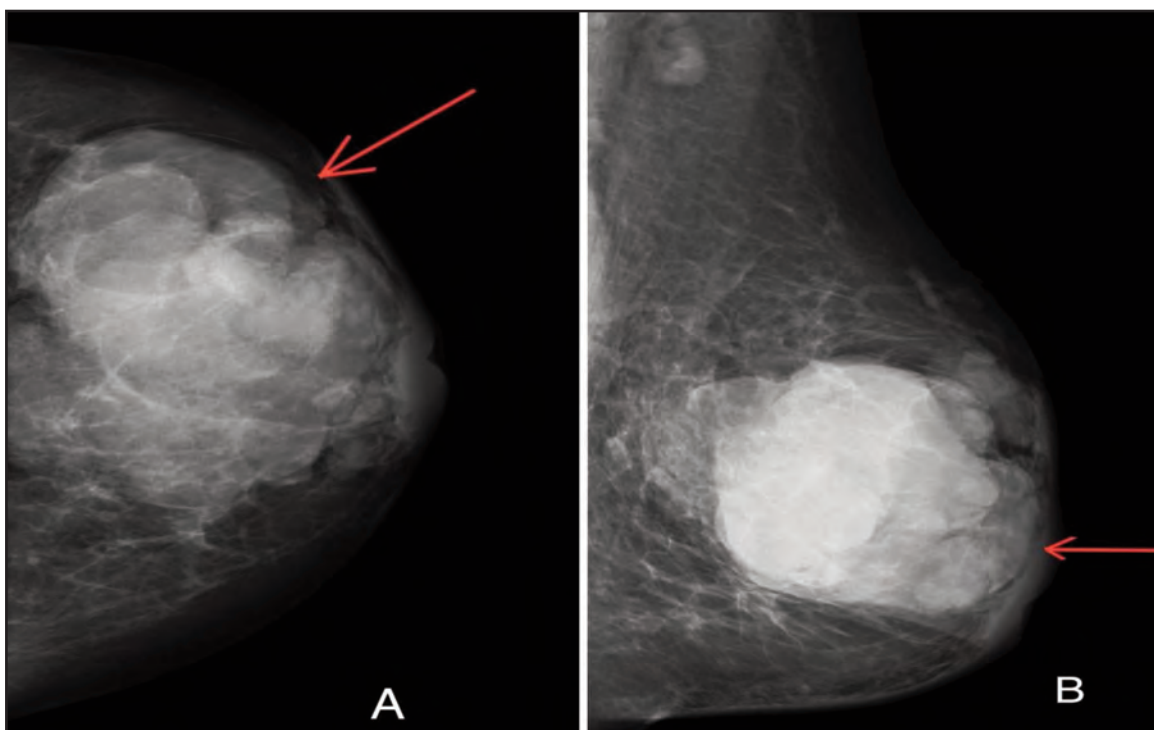


Fig. 2: (A-Left CranioCaudal view, B-Left MediolateralOblique view) Irregular lobulated high density lesion seen occupying all quadrants of the left breast with architectural distortion

specimens were sent for further histopathological evaluation, and subsequent report was consistent with angiosarcoma.

**DISCUSSION**

Breast cancer remains the most common cancer among Malaysian women, with angiosarcoma being one of its rarest histological subtypes. Primary BA typically occurs in younger women aged 30–50 years, whereas secondary BA usually affects older women aged above 60 years and arises in previously irradiated tissue.<sup>8</sup> Angiosarcoma is an extremely rare entity with breast being one of the commonest sites.<sup>2-4</sup> The incidence rate of BA accounted to be less than % among all the other breast malignancies.<sup>2,3</sup> It is further classified into Primary BA and secondary BA.<sup>1-3</sup> Primary BA has an incidence rate of less than 0.04%, sporadic in origin and with a mean age of occurrence 30-50 years old.<sup>3,5,6</sup>

BA demonstrates highly aggressive behaviour with early hematogenous spread to lungs, bones, and liver. Lymphatic spread is less common. Genetic alterations such as BRCA1 and BRCA2 mutations have been implicated in some cases of secondary BA.<sup>4,5,7,9</sup>

Generally, BA exhibits aggressive growth as compared to other breast malignant tumors with poor prognosis.<sup>1,3,10</sup> Studies show point mutations in BRCA1 and BRCA2 genes are often associated with secondary BA, wherein there is loss in endeavoring protection against radiation induced DNA damage.<sup>11,12</sup> Another study by Emanuela et al. shows a close relation between p53 gene down regulation, vascular endothelial growth factor (VEGF) over expression in BA origin.<sup>11</sup> Though there is molecular relevance, the pathogenic rarity of BA remains unclear.<sup>13</sup> There are reports with suggestive correlation of BA with chronic lymphoedema, chronic infection, and trauma.<sup>11</sup> Besides there are reported

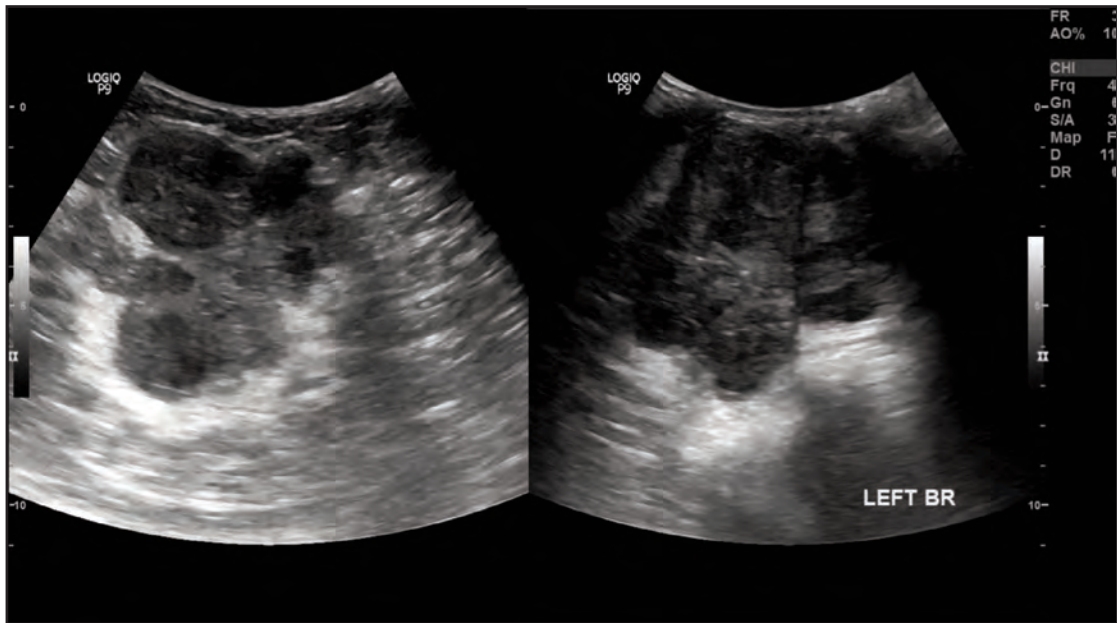


Fig. 3: (US Breast)



Fig. 4: (CECT Thorax)



Fig. 5: Post radical mastectomy with large chest wall defect



Fig. 6: Reverse abdominoplasty technique used for wound closure

cases of BA among pregnant women and hypothesized to be having possible hormonal triggers.<sup>4,13</sup> However still lack sufficient data confirming all these relevance.<sup>11,13</sup> BA in patients with chronic lymphoedema often termed as Stewart-Treves Syndrome.<sup>1,2,5</sup>

Patients with Primary BA typically present with rapidly growing palpable lump ( $\geq 4\text{cm}$ ) over the breast.<sup>5,13</sup> Often the mass is painless in nature.<sup>5,9</sup> A study by Katrina et al shows a mean tumor size of 5.9cm<sup>4</sup>. Occasionally, the mass is associated with purplish-bluish discoloration of overlying skin, which is being cognate to the vascular nature of the tumor.<sup>9,11,13</sup> Whereas in secondary BA predominantly affecting elderly women often patients present with complaints of bruising, ecchymosis or nodular like lesion over previous surgical site.<sup>4,5,13</sup> In contrast to primary BA, the lesions here are confined to the dermal layer and occasionally extend to breast parenchyma.<sup>13</sup>

Habitually BA exhibits metastasis via hematogenous route, though lymphatic spread is possible but unusual.<sup>5,14,15</sup> Common sites involving bone, liver, soft tissue structures and lymph nodes<sup>4,14</sup> have been reported. A retrospective study conducted by Aron Hui et al . shows, out of 14 cases studied, lungs were the commonest sites of involvement in both primary and secondary BA.<sup>5</sup>

Imaging is an important modality part of breast cancer work-up.<sup>8</sup> Mammography and USG Breast may not show specific characteristics attributing to BA, wherein the findings may be persistent with other malignant breast tumors.<sup>7,10</sup> USG of breast may show well circumscribed, ill-defined mass with hyper- or hypo-ecogenicity.<sup>9,10</sup> Mammographically non-specific, ill-defined with focal asymmetry commonly associated, occasionally calcification features.<sup>10</sup> Even in our case, the lesion was reported as lobulated, heterogenous mass with irregular architecture. Various studies show that magnetic

resonance imaging (MRI) has been the best imaging modality for BA as it can identify the lesions that were occult to mammography.<sup>7,10</sup> BA characteristically have low intensity on T1W and high intensity on T2W images.<sup>9</sup> However, MRI was not performed for our patient pertaining to limited resources in the secondary level hospital.

Fine needle aspiration cytology (FNAC) has a high rate of false negatives and is often misleading due to close similarities to other breast abnormalities, hence core needle biopsies are recommended in the case of BA.<sup>10</sup> In our patient, tru-cut biopsy was performed as a part of histopathological assessment.

These BA generally arise from endothelium, lining of vascular channels.<sup>4</sup> This is attributed to their nature of rapidly proliferating and infiltrating into surrounding connective tissues.<sup>3</sup> BA is typically positive for markers such as CD31, CD34 and VIII-related markers.<sup>11,15</sup> These are indicative markers for endothelial differentiation related to their vascular origin.<sup>11</sup> CD31 reported to be more specific, whereas CD34 marker more sensitive in BA.<sup>9</sup> In relation to that, our patient's biopsy sample shows to be positive for CD31 marker.

According to the degree of differentiation, BA is classified into three levels namely low-, intermediate- and high grade.<sup>13</sup> Furthermore, certain studies show a close correlation between histological grading in patients with primary BA and prognosis.<sup>10,13</sup> In most cases primary BA are associated with high tumor grade with positive margins.<sup>10,13</sup>

There is a lack of clear guidelines for surgical management of BA pertaining to their rarity.<sup>7,13</sup> However, a more rational surgical approach with mastectomy remains the mainstay treatment for primary and secondary BA with an aim to achieve surgical R<sup>0</sup> resection.<sup>3,4,13,15</sup> Though mastectomy is

preferable, study shows those who underwent BCS did not show worse prognosis.<sup>3,9,15</sup> Hence BCS are being suggested for small grade 1 lesions.<sup>4</sup> Axillary clearance remains controversial as BA usually don't have nodal involvement, thereby indicated in those selective cases with clinical or radiographic nodal involvement.<sup>9,10,11,13,15</sup> Another study by Ran An et al. shows no significant difference in survival rates among those who underwent simple mastectomy and modified radical mastectomy.<sup>13</sup>

In our patient, radical mastectomy was done, and tumor resection leading to creating a large chest wall defect. Hence instead of primary wound closure, reverse abdominoplasty technique was used.

Post operative adjuvant chemo radiation has been a controversial discussion due to limited data available.<sup>15</sup> However, few studies show patients receiving adjuvant radiotherapy in large doses (>50Gy) postoperatively have better locoregional control as well as being beneficial in combating microscopic positive margin.<sup>7,14,15</sup> Risk of radiation induced angio sarcoma has been a concern, thereby those receiving radiotherapy require closer long-term follow-up.<sup>15</sup> A series shows doxorubicin-based chemotherapy agents are being suggested as first line adjuvant chemotherapy post mastectomy.<sup>11</sup> Another series has reported the usage of gemcitabine and docetaxel as neoadjuvant therapy, showing a significant regression over skin lesion.<sup>16</sup>

Generally, patients with BA have poor prognosis and truly depend on the tumor grading.<sup>4,7,16</sup> For grade 1 tumors, a disease-free survival of 5 years is around 76% in contrast to grade 3 tumors which is only 15%<sup>4</sup> Few studies revealed that secondary BA has poorer prognosis compared to primary BA with survival rate of 32%.

## CONCLUSION

Breast angiosarcoma is a rare and aggressive malignancy with diagnostic challenges due to nonspecific clinical and imaging features. Mastectomy remains the primary treatment option, aiming for negative surgical margins. Axillary clearance is not routinely indicated unless nodal involvement is suspected. The role of adjuvant radiotherapy and chemotherapy remains controversial. Greater clinical awareness and multicentre data are needed to standardize management and improve survival outcomes.

## CONFLICT OF INTEREST

The authors declare no conflict of interest.

## ETHICAL STATEMENT

Patient's consent and permission has been obtained to publish this case report and accompanying images.

## REFERENCES

1. Scow JS, Reynolds CA, Degnim AC, et al. Primary and secondary angiosarcoma of the breast: the Mayo Clinic experience. *J Surg Oncol* 2010; 101(5): 401-7.
2. Vorburger SA, Xing Y, Hunt KK, et al. Angiosarcoma of the breast. *Cancer* 2005; 104(12): 2682-8.
3. Abdou Y, Elkhanany A, Attwood K, Ji W, Takabe K, Opyrchal M. Primary and secondary breast angiosarcoma: a single center report and a meta-analysis. *Breast Cancer Research and Treatment*. 2019; 178: 523-33.
4. Glazebrook KN, Magut MJ, Reynolds C. Angiosarcoma of the breast. *American Journal of Roentgenology*. 2008; 190(2): 533-8.
5. Hui A, Henderson M, Speakman D, Skandarajah A. Angiosarcoma of the breast: a difficult surgical challenge. *The Breast*. 2012; 21(4): 584-9.
6. Cozen W, Bernstein L, Wang F, Press MF, Mack TM. The risk of angiosarcoma following primary breast cancer. *British journal of cancer*. 1999; 81(3): 532-6.
7. Arora TK, Terracina KP, Soong J, Idowu MO, Takabe K. Primary and secondary angiosarcoma of the breast. *Gland surgery*. 2014; 3(1): 28.
8. Tan MM, Jamil AS, Ismail R, Donnelly M, Su TT. Breast cancer and breast cancer screening use—beliefs and behaviours in a nationwide study in Malaysia. *BMC public health*. 2023; 23(1): 1319.
9. Varghese B, Deshpande P, Dixit S, Koppiker CB, Jalnapurkar N. Primary angiosarcoma of the breast: a case report. *Journal of Radiology Case Reports*. 2019; 13(2): 15.
10. Arora J, Singh P, Singh S, Goel R. Rare case of bilateral primary breast angiosarcoma and review of literature. *Indian Journal of Breast Imaging*. 2025; 2(2): 55-62.
11. Esposito E, Avino F, di Giacomo R, Donzelli I, Marone U, Melucci MT, Rinaldo C, Ruffolo F, Saponara R, Siani C, Tortoriello R. Angiosarcoma of the breast, the unknown—a review of the current literature. *Translational Cancer Research*. 2019; 8(Suppl 5): S510.
12. West JG, Weitzel JN, Tao ML, Carpenter M, West JE, Fanning C. BRCA mutations and the risk of angiosarcoma after breast cancer treatment. *Clinical breast cancer*. 2008 Dec 1;8(6):533-7.
13. An R, Men XJ, Ni XH, Wang WT, Wang CL. Angiosarcoma of the breast: a review. *Heliyon*. 2024; 10(3).
14. Young RJ, Brown NJ, Reed MW, Hughes D, Woll PJ. Angiosarcoma. *The lancet oncology*. 2010 Oct 1;11(10):983-91.
15. Badak B, Yılmaz AŞ, Yurdakul MM, Seker NS, Albayrak F. Angiosarcoma of the Breast: Case Report. *Osmangazi Tıp Dergisi*.; 47(1): 146-50.
16. Gurleyik E, Yekenkurul E, Gursoy F, Gonullu E. Radiation-induced angiosarcoma of the breast: A case report. *International Journal of Surgery Case Reports*. 2024; 123: 110253.

# A silent impostor: Neurosyphilis mimicking incomplete oculomotor nerve palsy

Wan Mohd Redzuan Wan Hassan, MBBCh<sup>1,3</sup>, Julieana Muhammed, MMed<sup>3</sup>, Hor Jyh Yung, MRCP<sup>2</sup>, Wong Chee Keong, MRCP<sup>2</sup>, Abdul Salim Ismail, MMed<sup>1</sup>, Kow Wen Jin, MBBS<sup>1</sup>, Syed Anwar Syed Hussain, MBBS<sup>2</sup>

<sup>1</sup>Department of Ophthalmology, Hospital Pulau Pinang, <sup>2</sup>Department of Neurology, Hospital Pulau Pinang, <sup>3</sup>Department of Ophthalmology and Visual Science, School of Medical Sciences, Universiti Sains Malaysia, Kubang Kerian, Kelantan

## SUMMARY

Acquired isolated oculomotor nerve palsy (ONP) is a commonly encountered clinical entity in ophthalmology. While most cases are due to microvascular ischemia, the diagnosis of ONP requires careful evaluation for alternate life-threatening etiologies. We share our experience in diagnosing and managing a case of neurosyphilis presenting as unilateral oculomotor nerve palsy with bilateral pupil involvement (Light-Near dissociation) in a healthy 44-year-old man in whom aneurysmal compression was initially suspected. Investigations later revealed the diagnosis of neurosyphilis. Neurosyphilis is an extremely rare cause of isolated ONP and seldom reported in the literature. Timely recognition of this disease by ophthalmologists can help orient patients to the appropriate neurology and infectious disease services.

## INTRODUCTION

Neurosyphilis, a rare complication of *Treponema pallidum* infection, can affect the central nervous system in various ways. While it typically manifests as cognitive decline, meningovascular disease, or tabes dorsalis, isolated third cranial nerve palsy (ONP) is an uncommon presentation that can be mistaken for more prevalent conditions like aneurysmal compression or microvascular ischemia.

Risk factors for neurosyphilis include untreated syphilis, Human Immunodeficiency Virus (HIV) infection, immunosuppression, and high-risk sexual behaviour. Although it is more frequently observed in HIV-positive individuals, its occurrence in immunocompetent patients highlights the importance of considering it in differential diagnoses. The increasing prevalence of syphilis worldwide necessitates awareness of its diverse clinical features.

This case report aims to emphasize the diagnostic challenges associated with neurosyphilis presenting as isolated ONP with bilateral pupil involvement in an HIV- negative patient. Such a presentation is rarely documented, making early recognition and appropriate investigation critical for timely intervention.

What distinguishes this case is the bilateral pupil involvement, a feature seldom reported in neurosyphilis-associated ONP. Additionally, the patient was

immunocompetent and had no significant comorbidities, reinforcing the need to consider neurosyphilis in patients with unexplained cranial neuropathies. Early serological and CSF testing can facilitate prompt diagnosis and treatment, improving patient outcomes.

## CASE PRESENTATION

A 44-year-old healthy male visited the clinic reporting a sudden drooping of the left eyelid accompanied by blurred vision of three days duration. He had no additional neurological symptoms, and his review of neurological systems was normal. He is allergic to paracetamol and otherwise has no notable past medical history, does not smoke, and has not used any prior medications. Both his ocular and family histories were unremarkable. He had history of multiple unprotected sexual encounters with multiple partners many years ago. However, he denied any history of blood transfusions or intravenous drug use.

During the examination, he exhibited exotropia, significant hypotropia, and pronounced deficits in elevation, adduction, and depression of the left eye. These findings were consistent with the Hess chart results (Figure 1 and Figure 2). There was partial blepharoptosis. His uncorrected visual acuity was 6/9 in the right eye and 6/18 in the left. Anisocoria was noted, with the right pupil measuring 5 mm and the left 7 mm, both showing poor reactivity to bright light. Pupil evaluation indicated light-near dissociation. Nuclear cataracts are noted in both eyes, predominantly affecting the left eye. Otherwise, the fundoscopic examination was unremarkable bilaterally.

Based on the patient's clinical symptoms, aneurysmal compression was initially suspected, prompting an urgent computed tomography angiography (CTA) of the brain. However, the results were unremarkable. Blood tests revealed a positive Syphilis Rapid Plasma Reagin (RPR) with a titre of 1:64, while testing for human immunodeficiency virus (HIV) was negative.

The patient was referred to the neurology team, where a lumbar puncture was performed. Cerebrospinal fluid (CSF) analysis confirmed a positive Venereal Disease Research Laboratory (VDRL) test with a titre of 1:1. Magnetic Resonance Imaging (MRI) showed no focal enhancing brain parenchymal lesions or abnormal leptomeningeal

This article was accepted: 24 November 2025

Corresponding Author: Julieana Muhammed

Email: drjulieana@usm.my

**Table I: Summary of selected cases of neurosyphilis presenting as oculomotor nerve palsy, supported by magnetic resonance imaging (MRI) findings**

Author	Year	Age	Sex	HIV	Palsy	Pupil Involving	Pupil Involving	Clinical Outcomes
Vogt et al <sup>7</sup>	1993	44	F	-	Incomplete	Yes	Hyperintense lesion in the region of the exit of CN III from the brain stem in T2 (enhancing)	Resolved
Seeley et al <sup>2</sup>	2004	54	M	-	Complete	Yes	Isointense lesion at the base of the midbrain tracing the course of CN III into the cavernous sinus in T1 and T2 (enhancing)	Partially resolved
Corr et al <sup>5</sup>	2004	22	F	+	Complete OD Incomplete OS	Yes (OU)	Marked thickening of both CN III in T2 (enhancing)	Resolved
Hess et al <sup>4</sup>	2013	39	M	+	Complete	Yes	Hyperintense enlargement of CN III in the interpeduncular cistern in T2-FLAIR (enhancing)	Partially resolved
Sung Mo Kang et al <sup>3</sup>	2015	43	M	-	Complete	Yes	Diffuse thickening of CN III in T2 (enhancing)	Partially resolved
Silva et al <sup>6</sup>	2018	29	M	+	Complete	Yes	Diffuse thickening of the cisternal portion of CN III in T2 (enhancing)	Partially resolved
Antaki et al <sup>1</sup>	2020	47	M	-	Complete	Yes	Enlargement of CN III in the interpeduncular and suprasellar cisterns in T2 (enhancing)	Symptomatic improvement
Redzuan et al	2025	44	M	-	Incomplete	Yes	No focal enhancing brain parenchymal lesion or abnormal leptomeningeal enhancement	Partially resolved

Abbreviations: HIV = human immunodeficiency virus; MRI = magnetic resonance imaging; F = female; M = male; Oculomotor nerve = third cranial nerve or CN III; T1 = T1-weighted images; T2 = T2-weighted images; FLAIR = Fluid-attenuated inversion recovery sequence; OD = right eye; OS = left eye; OU = both eyes. Enhancement refers to postgadolinium enhancement in T1-weighted images.

enhancement. A diagnosis of neurosyphilis was established, and treatment was initiated with intravenous penicillin G (4 million units every 4 hours) for two weeks, followed by intramuscular benzathine penicillin (2.4 million units weekly) for three doses.

At the two-month follow-up, the patient's condition showed gradual improvement, though mild blepharoptosis persisted. Eye movement had significantly improved, with only minimal residual deficits in elevation, adduction, and depression. (Figure 3).

## DISCUSSION

In clinical practice, an isolated oculomotor nerve palsy often prompts an evaluation for aneurysmal compression, especially involving the posterior communicating artery. As seen in Antaki et al. and our case, urgent computed tomography angiography (CTA) was performed in such cases but did not reveal any vascular abnormalities.<sup>1</sup> This highlights the limitations of neuroimaging alone in diagnosing neurosyphilis.

Given its ability to mimic other neurological conditions, serological testing for syphilis is crucial when the cause of cranial nerve palsy remains unclear. There have been reported cases where the Rapid Plasma Reagin (RPR) or Venereal Disease Research 1–3 Laboratory (VDRL) tests played a pivotal role in identifying neurosyphilis.<sup>4,5</sup> Furthermore, cerebrospinal fluid (CSF) analysis is essential to confirm active neurosyphilis, particularly in cases where MRI findings are inconclusive.

Neurosyphilis is more frequently reported in HIV-positive individuals likely due to impaired immune response.<sup>4,6</sup> The interplay between HIV and neurosyphilis may contribute to a more aggressive or atypical presentation. However, cases in HIV-negative individuals suggest that neurosyphilis should not be overlooked in immunocompetent patients, as demonstrated in our case.<sup>1,3</sup>

Most reported cases had pupil involvement, reinforcing the classical feature of a “syphilitic pupil”.<sup>4,6,7</sup> However, Sung Mo Kang et al. documented a case of third nerve palsy with bilateral pupil involvement with light near dissociation, which is similar in our case, demonstrating variability in presentation.<sup>3</sup>

Standard treatment with intravenous penicillin G followed by intramuscular benzathine penicillin remains effective.<sup>1,4,6</sup> Improvement is often seen within weeks to months, but some patients have residual deficits, such as persistent mild ptosis or ocular movement limitations.<sup>1,3</sup> The prognosis depends on early diagnosis and treatment initiation; delayed treatment may lead to permanent deficits.

From a public health standpoint, the increasing incidence of syphilis globally including among heterosexual, HIV-negative men highlights the need to broaden screening criteria beyond traditionally defined high-risk groups. Awareness of neurosyphilis as a potential, albeit rare, cause of cranial neuropathies should be heightened among all clinicians, not only those in infectious disease specialties.



## CONCLUSIONS

Isolated third cranial nerve palsy caused by neurosyphilis is a rare but important clinical entity that can easily elude diagnosis due to its variable imaging findings and its ability to mimic other neurological conditions, living up to its reputation as the 'great impostor'. This case illustrates that even in immunocompetent, otherwise healthy individuals, neurosyphilis can present with pupil-involving cranial neuropathies that mimic more common aetiologies such as aneurysmal compression or microvascular ischemia.

A high index of suspicion, guided by a careful history including sexual exposure and subtle clinical signs such as light-near dissociation, is crucial. Routine inclusion of syphilis serology in the diagnostic workup for unexplained ONP may prevent misdiagnosis and facilitate early intervention.

Timely cerebrospinal fluid (CSF) analysis and initiation of standard penicillin therapy can lead to substantial clinical recovery, although some residual deficits may persist. This reinforces the importance of early recognition and multidisciplinary management.

Given the ongoing resurgence of syphilis worldwide, healthcare providers across all disciplines should maintain vigilance for its atypical presentations. Future clinical guidelines may benefit from incorporating syphilis testing as a routine component in the evaluation of cranial nerve palsies. Additional research into the clinical and radiological spectrum of neurosyphilis in HIV-negative populations is warranted to better understand its manifestations and optimize outcomes.

## REFERENCES

1. Antaki F, Bachour K, Trottier M, Letourneau-Guillon L, Rouleau J. Neurosyphilis masquerading as oculomotor nerve palsy in a healthy middle-aged man: Case report and review of the literature. *IDCases* 2021; 25: e01237.
2. Seeley WW, Venna N. Neurosyphilis presenting with gummatous oculomotor nerve palsy. *J Neurol Neurosurg Psychiatry*. 2004; 75(5): 789.
3. Sung Mo Kang HIP. Neurosyphilis Presenting Unilateral Oculomotor Nerve Palsy and Bilateral Pupil Involvement. *J Clin Exp Ophthalmol*. 2015; 06(01): 1000398.
4. Hess CW, Rosenfeld SS, Resor SR. Oculomotor Nerve Palsy as the Presenting Symptom of Gummatous Neurosyphilis and Human Immunodeficiency Virus Infection Clinical Response to Treatment Figure 2. *Magnetic Resonance Imaging of the Brain at Follow-Up*. 2013; 70(12) 1582-3.
5. Corr P, Bhigjee A, Lockhat F. Oculomotor nerve root enhancement in meningovascular syphilis. *Clin Radiol*. 2004; 59(3): 294-6.
6. Sá E Silva H, Paulo CO, Duarte F, Abreu RC, Neves I, Moniz P. Teaching NeuroImages: Gummatous neurosyphilis: An atypical presentation in a patient with HIV. *Neurology*. 2018; 90(10): e913-e914.
7. Yogi T, Dresel S, Iller HL, Bergman C, Reimers C, Lissner J. Third Cranial Nerve Palsy Caused by Gummatous Neurosyphilis: MR Findings. *JNR Am J Neuroradiol* 1993; 14(6): 1329-31.

# Continuous renal replacement therapy in a post-bentall procedure patient complicated by sepsis and acute kidney injury: A case report

Budiana Rismawan, Ani Haryani

Universitas Padjadjaran, Bandung, Jawa Barat Indonesia

## SUMMARY

**Background:** Acute kidney injury (AKI) frequently complicates major cardiac surgery and is associated with significant morbidity and mortality. In complex aortic procedures such as the Bentall operation, the risk is further amplified by prolonged cardiopulmonary bypass, systemic inflammation, and postoperative hemodynamic fluctuations. When septic shock develops early after surgery and renal dysfunction may progress rapidly, the likelihood of Kidney Disease: Improving Global Outcomes (KDIGO) stage 3 AKI requiring renal replacement therapy increases substantially. Continuous renal replacement therapy (CRRT) provides gradual solute removal and hemodynamic stability, making it preferable in unstable postoperative patients. **Case Presentation:** A 58-year-old female underwent a Bentall procedure for an ascending aortic aneurysm with severe aortic regurgitation. On postoperative day three, she developed early septic shock complicated by rapidly progressive acute kidney injury requiring continuous renal replacement therapy. Due to hemodynamic instability and metabolic derangement, CRRT was initiated, resulting in stabilization of the patient's metabolic status, improvement in hemodynamics, and gradual recovery of renal function. The patient ultimately regained kidney function and was discharged without the need for ongoing renal replacement therapy. **Conclusions:** This case demonstrates the successful early use of CRRT in septic shock-associated AKI following a Bentall procedure. Key novel aspects include the complexity of postoperative hemodynamics, feasibility of CRRT soon after major aortic surgery, and rapid renal recovery despite severe AKI. Individualized CRRT prescription and careful hemodynamic guidance were crucial for ensuring safety and metabolic control.

## INTRODUCTION

Cardiac surgery-associated acute kidney injury (CSA-AKI) remains a major postoperative complication and significantly contributes to morbidity, mortality, and prolonged hospital stay.<sup>1,2</sup>

The incidence of CSA-AKI varies depending on the type and complexity of surgery, patient comorbidities, and perioperative factors, but it frequently affects a substantial proportion of patients undergoing major cardiac procedures.<sup>1,2</sup> Complex aortic root surgeries, including the Bentall operation, are particularly associated with higher risk

due to prolonged cardiopulmonary bypass duration, ischemia-reperfusion injury, and heightened inflammatory response.<sup>1,2</sup>

The superimposition of sepsis further amplifies the risk and severity of AKI by introducing additional inflammatory and hemodynamic insults.<sup>3,4</sup> Sepsis-associated vasodilation, endothelial dysfunction, and microcirculatory disturbances compromise renal perfusion and exacerbate tubular injury.<sup>3,4</sup> In advanced stages of AKI, especially when accompanied by hemodynamic instability or refractory metabolic derangement, renal replacement therapy becomes a critical component of supportive management.<sup>2,4</sup>

Continuous renal replacement therapy has emerged as the modality of choice in critically ill patients with unstable hemodynamics.<sup>3,4</sup> Unlike intermittent hemodialysis, CRRT facilitates slow and continuous solute clearance and fluid removal, reducing the risk of abrupt shifts in intravascular volume and osmolarity.<sup>3,4</sup> Furthermore, the use of regional citrate anticoagulation has gained prominence because of its favorable bleeding profile and ability to prolong filter lifespan, which is particularly advantageous in the postoperative cardiac surgery setting.<sup>4,5</sup>

This report presents a rare and complex case characterized by the development of early fulminant septic shock and KDIGO stage 3 AKI within the first three postoperative days following a Bentall procedure, necessitating early initiation of continuous renal replacement therapy, highlighting unique hemodynamic challenges, individualized prescription strategies, and comparison with existing CRRT literature.

## CASE PRESENTATION

A 58-year-old female with a history of hypertension and bicuspid aortic valve disease was admitted for elective surgical correction of an ascending aortic aneurysm with severe aortic regurgitation. Preoperative evaluation showed stable renal function with a serum creatinine level of 0.97 mg/dL and estimated glomerular filtration rate of 82 mL/min/1.73 m<sup>2</sup>. There was no prior history of chronic kidney disease.

The patient underwent a Bentall procedure with composite graft replacement using a mechanical valved conduit. Cardiopulmonary bypass lasted 185 minutes, and aortic

*This article was accepted: 05 January 2026*

*Corresponding Author: Ani Haryani*

*Email: anestharyani@gmail.com*

**Table I: Hemodynamic and Renal Parameter Trends From POD-1 to POD-11**

POD	MAP (mmHg)	NE (µg/kg/min)	UO (mL/h)	K <sup>+</sup> (mmol/L)	Creatinine (mg/dL)
1-2	65-70	0.00	50-60	3.8	0.97
3-4	70-75	0.05	20-30	6.1	4.2
5-6	72-80	0.03	150	4.5	3.9
7-8	68-70	0.02	50-80	3.3	2.8
9	70-75	0.01	30-50	3.1	3.8
10	75-80	0.00	80-100	4.1	2.5
11	70-75	0.00	70-80	4.0	2.9

MAP = mean arterial pressure; NE = norepinephrine; UO = urine output; K<sup>+</sup> = potassium.

**Table II: Renal and Hemodynamic Response After CRRT**

Parameter	Pre-CRRT	24 h	72 h
MAP (mmHg)	65	72	75
UO (mL/h)	20	50	80
K <sup>+</sup> (mmol/L)	6.1	4.5	3.9
Creatinine (mg/dL)	4.2	3.6	2.8
CRP (mg/L)	50.49	27.5	18.5
PCT (ng/mL)	5.2	3.9	2.4

CRP = C-reactive protein; PCT = procalcitonin.

**Table III: CRRT Prescription**

Variable	Value
Mode	CVVHDF
Blood flow rate	100-120 mL/min
Dialysate flow	800 mL/h
Replacement fluid	500 mL/h pre-filter + 200 mL/h post-filter
Net ultrafiltration	50 mL/h
Effluent dose	25-30 mL/kg/h
Anticoagulation	Regional citrate anticoagulation
Filter lifespan	>48 h

**Table IV: Antimicrobial therapy timeline**

Day	Antibiotic	Dose	Rationale
POD 3	Meropenem	Standard	Empirical therapy for septic shock
POD 3	Levofloxacin	Standard	Empirical dual coverage
POD 4	Meropenem discontinued	—	Culture result
POD 4	Levofloxacin discontinued	—	Culture result
POD 4 → onward	Amikacin	1 g/day	Susceptibility-guided targeted therapy

cross-clamp time was 140 minutes. The intraoperative period was uneventful, and transfusion requirements were minimal. Postoperatively, she was transferred to the intensive care unit and initially maintained stable hemodynamics on low-dose norepinephrine, which was successfully weaned within 24 hours.

On postoperative day three, the patient developed high-grade fever, tachycardia, and hypotension despite fluid resuscitation and requiring norepinephrine. Urine output progressively declined to less than 0.3 mL/kg/h, and biochemical analysis revealed leukocytosis, elevated lactate, hyperkalemia, metabolic acidosis, and a significant rise in serum creatinine to 4.2 mg/dL. Chest imaging demonstrated a new right basal infiltrate, and blood cultures grew *Klebsiella pneumoniae*. A diagnosis of septic shock complicated by KDIGO stage 3 AKI was established.

Given the hemodynamic instability and progressive metabolic derangements, CRRT was initiated using Continuous Venovenous Hemodiafiltration (CVVHDF) mode, QB: 100-120 mL/min, dialysate: 800 mL/h, replacement: 500 mL/h pre-filter + 200 mL/h post-filter, net UF: 50 mL/h, effluent dose: 25-30 mL/kg/h, filter life: >48 hours, no clotting. Vascular access was achieved via a right femoral double-lumen catheter. Regional citrate anticoagulation was employed with continuous monitoring of systemic and post-filter ionized calcium levels.

Fluid balance was initially maintained at a neutral to slightly positive level to ensure adequate perfusion, then gradually transitioned to a negative balance as cardiovascular stability improved. No episodes of intradialytic hypotension occurred, and filter lifespan averaged 52 hours.

After seven days of CRRT, vasopressor support was discontinued, metabolic parameters stabilized, and urine



**Fig. 1:** Chest X-ray on postoperative day (POD) 1 (left) and POD 3 (right) demonstrating progressive radiographic features consistent with pneumonia

output progressively improved. The patient was transitioned to sustained low-efficiency dialysis for two sessions before complete discontinuation. Renal function showed steady recovery with stable hemodynamics and satisfactory urine output.

## DISCUSSION

This case illustrates the convergence of CSA-AKI and septic shock early after a Bentall procedure—an uncommon but devastating clinical scenario driven by prolonged bypass time, systemic inflammation, vasopressor use, and sepsis-related microcirculatory impairment. The Bentall procedure, originally described by Bentall and De Bono, is a complex aortic root replacement technique, and despite improved early survival, postoperative morbidity remains substantial, particularly in patients who develop AKI and septic shock.<sup>6</sup>

### CSA-AKI and Sepsis Interaction

AKI after cardiac surgery is associated with worse short- and long-term outcomes, including increased mortality and prolonged hospitalization.<sup>1,2</sup> Sepsis acts as an independent contributor to renal dysfunction by intensifying systemic inflammation, causing microcirculatory failure, and promoting renal hypoperfusion.<sup>3,4</sup> This dual insult significantly increases the severity of kidney injury and the likelihood of requiring RRT. In our case, inflammatory markers were available, and both CRP and procalcitonin (PCT) demonstrated a decline following CRRT initiation, indicating attenuation of systemic inflammation during treatment. This trend aligns with findings from Wu et al., who reported that CRRT significantly reduced inflammatory mediators in sepsis-associated AKI. Specifically, CRP levels decreased in two treatment groups after CRRT.<sup>7</sup>

### Choice of RRT Modality

In this patient, CRRT was favored due to vasopressor-dependent shock and the need for gradual solute and fluid management.<sup>3,4</sup> Although studies demonstrate comparable mortality between intermittent and continuous modalities, CRRT offers superior hemodynamic tolerance and more controlled metabolic correction, which is critical in unstable postoperative patients.<sup>3,4</sup>

### Anticoagulation Strategy

Regional citrate anticoagulation provided several advantages. By chelating calcium within the extracorporeal circuit, RCA prevented clot formation while minimizing systemic anticoagulation effects.<sup>4,5</sup> This approach significantly reduced bleeding risk and prolonged filter lifespan, which is especially relevant in patients shortly after major cardiac surgery where surgical sites remain vulnerable to hemorrhage.<sup>4,5</sup>

The observed filter lifespan of 52 hours in our case aligns with previously reported benefits of RCA in critically ill populations, supporting its use as a first-line anticoagulation strategy during CRRT.

### Dose and Fluid Strategy

An effluent dose of 20–25 mL/kg/h has been widely accepted as adequate for achieving metabolic control without increasing adverse effects.<sup>3,4</sup> In this patient, the chosen dose effectively corrected hyperkalemia and metabolic acidosis while maintaining cardiovascular stability. The fluid strategy was tailored to evolving hemodynamics, ensuring optimal tissue perfusion without precipitating volume overload or hypoperfusion. The randomized controlled trial by Park et al. demonstrated that although BIA (bioimpedance analysis)-guided ultrafiltration achieved higher nominal fluid removal than conventional strategies, it did not improve target volume reduction or clinical outcomes.<sup>8</sup> These findings suggest that, in sepsis-associated AKI, hemodynamic stability and infection control may be more critical determinants of outcome than the degree of fluid removal alone.

### Timing CRRT

In our case, early CRRT was initiated during significant metabolic and hemodynamic instability, resulting in prompt correction of acidosis, hyperkalemia, and improved perfusion. This favorable response supports the concept that timely CRRT may attenuate ongoing renal injury driven by inflammation and fluid imbalance, indicating potential value in earlier initiation among high-risk septic patients. The CRTSAKI Study, highlighted the persistent uncertainty regarding optimal CRRT timing in sepsis-associated AKI, noting that early renal injury may still be reversible and that intervention prior to advanced tubular damage could offer clinical benefit.<sup>9</sup>

### Clinical Implications

This case reinforces several practical lessons:

- CRRT is particularly beneficial in hemodynamically unstable postoperative cardiac surgery patients with septic shock and severe AKI and Early fulminant septic shock and KDIGO stage 3 AKI occurring shortly after a Bentall procedure, a scenario rarely reported.
- Regional citrate anticoagulation reduces bleeding risk and prolongs filter life, enhancing safety and efficiency.
- An effluent dose of 20–25 mL/kg/h provides effective metabolic control without unnecessary complications.
- Individualized fluid balance management is essential for optimizing renal recovery and hemodynamic stability.
- Rapid renal recovery despite severe sepsis-associated AKI.

### CONCLUSIONS

CRRT was safe and effective in this Bentall patient with SA-AKI and hemodynamic instability. Individualized prescription, careful monitoring, and early initiation allowed metabolic stabilization and renal recovery. This case provides unique clinical insights for managing complex postoperative patients not represented in major CRRT trials.

### INFORMED CONSENT

Written informed consent was obtained from the patient for publication of this case report and any accompanying data.

### CONFLICTS OF INTEREST

The authors declare no conflicts of interest.

### REFERENCES

1. Wang X, Bao R, Lan Y, Zhao Z, Yang X, Wang Y, Quan Z, Wang J, Bian J. The incidence, risk factors, and prognosis of acute kidney injury in patients after cardiac surgery. *Front Cardiovasc Med.* 2024; 11: 1396889.
2. Duplechin MO, Folds GT, Duplechin DP, Ahmadzadeh S, Myers SH, Shekoochi S, et al. Prevention and management of perioperative acute kidney injury: a narrative review. *Diseases.* 2025; 13(9): 295.
3. Evans L, Rhodes A, Alhazzani W, Antonelli M, Coopersmith CM, French C, et al. Surviving sepsis campaign: international guidelines for management of sepsis and septic shock 2021. *Intensive Care Med.* 2021; 47(11): 1181-247.
4. Kidney Disease: Improving Global Outcomes (KDIGO) Acute Kidney Injury Work Group. KDIGO clinical practice guideline for acute kidney injury. *Kidney Int.* (2012).
5. Jacobs R, Verbrugghe W, Dams K, Roelant E, Couttenye MM, Devroey D, et al. Regional citrate anticoagulation in continuous renal replacement therapy: is metabolic fear the enemy of logic? A systematic review and meta-analysis of randomised controlled trials. *Life (Basel).* 2023; 13(5): 1198.
6. Al-Mudhaffar SS, Alwan A, Ouj R, et al. Bentall procedure as a lifesaving surgery: a single center experience. *Med Int (Lond).* 2023; 3(1): 8.
7. Wu S, Xu T, Wu C, Lei X, Tian X. Continuous renal replacement therapy in sepsis-associated acute kidney injury: Effects on inflammatory mediators and coagulation function. *Asian J Surg.* 2021; 44(10): 1254-9.
8. Park CH, Koh HB, Lee JH, Jung HY, Ha J, Kim HW, Park JT, Han SH, Kang SW, Yoo TH. Volume control strategy and patient survival in sepsis-associated acute kidney injury receiving continuous renal replacement therapy: a randomized controlled trial with secondary analysis. *Sci Rep.* 2024; 14(1): 14284.
9. Chen WY, Cai LH, Zhang ZH, Tao LL, Wen YC, Li ZB, Li L, Ling Y, Li JW, Xing R, Liu XY, Lin ZD, Deng ZT, Wang SH, Lin QH, Zhou DR, He ZJ, Xiong XM. The timing of continuous renal replacement therapy initiation in sepsis-associated acute kidney injury in the intensive care unit: the CRTSAKI Study (Continuous RRT Timing in Sepsis-associated AKI in ICU): study protocol for a multicentre, randomised controlled trial. *BMJ Open.* 2021; 11(2): e040718.

# Inherited malignant brain tumour: A case of constitutional mismatch repair deficiency

Sugan Selvanathan, MD<sup>1</sup>, Teh Kok Hoi, MRCPCH<sup>2</sup>, Teh Chair Ying, MRCPCH<sup>2</sup>, Subasri Armon, MPath<sup>1</sup>

<sup>1</sup>Department of Pathology, Hospital Kuala Lumpur, Ministry of Health Malaysia, <sup>2</sup>Department of Paediatrics Haematology-Oncology, Hospital Tunku Azizah, Ministry of Health Malaysia

## SUMMARY

**Constitutional Mismatch Repair Deficiency (CMMRD) is a cancer-predisposing syndrome with high morbidity and mortality caused by biallelic pathogenic variants in one of the mismatch repair genes resulting in a broad spectrum of early onset of malignancies. Here we report a case of CMMRD with homozygous variant in the MSH6 gene manifesting as medulloblastoma in a child, born to first-degree consanguineous. CMMRD associated skin change resembling Neurofibromatosis type 1, are concurrently observed. Familiarity with CMMRD clinical presentations for screening and early detection of its related malignancies, in families affected by this form of inherited germline mutation is of clinical importance.**

## INTRODUCTION

Childhood brain tumour is the second commonest type of cancer in individuals aged 0-24 years globally causing significant morbidity and mortality.<sup>1</sup> Based on the 10-year report of the Malaysia National Cancer Registry on the incidence of childhood cancer from the year 2007-2016, brain and central nervous system tumours are the second commonest tumours for the children between 0-14 years.<sup>2</sup> Majority of brain and other CNS tumours in children and adolescents are malignant (age-adjusted incidence of 3.55 per 100,000) while non-malignant brain and other CNS tumours are less common (age-adjusted incidence of 2.60 per 100,000).<sup>3</sup> Several brain tumours such as gliomas, medulloblastomas, and vestibular schwannomas are associated with tumour predisposition syndromes.<sup>4</sup> Among the predisposition syndromes, Constitutional Mismatch Repair Deficiency (CMMRD) is rare. CMMRD is a distinct condition caused by biallelic pathogenic variant in one of these mismatch repair (MMR) genes-*MLH1*, *MSH2*, *MSH6*, or *PMS2*. Children with this syndrome present with a broad spectrum of tumours including haematological, brain, and gastrointestinal tract tumours. They have dermatological findings such as café-au-lait macules (CALM), neurofibromas and axillary freckling commonly seen in children with NF-1.<sup>5</sup> Ash leaf macules can also be found in children with Tuberous sclerosis. Parental consanguinity significantly increases birth incidence from 1 in a million for untreated parents to 110 times higher in parents consanguineous.<sup>7</sup>

## CASE PRESENTATION

An 8 year old boy of Indian descent, born to consanguineous parents initially presented to a tertiary hospital with occipital headaches for 2 weeks associated with episodes of daily morning vomiting, blurring and double vision. He subsequently developed right hemiparesis. His parents are first cousins- with 3 living children. Their deceased second son was diagnosed with T cell lymphoblastic lymphoma at 1½ years old who succumbed at 5½ years old due to disease relapse. Diagram 1 shows the pedigree chart of his family and the affected children. Physical examination of this boy was remarkable for several café-au-lait macules (CALM) and some ashleaf hypopigmented macules on the trunk. (Figure 1).

Computed Tomography (CT) scan of the brain showed faint hyperdense mass in the right posterior cranial fossa 3.9 x 3.8 x 3.2-cm causing acute obstructive hydrocephalus. An urgent ventriculoperitoneal (VP) shunt was inserted. MRI of the brain and spine, post-VP insertion showed a well-defined heterogeneous solid mass in the right cerebellum measuring 4.3 x 5 x 3.6-cm with restricted diffusion and cerebellar tonsil herniation of 1.1cm.

Right suboccipital craniotomy and tumour debulking was performed. Histopathological examination (HPE) confirmed the diagnosis of Large cell/ anaplastic medulloblastoma, SHH-activated and TP53 mutant (CNS WHO grade 4). Microscopically (Figure 3), the cells moderate nuclear pleomorphism, with large round to angulated nuclei, stippled chromatin, conspicuous nucleoli and moderate eosinophilic cytoplasm. Nuclear moulding and cell wrapping were also observed. The mitotic figures were brisk with high proliferative index (Ki67) of 80%. Intervening fibrous tissue was readily seen in the tumour but no typical nodular pattern was observed. No obvious rhabdoid cells or rosette patterns were encountered. The cells expressed Synaptophysin, CD56, YAP1, GAB1, p53-mutant, intact INI1, Flt1, NeuN and LIN28A as shown in Figure 4. They did not express GFAP, LCA, CD20, CD79 alpha, nuclear Beta-catenin and CD99.

He recovered well post-operatively with only right-sided intention tremor. However, repeat post-surgery MRI brain revealed significant residual tumour consisting of two

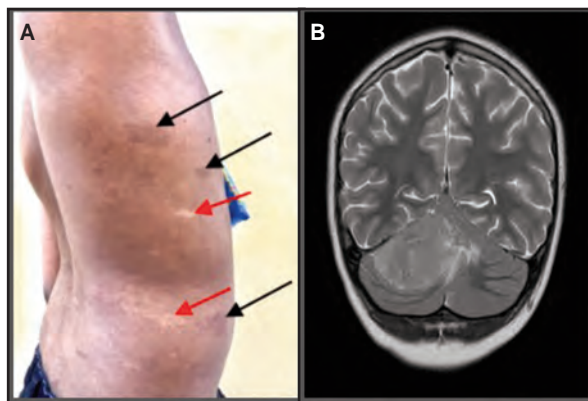
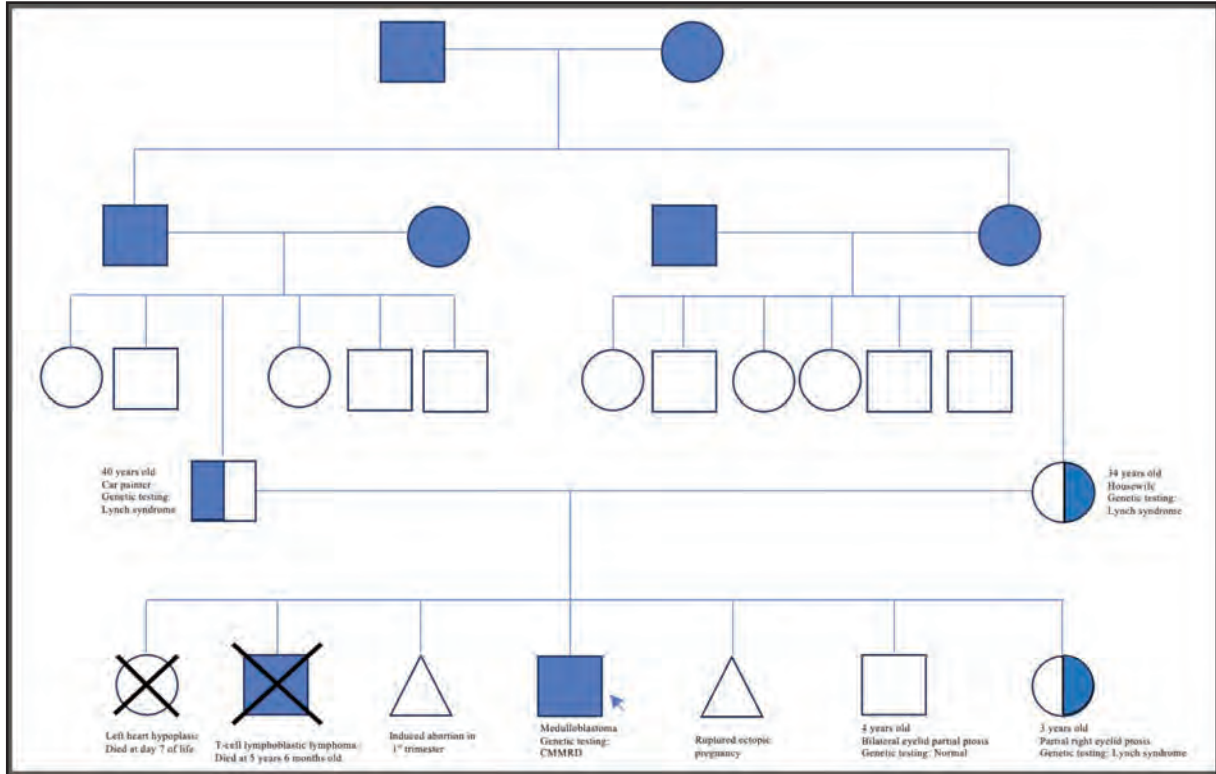


**Fig. 1:** Picture on the left (A) showing café au lait macules (black arrows) and ashleaf hypopigmented macules (red arrows) on the lumbar region. Picture on the right (B) shows the pre-op MRI brain (T1, T2 and T2 flare) showed a well-defined heterogeneous solid lesion (red arrow-head) in the right cerebellum with restricted diffusion and cerebellar tonsil herniation

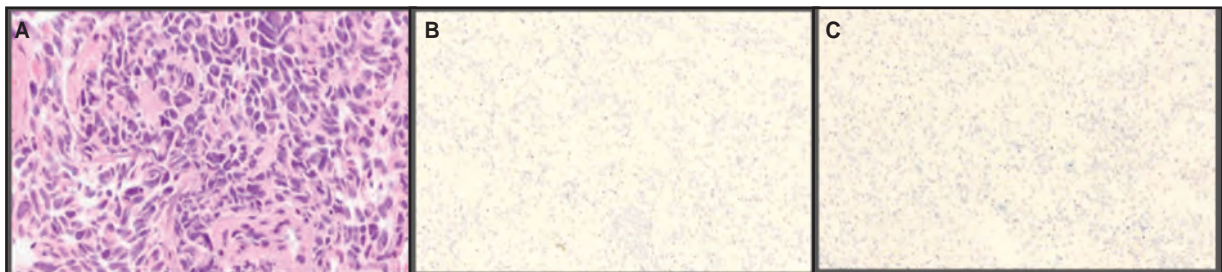


**Fig. 2:** Picture A shows Haematoxylin and eosin (H&E) stain of the tumour cells of the posterior fossa tumour exhibiting moderate nuclear pleomorphism, with large round to angulated nuclei, stippled chromatin, conspicuous nucleoli and moderate eosinophilic cytoplasm. Nuclear moulding and cell wrapping were observed. Picture B and C shows Mismatch Repair (MMR) immunohistochemistry protein expression of neoplastic and non-neoplastic cells show loss of nuclear expression to MSH2 (B) and MSH6 (C)

enhancing masses at the right cerebellar resection bed, measuring 2.3 x 2.4 x 1.8-cm and 1.3 x 1.9 x 1.9-cm respectively. Posterior fossa craniectomy and tumour excision was performed. Gross total excision was achieved. Histomorphological findings were similar with the completion surgery.

Based on parental consanguinity, history of haematological malignancy in the sibling and skin pigmentary changes in the patient, cancer predisposition syndrome such as CMMRD syndrome was suspected. Hence immunohistochemistry (IHC) staining by Ventana for MMR proteins of MSH2, MSH6, MLH1 and PMS2 was performed as a screening using Benchmark ULTRA Ventana platform on the sections from formalin fixed paraffin embedded tumour specimen. This revealed a loss of MSH2 and MSH6 proteins in both the neoplastic and surrounding non-neoplastic cells (Figure 5). The sequencing analysis and deletion/duplication testing of 84 target genes from the combination of Invitae Multi-Cancer Panel and Invitae Common Hereditary Cancers Panel was performed on the patient's blood sample using Illumina technology in Invitae Corporation. The results revealed homozygous pathogenic variant in MSH6 (c.3731T>G), affirming the diagnosis of CMMRD syndrome. Family screening was performed revealing both parents and a living younger sister having heterozygous pathogenic variant for the MSH6 variant gene confirming the diagnosis of Lynch syndrome.

Finally, a right frontal Ommaya reservoir was inserted and his left ventriculo-peritoneal shunt ligated for adjuvant intraventricular chemotherapy given concurrently with systemic chemotherapy.

## DISCUSSION

The rarity of CMMRD and its diverse clinical manifestations pose both diagnostic and management challenges. According to literature, most cases of CMMRD (~60%) result from a mutation in Mismatch Repair Genes of *PMS2* followed by *MSH6* (20–30% cases) and *MLH1/MSH2* genes (10–20%).<sup>8</sup> MMR proteins recognize and repair mismatched nucleotide insertions or deletions during DNA replication. MMR deficiency facilitates the accumulation of genetic changes and consequently leads to the development of cancer.<sup>7</sup>

The tumour spectrum for this syndrome includes haematological malignancies, brain or central nervous system tumours, Lynch syndrome (LS)-associated tumours and other malignancies. LS-associated tumours include tumours from the colorectal, small bowel, endometrial, ureter<sup>8</sup>, renal pelvis, biliary tract, stomach and bladder.<sup>7</sup> The initial age at diagnosis of CMMRD-related tumours is 0.4 to 39 years with 80% occurring before 18 years old.<sup>7</sup> Wimmer et al., reported the median age of 9.5 years for brain tumours, 5 years for haematological malignancies, 16 years for LS-associated cancers. The mean age at first diagnosis of a malignancy is 9 years old. Individuals with CMMRD are

known to be at high risk of developing a second malignancy at a later age usually during adulthood.

Brain tumours associated with CMMRD syndrome include high-grade gliomas, medulloblastomas and CNS embryonal tumours. In our case, the patient had Large cell/ anaplastic medulloblastoma, SHH-activated and *TP53* mutant (CNS WHO grade 4). Medulloblastoma, an embryonal tumour of the cerebellum is the most common malignant brain tumour in childhood. Most cases (95%) are sporadic in origin, with a few WNT medulloblastoma associated with Turcot syndrome and SHH medulloblastoma associated with Gorlin syndrome. In CMMRD syndrome the SHH signalling pathway is affected with a mutated *TP53* gene. Pathogenic variants DNA repair genes have been associated with medulloblastoma. In a study by Trubicka, J et al., six potentially new pathogenic variants were identified which included MSH2 (p.A733T and p.V606I), RAD50 (p.R1093\*), FANCM (p.L694\*), ERCC2 (p.R695C) and EXO1 (p.V738L). The same study provides preliminary evidence for a link between defects in DNA repair genes and treatment-related toxicity in children with medulloblastoma.

As mentioned earlier, CMMRD syndrome poses diagnostic challenges, as it often overlooked or undiagnosed; partly due to a lack of awareness among clinicians. In 2013, the European consortium 'Care for CMMRD' (C4CMMRD) proposed a three-point scoring system that should trigger diagnostic evaluation of CMMRD syndrome.<sup>6</sup>

Typically, immunohistochemistry (IHC) staining is used as a screening tool followed by germline mutation analysis for confirmation of CMMRD. However, due to limited availability of germline testing, IHC of MMR proteins is proposed as an ancillary diagnostic test for CMMRD.<sup>7</sup> To confirm CMMRD by IHC, loss of MMR expression in all cells of the investigated tissue (neoplastic and non-neoplastic cells) should be observed. In general, a truncating mutation in *PMS2* or *MSH6* will result in isolated loss of these proteins, whereas a mutation in *MLH1* or *MSH2* will lead to concurrent loss of MLH1/*PMS2* or MSH2/*MSH6* protein expressions respectively, since *MLH1* and *MSH2* are obligatory partners in the formation of MLH1/*PMS2* and MSH2/*MSH6* heterodimers.<sup>7</sup>

In 2021, a set of diagnostic criteria consisting of MMR germline results, ancillary test and clinical manifestations was recommended by C4CMMRD consortium. Ancillary tests include assays showing microsatellite instability (MSI) in constitutional tissue[6], functional assays showing loss of MMR activity and MMR immunohistochemistry (IHC) showing loss of MMR protein expression. Patient who fulfil the diagnostic criteria warrants CMMRD surveillance.

Besides tumours, CMMRD patients often have café-au-lait macules (CALM). They may also have neurofibromas and axillary freckling[7]. Most of these patients have multiple (two or more) CALMs-but they do not always have  $\geq 6$  CALM

needed for diagnosis of Neurofibromatosis Type 1 (NF1). A study suggested that CALM in CMMRD could be distinguished from CALM in NF1 by experienced physicians through the degree of pigmentation and shape.<sup>8</sup> It has been hypothesised that NF1 gene is a frequent somatic target in CMMRD.<sup>7</sup>

Genetic counselling should be offered to parents before germline testing of the affected child, including information on potential risk of recurrence and consequences of heterozygous mutation in both parents. Predictive testing should be offered to all family members once a mutation has been identified. The family must be informed of the potential therapeutic implications and of the high risk of second malignancy if the patient is positive. Preferentially, targeted gene mutation analysis is performed. In cases where tumour tissue is not available for IHC analysis or the results are inconclusive, mutation analysis of blood samples by genetic sequencing method can also be considered.<sup>8</sup>

Monitoring patients with CMMRD presents a formidable challenge due to the broad spectrum of associated malignancies.<sup>9</sup> Developing a specific surveillance protocol is particularly daunting given this complexity. Nevertheless, once an early diagnosis of CMMRD is confirmed, regular and vigilant screening becomes imperative to detect other CMMRD-related malignancies. This surveillance protocol should encompass a rigorous clinical evaluation, including a full blood count and monitoring of carcinoembryonic antigen (CEA) levels. Additionally, MRI of the brain, lower gastrointestinal endoscopy, and transvaginal ultrasound for endometrial and ovarian cancers should be integral components of this comprehensive screening approach. Implementing such a proactive strategy is paramount for the early detection and management of potential malignancies. Accurate and early diagnosis of CMMRD has important implications in the management of the patients and their families. Clinicians should consider conducting IHC staining of MMR proteins and gene analysis in children with brain tumors and presents with clinical criteria as mentioned above. An accurate diagnosis is pre-requisite for surveillance and improved survival for patients and their families.

## CONCLUSION

Navigating the intricacies of Constitutional Mismatch Repair Deficiency (CMMRD) syndrome demands a proactive and multidisciplinary approach. This rare syndrome, characterized by its diverse clinical manifestations driven by mutations in Mismatch Repair (MMR) genes, underscores the critical need for early and precise diagnosis. Despite the challenges posed by the syndrome's rarity and the wide spectrum of associated malignancies, diligent surveillance is paramount. By implementing these strategies, we can optimize the management and surveillance of CMMRD, significantly enhancing patient outcomes. With its unique presentation, including but not limited to skin abnormalities, brain tumors, and haematological malignancies, CMMRD requires a comprehensive and tailored approach. This approach not only improves patient care but also contributes to the growing body of knowledge surrounding this complex syndrome, fostering advancements in its understanding and treatment.

## DISCLOSURE

Consent was obtained from the patient's parents for this study. All authors contributed to manuscript drafting. All authors read and approved the final manuscript. The authors declare no conflict of interest.

## ETHICAL APPROVAL

The Medical Research and Ethics Committee (MREC), Ministry of Health Malaysia (MOH) has deemed that this study does not require ethical approval.

## ACKNOWLEDGEMENT

The authors would like to thank the Director General of Health Malaysia for the permission to publish this paper.

## REFERENCES

1. Raja N, Hayes L, Basta N, McNally RJQ. International trends in the incidence of brain tumours in children and young-adults and their association with indicators of economic development. *Cancer Epidemiology*. 2021; 74: 102006.
2. Raman, S. Et Al. (Eds) (2021) *The Incidence Of Childhood Cancer In Malaysia 2007-2016*. Institut Kanser Negara, Putrajaya.
3. Farouk Sait S, Walsh MF, Karajannis MA. Genetic syndromes predisposing to pediatric brain tumors. *Neuro-Oncology Practice*. 2021; 8(4): 375-90.
4. Wimmer K, Etzler J. Constitutional mismatch repair-deficiency syndrome: have we so far seen only the tip of an iceberg? *Human Genetics*. 2008; 124(2): 105-22.
5. Wang Q, Montmain G, Ruano E, Upadhyaya M, Dudley S, Liskay RM, et al. Neurofibromatosis type 1 gene as a mutational target in a mismatch repair-deficient cell type. *Human genetics [Internet]*. 2003; 112(2): 117-23.
6. Abedalthagafi M. Constitutional mismatch repair-deficiency: current problems and emerging therapeutic strategies. *Oncotarget [Internet]*. 2018; 9(83).
7. Wimmer K, Rosenbaum T, Messiaen L. Connections between constitutional mismatch repair deficiency syndrome and neurofibromatosis type 1. *Clinical Genetics*. 2017 Jan 10; 91(4): 507-19.
8. González-Acosta M, Marín F, Puliafito B, Bonifaci N, Fernández A, Navarro M, et al. High-sensitivity microsatellite instability assessment for the detection of mismatch repair defects in normal tissue of biallelic germline mismatch repair mutation carriers. *Journal of Medical Genetics [Internet]*. 2020 Apr 1 [cited 2024 Jan 26]; 57(4): 269-73.
9. Sameen Bin Naeem, Ullah N, Mussadique Ali Jhatial, S. Mudassar Muzaffar, Abbas M, Iftikhar IH, et al. Constitutional Mismatch Repair Deficiency (CMMRD) Syndrome: A Case Report of a Patient With Multiple Metachronous Malignancies. *Cureus*. 2023;.
10. Trubicka J, Žemojtel T, Hecht J, Falana K, Piekutowska-Abramczuk D, Płoski R, et al. The germline variants in DNA repair genes in pediatric medulloblastoma: a challenge for current therapeutic strategies. *BMC Cancer*. 2017; 17(1).

# Shadows of a triad: Exploring the gaps in miller fisher syndrome

Wan Mohd Redzuan Wan Hassan<sup>1,2</sup>, Julieana Muhammed<sup>2</sup>, Hor Jyh Yung<sup>3</sup>, Wong Chee Keong<sup>3</sup>, Abdul Salim Ismail<sup>1</sup>, Nurul Najihah Khalid Alwalid Dziyauiddin<sup>3</sup>, Mohammad Syafiq Idris<sup>3</sup>

<sup>1</sup>Department of Ophthalmology, Hospital Pulau Pinang, Malaysia, <sup>2</sup>Department of Ophthalmology and Visual Science, School of Medical Sciences, Universiti Sains Malaysia, Kubang Kerian, Kelantan, Malaysia, <sup>3</sup>Department of Neurology, Hospital Pulau Pinang, Malaysia

## SUMMARY

We describe a case of incomplete Miller Fisher Syndrome (MFS) in a 36-year-old previously healthy woman who presented with three days of binocular diplopia accompanied by internal ophthalmoplegia and horizontal nystagmus, preceded by a week of distal paraesthesia without an infectious prodrome. Clinical examination revealed non-reactive mid-sized pupils, mild limitations in ocular motility, bilateral non-fatigable ptosis, distal sensory impairment, and generalized areflexia, in the absence of ataxia. Neuroimaging and nerve conduction studies were unremarkable. Cerebrospinal fluid analysis demonstrated albumin–cytological dissociation, and serum anti-GQ1b IgG antibodies were positive, supporting the diagnosis of an incomplete MFS variant. The patient was treated with intravenous immunoglobulin (0.4 g/kg/day for 5 days), with progressive clinical improvement noted over two weeks. This case highlights the importance of recognising atypical MFS presentations, particularly those dominated by internal ophthalmoplegia without ataxia, and emphasizes the diagnostic utility of anti-GQ1b serology in incomplete variants.

## INTRODUCTION

Gullain-Barre Syndrome (GBS) is an autoimmune disorder with the most common clinical presentation of neuromuscular weakness. Acute inflammatory demyelinating polyradiculoneuropathy (AIDP) is the most commonly occurring subtype in North America and Europe accounting for about 90% of all cases. However, in other parts of the world (Asia, Central and South America) axonal variants of GBS i.e. acute motor axonopathy (AMAN) and acute motor sensory axonopathy (AMSAN) are found to represent 30% to 47% of cases.<sup>1</sup>

A rare clinical variant of GBS, known as Miller Fisher Syndrome (MFS) is an acute immune-mediated demyelinating polyneuropathy which features were first identified by James Collier in 1932 and described it as a unique classical triad of symptoms including ophthalmoplegia, ataxia and areflexia. Miller Fisher later characterized it in 1956, classifying it as a unique entity within the GBS spectrum. The predominant features of MFS are ophthalmoplegia and ataxia, with a peripheral neuropathy being only a very mild clinical feature.

Biochemically, there is elevated cerebrospinal fluid (CSF) protein and presence of ganglioside GQ1b antibody.<sup>2</sup> This is in contrast with classical GBS, where weakness and sensory disturbance are usually the presenting features.<sup>3</sup> We share our experience in diagnosing and managing a case of incomplete Miller Fisher Syndrome without ataxia, emphasizing the role of anti-GQ1b serology in confirming incomplete variants.

## CASE PRESENTATION

A 36-year-old healthy female lady presented with seeing double images at near and far distance for three days duration. She was found to have internal ophthalmoplegia with horizontal nystagmus. Further history revealed that it was preceded by bilateral upper and lower limb numbness for one week. There was no prior history of upper respiratory tract infection or gastrointestinal symptoms. She denied any photophobia or using any eyedrops.

Uncorrected visual acuity was 6/9 bilaterally, no reduced contrast sensitivity and colour vision documented. Ocular examination revealed non-reactive mid-size pupils with horizontal nystagmus. No flutter or opsoclonus seen. There was no light-near dissociation noticed. Ocular motility was mildly limited at dextro-version, dextro-elevation and elevation. Bilateral eye also revealed mild bilateral non-fatigable blepharoptosis. Otherwise, fundus bilaterally was unremarkable. Neurological examination revealed reduced sensation in glove and stocking distribution with areflexia without presence of ataxia. Electrophysiologically there is no evidence of large fibre neuropathy on nerve conduction study. Magnetic Resonance Imaging (MRI) Brain and orbit is normal. She was given intravenous immunoglobulin 0.4g/kg for 5 days and her condition gradually improved after 2 weeks on follow up with residual diplopia at near (Figure 1). Cerebrospinal Fluid (CSF) studies showed albumin-cytological dissociation. Serum anti-GQ1b IgG is positive.

## DISCUSSION

A diagnosis of MFS can be made with compatible clinical history taking, cardinal symptoms, normal findings on CT or MRI, and presence of albumin-cytologic dissociation (hyperproteinorrhachia without pleocytosis) in the CSF of affected patients. Antibodies against ganglioside GQ1b are

This article was accepted: 08 December 2025

Corresponding Author: Julieana Muhammed

Email: drjulieana@usm.my



**Fig. 1:** showed mild ocular motility limitation at dextro-version, dextro-elevation and elevation

detected in the acute-phase sera in more than 90% of MFS cases which is useful for confirmation of MFS in this case.<sup>4</sup>

Diagnosis is usually based on clinical history, and the infectious antecedent appears to be present in the majority of patients: previous infection of the upper respiratory apparatus is most frequent (56–76% of patients). Gastrointestinal infection (4%), typical of classical GBS, and isolated fever (2%) are rarer.<sup>5</sup> However, our patient didn't have any preceding symptoms of illness. Although initial symptoms include progressive symmetrical paraesthesias in the upper and lower limbs, patients can also complain of diplopia without blurring of vision as the first symptom which bring her to our attention. Other symptoms include distal weakness, and absent deep tendon reflexes. This highlights that although the defining features of ataxia, ophthalmoplegia, and areflexia are generally required for the diagnosed as MFS, other symptoms and signs may be present without one of the classical triad and confound a clinician's diagnostic decision making.

The most common differentials for MFS include myasthenia gravis. However, absence of fatigability and bulbar symptoms makes myasthenia gravis less likely in this case. GQ1b ganglioside complex is most often associated with MFS, positive in over 90% of patients with MFS and is not present in unaffected individuals.<sup>6</sup> It is now known that elevated anti-GQ1b antibody production can be seen within a spectrum of conditions, including acute ophthalmoparesis, Bickerstaff's brainstem encephalitis, and Guillain-Barre syndrome, in addition to MFS.<sup>7</sup> Its high occurrence in patients with MFS is very useful for the diagnosis especially in incomplete type of MFS.

To our knowledge, only two previous cases of MFS presenting with internal ophthalmoplegia as first presentation has been documented. The first case was a woman with typical MFS whose initial manifestation was blurred vision because of bilateral tonic pupils. Investigations, including brain imaging, cerebrospinal fluid examination and nerve conduction studies were normal except for elevated serum levels of immunoglobulin G anti-GQ1b antibody. During the disease, she subsequently developed bilateral sixth and seventh nerve palsies, gait ataxia, and areflexia.<sup>8</sup> However, in our patient, there is no ataxia.

The second case was an elderly lady who presented with internal ophthalmoplegia as most notable feature, consisting of mid-sized non-reactive pupils, as well as fronto-orbital headache. The patient had a history of upper respiratory tract infection a week before symptoms and subsequently developed classical triad of ophthalmoparesis, ataxia and areflexia. Among ophthalmoplegias, internal ophthalmoplegia is much less common than external ophthalmoplegia. There are very few references in the literature regarding isolated internal ophthalmoplegia without external involvement. Pupillary disorders in MFS can be seen in up to 50% of cases, tend to progress independently of the presence of external ophthalmoplegia, and usually resolve in a significantly shorter period than external ophthalmoplegia. These findings suggest that the involvement of pupil-motor fibers is independent of lesions in the other subdivisions of the oculomotor nerve.<sup>9</sup>

Pupillary abnormalities like mydriasis and light-near dissociation, though rare, correlate strongly with anti-GQ1b antibodies. These antibodies target gangliosides enriched in ocular motor nerves and autonomic pathways, with cross-reactivity to GT1a potentially disrupting sympathetic

innervation of the iris.<sup>10</sup> Such mechanisms may underlie atypical autonomic features, including bilateral mydriasis, in MFS. This explains the presence of pupillary involvement in our case.

### CONCLUSIONS

This case highlights pupillary involvement in a case of mild upper and lower limb weakness or numbness and areflexia should lead the clinician to the suspicion of Miller Fisher syndrome. Early recognition with timely treatment can lead to early recovery with good prognosis without residual deficit.

### REFERENCES

1. Sudulagunta SR, Sodalagunta MB, Sepehrar M, Khorram H, Bangalore Raja SK, Kothandapani S, Noroozpour Z, Aheta Sham M. Guillain-Barré syndrome: clinical profile and management Ger Med Sci. 2015; 13: Doc16.
2. Pan J, Zheng N, Yu D, Jiang H, Zhou Y. Unilateral Ophthalmoplegia in anti-GQ1b antibody syndrome: case report and systematic literature review. Front Immunol. 2025; (16): 1669821.
3. Yadav P, Vaishali Kuchewar, Bhusari N, Yadav T. Integrated treatment approach to Miller Fisher syndrome, a variant of Guillain-Barre syndrome – A case report. J Ayurveda Integr Med. 2025; 16(4).
4. Yu H, Ding M, Cao Q, Zhou R, Yao J, Fu R, et al. Clinical Features and Differences of Miller Fisher Syndrome in Southern China: Retrospective Analysis of 72 Patients in 13 Provinces of Southern China. Journal of Clinical Neurology (Korea). 2023; 19(6): 589-96.
5. Noioso CM, Bevilacqua L, Acerra GM, Della Valle P, Serio M, Vinciguerra C, et al. Miller Fisher syndrome: an updated narrative review. Vol. 14, Frontiers in Neurology. Frontiers Media SA; 2023.
6. Miller JAL, Spyropoulos A, Jaros E, Galban-Horcajo F, Whittaker RG, Willison HJ. Anti-GQ1b ganglioside positive Miller Fisher syndrome – evidence of paranodal pathology on nerve biopsy. J Neuromuscul Dis. 2014; 1(2): 191-5.
7. Alvin Liu TY, Ravindra Patel V. Unique presentation of anti-GQ1b antibody syndrome. Vol. 51, Canadian Journal of Ophthalmology. Elsevier B.V.; 2016; e116-9.
8. Bae JS, Kim JK, Kim SH, Kim OK. Bilateral internal ophthalmoplegia as an initial sole manifestation of Miller Fisher syndrome. J Clin Neurosci. 2009; 16(7): 963-4.
9. Terry López O, Sagarra Mur D, Gutiérrez Álvarez AM, Jiménez Corral C. Internal ophthalmoplegia as the initial symptom of Miller-Fisher syndrome. Vol. 29, Neurologia. Spanish Society of Neurology; 2014; 504-5.
10. Yang F, Tian Z, Lu Y, Li Y, Liu K. Miller-Fisher syndrome subtype with isolated bilateral mydriasis: a pediatric case report. BMC Neurol. 2025; 25(1).

# A rare presentation of paracentral acute middle maculopathy during early gestation

Siti Hajar Darussalam, MD<sup>1,2</sup>, Amirah Mohammad Razali, Dr Ophth<sup>2</sup>, Teck Chee Cheng, Dr Ophth<sup>1</sup>, Jemaima Che Hamzah, PhD<sup>1</sup>, Mohammad Mohd Isa, MSurgOphthal<sup>2</sup>

<sup>1</sup>Department of Ophthalmology, Faculty of Medicine, Universiti Kebangsaan Malaysia, Malaysia, <sup>2</sup>Department of Ophthalmology, Faculty of Medicine and Health Sciences, Universiti Putra Malaysia, Malaysia

### SUMMARY

Paracentral acute middle maculopathy (PAMM) is a rare ischemic pathology affecting the macula, specifically the middle retinal layers. Patients often present with an acute onset of paracentral scotoma, but some may be asymptomatic. It is most often seen in patients with vascular risk factors or retinal vascular occlusive disease. PAMM is exceedingly rare in pregnancy and is commonly overlooked during clinical examination. Diagnosis is usually made with the support of Optical Coherence Tomography (OCT) or Optical Coherence Tomography Angiography (OCTA) imaging. We report a case of PAMM in a young, healthy pregnant woman who complained of sudden onset of unilateral paracentral scotoma and exhibited imaging features of PAMM. Her systemic workup was unremarkable, and she was managed conservatively with close monitoring. She achieved complete resolution by seven weeks postpartum. This case emphasizes the clinical relevance of considering PAMM in the causes for pregnant patients presenting with acute visual symptoms. The combined use of OCT and OCTA is key in identifying PAMM, especially when fundus findings are subtle and other vascular retinopathies are not evident.

### INTRODUCTION

Paracentral acute middle maculopathy (PAMM) was first reported in 2013 by Sarraf et al, identifying it as a subdivision of acute macular neuroretinopathy (AMN).<sup>1</sup> Advances in spectral-domain Optical Coherence Tomography (SD-OCT) have greatly improved the ability to localize lesions in AMN. PAMM is considered an uncommon retinal vascular condition, typically identified on SD-OCT as a hyperreflective band at the level of the inner nuclear layer (INL).<sup>2</sup> The typical clinical presentation of PAMM is an acute paracentral scotoma with preserved central acuity. Since fundus examination usually reveals only subtle or non-specific changes, Optical Coherence Tomography (OCT) and Optical Coherence Tomography Angiography (OCTA) are often required to establish the diagnosis.<sup>3</sup> However, access to these imaging is often limited, thus leading to the condition being underdiagnosed in routine practice.

Although the pathogenesis of PAMM remains incompletely understood, several factors have been identified, which include systemic or pharmacologic vasoconstrictors, such as adrenaline and caffeine, as well as hormonal influences like

oral contraceptive use. Moreover, retinal vascular causes include diabetic retinopathy, central retinal vein occlusion, branch retinal artery occlusion and sickle cell retinopathy.<sup>2</sup> Reports of PAMM during pregnancy are uncommon, with proposed mechanisms including a hypercoagulable state of pregnancy, maternal anaemia, and systemic hypotension, all of which may contribute to retinal ischaemia. Given its non-specific presentation and rarity in pregnancy, we report a case of PAMM occurring in early gestation in a healthy young woman without vascular risk factors, emphasizing the clinical and imaging features that facilitated the diagnosis.

### CASE PRESENTATION

A healthy 33-year-old primigravida, at 10 weeks of gestation, with no prior medical illness, complained of right temporal paracentral scotoma for one week. The symptom was described as a persistent "glitch of light" obscuring her visual field. She otherwise had no other ocular or neurological symptoms. She was normotensive throughout pregnancy. On examination, visual acuity was bilaterally 6/6, with no relative afferent pupil defect. The anterior segment examination revealed normal findings with intraocular pressure of 14mmHg bilaterally. Funduscopy examination of the right eye showed a slight elevation nasal to the fovea. The left fundus appeared normal. There was an enlarged blind spot in the right Humphrey visual field (HVF) test (Figure 1).

Meanwhile, the right OCT of the macula showed a hyperreflective band nasal to the fovea, confined to the INL, findings characteristic of PAMM (Figure 2a). OCT angiography (OCTA) detected a diminished flow at the site of the lesion (Figure 2b). Systemic investigations, including blood pressure monitoring, fasting blood sugar, lipid profile, echocardiography, and carotid ultrasound Doppler, showed no abnormalities. Thus, a diagnosis of PAMM was derived, and she was followed up closely. During follow-up, her scotoma gradually improved, accompanied by a progressive reduction in the lesion on OCT. At seven weeks postpartum, the patient experienced minimal residual scotoma, with complete resolution of the hyperreflective band and normal OCTA (Figure 3).

### DISCUSSION

Acute onset of visual disturbance during pregnancy is concerning as it may reflect a potentially serious underlying

*This article was accepted: 03 January 2026*

*Corresponding Author: Muhammad Mohd Isa*

*Email: mmi@upm.edu.my*

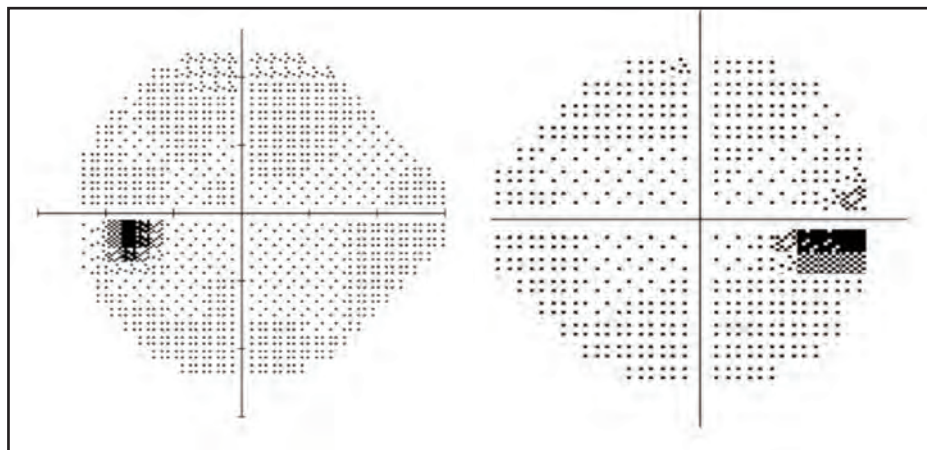


**Fig. 1:** HVF\* of the right eye shows an enlarged blind spot on presentation, whereas the left eye Humphrey Visual Field appears normal.

\*HVF, Humphrey Visual Field.

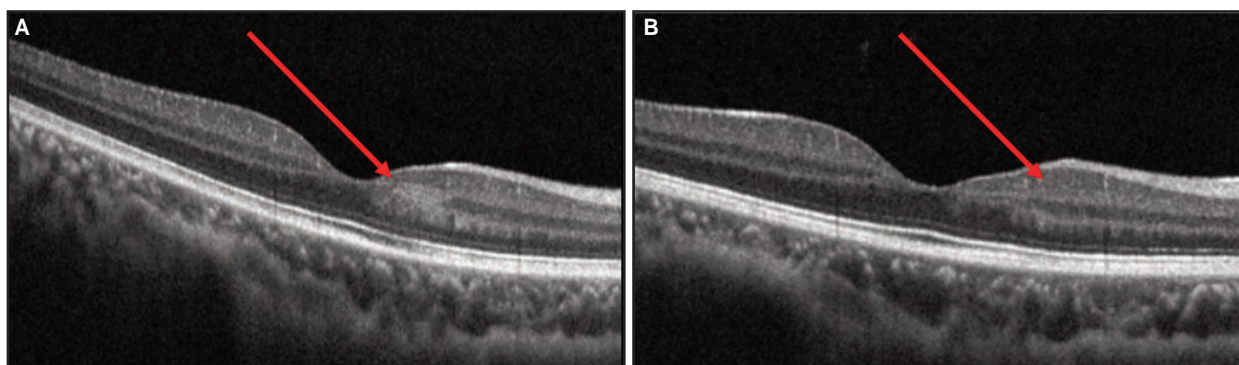


**Fig. 2:** A) OCT+ of the right macula revealed a hyperreflective band nasal to the fovea, which involved INL‡ on presentation. B) At seven weeks postpartum, OCT+ of the macula demonstrated the disappearance of the previously noted nasal parafoveal hyperreflective band, without evidence of retinal layer thinning.

†OCT, Optical Coherence Tomography; ‡INL, inner nuclear layer.

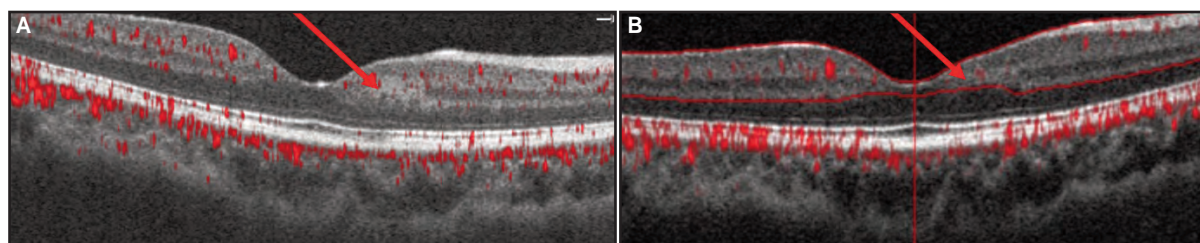


**Fig. 3:** A) OCTA§ of macula revealed flow attenuation that matched the location of the lesion at initial presentation. B) No more abnormality seen on OCTA§ of the macula.

§OCTA, Optical Coherence Tomography Angiography.

pathology. Such scenarios frequently impose a considerable dilemma for clinicians in both diagnosis and management. Visual impairment in pregnancy often happens, resulting from severe hypertensive complications or the physiologic hypercoagulable state, both of which lead to a significant risk to ocular wellbeing.<sup>4</sup> PAMM occurring during pregnancy is highly unusual. Typical cases of PAMM are usually associated with older age, underlying vascular risk factors, systemic diseases, or retinal arterial occlusive diseases. In contrast, our patient was young and otherwise healthy, with pregnancy identified as the only plausible contributing factor.<sup>2</sup>

To date, there have only been two reported cases of PAMM occurring during pregnancy. It was first documented by Pencen et al., who involved a 29-year-old pregnant woman with no known medical illness, who developed a paracentral scotoma during a presyncope hypotensive episode. OCTA showed evidence of retinal infarction, revealing a persistent reduction in deep retinal capillary perfusion with subsequent atrophy of the INL. It was postulated that a combination of hypotension, anaemia, and the hypercoagulability that happens during pregnancy may have contributed to the development of PAMM in this patient.<sup>5</sup>

Another author proposed that the mechanism behind PAMM involves an imbalance in retinal oxygen dynamics. The reduced blood flow velocity and lower oxygen saturation at the venular pole lead to increased oxygen extraction from the retinal arterial circulation, resulting in ischemic damage to the middle retinal layers. This is evidenced by findings consistent with OCTA that showed disruption of the deep capillary plexus and decreased vascular density in the superficial capillary plexus, indicating a more severe degree of microvascular compromise in PAMM.<sup>6</sup>

Nevertheless, PAMM does not directly lead to these changes, as the superficial plexus operates independently from the deep retinal circulation. Instead, this pattern likely results from a shared systemic cause, such as hypertension, as simultaneous microvascular alterations occur throughout the retina.

PAMM typically presents with a sudden paracentral scotoma, which may be accompanied by blurred vision. PAMM lesions are situated in the deeper parafoveal retina and appear grayish white, which is distinguished from cotton wool spots. However, due to their minimal visibility, these lesions are often missed during routine fundus examinations and are more reliably visualized with SD-OCT using near-infrared reluctance imaging.<sup>3</sup>

Type 1 PAMM is marked by the involvement of retinal structures above the outer plexiform layer (OPL), which is likely corresponding to vascular compromise in the superficial or intermediate capillary plexus.

The characteristic feature of PAMM is the presence of a hyperreflective band extending across the middle retinal layers. PAMM can be divided into two patterns based on the location of the lesion. Type 1 involves the superficial or

intermediate capillary plexus, affecting retinal layers above the OPL. In contrast, Type 2 affects the layers beneath OPL, consistent with ischaemia originating from the deep capillary plexus.<sup>1</sup>

With the emergence of OCTA, the underlying pathophysiology of PAMM is now better understood. Recent studies suggest that hypoperfusion of the deep capillary plexus is a key feature during the acute stage of the disease. This helps explain the pattern of selective INL injury seen in acute PAMM and the ongoing thinning of this layer in the chronic stage.<sup>7</sup> OCTA has become essential for differentiating Type 1 and Type 2 PAMM, as its imaging findings reveal ischemic damage at the intermediate and deep capillary plexus levels, accounting for the characteristic lesion patterns observed.<sup>3</sup>

Clinical reports have linked symptomatic PAMM to a variety of pharmacological agents, as well as numerous ocular and systemic disorders. Recent findings indicate that small lesions, although sharing the typical morphology of PAMM, often occur without symptoms and are typically diagnosed retrospectively, after the lesion has resolved.<sup>6</sup> These small PAMM lesions frequently appear in patients with retinal vein occlusions, hypertension, diabetes (with or without retinopathy), underlying cardiovascular disease, or elevated vascular risk.<sup>8</sup> Various ocular and systemic conditions have been linked to PAMM through their effects on the retinal circulation. Examples include compressive ocular ischemia, hematological disorders such as sickle cell disease, trauma related entities such as Purtscher's retinopathy, inflammatory vasculitis, and systemic conditions including uncontrolled hypertension, migraine, and even viral upper respiratory infections. The diversity of underlying causes supports the idea that PAMM should be reviewed not as a distinct disease, but rather as a manifestation of retinal vascular compromise reflecting broader systemic or ocular circulatory dysfunction. In this regard, PAMM could serve as a clinical marker of vascular morbidity or as an indicator within the spectrum of retinal vascular disorders.<sup>9</sup>

In distinguishing PAMM from optic neuritis, standard clinical tests such as visual acuity, color vision, RAPD, and visual field assessment are useful. However, if results are inconclusive, clinicians should consider a retinal cause as a potential explanation. In practice, OCT and OCTA are highly valuable for confirming whether the optic nerve or retina is involved, helping to prevent unnecessary investigations- a particularly important factor during early pregnancy. Moreover, OCTA provides insights into the vascular pathophysiology of PAMM.

Although PAMM lesions typically resolve over time, most patients continue to experience scotomas. As the condition evolves, OCT imaging reveals that the hyperreflective band usually disappears within a few months, often followed by thinning and distortion of the INL and OPL of the middle retina.<sup>1</sup> Additional changes may include excavation of the inner retinal surface and thickening of the ONL.<sup>10</sup> After the lesion resolves, OCTA often shows areas of capillary dropout and structural disruption of the deep capillary plexus,

highlighting the chronic vascular consequences of PAMM.<sup>10</sup> Fundus fluorescein angiography generally does not provide further detail about PAMM lesions but remains helpful in excluding ischemic conditions related to other disorders.

PAMM may be the only ocular indicator of an underlying systemic microvascular disorder, even in patients with no obvious comorbidities. As a result, a thorough systemic evaluation is essential to rule out possible cardiovascular risk factors. Early identification and prompt treatment can help reduce mortality. However, when assessing young individuals with sudden unilateral visual impairment and normal fundus, clinicians must also consider the possibility of an underlying retinal disorder.

### CONCLUSION

Although uncommon, PAMM should be considered as an important cause of paracentral scotoma even in healthy pregnant women without known vascular risk factors. OCT and OCTA are critical for early detection, monitoring disease progression, and excluding other possible causes. Although no specific treatment is available, prompt recognition of PAMM and evaluation of systemic risk factors, particularly cardiovascular and hematological abnormalities, are essential for optimal patient management.

### REFERENCES

1. Sarraf D, Rahimy E, Fawzi AA, Sohn E, Barbazetto I, Zacks DN et al. Paracentral acute middle maculopathy: a new variant of acute macular neuroretinopathy associated with retinal capillary ischemia. *JAMA Ophthalmol.* 2013; 131(10).
2. Shah D, Saurabh K, Roy R. Multimodal imaging in paracentral acute middle maculopathy. *Indian J Ophthalmol.* 2018; 66(8): 1186-8.
3. Scharf J, Freund KB, Sadda S, Sarraf D. Paracentral acute middle maculopathy and the organization of the retinal capillary plexuses. *Prog Retin Eye Res.* 2021; 81: 100884.
4. Digre KB, Kinard K. Neuro-ophthalmic disorders in pregnancy. *Continuum.* 2014; 20(1): 162-76.
5. Pecan PE, Smith AG, Ehlers JP. Optical coherence tomography angiography of acute macular neuroretinopathy and paracentral acute middle maculopathy. *JAMA Ophthalmol.* 2015; 133(12): 1478-80.
6. Kulikov AN, Maltsev DS, Leongardt TA. Retinal microvasculature alteration in paracentral acute middle maculopathy and acute macular neuroretinopathy: a quantitative optical coherence tomography angiography study. *Retin Cases Brief Rep.* 2020; 14(4): 343-51.
7. Nemiroff J, Kuehlewein L, Rahimy E, Tsui I, Doshi R, Gaudric A et al. Assessing deep retinal capillary ischemia in paracentral acute middle maculopathy by optical coherence tomography angiography. *Am J Ophthalmol.* 2016; 162: 121-32.
8. Maltsev DS, Kulikov AN, Burnasheva MA, Chhablani J. Prevalence of resolved paracentral acute middle maculopathy lesions in fellow eyes of patients with unilateral retinal vein occlusion. *Acta Ophthalmol.* 2020; 98(1): e22-8.
9. Madala S, Adabifirouzjaei F, Lando L, Yarmohammadi A, Long CP, Bakhoun CY et al. Retinal ischemic perivascular lesions are a biomarker of cardiovascular disease. *Ophthalmol Retina.* 2022; 6(9): 865-7.
10. Nakamura M, Katagiri S, Hayashi T, Aoyagi R, Hasegawa T, Kogure A et al. Longitudinal follow-up of two patients with isolated paracentral acute middle maculopathy. *Int Med Case Rep J.* 2019: 143-9.

# Huge tubo-ovarian abscess with elevated CA-125 pre-operative diagnosis dilemma: A case report

Su Chok Kim, MD<sup>1</sup>, Yew Tze Wei, MRCOG<sup>1</sup>, Tze Cheng Yew, MRAD<sup>2</sup>, Harris Roland Demong, MOG<sup>1</sup>

<sup>1</sup>Department of Obstetrics and Gynaecology, Hospital Miri, Miri, Sarawak, Malaysia, <sup>2</sup>Department of Radiology, Hospital Melaka, Melaka, Malaysia

### SUMMARY

**Atypical clinical presentation and imaging features of tubo-ovarian abscess (TOA) may resemble pelvic malignancy, in addition to elevated CA-125, which may further cause diagnostic and treatment dilemmas. This case report highlights a postoperatively confirmed TOA case. Here we share a case of a lady with huge abdominal distension due to ovarian mass as evidenced by radiological imaging, and an elevated CA-125 level. Due to obstructive uropathy and bilateral mild hydronephrosis, an urgent staging laparotomy was performed and uncovered a 4-liter pus-filled mass. Histopathology revealed likely to be a tubo-ovarian abscess. Factors such as huge abscess size and patient demographics play a huge role in this case due to arising complications, favouring operative intervention as part of the treatment.**

### INTRODUCTION

A tubo-ovarian abscess (TOA) develops when an encapsulated collection of pus forms within an infected fallopian tube and ovary, and it can become life-threatening if rupture occurs. TOA commonly arises as a complication of pelvic inflammatory disease (PID), although in some cases, a TOA may itself be the initial presentation leading to a diagnosis of PID. While TOA is more frequently observed in reproductive-age women, cases have also been reported in postmenopausal women. Its atypical clinical presentation and variable imaging characteristics may mimic pelvic malignancy or other non-gynaecological conditions, and an elevation in CA-125 may further complicate preoperative diagnosis and management. This case report discusses a postoperatively confirmed TOA, highlighting its clinical presentation, diagnostic challenges, and management considerations.

### CASE PRESENTATION

A 20-year-old, Para 1, woman came into the hospital, with a month-long history of abdominal distension, early satiety, and lethargy. She has normal, regular menses without any dysmenorrhoea or history of chronic pelvic pain. Although afebrile without pain, vaginal discharge, or altered bowel habits, she showed tachycardia and a term-size distended, non-tender abdomen. Transabdominal ultrasound showed a huge unilocular cystic mass, homogeneous echogenic content without any obvious solid area, papillary projection,

or significant Doppler flow, and bilateral mild hydronephrosis. Raised leucocytes with elevated CA-125 level were noted (116 U/mL; normal value, <35 U/mL), while the levels of other tumour markers (α-fetoprotein, carcinoembryonic antigen, β-human chorionic gonadotropin, and CA 19-9) were within normal limits. Diagnostic CT imaging (Figure 1) revealed a huge pelvic cyst measuring 20.7cm x 28.3cm x 27.8cm (AP x W x CC), likely of ovarian origin, causing obstructive uropathy and bilateral mild hydronephrosis. Urgent staging laparotomy was performed and uncovered a 4-liter pus-filled mass adhered to surrounding structures, leading to a right salpingo-oophorectomy. She was given intravenous tazosin for 7 days postoperatively and discharged well with oral amoxicillin-clavulanic acid for 7 days. Histopathology revealed chronic inflammation without malignancy of right ovarian cyst with chronic salpingitis, likely to be a huge right tubo-ovarian abscess case. Pus culture and sensitivity test showed no significant pathogens.

### DISCUSSION

Tubo-ovarian abscess (TOA) poses a significant preoperative diagnostic challenge due to its varied and non-specific clinical presentation, often making it difficult to distinguish from other gynaecological pathologies as well as several non-gynaecological conditions with overlapping symptoms. In this case, the marked abdominal distension caused by a large pelvic mass, together with radiological imaging findings and a raised CA-125 level, was highly suggestive of ovarian malignancy.<sup>1,2</sup> Relying on CA-125 alone to differentiate benign from malignant pelvic masses has limited diagnostic value, particularly in premenopausal women.<sup>1</sup> Therefore, correlation with the overall clinical picture, including symptoms, laboratory parameters, imaging features, patient factors, and associated complications, is essential in guiding the management plan for this case.

CA-125 is a relatively useful tumor marker for epithelial ovarian cancer,<sup>3</sup> and an elevated level often raises suspicion for malignancy when an adnexal mass is identified. However, CA-125 can also be increased in numerous benign and inflammatory gynaecological conditions, particularly in premenopausal women with sexual activity, such as endometriosis, benign ovarian cysts, pelvic inflammatory disease, omental inflammation from a ruptured dermoid cyst, as well as during menstruation and pregnancy. It may

*This article was accepted: 15 December 2025*

*Corresponding Author: Su Chok Kim*

*Email: jeremiahsu@gmail.com*

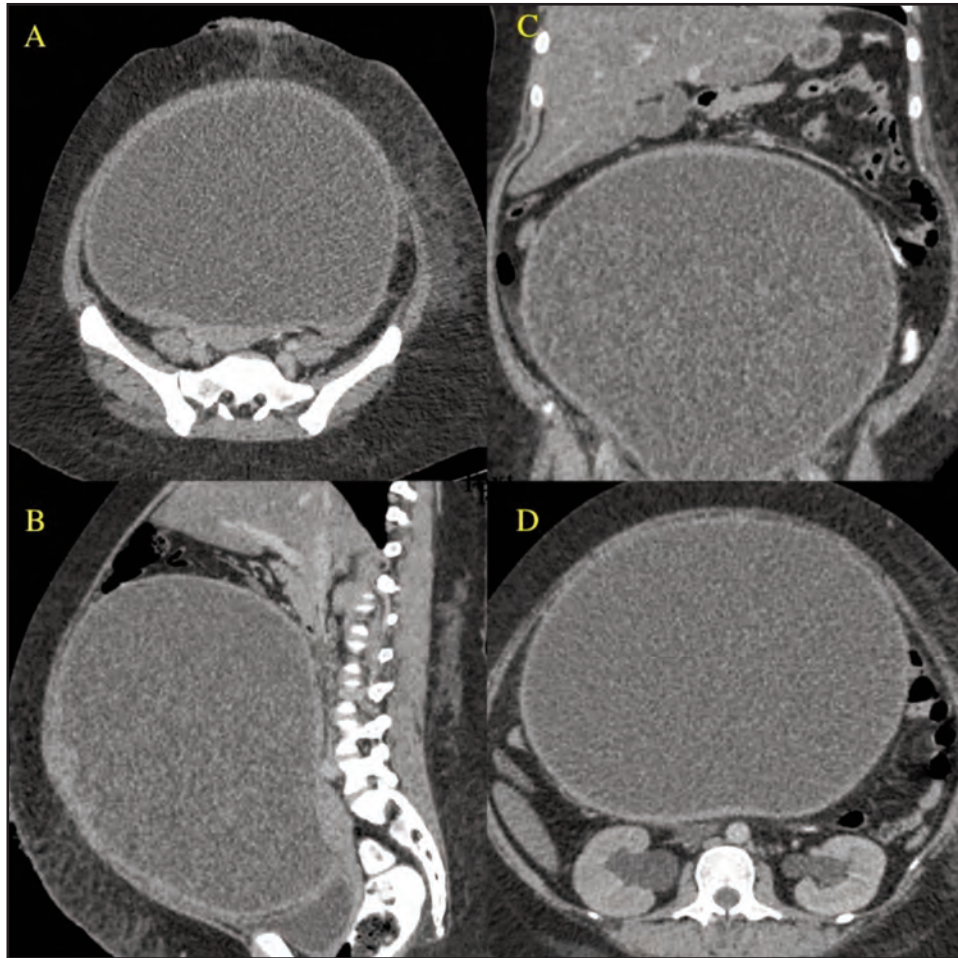


**Fig. 1:** CT TAP findings. A: transverse view at pelvic level. B: Sagittal view, showing displacement of visceral organs superiorly. C: Transverse view at hepatosplenic level. D: transverse view at renal level showing mild hydronephrosis. CECT abdomen and pelvis in axial, coronal and sagittal views showing a huge peripherally enhancing unilocular cystic mass measuring 20.7 x 28.3cm x 27.8cm (AP x W x CC) arising from pelvis till right subhepatic region. There is no septation, papillary projection, calcification enhancing solid or fat component within. It results in bilateral mild hydronephrosis.

also be elevated in non-gynaecological conditions including peritonitis, and hepatic or pulmonary diseases.<sup>1,2</sup> Its elevation may be caused by peritoneal irritation, regardless of whether the underlying cause is benign or malignant.<sup>3</sup> In this case, the atypical clinical presentation (marked abdominal distension without fever, together with elevated leukocyte count and raised CA-125) could mimic an ovarian malignancy and should be considered in the differential diagnosis.<sup>3</sup>

Endometriomas are typically described as homogeneous, hypoechoic ovarian lesions, and most exhibit diffuse low-level internal echoes, multilocularity, and hyperechoic wall foci, although their ultrasonographic appearance can vary.<sup>4</sup> Endometrioma is unlikely in this case, as the patient reports normal, regular menses and does not demonstrate chronic pelvic pain or other common clinical features of endometriosis, such as dysmenorrhoea, dyspareunia, dysuria, dyschezia, or infertility.<sup>5</sup> An infected endometrioma could be considered; however, the patient was afebrile, and such lesions rarely present with rapid, marked abdominal distension over the course of one month.

Ultrasonography is the first-line diagnostic modality for evaluating pelvic masses,<sup>2</sup> and transvaginal ultrasonography have a high negative predictive value in assessing ovarian tumours.<sup>6</sup> According to the IOTA-ADNEX model, incorporating the clinical predictors (20-year-old patient, CA-125 level of 116 U/mL, and referral to a centre with gynaecologic oncology services) and ultrasound predictors (maximum tumour diameter of 28 cm; absence of solid components, cyst locules, papillary projections, acoustic shadows, and ascites), the estimated probability of a benign ovarian tumour in this case is 88.5%. Typical ultrasonographic features of a TOA include a solid, cystic, or complex adnexal mass with surrounding fluid collections.<sup>7</sup> However, preoperative diagnosis of this huge 28 cm mass, such as in this case, is challenging with ultrasonography alone. While the IOTA system offers standardized terminology for adnexal mass characterization, the definitive diagnosis and management of this huge mass depend heavily on clinical presentation, tumor markers, and laboratory findings, and therefore extend beyond the scope of IOTA classification rules.

MRI has been shown to be superior to ultrasonography and CT in characterizing pelvic pathologies, with overall diagnostic accuracies of 97%, 77%, and 87%, respectively.<sup>6</sup> While CT is less ideal for soft tissue discrimination in pelvic masses, it remains valuable for identifying fatty and calcified components, as well as assessing the overall extent of large masses, as demonstrated in this case.<sup>6</sup>

A staging laparotomy was chosen in this case due to compressive complications, including obstructive uropathy and bilateral mild hydronephrosis. Intraoperatively, a 4-liter pus-filled TOA was found adherent to surrounding structures, necessitating a right salpingo-oophorectomy as the right fallopian tube and ovary were already unhealthy and unsalvageable. A minimally invasive approach was not feasible given the massive 28 cm lesion, which significantly increased the risk of injury to adjacent visceral organs and inadvertent puncture of the mass due to the poor laparoscopic working window. Although conservative management with antibiotics is the first-line treatment for any small TOA, an abscess measuring more than 5 cm is associated with poorer response to medical therapy, and surgical intervention or drainage is generally recommended when the abscess exceeds 8 cm.<sup>8,9,10</sup>

Surgical drainage is not ideal in this case, as it may not ensure complete evacuation of the 28 cm TOA compared with smaller TOAs. The significantly larger size increases the risk of intra-abdominal spillage or residual content leaking from the collapsed capsule after drainage. This may lead to recurrence, peritonitis, and subsequent visceral adhesions, which can contribute to chronic pelvic pain and impair fertility preservation. Furthermore, there remains a possibility of an underlying adnexal malignancy that may not be recognised prior to surgery. All these potential complications were taken into consideration in determining the management for this case, especially given that there are yet no reported or published cases addressing the management of a TOA of this size.

Interestingly, a review has reported better outcomes for smaller TOAs when managed with minimally invasive approaches compared with conservative treatment with antibiotics alone.<sup>9</sup> In this case, the patient received 14 days of broad-spectrum antibiotics postoperatively and was subsequently discharged in good condition. Other factors associated with poor response to medical treatment include age over 40 years, elevated initial white blood cell count, and smoking history.<sup>8</sup> Postoperative recovery with antibiotics was successful, reinforcing the importance of surgical intervention when conservative management may be inadequate.

## CONCLUSION

This case contributes valuable insight by presenting an uncommon manifestation of TOA and demonstrating the importance of a multidisciplinary approach in achieving successful management. Although the patient's symptoms and clinical findings initially suggested an ovarian tumour rather than a TOA, this case underscores the significant diagnostic challenges associated with TOA in the preoperative setting. The unusually large abscess size, associated complications, and patient demographics were key factors influencing the decision to proceed with operative intervention as the primary management strategy. This approach aimed not only to treat the underlying pathology but also to preserve fertility and protect adjacent vital organs. This report may assist clinicians in managing huge TOA cases and encourage further reporting to inform future practice, improve outcomes, and guide management strategies for atypical presentations.

## ACKNOWLEDGMENT

The authors would like to thank the patient for agreeing to publish this case.

## DECLARATION

The authors declare no conflict of interest related to this report.

## REFERENCES

1. Ranjan R, Katiyar S, Kumar A, Mishra J. Benign pelvic masses associated with raised CA-125 level: radiological pathological correlation. *Int J Sci Stud* 2015; 3: 28-32.
2. Asher V, Hammond R, Duncan TJ. Pelvic mass associated with raised CA 125 for benign condition: a case report. *World J Surg Oncol*. 2010; 16(8): 28.
3. Meden H, Fattahi-Meibodi A. CA 125 in benign gynecological conditions. *Int J Biol Markers* 1998; 13(4): 231-7.
4. Woodward PJ, Sohaey R, Mezzetti Jr. TP. Endometriosis: Radiologic-Pathologic Correlation *RadioGraphics* 2001; 21: 193-216.
5. National Institute for Health and Care Excellence (NICE). Endometriosis: diagnosis and management. NICE. <https://www.nice.org.uk/>. 16 Apr 2024. Accessed on 9 Dec 2025.
6. Kim SH, Kim SH, Yang DM, Kim KA. Unusual causes of tubo-ovarian abscess: CT and MR imaging findings. *Radiographics* 2004; 24(6): 1575-89.
7. Togashi K. Ovarian cancer: the clinical role of US, CT, and MRI. *Eur Radiol* 2003; 13 Suppl 4: L87-104.
8. Greenstein Y, Shah A, Vragovic O, Cabral H, Soto-Wright V, Borgatta L, Kuohung W. Tuboovarian abscess. Factors associated with operative intervention after failed antibiotic therapy. *The Journal of reproductive medicine* 2013; 58(3-4): 101-6.
9. Goje O, Markwei M, Kollikonda S, Chavan M, Soper DE. Outcomes of Minimally Invasive Management of Tubo-ovarian Abscess: A Systematic Review. *J Minim Invasive Gynecol*. 2021; 28(3): 556-64.
10. Akıncı GE, Bornaun I, Güven HZ. Management and complications of tubo-ovarian abscesses: a brief literature review. *Eur Res J*. 2024. doi: 10.18621/eurj.1467569

# Case report of hyperemesis gravidarum: Hormonal change due to pregnancy and hypothyroidism

Soedarsono Hadipranata, MD, SpOG<sup>1</sup>, Nieke Andina Wijaya, MD, SpDVE<sup>2</sup>, Shod Abdurrachman Dzulkarnain, MD, MBIomed<sup>2</sup>

<sup>1</sup>University of Surabaya / UBAYA Hospital, Surabaya, East Java, <sup>2</sup>Faculty of Medicine, Universitas Negeri Surabaya, Surabaya, East Java

## SUMMARY

Hyperemesis gravidarum (HG) is an extreme form of nausea and vomiting in pregnancy, often leading to severe dehydration, electrolyte imbalances, and significant weight loss, posing risks for both maternal and fetal health. In this report, we present a complex case of a 32-year-old woman at 16 weeks of gestation with HG complicated by suspected gastroparesis and subclinical hypothyroidism. The patient reported unrelenting nausea, vomiting over seven times daily, abdominal fullness, and a substantial weight loss of 8 kg. She exhibited symptoms of weakness, tingling in her limbs, and a three-day history of constipation, highlighting the debilitating nature of HG compounded by delayed gastric emptying. Laboratory results revealed mild anemia, electrolyte imbalances, and elevated TSH, indicating subclinical hypothyroidism. Imaging confirmed superficial gastritis and esophagitis, adding to the diagnostic complexity. Management included antiemetics, levothyroxine, and prokinetic agents, aiming to stabilize her condition and support nutritional intake. This case underscores the multifaceted approach required for HG management, particularly when concurrent conditions like gastroparesis and hypothyroidism are present. Early and accurate diagnosis is crucial to avoid complications such as malnutrition, intrauterine growth restriction, and preterm birth. A multidisciplinary approach, incorporating obstetric, endocrinological, and gastrointestinal care, is essential in optimizing outcomes for both mother and fetus. Through this case, we explore the interconnected pathophysiology of HG, gastroparesis, and hypothyroidism in pregnancy, highlighting the need for vigilant monitoring and personalized management to address the complex symptoms and prevent severe maternal-fetal outcomes.

## INTRODUCTION

Hyperemesis gravidarum (HG) is a severe manifestation of nausea and vomiting in pregnancy, surpassing typical morning sickness in intensity and persistence. It is marked by excessive vomiting, dehydration, electrolyte imbalances, and substantial weight loss, affecting approximately 0.3–2% of pregnancies.<sup>1</sup> Early differentiation between HG and normal pregnancy-related nausea and vomiting is critical, as HG can lead to serious maternal and fetal complications. Gastroparesis may complicate HG due to its delayed gastric emptying, which can aggravate symptoms of nausea, vomiting, and early satiety.<sup>2</sup> Pregnancy-related hormonal changes, particularly increased progesterone levels, can exacerbate or trigger gastroparesis, complicating nutritional

intake and management. Gastroparesis in pregnancy requires dietary adjustments, prokinetic agents, and careful monitoring to mitigate risks such as dehydration and malnutrition. Additionally, subclinical hypothyroidism may exacerbate symptoms such as fatigue, constipation, and nausea, complicating the differential diagnosis of gastrointestinal distress in pregnancy.<sup>3</sup> Thyroid hormone plays a vital role in metabolic and gastrointestinal regulation, and untreated subclinical hypothyroidism is associated with increased risks of preterm delivery, preeclampsia, and low birth weight.<sup>2</sup>

Management strategies for HG and associated conditions require a personalized, multifaceted approach, often including antiemetics, proton pump inhibitors, and sucralfate to control gastrointestinal symptoms. Hydration, electrolyte replacement, and, in severe cases, intravenous fluids are essential to address dehydration and prevent malnutrition. Nutritional support is a cornerstone of ensuring adequate intake and safeguarding fetal development and maternal health. Despite appropriate management, HG and its associated complications can lead to significant maternal and fetal risks. Maternal complications include dehydration, nutritional deficiencies, and electrolyte imbalances, which may result in further cardiovascular, renal, or metabolic issues if not carefully managed. Fetal complications are also of concern, particularly in cases of poorly controlled HG, as the condition can lead to intrauterine growth restriction (IUGR), preterm birth, and in some extreme cases, fetal death.<sup>4</sup>

The objectives of this case report are to highlight the clinical challenges and diagnostic complexities encountered in a pregnant patient presenting with hyperemesis gravidarum, suspected gastroparesis, and subclinical hypothyroidism. Specifically, the report aims to discuss the pathophysiology and differential diagnosis of severe pregnancy-related nausea and vomiting, explore the impact of coexisting conditions such as gastroparesis and hypothyroidism on management, and evaluate the therapeutic approach, including pharmacologic and supportive treatments.

## CASE PRESENTATION

### Investigation

A 32-year-old pregnant woman, currently at 16 weeks of gestation, presented with persistent nausea and vomiting that had progressively worsened over the past three days. She reported experiencing more than seven episodes of vomiting

*This article was accepted: 22 December 2025*

*Corresponding Author: Soedarsono Hadipranata*

*Email: dr.soedarsono@gmail.com*

**Table I. Laboratory Results Supporting the Diagnosis**

Parameter	26/05/24	18/06/24	19/08/24	05/09/24	07/10/24	11/10/24	01/11/24	Notes/Interpretation
Hemoglobin (Hb)	11.9	12.3	11.8	12.1	11.7	10	11.7	Mild decrease in Hb, consistent with weight loss and possible malnutrition due to hyperemesis gravidarum. Decrease in hematocrit, potentially linked to dehydration or poor intake. Slightly elevated WBC in some tests may indicate mild stress or infection. Within normal range, no signs of significant bleeding or clotting abnormalities. Mild hyponatremia, possibly from dehydration due to vomiting and fluid loss. Mild hypokalemia, potentially due to vomiting and electrolyte loss. Elevated glucose level, likely due to stress, dehydration, and possible ketone production. Proteinuria could indicate renal stress, possibly due to dehydration and hypovolemia. Elevated ketones, suggesting dehydration or prolonged fasting from vomiting. Elevated TSH and normal FT4, indicating subclinical hypothyroidism, which may exacerbate symptoms of hyperemesis gravidarum.
Hematocrit (Hct)	36%	37.4%	36.2%	34.5%	35.8%	29%	36%	
Leukocytes (WBC)	6.9	7.88	10.8	10.6	8.8	6.64	9.3	
Platelets (Plt)	236	300	297	304	269	222	282	
Sodium (Na)	140	140	136	134.5	-	131	134	
Potassium (K)	3.3	4.1	4.3	3.5	-	2.8	3.3	
Random glucose levels	-	-	-	-	-	-	132	
Urine: Protein	-	Neg	(+)1	(+)1	(+)2	-	(+)1	
Urine: Ketones	-	Neg	(+)4	(+)1	(+)4	-	(+)3	
TSH	-	-	-	-	-	-	5.1	
FT4	-	-	-	-	-	-	1.25	

**Table II: Differential Diagnoses and Respective Considerations**

Diagnosis	Differential Diagnoses
Hyperemesis gravidarum	<ul style="list-style-type: none"> <li>• Gestational trophoblastic disease: Ruled out by normal imaging and hCG levels.</li> <li>• Pancreatitis: Excluded by normal amylase and lipase levels.</li> <li>• Metabolic disorders: No metabolic acidosis or hallmark features.</li> </ul>
Suspected gastroparesis	<ul style="list-style-type: none"> <li>• Intestinal obstruction or infections: Imaging and endoscopy ruled out mechanical obstructions or infections.</li> <li>• Autonomic neuropathy: No diabetes or neurological history.</li> <li>• Mechanical obstruction: Excluded by imaging and endoscopy.</li> <li>• Medication-induced gastroparesis: No history of anticholinergic or opioid use.</li> </ul>
Subclinical hypothyroidism	<ul style="list-style-type: none"> <li>• Central hypothyroidism: Excluded by normal FT4 levels.</li> <li>• Euthyroid sick syndrome: Unlikely without signs of critical illness.</li> <li>• Transient gestational hypothyroidism: Less likely due to persistence beyond the first trimester.</li> </ul>

per day, particularly after meals. Additional symptoms included abdominal fullness, intermittent abdominal pain, frequent belching, weakness, and tingling sensations in her limbs. Over the course of her pregnancy, she experienced a significant weight loss of 8 kg and had not had a bowel movement for three days.

The patient's medical history included chronic gastritis and a prior diagnosis of cholecystitis. She had been hospitalized multiple times for similar symptoms during previous pregnancies, initially attributed to normal pregnancy-related conditions. Previous interventions included treatments with antiemetics, proton pump inhibitors, and steroids, but these failed to alleviate her symptoms and instead led to progressive worsening.

On physical examination, the patient appeared dehydrated and malnourished, with a weight of 52 kg, a height of 168 cm, and a BMI of 18.4, indicating underweight status. Her vital signs were as follows: blood pressure 106/64 mmHg, respiratory rate 20 breaths per minute, heart rate 58–65 beats per minute, and axillary temperature 36.1°C.

Abdominal examination revealed a soft, non-distended abdomen with mild tenderness localized to the epigastric region. No guarding, rebound tenderness, or palpable masses were noted. Percussion was tympanic over the epigastric area, and auscultation revealed hypoactive bowel sounds, suggestive of delayed gastric emptying. Neurological evaluation identified slightly reduced motor strength (4/5) in the lower extremities, mild paresthesia in both hands and

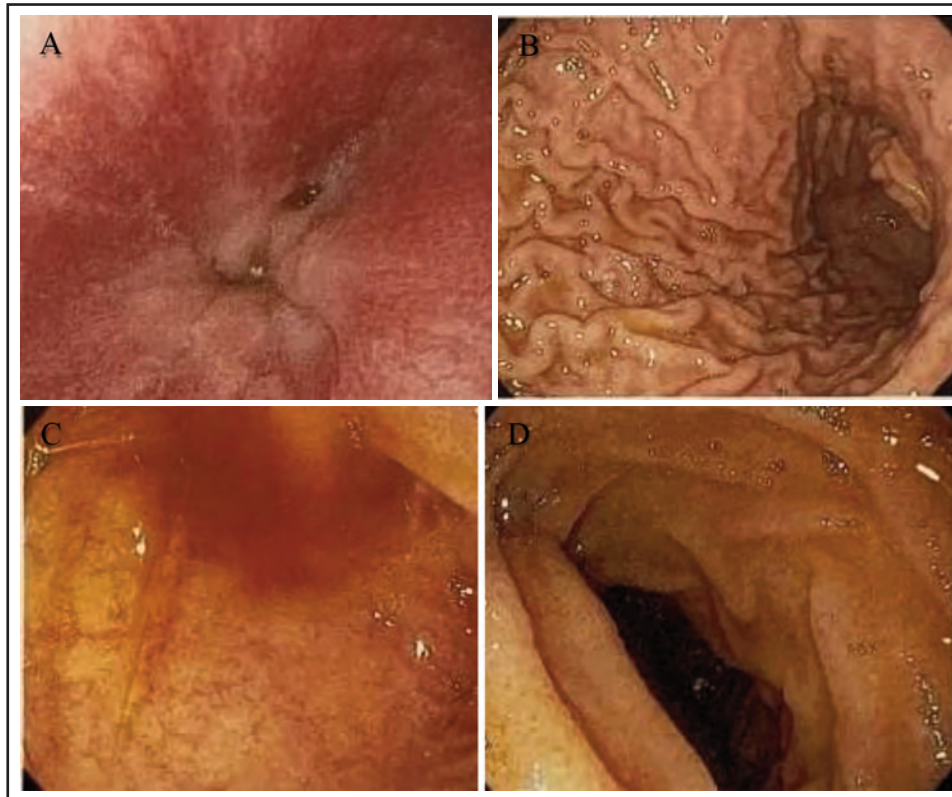


**Fig. 1:** Endoscopy Evaluation. A. hyperemic esophagus; B. hyperemic gaster; C. hyperemic bulbus of duodenum; D. hyperemic duodenum mucous

feet, and normal deep tendon reflexes. Other systemic findings included dry mucous membranes, reduced skin turgor, delayed capillary refill (3 seconds), and no edema in the extremities. Cardiovascular and respiratory examinations were unremarkable.

Laboratory tests revealed mild decreases in hemoglobin (Hb: 10–11.9 g/dL) and hematocrit (Hct: 29–37%), mild hyponatremia (131–140 mEq/L), and hypokalemia (2.8–4.3 mEq/L). Urinalysis showed positive ketones and proteinuria (+1 to +2), and random blood glucose was mildly elevated at 132 mg/dL. Thyroid-stimulating hormone (TSH) was elevated at 5.1 mIU/L, indicating subclinical hypothyroidism. Imaging and endoscopic evaluation demonstrated hyperemic mucosa in the esophagus, stomach, and duodenum, but no evidence of infection or malignancy.

From a psychosocial perspective, the patient expressed significant stress and anxiety related to her persistent symptoms and their potential impact on her ability to care for herself and her baby. Financial concerns and limited availability of her husband, due to work commitments, exacerbated her emotional burden. However, she reported some emotional and physical support from her mother. A family history revealed hypothyroidism in her mother and postpartum depression in a maternal aunt.

### Diagnosis

The diagnostic process for this case involved a combination of physical examination, laboratory testing, urine analysis, imaging, and endoscopic evaluation. Physical examination

(PE) findings indicated moderate dehydration, malnutrition (BMI: 18.4 kg/m<sup>2</sup>), hypoactive bowel sounds suggestive of delayed gastric emptying, and mild paresthesia in the extremities. Laboratory results showed mild anemia, hyponatremia, hypokalemia, positive urine ketones and proteinuria, elevated random blood glucose, and an increased TSH level (5.1 mIU/L), consistent with subclinical hypothyroidism. Endoscopic findings revealed hyperemic mucosa in the esophagus, stomach, and duodenum, supporting the suspicion of gastroparesis but ruling out structural obstructions, malignancy, or infection.

The case was challenging due to persistent, severe vomiting refractory to standard treatments like antiemetics, proton pump inhibitors, and steroids. The delayed diagnosis of gastroparesis further complicated management, as its clinical presentation overlapped significantly with hyperemesis gravidarum (HG). Additionally, the presence of subclinical hypothyroidism posed another layer of diagnostic complexity due to its potential exacerbation of symptoms such as nausea and delayed gastric motility.

### Treatment

The therapeutic approach for the patient focused on addressing her primary conditions: hyperemesis gravidarum, gastroparesis, and subclinical hypothyroidism, using a combination of pharmacologic and supportive interventions. For hyperthyroidism, the patient was prescribed levothyroxine at a dosage of 100 µg once daily. This medication was taken in the morning on an empty stomach, ideally 30-60 minutes before breakfast, accompanied by a

full glass of water to optimize absorption. Care was taken to avoid the intake of calcium or iron supplements within a 4-hour window of levothyroxine, as these could interfere with its absorption.

To manage the symptoms of gastroparesis and persistent nausea, the patient was prescribed metoclopramide, 10 mg per dose, to be taken three times daily, 30 minutes before meals. This medication promotes gastric emptying and helps reduce nausea and vomiting. However, treatment with metoclopramide was limited to a maximum of 12 weeks due to concerns about the risk of tardive dyskinesia with prolonged use. To address the gastric acid-related symptoms and prevent esophageal and gastric irritation, omeprazole was prescribed at a dosage of 20 mg twice daily, before breakfast and dinner. This proton pump inhibitor was taken to suppress gastric acid production and promote mucosal healing. Additionally, the patient was given sucralfate syrup at a dosage of 15 mL three times daily, to be taken 1 hour before meals and at bedtime. Sucralfate acts by forming a protective barrier in the stomach lining, helping to prevent further irritation and promoting healing of the mucosa. The patient was advised not to take antacids within 30 minutes before or after taking sucralfate, as this could interfere with its action.

Throughout the treatment process, adjustments were made based on the patient's clinical response. As her vomiting subsided and symptoms were managed, the focus shifted toward maintaining adequate hydration and nutrition, both crucial for her health and the health of the fetus. Regular monitoring was conducted to assess the effectiveness of the medications, with further interventions planned as necessary.

#### Follow-Up and Outcomes

Following the initiation of treatment, the patient experienced significant improvement in her condition. The vomiting subsided, and there was a general improvement in her symptoms after just two days of treatment. This positive response indicated that the combination of levothyroxine, metoclopramide, omeprazole, and sucralfate effectively addressed the primary issues of hyperemesis gravidarum and gastroparesis. Routine follow-up tests were conducted to monitor her progress, including repeat lab tests for thyroid function, electrolytes, and glucose, which showed stable results post-treatment. Imaging and clinical assessments also confirmed the absence of new complications.

Adherence to the prescribed treatment regimen was assessed during follow-up visits, with the patient reporting no significant adverse events, although she was closely monitored for any potential side effects, especially from metoclopramide. Given the nature of the medications, the patient was educated on the importance of timely and consistent medication administration, with particular attention to the timing of levothyroxine and the avoidance of antacids with sucralfate.

In the long term, maternal health shall be closely monitored, particularly regarding mental health, given the psychological toll of prolonged illness during pregnancy. Signs of postpartum depression or anxiety shall be assessed

following labor, and appropriate support shall be provided. Nutritional deficiencies shall be evaluated, particularly given the significant weight loss and vomiting the patient experienced in this pregnancy. The patient was advised to maintain ongoing dietary adjustments and medications to manage any possible symptoms of gastroparesis, ensuring both her health and the potential health of future pregnancies.

#### DISCUSSION

Hyperemesis gravidarum (HG) is a severe form of pregnancy-related nausea and vomiting, distinct from common morning sickness due to its intensity, duration, and associated complications such as weight loss and dehydration.<sup>1</sup> Hormonal changes, particularly elevated levels of human chorionic gonadotropin (hCG), estrogen, and progesterone, play a crucial role in the pathophysiology of HG. Human chorionic gonadotropin, produced by the placenta, is believed to stimulate the vomiting center in the brain. Although essential for maintaining pregnancy, hCG levels peak early in gestation and are thought to be disproportionately elevated in women with HG, triggering more severe symptoms.<sup>5</sup>

Progesterone contributes to HG through its effects on the gastrointestinal tract. By relaxing smooth muscles, including the lower esophageal sphincter, progesterone causes delayed gastric emptying, increased gastric acid secretion, and gastric stasis, which exacerbate nausea and vomiting. Its effects on the autonomic nervous system may further alter gastric motility, contributing to fullness, dehydration, and malnutrition that can complicate pregnancy.<sup>6</sup> HG receptor mechanisms involve interactions between hormones, receptors, and signaling pathways. Estrogen can sensitize the vomiting center in the brainstem via estrogen receptor binding. Neurokinin-1 (NK1) receptor activation by substance P plays a key role in the emetic response. In HG, elevated hormone levels may disrupt neurotransmitter balance, enhancing symptom severity and persistence.<sup>7</sup>

Gastroparesis is characterized by delayed gastric emptying without mechanical obstruction and is an important differential diagnosis in severe nausea and vomiting during pregnancy.<sup>3</sup> Pregnancy-related hormonal changes, particularly elevated progesterone levels, play a significant role in its development. Progesterone induces smooth muscle relaxation throughout the gastrointestinal tract, reducing gastric motility and delaying gastric emptying, while also affecting the lower esophageal sphincter and increasing the risk of gastroesophageal reflux, which can exacerbate nausea and vomiting.<sup>8</sup> Anatomical and physiologic changes during pregnancy further contribute to delayed gastric emptying. As pregnancy progresses, uterine enlargement displaces and compresses the stomach and intestines, slowing gastric transit and worsening symptoms such as fullness, bloating, and postprandial discomfort. These effects are more pronounced in the second and third trimesters, when mechanical impedance of gastrointestinal function is greatest.<sup>2</sup> Rising progesterone levels interact with gastric smooth muscle receptors, including the progesterone receptor, leading to impaired motility. Pregnancy-related

autonomic changes, with increased sympathetic and reduced parasympathetic tone, further inhibit gastric emptying. Although compensatory neurohormonal responses such as increased motilin may occur, elevated progesterone levels and mechanical factors may overwhelm these mechanisms, preventing restoration of normal gastric emptying.<sup>8</sup>

Subclinical hypothyroidism, characterized by elevated TSH with normal FT4, reflects impaired thyroid hormone activity without overt clinical symptoms. Thyroid hormones (T4 and T3) are essential regulators of gastrointestinal motility, particularly during pregnancy. Increased TSH suggests insufficient thyroid hormone action, which can slow gastrointestinal transit. Thyroid hormones act via thyroid hormone receptors (TRs) in gastrointestinal smooth muscle cells to regulate contraction and relaxation necessary for normal peristalsis; reduced hormone activity therefore results in delayed gastric emptying and constipation.<sup>9</sup>

The gastrointestinal effects of hypothyroidism are primarily mediated through altered motility. Thyroid hormones stimulate smooth muscle contraction via TRs and  $\beta$ 1- and  $\beta$ 2-adrenergic receptor pathways. In subclinical hypothyroidism, reduced thyroid hormone availability decreases  $\beta$ -adrenergic receptor activity, leading to impaired motility. Thyroid hormones also regulate gastrointestinal hormones such as motilin and gastrin, and their imbalance may further exacerbate nausea, bloating, and delayed gastric emptying. Thyroid hormone deficiency additionally affects gastrointestinal function through modulation of the autonomic and enteric nervous systems. Normally, thyroid hormones promote parasympathetic activity and coordinated gut motility. In subclinical hypothyroidism, relative sympathetic predominance and altered enteric neurotransmitter release, including serotonin dysregulation, contribute to reduced motility and prolonged transit time.<sup>9</sup>

Management of hyperemesis gravidarum (HG) focuses on symptom control and prevention of dehydration, electrolyte imbalance, and malnutrition. Pharmacological therapy is central. Metoclopramide acts as both a dopamine D2 receptor antagonist in the chemoreceptor trigger zone and a prokinetic agent in the gastrointestinal tract via serotonin receptors (5-HT<sub>3</sub> and 5-HT<sub>4</sub>). This dual central and peripheral action reduces nausea and vomiting while improving gastric motility and delayed gastric emptying, alleviating bloating and supporting nutrient absorption critical for maternal and fetal health.<sup>5</sup>

Proton pump inhibitors such as omeprazole are commonly added to address acid-related symptoms. By irreversibly inhibiting the H<sup>+</sup>/K<sup>+</sup>-ATPase in gastric parietal cells, omeprazole reduces gastric acid secretion, which may be increased due to prolonged vomiting. Acid suppression provides relief from reflux symptoms and reduces the risk of esophagitis and ulcer formation, reflecting the molecular basis of acid-mediated mucosal injury in HG. Non-pharmacological measures remain essential. HG carries a substantial psychological burden, and anxiety or stress may exacerbate symptoms via the gut-brain axis and activation of the hypothalamic-pituitary-adrenal axis. Psychological support and dietary modifications, including small frequent

meals and avoidance of triggers, can reduce gastric distension and improve gastric emptying, complementing pharmacological therapy.<sup>10</sup>

This case report highlights the diagnostic and management challenges in a pregnant patient with hyperemesis gravidarum (HG), gastroparesis, and subclinical hypothyroidism. HG, characterized by severe nausea and vomiting, poses significant risks to maternal and fetal health, exacerbated by gastroparesis, which delays gastric emptying, and subclinical hypothyroidism, which can worsen gastrointestinal symptoms. Diagnosing these conditions is challenging, especially distinguishing between normal pregnancy changes and pathological symptoms. Effective management involved anti-nausea medications, prokinetic agents, thyroid hormone replacement, and nutritional support. A multidisciplinary approach was essential to prevent complications like dehydration and fetal growth restriction. This case underscores the importance of individualized care and thorough evaluation of thyroid function in pregnant women, while also highlighting the need for further research to explore the complex interplay of gastrointestinal, hormonal, and metabolic factors in pregnancy.

#### ACKNOWLEDGMENT

We appreciate the assistance of all staff from the Medical Record Installation of Ubaya Hospital, Surabaya.

#### FINANCIAL DISCLOSURE

The authors declared that this study has received no financial support.

#### CONFLICT OF INTEREST

The authors have no conflicts of interest to declare.

#### REFERENCES

1. Fassett MJ, Peltier MR, Lopez AH, Chiu VY, Getahun D. Hyperemesis Gravidarum: Risk of Recurrence in Subsequent Pregnancies. *Reprod Sci.* 2023; 30(4): 1198-206.
2. Moosavi S, Min YW, Wong M, Rezaie A. Gastroparesis in pregnancy. *Am J Obstet Gynecol.* 2023; 228(4): 382-94.
3. Sullivan A, Temperley L, Ruban A. Pathophysiology, Aetiology and Treatment of Gastroparesis. *Dig Dis Sci.* 2020; 65(6): 1615-31.
4. Adane KD, Zerga AA, Gebeyehu FB, Ayele FY. Proportion of hyperemesis gravidarum and associated factors among pregnant women admitted into the obstetrics ward at Akesta general hospital, North East Ethiopia. *PLoS One.* 2023; 18(2 February): 1-10.
5. Geeganage G, Iturrino J, Shainker SA, Ballou S, Rangan V, Nee J. Emergency department burden of hyperemesis gravidarum in the United States from 2006 to 2014. *AJOG Glob Reports.* 2023; 3(1): 1-7.
6. Fejzo M, Rocha N, Cimino I, Lockhart SM, Petry CJ, Kay RG, et al. GDF15 linked to maternal risk of nausea and vomiting during pregnancy. *Nature.* 2024; 625(7996): 760-7.
7. Fejzo MS. Hyperemesis gravidarum theories dispelled by recent research: a paradigm change for better care and outcomes. *Trends Mol Med.* 2024; 30(6): 530-40.

## Case Report

8. Sprouse J, Sampath C, Gangula PR. Role of sex hormones and their receptors on gastric Nrf2 and neuronal nitric oxide synthase function in an experimental hyperglycemia model. *BMC Gastroenterol.* 2020; 20(1): 1-16.
9. Chen A, Luo Z, Zhang J, Cao X. Emerging research themes in maternal hypothyroidism: a bibliometric exploration. *Front Immunol.* 2024; 15(March): 1-20.
10. Jansen LAW, Shaw V, Grooten IJ, Koot MH, Dean CR, Painter RC. Diagnosis and treatment of hyperemesis gravidarum. *C Can Med Assoc J.* 2024; 196(14): E477-85.

# Miller fisher syndrome mimicking cavernous sinus thrombosis and thyroid eye disease: A diagnostic dilemma in a hyperthyroid patient

Nur Azureen Mohd Ali, MBBS<sup>1,2</sup>, Julieana Muhammed, MMed<sup>2</sup>, Farhana Ibrahim, MD<sup>1</sup>

<sup>1</sup>Department of Ophthalmology Hospital Tuanku Ja'afar Seremban, Negeri Sembilan Malaysia, <sup>2</sup>Department of Ophthalmology and Visual Science, School of Medical Sciences, Health Campus, Universiti Sains Malaysia, Kubang Kerian, Kelantan, Malaysia

## SUMMARY

**Introduction:** Miller Fisher Syndrome (MFS), a variant of acute inflammatory demyelinating polyneuropathy (AIDP), may mimic orbital diseases such as cavernous sinus thrombosis (CST) and thyroid eye disease (TED), creating significant diagnostic challenges. **Case presentation:** A 65-year-old hyperthyroid male who presented with bilateral eye pain, right (RE) lid drooping, left eye (LE) proptosis, diplopia, and gait instability. Examination revealed ophthalmoplegia and conjunctival injection bilaterally, complete RE ptosis, LE proptosis, and preserved optic nerve function. Neurological assessment demonstrated areflexia, involvement of cranial nerves III, IV, VI, and left VII, and positive cerebellar signs. Contrast-enhanced CT imaging showed left eye proptosis with bilateral cavernous sinus opacification. Cerebro-spinal fluid analysis revealed positive anti-ganglioside GQ1b antibodies, confirming MFS. He was treated with intravenous immunoglobulin (IVIg) and systemic antibiotics, with marked neurological and ocular improvement over six weeks. **Conclusion:** MFS can present with orbital features seen in CST and TED, awareness of neurogenic signs, particularly areflexia and preserved optic nerve function is crucial. Anti-GQ1b antibodies remain key to definitive diagnosis.

## INTRODUCTION

MFS is a rare autoimmune neuropathy characterized by the triad of ophthalmoplegia, areflexia, and ataxia.<sup>1,2</sup> It is considered a variant of Guillain-Barré Syndrome (GBS) and is often associated with anti-GQ1b antibodies.<sup>1,4</sup> The overlapping clinical features of MFS with other orbital pathologies such as CST and TED can complicate the diagnostic process.<sup>3</sup> We present a case initially suspected to be CST and TED, emphasising the importance of thorough neurological evaluation in atypical ophthalmic presentations.

## CASE PRESENTATION

A 65-year-old hyperthyroid male and chronic smoker presented with bilateral eye pain, RE swelling and redness, progressive drooping of the right eyelid, diplopia, headache, vomiting, and unsteady gait. Visual acuity was 6/12 in the RE and 6/24 in the LE. Pupillary response were normal with no

relative afferent pupillary defect. Optic nerve function was preserved.

Examination revealed RE ptosis and axial LE axial proptosis (Figure 1). Extraocular movements were restricted in all directions bilaterally. The conjunctiva was injected, but there was no anterior chamber inflammation or raised intraocular pressure. Fundus examination was unremarkable.

Neurological assessment demonstrated global areflexia, involvement of cranial nerves III, IV, VI, and left VII, positive cerebellar signs, and impaired tandem gait.

A contrast-enhanced CT of the brain and orbits revealed LE proptosis and bilateral cavernous sinus opacification (Figure 2). Lumbar puncture and CSF analysis showed positive anti-GQ1b antibodies, confirming MFS.

He was treated with a five-day course of IVIg and empirical systemic antibiotics. After six weeks, the patient's ophthalmoplegia resolved, RE ptosis improved, and LE proptosis reduced. Neurologically, reflexes returned, gait normalized, and only a mild left VII cranial nerve palsy remained.

## DISCUSSION

This case illustrates how MFS can masquerade as orbital pathology due to overlapping signs of ptosis, ophthalmoplegia, and proptosis. Although the initial presentation resembled CST or TED, the bilateral symmetrical ophthalmoplegia, preserved optic nerve function and associated systemic neurological findings were atypical for primary orbital disease. These key features prompted consideration of a neurogenic aetiology rather than an isolated orbital disorder.

Recent literature has expanded understanding of anti-GQ1b antibody syndromes, emphasising their diagnostic value in atypical neuro-ophthalmic presentations.<sup>6</sup> Updated reviews on Guillain-Barré variants also highlight the broad clinical spectrum of MFS and reinforce the need to recognise mimics early.<sup>7</sup>

*This article was accepted: 22 December 2025*  
Corresponding Author: Julieana Muhammed  
Email: drjulieana@usm.my

**Table I: Differentiating features of MFS, CST and TED**

Features	MFS	CST	TED
Onset	Acute, post-infectious	Acute, rapidly progressive	Subacute to chronic
Pain	Mild or absent	Severe	Usually mild
Optic nerve involvement	Rare	Common	Possible
Areflexia	Present	Absent	Absent
Ataxia	Common		
Cranial nerve palsies	II, IV, VI, VII common	III, IV, V1, V2, VI	Restrictive myopathy
Proptosis	Rare, mild	Possible	Common
Systemic features	Neurogenic	Fever, sinusitis	Hyperthyroid
Anti-GQ1b antibodies	Positive	Negative	Negative
Response to IVIg	Good	No	Variable
Imaging	Usually normal	Cavernous sinus changes	EOM enlargement with tendon sparing

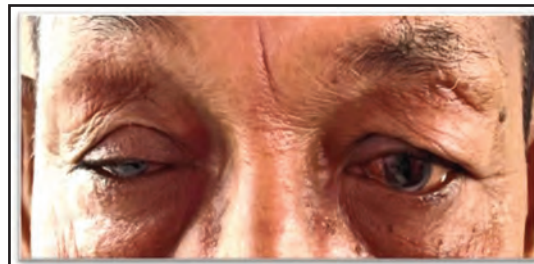


**Fig. 1:** Clinical photograph showing right upper eyelid ptosis and left axial proptosis at initial presentation

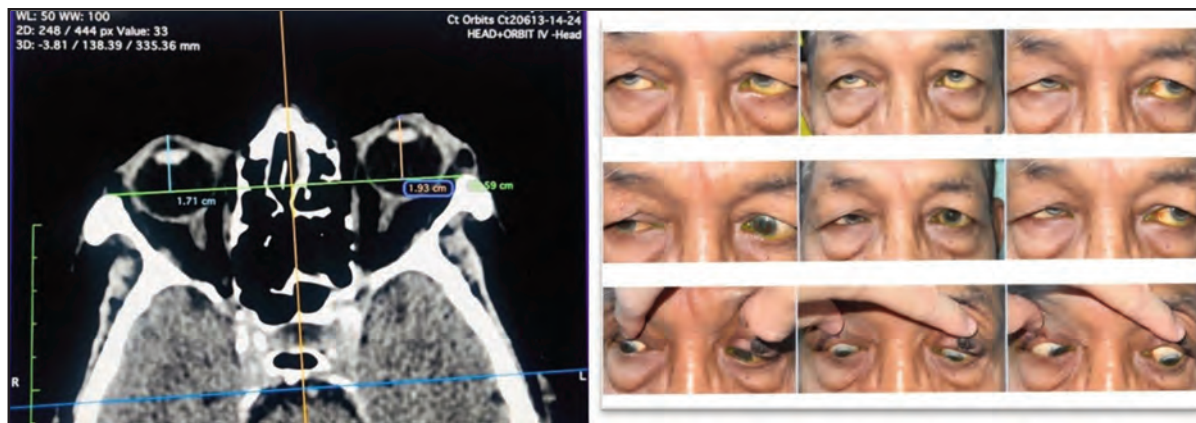


**Fig. 2:** Initial Contrast-enhanced CT orbit demonstrating LE proptosis and bilateral cavernous sinus opacification (A). Sixth-week post-IVIg treatment, marked resolution of ophthalmoplegia and improvement in ptosis and proptosis (B). – Post-treatment imaging not done

Misdiagnosis of MFS may lead to delayed immunotherapy and unnecessary investigations or treatments. Early testing for anti-GQ1b antibodies is therefore crucial, as these antibodies are highly specific for MFS and correlate with disease severity.<sup>1,5</sup>

Radiological findings in MFS are often nonspecific with imaging changes frequently reflecting mimicking pathology rather than the underlying neuropathy. CT findings may be misleading, as cavernous sinus fullness can be present even in non-thrombotic conditions. In this case, imaging suggested CST, illustrating the diagnostic overlap.

From an ophthalmic standpoint, MFS can present with findings similar to CST and TED, such as ptosis, ophthalmoplegia, and proptosis (Table 1). The presence of systemic neurological signs, such as ataxia and areflexia, should prompt consideration of a neurological etiology.

While intravenous immunoglobulin is the standard of therapy, residual cranial nerve deficits may persist.<sup>2,4</sup> In our case, the persistence of LE proptosis in our case raises the possibility of concurrent TED, especially given the patient’s hyperthyroidism and a dual pathology of TED overlapping with MFS may be considered. Further orbital imaging or TSH-receptor antibody testing may help clarify whether TED contributed to the presentation. This highlights the importance of monitoring for dual pathology in patients with underlying thyroid disease and the need for ongoing monitoring to distinguish residual orbital pathology from neurological recovery.

This case underscores the value of multidisciplinary collaboration, particularly between ophthalmologists, neurologists, and radiologists in evaluating atypical presentations, thereby ensuring timely diagnosis and optimal management.

### CONCLUSION

Miller Fisher Syndrome can closely mimic orbital diseases such as CST and TED, awareness of neurogenic clues, particularly areflexia and preserved optic nerve function, is essential. Anti-GQ1b antibodies remain key to definitive diagnosis.

### PATIENT CONSENT

Written informed consent was obtained from the patient for publication of this case report and accompanying images.

### CONFLICT OF INTEREST

The authors declare no conflict of interest.

### REFERENCES

1. Odaka M, Yuki N, Hirata K. Anti-GQ1b IgG antibody syndrome: clinical and immunological range. *Journal of Neurology, Neurosurgery & Psychiatry*, 2001; 70(1): 50-5.
2. Mori M, Kuwabara S, Fukutake T, Yuki N, Hattori T. Clinical features and prognosis of Miller Fisher syndrome. *Neurology*, 2001; 56(8): 1104-6.
3. Tilikete C, Vighetto A. Ophthalmoplegia in GBS and related disorders. *J Neuroophthalmol*. 2005; 25(4): 308-13.
4. Yuki N, Hartung HP. Guillain-barré syndrome. *New England Journal of Medicine*, 2012; 366(24): 2294-304.
5. Koga M, Yuki N, Hirata K. Antecedent symptoms in Guillain-Barré syndrome: an important indicator for clinical and serological subgroups. *Acta neurologica scandinavica*, 2001; 103(5): 278-87.
6. Sato Y, Yuki N. Anti-GQ1b antibody syndrome: clinical and immunological update. *Neurol Neuroimmunol Neuroinflamm*. 2021; 8(3): e973.
7. Doets AY, Verboon C, van den Berg B, Harbo T, Cornblath DR, Willison HJ, et al. Guillain-Barré syndrome and variants: a systematic review and update. *Lancet Neurol*. 2020; 19(10): 923-36.

# Placental-site trophoblastic tumor with deep myometrial invasion - a rare entity: The Malaysian experience

Pei Yoke Wang, MBBS<sup>1</sup>, Mohd Faizal Ahmad, MD<sup>2</sup>, Mohamad Faiz Mohamed Jamli, MBBS<sup>1</sup>, Marliza Hadzar, MD<sup>3</sup>, Eng Ngen Chong, MD<sup>4</sup>, Chee Meng Yong, MD<sup>5</sup>

<sup>1</sup>Department of ObGyn, Hospital Tuanku Ja'afar, Seremban Negeri Sembilan, Malaysia, <sup>2</sup>Advanced Reproductive Centre (ARC), Hospital Canselor Tuanku Mukhriz (HCTM) UKM, Faculty of Medicine, National University of Malaysia Cheras, Kuala Lumpur, Malaysia, <sup>3</sup>Department of Pathology, Hospital Tuanku Ja'afar, Seremban Negeri Sembilan, Malaysia, <sup>4</sup>Department of Radiology, Hospital Tuanku Ja'afar, Seremban Negeri Sembilan, Malaysia, <sup>5</sup>Department of ObGyn, Hospital Ampang, Selangor, Malaysia

### SUMMARY

A placental-site trophoblastic tumor (PSTT) is a sporadic form of gestational trophoblastic neoplasm characterized by minimal secretion of beta-hCG and notable resistance to chemotherapy. This report presents the case of a 43-year-old multiparous woman with a previous initial diagnosis of an arteriovenous malformation (AVM). The patient exhibited recurrent episodes of abnormal uterine bleeding (AUB) accompanied by rising beta-hCG levels following successful embolization. The subsequent assessment revealed a vascular intrauterine mass measuring at least 5 cm, accompanied by an elevated serum beta-hCG level. Option of definitive treatment - total abdominal hysterectomy was offered for optimal management and precision in diagnosis via histopathological assessment. The histopathological analysis confirmed the diagnosis of PSTT. As the initial beta-hCG was declining following surgical intervention, initiation of methotrexate (MTX) treatment was done. However, the lack of clinical response necessitates escalation to EMA/CO chemotherapy; hence, complete remission is achieved. To date, our patient remains disease-free with no evidence of early recurrence or metastasis. Thus, we highlight the critical importance of histopathological evaluation in women presenting with persistent bleeding, even in the presence of low beta-hCG levels. The characteristics of AVM can hinder early diagnosis; thus, the critical value of beta-hCG should be emphasized in assisting this rare diagnosis of PSTT. Additionally, we emphasize the potential for ovarian preservation following definitive treatment and the efficacy of multi-agent EMA/CO chemotherapy over single-agent methotrexate in managing high-risk PSTT patients aiming for early remission.

### INTRODUCTION

A placental-site trophoblastic tumor (PSTT) is the rarest type of malignant gestational trophoblastic tumor. Since its first formal description by Scully in 1976, fewer than 350 well-documented cases have been published worldwide; its incidence is estimated at roughly 1 in 50,000–100,000 pregnancies, though the true rate may be higher due to misclassification of indolent lesions.<sup>1</sup> Clinically, PSTT arises from intermediate trophoblasts at the implantation site, which generally serve to anchor the placenta and remodel the maternal spiral arterioles. These cells produce human

placental lactogen (hPL) and inhibin  $\alpha$  more readily than beta human chorionic gonadotropin ( $\beta$  hCG), resulting in low  $\beta$  hCG levels and potential diagnostic confusion. Biologically, PSTT occupies an intermediate niche between benign placental site nodules and aggressive choriocarcinoma; it grows relatively slowly with a “pushing” myometrial invasion pattern and later metastasis (commonly to lung, pelvis, brain, liver), yet is relatively resistant to single agent chemotherapy once metastatic.<sup>2</sup> To date, the pathologists identify PSTT by sheets of monomorphic intermediate trophoblasts with abundant eosinophilic cytoplasm, distinct cell membranes, and absence of chorionic villi; immunohistochemistry is pivotal, with diffuse hPL and cytokeratin, patchy  $\beta$  hCG, and a Ki 67 index typically 5–30%, helping distinguish PSTT from epithelioid leiomyosarcoma, epithelioid trophoblastic tumour (ETT), and placental site nodule.<sup>3</sup> Consequently, management principles differ markedly from those for choriocarcinoma or invasive moles. Surgery is the primary modality because complete excision offers the highest likelihood of cure while avoiding multi agent chemotherapy toxicities based on international guidelines recommendation.<sup>4</sup> Nevertheless, controversy persists over surgical extent either simple hysterectomy versus hysterectomy with bilateral salpingo oophorectomy and/or lymphadenectomy and indications for adjuvant treatment. Current FIGO and NCCN guidance supports considering adjuvant EMA/CO (etoposide, methotrexate, dactinomycin, cyclophosphamide, vincristine) or other multi agent regimens when histopathologic risk factors are present, including deep myometrial/serosal invasion, lymphovascular space involvement, high mitotic index, and an interval >4 years since prior pregnancy.<sup>4</sup> Thus, managing PSTT is challenging, particularly ensuring precise diagnosis to guide appropriate therapy. Our case consolidates current evidence and underscores the importance of revisiting the initial diagnosis to offer accurate management. Thorough counselling and judicious refinement of diagnostic modalities are paramount.

### CASE PRESENTATION

#### Background Clinical Presentation

A 43-year-old woman with no known medical illnesses and a history of three childbirths (the last one occurring eight

This article was accepted: 25 December 2025

Corresponding Author: Pei Yoke Wang

Email: wpy713@yahoo.com

months ago via spontaneous vaginal delivery) presented for evaluation. She had a healthy baby boy without any complications during her antenatal, intrapartum, or postpartum periods. She was doing well until she started taking a hormonal contraceptive pill 40 days after giving birth. Following this, she began to experience irregular bleeding despite adhering to her contraceptive schedule. Consequently, she was assessed at an outpatient gynecology clinic for possible abnormal uterine bleeding (AUB) and expressed interest in exploring other contraceptive methods. Her bleeding pattern had been erratic for the past six months, but she reported no constitutional symptoms or changes in bowel habits. She denied experiencing any symptoms of anemia, such as lethargy or palpitations. A basic assessment confirmed that she was not anemic, with a clinical hemoglobin level between 11-12 g/dL. Her abdomen was soft and non-tender. A speculum examination revealed blood but showed a normal cervical contour with no polyps or abnormal growths. A pelvic examination yielded normal findings: the uterus was non-tender and non-palpable, and both adnexa appeared unremarkable.

A bedside transvaginal ultrasound (USG) was performed, revealing a 5.0 x 4.8 cm heterogeneously echogenic, highly vascular mass occupying the uterine cavity. The uterus was noted to be bulky, and a right hemorrhagic cyst measuring less than 4 cm was observed. The left ovary was of normal size, and no free fluid or adnexal mass was documented during the initial scan. Suspecting retained products of conception (POC), serum  $\beta$ -hCG concentrations were checked and found to be elevated at approximately 140 mIU/mL. Further imaging with pelvic Magnetic Resonance Imaging (MRI) was conducted, which when compared with the previous pelvic ultrasound, suggested a uterine arteriovenous malformation (AVM) with intrauterine bleeding/ hematoma of variable ages despite the elevated baseline levels of beta-hCG (Figure 1). She subsequently underwent uterine embolization for the AVM without any complications. A follow-up schedule was established, including ongoing monitoring of beta-hCG levels, which initially showed a declining trend, along with normal gynecological findings on bedside USG scanning. After six months, she was deemed well and discharged for community clinic follow-up as per local protocol.

Unfortunately, three months later, she experienced five weeks of amenorrhea despite consistent use of hormonal contraceptives. Suspecting a possible pregnancy, she sought medical attention and presented with findings similar to those of her previous AVM. Imaging revealed a uterine mass located within the endometrium, measuring 3.7 x 3.6 cm, with evidence of vascularity found in both the anterior and posterior myometrium (Figure 2). Her beta-hCG level was measured at 6464 mIU/mL during her initial diagnosis. A comprehensive imaging workup, including a computed tomography scan of the thorax, abdomen, and pelvis, was offered, which revealed findings similar to those in the recent USG result with no evidences of possible metastasis. A comparison of CT scan findings was reviewed. Otherwise, her beta-hCG levels remained elevated, fluctuating between 6204 and 6464 mIU/L. The trend of beta hCG level were summarized (Table I). She was counselled regarding

definitive management, and a potential recurrence of the AVM was discussed. The risks of bleeding from a possibly aggressive AVM within one year of embolization, along with the necessity for histopathological evaluation due to her high beta-hCG levels, were communicated before surgical intervention, which she agreed to. As planned, she underwent an elective total abdominal hysterectomy with bilateral salpingectomy and right ovarian cystectomy. Intraoperatively, we examined both ovaries and found them to be clinically normal. Thus, we opted for the decision to preserve them, given her age, to prevent the risk of surgical menopause. Otherwise, the operation was uneventful, with minimal blood loss and no intraoperative or postoperative complications occurring.

#### Diagnostic Evaluation Following Operative Intervention

The anatomical assessment revealed a cross-section of the uterine wall from the cervical to the fundus, which exhibited a variegated mass; the area near the fundus was reported to be painful. Microscopic evaluation revealed infiltrative sheets of predominantly mononuclear intermediate trophoblast, along with scattered multinucleated cells that invaded the myometrium. This invasion separated the smooth muscle cells and extended from the upper to the lower uterine wall, accompanied by extensive necrosis and hemorrhage. The atypical trophoblasts displayed significant nuclear atypia, characterized by coarse chromatin and some cells possessing prominent nucleoli, along with amphophilic to eosinophilic cytoplasm. Additionally, the mitotic activity was brisk and aberrant, with 16 instances observed per 10 high-power fields (hpf). Vascular invasion was prominent, with tumor cells replacing the walls of the myometrial vessels. However, no malignant trophoblast was observed breaching the serosal layer. The malignant trophoblasts exhibited focal expression of human chorionic gonadotropin (hCG) but did not express SALL4. A focal area with normal endometrial tissue, mainly composed of tubular glands lined by stratified columnar epithelium, was noted (Figure 3). In contrast, other structures, including the cervix, both fallopian tubes, and parametrium, appeared unremarkable. The right ovarian cyst was identified as a corpus luteum. Based on the operative and histopathological examination, the final diagnosis was concluded as Placental Site Trophoblastic Tumor (PSTT), classified at least as stage I.

#### Clinical Management

Postoperatively, the patient was stable, and her beta-hCG levels were monitored in an outpatient setting. Initially, no adjuvant chemotherapy was administered. However, after two months, her beta-hCG levels began to rise, prompting the initiation of single-agent methotrexate (MTX). Following the second cycle of MTX, her beta-hCG levels became undetectable. Unfortunately, subsequent monitoring indicated an increase in beta-hCG, raising concerns about potential tumor recurrence or resistance, although she remained asymptomatic. To further investigate, a Positron Emission Tomography (PET) scan was conducted, revealing a hypodense, amebolic lesion in the left adnexa, indicative of a left ovarian cyst measuring 7.8 x 6.6 x 7.1 cm. The PET results could not definitively confirm the presence of metastatic disease; however, they did show a localized area of increased absorption of the radioactive tracer,

**Table I: The beta-hCG level trend**

Initial Diagnosis						
Date	4.8.23	14.8.23	28.8.23	13.9.23	26.9.23	10.10.23
Level	140	150.7	36.7	22	13.6	7.6
Prior Op						
Date	1.10.24	8.10.24	15.10.24	6.11.24	12.11.24	19.11.24
Level	3837.1	550.8	154.9	43.1	55.4	71.6
During MTX						
Date	29.11.24	18.12.24	5.1.25	22.1.25		
Level	124.5	15.2	4.5	4		
Prior EMA/CO						
Date	24.2.25	10.3.25	27.3.25	6.4.25		
Level	42.6	406.4	4177.7	6425.6		
During EMA/CO						
Date	10.4.25	2.5.25	21.5.25	29.5.25	13.6.25	25.6.25
Level	8080.37	3748.74	1265.31	1074.12	368.83	81.01
During EMA/CO						
Date	30.6.25	15.7.25	4.8.25	12.8.25	20.8.25	8.9.25
Level	48.46	10.32	5.25	3.42	1.32	<1.2

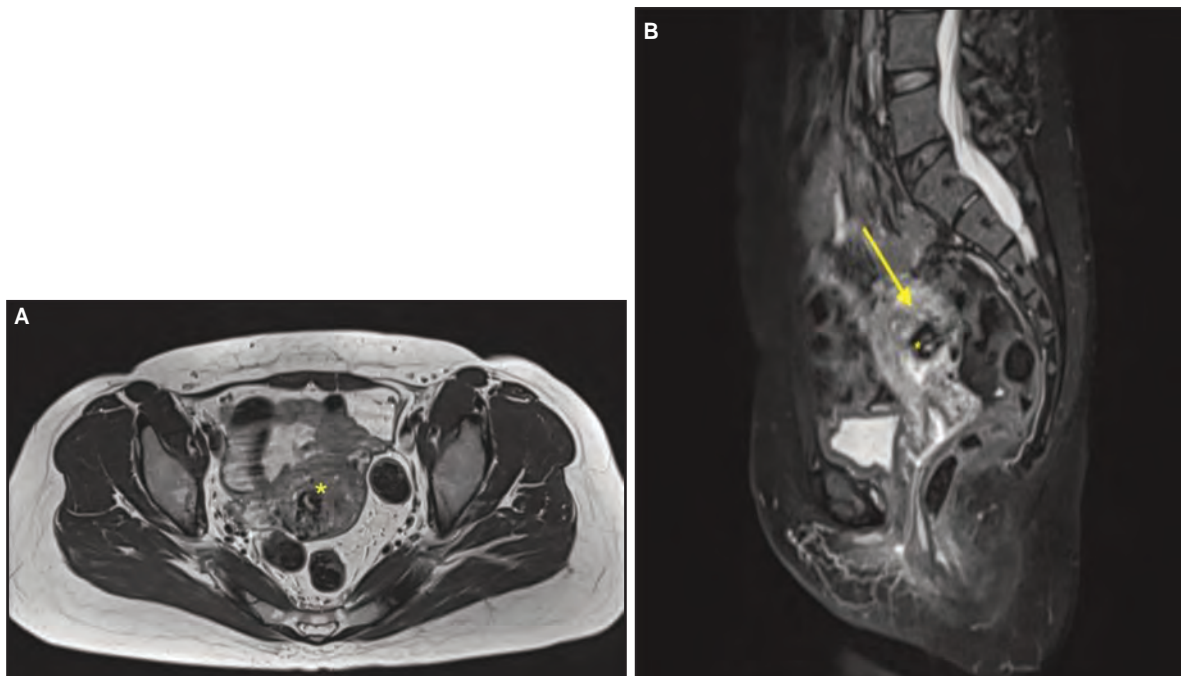


**Fig. 1:** A - T2W image show myometrium invasion by the AVM (\*)  
 B - Sagittal T2 STIR image (MRI 1.8.2023) shows signal void lesion (\*) within the myometrium of uterus (arrow) suggestive of AVM invading the posterior uterine wall myometrium.

fluorodeoxyglucose (FDG), at the left vertebral body without any evident lytic or sclerotic changes, suggesting the possibility of bone metastasis. No other locations showed abnormal FDG uptake or definitive evidence of FDG-avid metastases. Based on the PET findings, she was scheduled for an oophorectomy. However, this procedure was canceled upon preoperative assessment, which indicated no evidence of a left ovarian cyst, suggesting that it may have resolved prior to the surgical intervention. Despite this, her beta-hCG levels continued to rise from 4000 to 6000. A subsequent CT TAP confirmed the absence of an ovarian cyst or adnexal mass. However, it did identify an enhancing intraspinal lesion at L2, which could not rule out the possibility of dural metastasis. To facilitate a more informed treatment approach, a multidisciplinary team (MDT) discussion was

held, including input from an oncologist and a pathologist. The EMA/CO adjuvant chemotherapy regimen was recommended to enhance disease control. Unfortunately, the patient developed severe neutropenia sepsis with myelosuppression after completing the second cycle of chemotherapy. In the subsequent cycle, the dosage was adjusted with deduction to 15% and viscritine was omitted. Targeting this regimen proved effective, as serum beta-hCG levels became normalized after the seventh cycle and a total of nine cycles of chemotherapy were given. She has remained well during the past six months of ongoing follow-up. Throughout this period, she has remained well, tolerating the side effects of the chemotherapy regimen effectively.

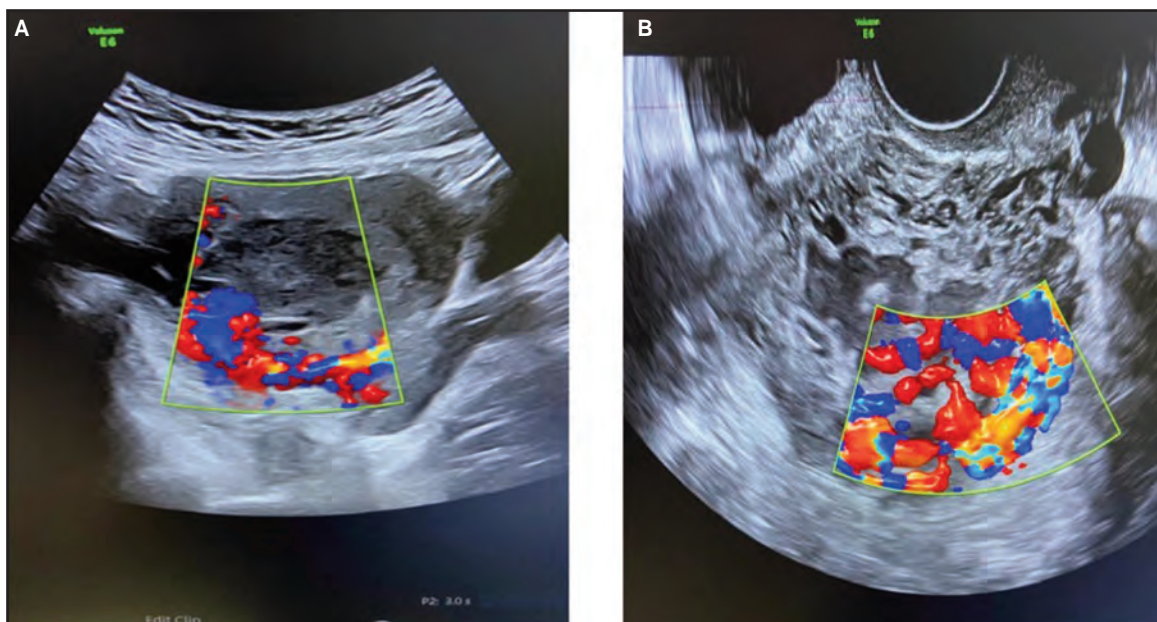


Fig. 2: A,B - The heterogeneously echogenic, highly vascular mass occupying the uterine cavity

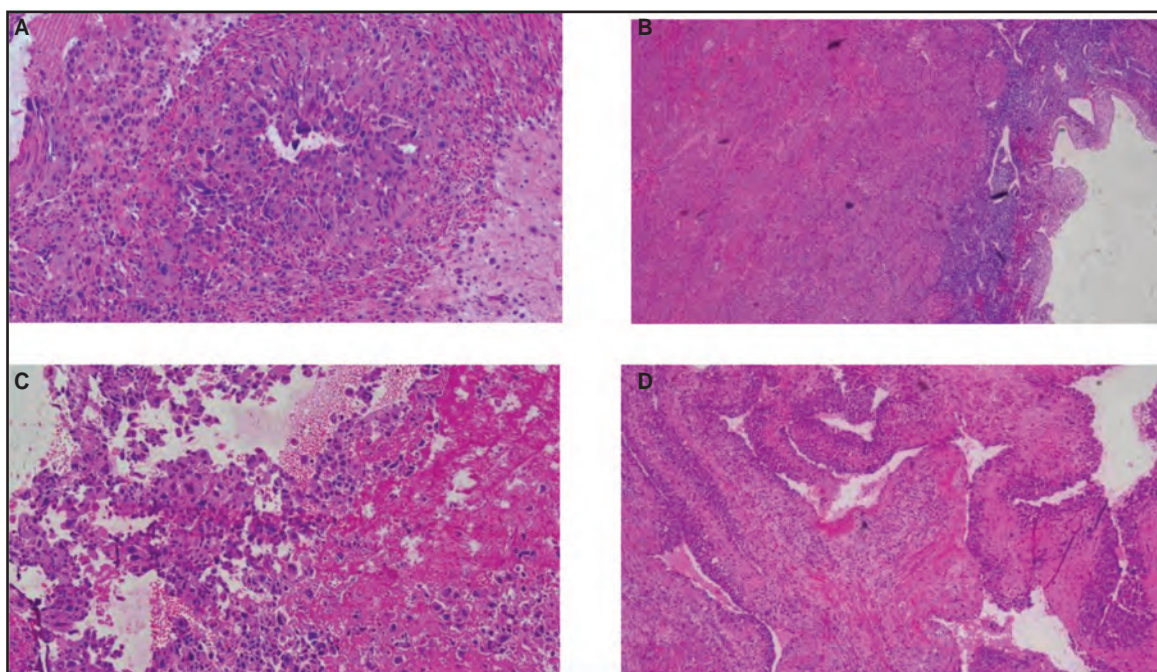


Fig. 3: A, B - Infiltrative sheets of predominantly mononuclear intermediate trophoblast, along with scattered multinucleated cells that invaded the myometrium, separated the smooth muscle cells and extended from the upper to the lower uterine wall, accompanied by extensive necrosis and haemorrhage.  
C,D - The malignant trophoblasts exhibited focal expression of hCG but did not express SALL4. A focal area with normal endometrial tissue, mainly composed of tubular glands lined by stratified columnar epithelium

### DISCUSSION

Our case highlights the potential diagnosis dilemma following the revision of AVM diagnosis to PSTT, which suggests that the low index of suspicion should be emphasized, especially in cases where beta-hCG is detected. However, it is not markedly high, ensuring that a possible PSTT diagnosis can be made in the initial stages.<sup>5</sup> Our case also underscores several diagnostic and therapeutic nuances

that distinguish PSTT from other gestational trophoblastic neoplasms. First, although the patient's six-month history of intermittent bleeding might be dismissed as abnormal uterine bleeding (AUB), the persistence of symptoms after delivery with raised  $\beta$ -hCG is considered pathological and should be explored.<sup>1,4</sup> As established, at least 70% of PSTT cases arise after an expected term delivery, and at least 15% follow abortion or miscarriage, making our patient's

antecedent event somewhat atypical.<sup>3</sup> In addition to that, her consistently low beta-hCG—a plateau around 250 mIU/mL—mirrors the tumor's modest secretory profile and highlights why biochemical surveillance alone can mislead diagnosis and management; incorporating hPL or inhibin  $\alpha$  into post pregnancy surveillance panels, where available, may improve early detection.

Thus, not surprisingly, our diagnosis is hindered, as it is based on imaging, mainly the MRI, which led to the initial diagnosis of AVM. From a radiological standpoint, Doppler ultrasonography (USG) is the primary investigative tool; however, its specificity is limited, as PSTT can resemble submucosal fibroids or arteriovenous malformations.<sup>6</sup> In contrast, MRI provides a superior assessment of myometrial depth and junctional zone disruption and is recommended whenever uterine preserving surgery is being considered or when decisions regarding adjuvant therapy depend on the depth of invasion. In our case, the MRI revealed disease adjacent to the serosa, prompting the surgical team to proceed with en bloc removal to avoid any potential tumor spill.<sup>7</sup>

A total or simple hysterectomy is the primary treatment for PSTT because they often don't respond well to chemotherapy. For localized disease, a total abdominal hysterectomy is often effective. Additionally, the choice to preserve both ovaries merits further discussion. Removing the ovaries through oophorectomy eliminates the rare possibility of hidden microscopic metastasis and any theoretical hormonal stimulus; however, estrogen and progesterone receptors are not consistently expressed in PSTT.<sup>8</sup> Furthermore, the sudden loss of ovarian function in a 43 year old can lead to a 2–3 fold increase in long term cardiovascular and osteoporotic complications.<sup>9</sup> In population based and multi institutional studies, no survival difference has been observed between ovarian preservation and oophorectomy in stage I PSTT, provided that adjuvant chemotherapy is administered when necessary.<sup>10</sup> Therefore, in our case, choosing to preserve the ovaries aligns with contemporary survivorship principles without compromising prognosis.

There is ongoing controversy regarding surgical procedures, particularly concerning lymph node assessment related to pelvic and para aortic nodal metastases, which are reported in up to ~10% of clinically localized PSTT/ETT cases. However, routine lymphadenectomy can increase operative time and morbidity without a clear survival benefit; sentinel node mapping with indocyanine green fluorescence is being evaluated and could rationalise staging while reducing routine lymphadenectomy. In our case, we opted not to perform routine lymphadenectomy based on current literature, and PET/CT showed no suspicious nodal involvement. Additionally, the patient has responded well to the EMA/CO regimen, as reported.<sup>1,7</sup>

In choosing the optimal chemotherapy, balancing outcomes and side effects is crucial. We escalated from MTX to EMA/CO based on overall diagnosis and risk factors following FIGO scoring which in her case consider high risk. She was starting with MTX to reduce toxicity but prepared to transition as  $\beta$  hCG rose. The EMA/CO's inclusion of etoposide and

cyclophosphamide targets DNA topoisomerase and alkylation pathways and achieves higher cytotoxic synergy, which may overcome resistance suggested by copy number gains in cell cycle regulators and drug efflux pumps. Nevertheless, EMA/CO entails significant short and long term toxicity—including myelosuppression, alopecia, premature ovarian insufficiency, and secondary leukaemia—necessitating informed consent and robust supportive care.<sup>2,7</sup> In our case, the patient experienced grade 4 neutropenia during cycle 2 (ANC  $<0.5 \times 10^9/L$ ), underscoring the value of vigilant monitoring, prompt G CSF, and dose adjustments such as withholding vincristine to mitigate further neutropenia.

Once a diagnosis of PSTT is confirmed, careful long term follow up is essential after completing chemotherapy. At least 25% of recurrences occur more than two years after remission, often at extra uterine sites.<sup>8</sup> In accordance with our local protocol, we implemented the FIGO endorsed surveillance plan: monthly  $\beta$  hCG for 12 months, then quarterly for four years, with annual chest radiographs and symptom triggered imaging.<sup>4</sup> Given evidence that PD L1 is expressed in roughly one third of PSTT specimens, we discussed enrolment in an immunotherapy registry should relapse occur, resources permitting.

Our case highlights a possible misdiagnosis of PSTT during the initial stages, primarily due to diagnostic challenges and limited resources. Lack of access to MRI and immunohistochemistry can delay diagnosis, and non availability of multi agent chemotherapy can defer treatment, leading to suboptimal outcomes. Establishing a local GTN network and a multidisciplinary trophoblastic disease board can improve pathways and outcomes, as demonstrated in our institution.

## CONCLUSION

As a conclusion, our case underscores the importance of vigilant clinical suspicion, image-guided staging, and histology-driven therapy in achieving a cure for PSTT. Tailored surgical conservatism—specifically, ovarian preservation—and judicious use of EMA/CO can maximize both oncologic and quality-of-life outcomes. Furthermore, ongoing research into molecularly targeted agents and immunotherapy is crucial for improving survival rates in advanced or recurrent cases.

## REFERENCES

1. Lucas R, Cunha TM, Santos FB. Placental site trophoblastic tumor: a case report and review of the literature. *J Radiol Case Rep.* 2015; 9(4): 14-22.
2. Zampacorta C, Pasciuto MP, Ferro B, Lucidi A, Maestro AS, Espinosa I, et al. Placental site trophoblastic tumor (PSTT): a case report and review of the literature. *Pathologica.* 2023; 115(2): 111-6.
3. Chaves MM, Maia T, Cunha TM, Veiga VF. Placental site trophoblastic tumour: the rarest subtype of gestational trophoblastic disease. *BMJ Case Rep.* 2020; 13(10).
4. Ngan HYS, Seckl MJ, Berkowitz RS, Xiang Y, Golfier F, Sekharan PK, et al. Diagnosis and management of gestational trophoblastic disease: 2021 update. *Int J Gynaecol Obstet.* 2021; 155 Suppl 1(Suppl 1): 86-93.

5. Horowitz NS, Goldstein DP, Berkowitz RS. Placental site trophoblastic tumors and epithelioid trophoblastic tumors: Biology, natural history, and treatment modalities. *Gynecol Oncol.* 2017; 144(1): 208-14.
6. Lin LH, Polizio R, Fushida K, Francisco RPV. Imaging in Gestational Trophoblastic Disease. *Semin Ultrasound CT MR.* 2019; 40(4): 332-49.
7. Seckl MJ, Sebire NJ, Fisher RA, Golfier F, Massuger L, Sessa C, et al. Gestational trophoblastic disease: ESMO Clinical Practice Guidelines for diagnosis, treatment and follow-up. *Ann Oncol.* 2013; 24 Suppl 6: vi39-50.
8. Lurain JR. Gestational trophoblastic disease II: classification and management of gestational trophoblastic neoplasia. *Am J Obstet Gynecol.* 2011; 204(1): 11-8.
9. Parker WH, Broder MS, Chang E, Feskanich D, Farquhar C, Liu Z, et al. Ovarian conservation at the time of hysterectomy and long-term health outcomes in the nurses' health study. *Obstet Gynecol.* 2009; 113(5): 1027-37.
10. Matsuo K, Machida H, Shoupe D, Melamed A, Muderspach LI, Roman LD, et al. Ovarian Conservation and Overall Survival in Young Women With Early-Stage Low-Grade Endometrial Cancer. *Obstet Gynecol.* 2016; 128(4): 761-70.

# A case report: Co-existence of uterine arteriovenous malformation with persistent trophoblastic disease – The diagnostic and management dilemmas

Rajkumar Chelladurai<sup>1</sup>, Kalavathy Subramaniam<sup>2</sup>

<sup>1</sup>Department of Obstetrics & Gynaecology, Hospital Tuanku Jaafar, Seremban, Negeri Sembilan, <sup>2</sup>Department of Obstetrics & Gynaecology, School of Medicine, IMU University, Seremban, Negeri Sembilan

### SUMMARY

Uterine arteriovenous malformation (UAVM) is a rare vascular anomaly characterised by abnormal connections between the uterine arteries and veins. It can be either congenital or acquired, often presenting with abnormal uterine bleeding. Persistent Trophoblastic Disease (PTD) is a form of gestational trophoblastic tumor, which is an uncommon pregnancy-related condition that can arise following a molar pregnancy or a normal pregnancy, due to retained trophoblastic tissue. Both conditions are rare and can potentially cause life-threatening hemorrhage independently. It is rare for both to coexist, and when they do, the diagnosis and management can be challenging, as exemplified in our patient.

### INTRODUCTION

Uterine Arteriovenous Malformation (UAVM) is a rare condition that can occur either congenitally or be acquired. It is described as abnormal connections that occur between the uterine arteries and veins with no intervening capillary.

Gestational Trophoblastic Disease (GTD) is a group of tumors that arise with either normal or abnormal pregnancies. It can be malignant or benign. Persistent Trophoblastic Disease (PTD) is when there is a persistent elevation of beta-human chorionic gonadotrophin ( $\beta$ -hCG) hormone after GTD, and it forms part of the condition referred to as Gestational Trophoblastic Neoplasia (GTN).<sup>1</sup> This rare condition arises after a molar pregnancy or after the loss of a pregnancy.

However, co-existence of UAVM with PTD is very rare but can be potentially life-threatening due to uncontrollable uterine bleeding that can harm the patient. This case report highlights a 35-year-old woman who was managed at Hospital Tuanku Ja'afar (HTJ) with both these conditions co-existing. The diagnosis and management of the woman were challenging but gratifying once the exact diagnosis was made. She had a spectrum of modalities for diagnosis and management that resulted in a good management outcome for her.

### CASE PRESENTATION

A 35-year-old woman, Para 0 + 1, was seen in the Obstetrics and Gynecology Clinic of HTJ for persistent vaginal bleeding

for about 1 month in May 2024. She is not known to have any medical problems.

She had a history of Evacuation of Retained Product of Conception (ERPOC) for incomplete miscarriage in October 2019. She had retained products of conception (POC) complicated with endometritis at that time. It was a 13-week spontaneous pregnancy loss with excessive vaginal bleeding. A transvaginal ultrasound had revealed POC within the endometrial cavity measuring 6 cm by 2.5 cm. She was pyretic at that time and was given intravenous broad-spectrum antibiotics. During the ERPOC procedure, she had bled excessively, and she was hypotensive intraoperatively. She had 4 units of packed red blood cells (RBCs) transfused during this admission and was discharged home well on the 4th day after the procedure when she was hemodynamically stable.

She did not conceive after that until May 2024, when she noted that her urine pregnancy test was positive. However, she was having lower abdominal pricking pain with irregular vaginal bleeding at that time. The General Practitioner who saw her did a transvaginal scan that revealed an intrauterine gestational sac that was irregular with no embryo seen. She was referred to HTJ for a missed miscarriage for further management.

The transvaginal scan showed an irregular intrauterine gestational sac with a  $\beta$ -hCG level of 398,322 mIU/ml. A diagnosis of partial mole was made. She had ERPOC with excessive blood loss. No vesicles to suggest molar pregnancy were noted at the procedure, and a repeat ultrasound post-evacuation showed an endometrial cavity that was thin and linear. The post-procedure hemoglobin was low, and she required 2 units of packed cell transfusions.

Post-procedure  $\beta$ -hCG had dropped to 39,549 mIU/ml. She was discharged home on the 3rd day after ERPOC with stable vitals and no vaginal bleeding. The transabdominal ultrasound before discharge showed mixed echogenicity within the uterine cavity measuring 1.3 cm in the mid-sagittal view.

During her review 3 weeks later in the gynecology outpatient clinic, she started to have excessive vaginal bleeding. Examination showed that she was bleeding and soaking

*This article was accepted: 27 December 2025*

*Corresponding Author: Kalavathy Subramaniam*

*Email: kalavathy@imu.edu.my; kalatsdp@yahoo.com*

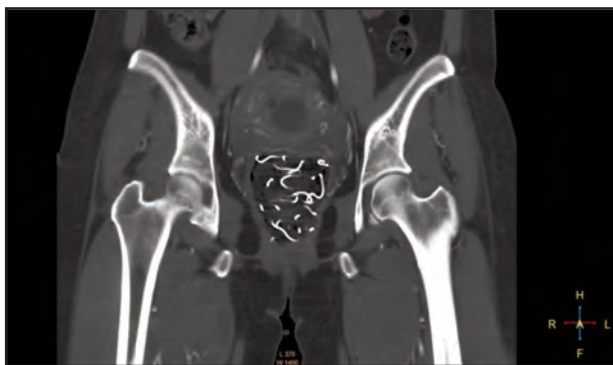


Fig. 1: CTA of the pelvis



Fig. 2: CTA of the pelvis

through her clothes and wetting the drapes. The speculum examination showed that there were about 50-100 ml of blood clots in the vaginal cavity. Transabdominal ultrasound revealed a retroverted uterus with thin endometrium. However, a homogenous mass measuring 3 cm by 1.8 cm with large tortuous vessels was noted over the anterior lower endometrial cavity extending into the myometrium. The Doppler uptake of the mass was high, with a Peak Systolic Velocity of 65 cm/s. The  $\beta$ -hCG, which had been done at the outpatient clinic two days prior, was 162,234 mIU/ml. A provisional diagnosis of Invasive Molar Pregnancy with possible UAVM was made.

She had an evacuation of the uterine cavity through a suction and curettage procedure that day under ultrasound guidance with Karmen's catheter size 6, to control her excessive vaginal bleeding. Her pre-operative hemoglobin was 8.8 gm/dL. There was minimal curetting with excessive bleeding post procedure requiring uterine massage, bimanual uterine compression, and Foley's catheter insertion with 60 ml of Normal Saline to control her uterine bleeding. She was also given intramuscular Syntometrine, intravenous Oxytocin Infusion, and intravenous Tranexamic Acid to control her bleeding. She lost about 1000ml of blood intraoperatively and required 1 unit of RBC transfusion post-procedure. The  $\beta$ -hCG post procedure was 5390 mIU/ml.

She was stable post-operatively and had an urgent Computed Tomography Angiography (CTA) of the pelvis at HTJ. The imaging revealed a rounded out-punching vascular structure at the lower anterior uterine body measuring 0.6 cm by 0.6 cm by 0.6 cm. (Figure 1 and Figure 2). This structure was most likely a UAVM. The patient was referred to Hospital Kuala Lumpur (HKL) radiology department with an available interventional radiologist for uterine artery embolization, as none were available in HTJ.

Bilateral uterine artery embolisation was done successfully at HKL. During the procedure, bilateral hypervascularity of the submucosal region of the lower uterine wall was noted. Patient recovered well post-procedure with no vaginal bleeding and was discharged home after 5 days following the procedure.

Her follow-up visits revealed that her  $\beta$ -hCG was trending downwards to 2152 mIU/ml and then to 788.5 mIU/ml. The histopathology of the endometrial curetting confirmed a

partial molar picture. However, the patient started having lower abdominal cramps with irregular vaginal bleeding, and the transvaginal ultrasound revealed a vascular lower uterine mass measuring 4.2 cm by 2.4 cm by 4.1 cm. Chest radiography was reported as unremarkable.

The International Federation of Gynecology and Obstetrics (FIGO) 2000 scoring system, was used to risk-stratify the patient. The score was 2, being positive for a history of pregnancy/miscarriage before the event, and tumor size between 3 to 5 cm.

She was started on intramuscular Methotrexate with folinic acid. She was planned for 6 chemotherapy cycles, and her  $\beta$ -hCG dropped from 214 mIU/ml to 114 mIU/ml to < 5 mIU/ml after the third cycle. The patient is still under gynecology outpatient follow-up. She is on a barrier method of contraception with no abnormal vaginal bleeding or positive transvaginal ultrasound findings. She plans for a pregnancy in 2026.

## DISCUSSION

Persistent molar tissues characterise PTD after a normal pregnancy, or molar pregnancy, or a miscarriage. It is associated with abnormal vaginal bleeding with abdominal pain, or cramps. The  $\beta$ -hCG does not return to normal levels and remains elevated. This was the scenario with the patient above, as her  $\beta$ -hCG levels were elevated even after evacuation of the uterus for partial mole.

UAVM is a rare condition, but it can be life-threatening because of uncontrollable vaginal bleeding. PTD is a more common condition found among Southeast Asians. However, for both PTD and UAVM to co-exist is even rarer. Very few case reports are available in the literature. Nandeesh and her group reported a similar case in 2022.<sup>2</sup> Their patient had uterine artery embolization after chemotherapy.

The diagnosis is complicated and challenging when there is co-existing UAVM with PTD because both share similar ultrasonic features. However, in UAVM, the PSV will be high, as seen in this patient. UAVM is a rare condition and may be congenital or acquired after uterine surgery, especially following an evacuation of the endometrial cavity. The UAVM in this patient most likely developed following her uterine evacuation in 2019. It is a potentially life-threatening

condition as patients can have profuse bleeding either spontaneously or following any uterine evacuation procedures. UAVM is best diagnosed with Color Doppler Ultrasound, where the PSV will be elevated more than 40 cm/s, as was seen in this patient. A confirmatory diagnosis can be made using CT angiography.<sup>3</sup> The diagnosis was confusing in this patient because the elevated  $\beta$ -hCG implied PTD. The patient was bleeding profusely, and to control it, evacuation of the uterus with minimal curetting was done. The intrauterine tamponade effect of the Foley's catheter controlled the bleeding.

Patients who wish to conserve the uterus can have uterine artery embolisation by an interventional radiologist. UAVM can result in heavy menstrual flow or life-threatening menstrual bleeding if untreated. Our patient had uterine artery embolisation for her UAVM. However, failures of uterine artery embolisation have been reported.<sup>4</sup>

Our patient's diagnosis was challenging as both conditions were co-existing. We proceeded with uterine artery embolization and then with chemotherapy as the  $\beta$ -hCG was persistently elevated.

#### CONCLUSION

Co-existing PTD with UAVM can be challenging to manage and diagnose. We need to have a high index of suspicion and excellent clinical acumen to diagnose the condition.<sup>5</sup> Early recognition and timely intervention were crucial in the management of this patient.

UAVM can be life-threatening due to uncontrollable bleeding.

Uterine artery embolisation is performed and recommended as a fertility-preserving measure for UAVM when expertise is available. Successful pregnancies with no increased risk for miscarriages, fetal growth restrictions or abnormal invasion of the placenta have been reported.<sup>6</sup> Single-agent chemotherapy is the accepted mode of management for low-risk PTD. A multidisciplinary approach is essential in achieving a good clinical outcome, as was seen in our patient.

#### ACKNOWLEDGEMENT

The authors would like to thank the Head of the Obstetrics & Gynaecology Department, HTJ, Negeri Sembilan, and the patient for the permission to publish this case report.

#### DECLARATION

Written consent for publication was obtained from the patient. All authors have no conflict of interest to declare. This manuscript has not received any funding.

#### REFERENCES

1. Tidy J, Seckl M, Hancock BW, on behalf of the Royal College of Obstetricians and Gynaecologists. Management of gestational trophoblastic disease. *BJOG*. 2021; 128: e1-e27.
2. Nandeeshia TD, Padmasri R. Uterine arteriovenous vascular malformation (AVM) masked by gestational trophoblastic disease (GTD): diagnostic challenge and subsequent treatment. *Int J Clin Obstet Gynaecol*. 2022; 6(4): 12-4.
3. Hashim H, Nawawi O. Uterine arteriovenous malformation. *Malay J Med Sci*. 2013; 20(2): 76-80.
4. Seo KJ, Kim J, Sohn IS, Kwon HS, Park SW, Hwang HS. Failed transarterial embolization of subserosal uterine arteriovenous malformation. *Obstet Gynecol Sci*. 2013; 56(5): 333-7.
5. Chen Y, Wang G, Xie F, Wang B, Tao G, Kong B, et al. Embolization of uterine arteriovenous malformation. *Iran J Reprod Med*. 2013; 11(2): 159-66
6. Eling R, Kent A, Robertson M. Pregnancy after uterine arteriovenous malformation-case series and literature review. *Australas J Ultrasound Med*. 2012; 15(3): 87-96.

# Optimizing care in caesarean scar pregnancy: Lesson from five cases with different management modalities

Siti Sarah Ahmad, MMed<sup>1</sup>, Sharifa Azlin Hamid, MMed<sup>1</sup>, Bavanandam Naidu, MMed<sup>1</sup>, Ismail Aliyas, MMed<sup>2</sup>

<sup>1</sup>Maternal Fetal Medicine Unit, Department of Obstetrics and Gynecology, Hospital Sultanah Bahiyah Alor Setar, Kedah,

<sup>2</sup>Gynaecology Unit, Department of Obstetrics and Gynecology, Hospital Sultanah Bahiyah Alor Setar, Kedah

## SUMMARY

Caesarean scar pregnancy (CSP) is a rare form of ectopic pregnancy that has been increasingly reported in recent years in parallel with the rising rate of caesarean section deliveries worldwide. CSP poses serious risks including uterine rupture, hemorrhage, hypovolemia, and even death if not properly diagnosed and managed. This report highlights the importance of early detection and appropriate treatment based on individual clinical presentation. We report five cases managed between November 2023 and April 2024, utilizing various approaches: systemic methotrexate, intragestational potassium chloride with multi-dose methotrexate, and surgical intervention. Despite one complication from a misdiagnosed CSP, all patients recovered without severe outcomes.

## INTRODUCTION

Caesarean Scar Pregnancy (CSP) is characterized by the implantation of trophoblastic tissue in the niche of a previous caesarean section site.<sup>2,3</sup> If untreated, CSP can progress to an abnormally invasive placenta.<sup>4</sup> The incidence of CSP ranges from 1 in 1,800 to 1 in 2,226<sup>1</sup> pregnancies and correlates with the increasing rate of caesarean sections.<sup>5</sup> The estimation cases diagnosed as CSP at our center is around 10 cases per year since 2022. Diagnosis typically involves ultrasound or magnetic resonance imaging. Optimal management of CSP should be conducted at tertiary centers with appropriate facilities and experienced professionals. Treatment options include local or systemic methotrexate (MTX)<sup>6</sup> administration or surgical interventions such as laparoscopy, hysterotomy, or hysterectomy.<sup>7,8</sup> This case series reviews five CSP cases managed at our hospital, detailing their clinical presentations, diagnostic processes, management strategies, and outcomes.

## CASE PRESENTATION

### Case Report 1:

A 32-year-old woman, gravida 4 para 3, with an uncertain conception date, presented to the Early Pregnancy Assessment Unit with a complaint of two months of amenorrhea and intermittent vaginal bleeding for the past week. Her obstetric history includes a caesarean delivery at 27 weeks' gestation four years ago due to bleeding from a low-lying placenta, which was complicated by hypovolemic shock. She also has a history of type 2 diabetes mellitus, diagnosed in 2020.

On examination, her abdomen was soft and non-tender with a well-healed Pfannenstiel scar, and her vital signs were stable. Ultrasound revealed a gestational sac measuring 35 x 21 mm, with no visible fetal pole, located at the cervico-isthmic junction at the anterior scar site. Color Doppler showed hypervascularity, and the anterior myometrium measured 3.4 mm in thickness. The diagnosis of Caesarean Scar Pregnancy (Type 1) was established, and the patient was counseled accordingly.

Conservative management with methotrexate (MTX) was chosen. Baseline blood investigations, including a full blood count, renal function tests, and liver function tests, were within normal limits. The patient's beta-human chorionic gonadotropin (hCG) level at admission was 21 mIU/mL. She received a single 50 mg dose of intravenous methotrexate. Follow-up included serial beta-hCG measurements and transvaginal scans. Her beta-hCG levels decreased to 15 mIU/mL, 8 mIU/mL, 8 mIU/mL, and 4 mIU/mL over 50 days post-treatment. A subsequent transvaginal scan showed no remaining gestational sac in the lower uterine segment. The patient remained well throughout the follow-up period.

### Case Report 2:

A 31-year-old female, gravida 3 para 1, with a history of miscarriage in 2020, presented with intermittent brownish vaginal spotting over the past month. Her obstetric history includes a caesarean delivery in 2020, followed by evacuation of retained products of conception later that year due to miscarriage. She also has a history of perimembranous ventricular septal defect (VSD) diagnosed in childhood, surgically repaired in 1994, and is currently under cardiology follow-up.

Upon admission, the patient's vital signs were stable, and her abdomen was non-tender. The cervical os was closed, with no active vaginal bleeding observed. Her beta-human chorionic gonadotropin (hCG) level was 52,530 mIU/mL, and other blood investigations were normal.

Ultrasound examination revealed a gestational sac positioned above the internal os in the lower uterus, bulging anteriorly, with the anterior myometrium measuring 3.8 mm in thickness. Doppler examination showed increased vascularity around the gestational sac and anterior myometrium. A live embryo with a crown-rump length (CRL) of 3.56 cm, corresponding to ten weeks and three days of gestation, was noted. Given these findings and the patient's

This article was accepted: 10 January 2026

Corresponding Author: Siti Sarah Ahmad

Email: sarahahmad2910@gmail.com

history of prior caesarean delivery, a diagnosis of Caeserean Scar Pregnancy (CSP) was strongly suspected.

Management included a transvaginal injection of potassium chloride (KCl) for fetal reduction, followed by a multi-dose systemic methotrexate (MTX) regimen of 1 mg/kg on days 1, 3, 5, and 7, with tetrahydrofolate 0.1 mg/kg on days 2, 4, 6, and 8. Serial beta-hCG levels decreased as follows: 1,087 mIU/mL, 690.1 mIU/mL, 166.3 mIU/mL, 230.1 mIU/mL, 56.5 mIU/mL, and <2.3 mIU/mL over three months. Follow-up ultrasound showed a regressing gestational sac. The patient remained well throughout the follow-up, with no complications reported.

*Case Report 3:*

A 38-year-old woman, gravida 4 para 3, at 6 weeks' gestation, presented with intermittent vaginal spotting over the past week. Her history includes three previous caesarean deliveries, with the most recent in 2021, which was uncomplicated. Initial assessment at 6 weeks' gestation showed an empty, regular gestational sac with a subchorionic hematoma measuring 2 x 1.8 cm, and she was managed conservatively.

The patient subsequently visited the emergency department twice at 7 and 8 weeks' gestation with increased vaginal bleeding. A transvaginal ultrasound at 7 weeks revealed a live embryo with a crown-rump length (CRL) of 9.8 mm, consistent with 7 weeks' gestation. She was diagnosed with a threatened miscarriage and continued conservative management.

At 10 weeks' gestation, the patient developed abdominal pain and increased vaginal bleeding. Ultrasound showed the placenta located anteriorly at the caesarean scar site, with indistinct separation between the myometrium and placental bed. Doppler ultrasound revealed multiple lacunae and significant hypervascularization. The subchorionic hematoma had increased in size from 2 x 2 cm to 5 x 6 cm. A singleton pregnancy with a CRL corresponding to 10 weeks' gestation and fetal heart activity was observed.

Following discussions with the couple, a decision was made to proceed with surgical intervention due to the risk of uterine rupture. The patient underwent an uncomplicated total hysterectomy with bilateral salpingectomy via laparotomy. Intraoperative findings included a gravid uterus approximately 16 weeks in size, with the gestational sac implanted in the niche area, and clots from the posterior part of the sac occupying the uterine cavity up to the fundus (Figure 1).

The patient was discharged in good condition on the third postoperative day but developed a surgical site infection on the 11th postoperative day, which was managed conservatively with antibiotics and wound care. Histopathological examination confirmed the diagnosis of caesarean scar pregnancy with focal features of placenta accreta.

*Case Report 4:*

A 37-year-old woman, gravida 4 para 2, with a history of

complete miscarriage in 2014, presented to our Early Pregnancy Assessment Unit with intermittent vaginal bleeding since early pregnancy. At 11 weeks' gestation, she was diagnosed with a missed miscarriage and managed conservatively. Her obstetric history includes two previous caesarean deliveries in 2014 and 2017, both due to acute fetal distress. Additionally, she was diagnosed with overt diabetes mellitus and essential hypertension early in this pregnancy.

At 14 weeks' gestation, a follow-up assessment raised suspicion of Caeserean Scar Pregnancy (CSP) when ultrasound revealed an irregular gestational sac measuring 6 x 4 cm, containing a fetal pole but no fetal heart activity. The sac was located in the lower part of the uterus and bulging anteriorly, with myometrial thickness measuring 5.3 mm. Doppler ultrasound indicated increased vascularity surrounding the sac. The patient's vital signs were stable, and no abdominal tenderness was noted. Her initial serum beta-human chorionic gonadotropin (hCG) level was 272 mIU/mL, with other blood parameters within normal limits.

After discussing management options, including systemic methotrexate (MTX) and surgical intervention, the patient and her husband opted for surgical management due to the patient's completed family and her inability to commit to regular follow-up. The patient underwent an uncomplicated total hysterectomy with bilateral salpingectomy via laparotomy (Figure 2).

Intraoperative findings revealed the gestational sac implanted in a niche area, embedded in the serosal layer of the uterus. The patient was discharged in good condition on the third postoperative day but later developed a surgical site infection, which required secondary suturing after antibiotic treatment. Histopathological examination confirmed caesarean scar pregnancy with early placenta accreta spectrum (increta).

*Case report 5:*

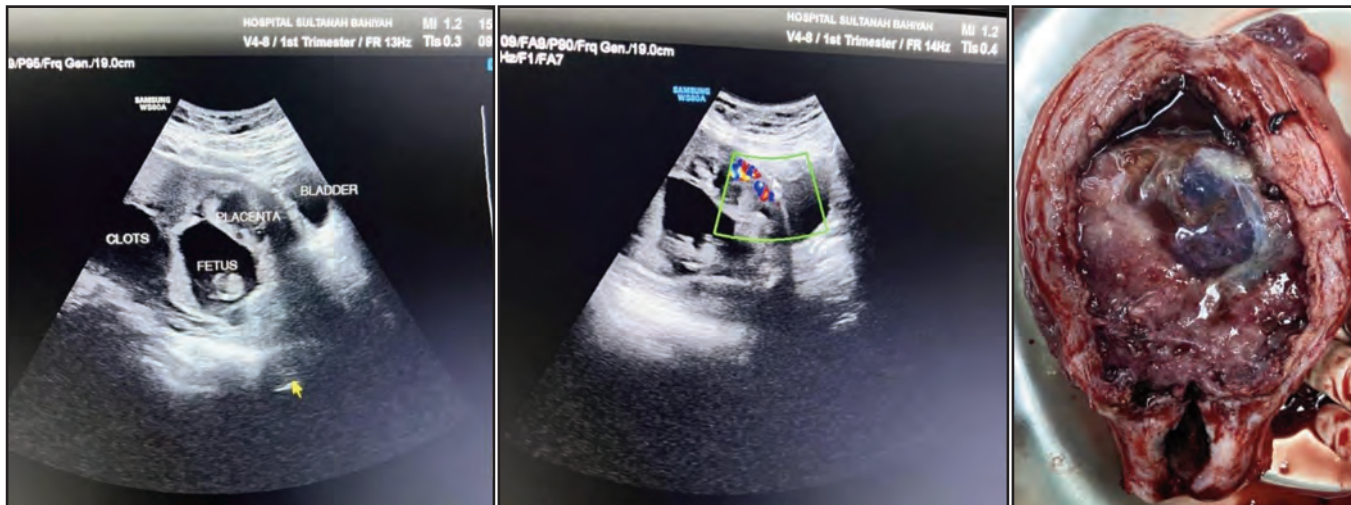
A 31-year-old woman, gravida 4 para 1+2, was referred to our center with a diagnosis of missed miscarriage at 11 weeks' gestation. She presented with three days of vaginal spotting. On physical examination, her vital signs were stable, and no abdominal tenderness was noted. Ultrasound revealed an anembryonic sac measuring 4.8 cm, confirming the diagnosis of missed miscarriage. The patient underwent evacuation of retained products of conception (ERPOC).

During the procedure, the patient experienced hypovolemic shock due to massive bleeding, likely secondary to a caesarean scar pregnancy. Intraoperative ultrasound showed a mixed echogenic collection in the lower uterus, likely blood clots, with thinning of the anterior myometrium over the scar site. The endometrial thickness was 8 mm. Despite uterotonic drugs, including oxytocin and carboprost, bleeding continued. A Foley balloon catheter was placed under ultrasound guidance for tamponade, inflated with 20 mL of sterile water, and removed 24 hours later.

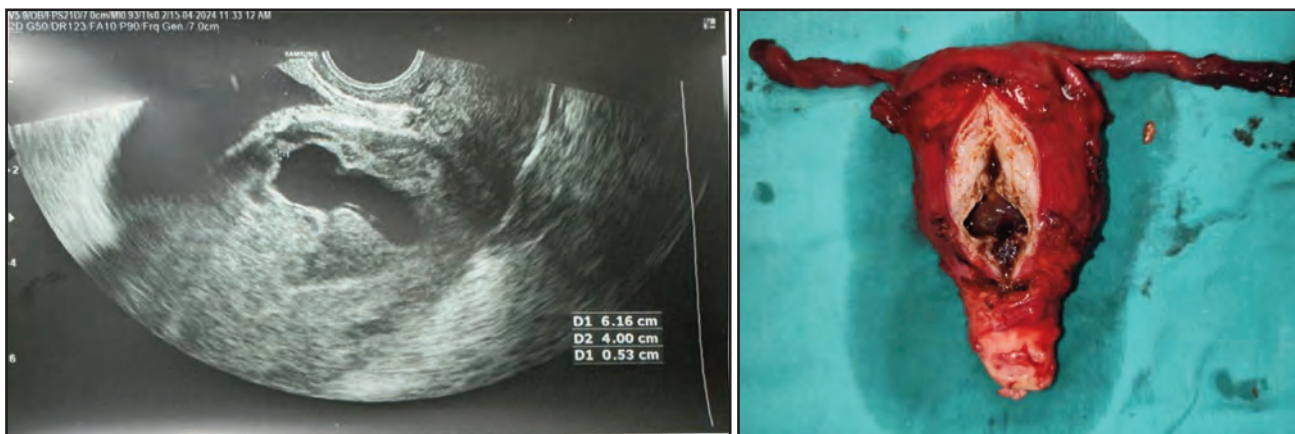
The patient's estimated blood loss was 1300 mL, and she was transfused with two units of packed red blood cells. Following the removal of the Foley balloon, no further excessive vaginal

Table I: Summary of clinical history, management and outcomes of the patients with Caesarean Scar Pregnancies

Clinical history	Patient 1	Patient 2	Patient 3	Patient 4	Patient 5
Age	32	31	38	37	31
Gravidity/parity	G4P3	G3P1+1	G4P3	G4P2+1	G4P1+2
Obstetric history	1 previous LSCS	1 previous LSCS and 1 ERPOC	3 previous LSCS	2 previous LSCS	1 previous LSCS and 1 ERPOC
Gestational age at presentation	Unsure of date	13 week	10week	14week	11week
CRL (mm)	-	68mm	42mm	16.1mm	-
Fetal heart activity	-	Present	Present	-	-
Pre treatment Bhcg	21mIU/ml	52530mIU/ml	-	272mIU/ml	36mIU/ml
Size of gestational sac (mm)	35x21mm	-	-	60x40mm	48x20mm
Management	Intravenous single dose methotrexate injection	Transvaginal potassium chloride for fetal reduction followed by systemic methotrexate injection (day 1,3,5,7)	Total abdominal hysterectomy bilateral salphingectomy	Total abdominal hysterectomy and bilateral salphingectomy	ERPOC-undiagnosed caesarean scar pregnancy, followed by single dose of intravenous
Outcome	No complication	Bhcg normalized after 3 month	Surgical site infection	Surgical site infection	Complicated with massive bleeding required balloon tamponade and blood transfusion
HPE	-	-	Consistent with caesarean scar pregnancy with features of focal placenta accreta	Consistent with caesarean scar pregnancy with early placenta accreta spectrum (increta)	Consistent with product of conception



**Fig. 1:** Ultrasound findings showed placenta located anteriorly at the caesarean scar site with indistinct separation between placenta and myometrium. Doppler ultrasound showed hypervascularization with presence of lacunae. Gross specimen revealed gestational sac implanted in the niche area with clots from posterior part of gestational sac occupying the uterine cavity



**Fig. 2:** Ultrasound findings noted irregular gestational sac located in the lower part of the uterus and bulging anteriorly with myometrial thickness of 5.3mm. Gross specimen showed gestational sac implanted in the niche area embedded in the serial layer of uterus

bleeding was observed. The patient received a single dose of methotrexate (50 mg) prior to discharge and was treated with broad-spectrum antibiotics. She was discharged in good condition on postoperative day 7. Follow-up showed normalization of beta-hCG levels and no additional complications with no significant abnormalities on ultrasound.

**DISCUSSION**

The diagnosis of Caesarean Scar Pregnancy (CSP) presents significant challenges, and its outcomes are highly dependent on both accurate diagnosis and appropriate management. CSP symptoms, are usually not specific<sup>2</sup> and often overlap with those of normal pregnancy or other gynecological conditions, contribute to the complexity of diagnosis. Common clinical findings is vaginal bleeding, low abdominal pain alone or combined with vaginal bleeding and however approximately one third of cases are asymptomatic.<sup>2</sup> Therefore, early detection and prompt intervention are critical to managing this condition effectively.

Imaging modalities, particularly ultrasound and magnetic resonance imaging (MRI), are indispensable in diagnosing CSP. First trimester transvaginal ultrasound plays an essential role in early diagnosis of CSP.<sup>8</sup> It is an optimal modality for evaluation of suspected CSP as it provides the highest image resolution.<sup>9</sup> The diagnostic ultrasound features of CSP include an empty uterine cavity and cervix with a normal endometrium and endocervical canal, alongside a gestational sac possibly containing an embryo or yolk sac positioned in the anterior part of the lower uterine segment at the site of the caesarean scar. A key characteristic is the presence of a thin or absent myometrial layer between the bladder wall and the gestational sac.

The primary management goals in CSP are to prevent life-threatening complications while preserving fertility whenever possible. However, the absence of standardized guidelines and limited evidence-based recommendations make treatment selection challenging. The management of CSP requires a personalized approach, considering factors such as clinical presentation, gestational age, grading of CSP, fetal viability, and the patient’s preferences.<sup>9</sup>

For stable, young patients wishing to preserve fertility, medical management with methotrexate (MTX) is often the preferred option. It can be given intramuscularly, intravenously, orally or locally under image guidance.<sup>8</sup> It is crucial to inform patients about all available alternatives, including their potential benefits, risks, and failure rates. Unlike established protocols for tubal pregnancies, there are no definitive guidelines for MTX use in CSP.<sup>10</sup> MTX may be administered as a single dose of 50 mg/m<sup>2</sup> body surface area (BSA) or through a multidose regimen—MTX 1 mg/kg on days 1, 3, 5, and 7, with tetrahydrofolate 0.1 mg/kg on days 2, 4, 6, and 8. Follow-up typically involves weekly serum beta-hCG measurements for three consecutive weeks, followed by bimonthly monitoring until levels are undetectable. In cases where medical treatment fails, surgical intervention becomes necessary.

Surgical treatment is the only choice when life threatening complication arise<sup>8</sup> and options include hysteroscopic resection, CSP excision with scar reconstruction, hysterotomy via laparoscopy or laparotomy, and hysterectomy. The choice of surgical method should be based on the surgeon's expertise and the patient's preferences.

In our case series, patients 1 and 2, both younger and stable, opted for medical management to preserve their fertility. MTX has been shown to be effective at a dose of 50mg/m<sup>2</sup> when beta-hCG level is less than 5000mIU/ml.<sup>8</sup> Single dose of MTX showed to be effective in a case no 1 as the pre treatment beta hCG was 21mIU/ml with no fetal cardiac activity. In a case with presence of fetal cardiac activity treatment with multi dose MTX therapy with intramniotic or intrafetal injection of potassium chloride have been propose by Gonzalez et al.<sup>8</sup> For a case 3, who presented with persistent symptoms such as abdominal pain and vaginal bleeding, required surgical management. Patient 4 also chose surgical intervention due to her inability to comply with the stringent follow-up required for medical therapy. Notably, patient 5, misdiagnosed with CSP and subsequently undergoing dilation and curettage, experienced severe hemorrhage, necessitating an additional procedure involving a Foley balloon catheter to control the bleeding. This case underscores the critical importance of accurate CSP diagnosis in determining appropriate management strategies and anticipating potential complications.

The conclusions drawn from this report are limited by the small number of cases. Larger, multi center studies are therefore warranted to better evaluate management strategies and outcomes, which may facilitate the development of national practice guidelines and standardized clinical algorithms for the management of caesarean scar pregnancies.

## CONCLUSION

Caesarean Scar Pregnancy (CSP) is a potentially life-threatening condition if left untreated. Early termination of pregnancy during the first trimester is generally recommended to mitigate risks. Our case series underscores the importance of early CSP detection and highlights the need for individualized treatment strategies based on the specific clinical circumstances of each patient. Accurate diagnosis and tailored management are essential to improving outcomes and minimizing complications in CSP cases.

## ACKNOWLEDGMENT

We are very grateful to the patients who involved in this study for their written informed consent to publish this case report.

## DECLARATION

The authors declare no conflicts of interest.

## REFERENCES

1. Seow KM, Huang LW, Lin YH, Lin MY, Tsai YL, Hwang JL. Caesarean scar pregnancy: issues in management. *Ultrasound Obstet Gynecol* 2004; 23(3): 247-53.
2. Gonzalez N, Tulandi T. Caesarean scar pregnancy: a systematic review. *J Minim Invasive Gynecol* 2017; 24(5): 731-8.
3. Royal College of Obstetricians and Gynaecologists. Diagnosis and management of ectopic pregnancy: Green-top Guideline No. 21. *BJOG* 2016; 123(13): e15-55.
4. Timor-Tritsch IE, Monteagudo A, Cali G, Palacios-Jaraquemada JM, Maymon R, Arslan AA, et al. Cesarean scar pregnancy and early placenta accreta share common histology. *Ultrasound Obstet Gynecol* 2014; 43(4): 383-95.
5. Betran AP, Ye J, Moller AB, Souza JP, Zhang J. Trends and projections of caesarean section rates: global and regional estimates. *BMJ Glob Health* 2021; 6(6): e005671.
6. Maymon R, Halperin R, Mendlovic S, Schneider D, Herman A. Ectopic pregnancies in a cesarean scar: review of the medical approach to an iatrogenic complication. *Hum Reprod Update* 2004; 10(6): 515-23.
7. Birch Petersen K, Hoffmann E, Rifbjerg Larsen C, Svarre Nielsen H. Cesarean scar pregnancy: a systematic review of treatment studies. *Fertil Steril* 2016; 105(4): 958-67.
8. Riaz RM, Williams TR, Craig BM, Myers DT. Cesarean scar ectopic pregnancy: imaging features, current treatment options, and clinical outcomes. *Abdom Imaging* 2015; 40(7): 2589-99.
9. Miller R, Timor-Tritsch IE, Gyamfi-Bannerman C; Society for Maternal-Fetal Medicine (SMFM). Society for Maternal-Fetal Medicine (SMFM) Consult Series #49: Cesarean scar pregnancy. *Am J Obstet Gynecol* 2020; 222(5): B2-14.
10. Cheung VY. Local methotrexate injection as the first-line treatment for cesarean scar pregnancy: review of the literature. *J Minim Invasive Gynecol* 2015; 22(5): 753-8.

# Isolated portal vein thrombosis as a rare complication of minimal change disease in nephrotic syndrome

Aini Izzati Abdullah, MD<sup>1</sup>, Hoong Heng Loh, MRCP<sup>2</sup>, Yik Shen Lim, MIntMed<sup>2</sup>, Siti Salwani Othman, DrRad<sup>3</sup>, Anim Md Shah, FRCP<sup>1</sup>

<sup>1</sup>Faculty of Medicine and Health Sciences, Universiti Putra Malaysia, <sup>2</sup>Department of Medicine, Hospital Kulim Malaysia, <sup>3</sup>Department of Radiology, Hospital Kulim Malaysia

### SUMMARY

Minimal change disease (MCD) accounts for the majority of idiopathic nephrotic syndrome, distinguished by significant proteinuria, oedema, and hypoalbuminemia. Although rare, thromboembolic complications like portal vein thrombosis (PVT) pose life-threatening risks owing to the hypercoagulable state of nephrotic syndrome. This report details a case of a 28-year-old man with histologically proven MCD who developed PVT during treatment. The patient reported symptoms of frothy urine while experiencing lower limb swelling on both sides and difficulty breathing. Both laboratory results and clinical assessments confirmed a full-blown relapsing nephrotic syndrome and hepatitis. Doppler ultrasound confirmed the presence of partial portal vein thrombosis. The combination treatment using both corticosteroids and anticoagulants led to complete remission of MCD and the resolution of PVT. This case aims to discuss the underdiagnosis of PVT as a thrombotic sequela of MCD while reviewing the best management approaches.

### INTRODUCTION

Minimal change disease (MCD) represents approximately 10-15% of idiopathic nephrotic syndrome cases in adults and is diagnosed based on the classic triad of heavy proteinuria, hypoalbuminemia and generalised oedema. While MCD appears benign on light microscopy – with negative immunofluorescence and diffuse effacement of podocyte foot processes on electron microscopy – and offers an excellent renal prognosis (>90% initial corticosteroid responses), it causes substantial morbidity from the nephrotic syndrome and its treatment regimen. Key complications include:

1. Thromboembolic complications: Venous thromboembolism is common, often as pulmonary embolism or deep vein thrombosis, with risk increasing at serum albumin <20g/L, due to losses of antithrombin III and protein C/S, plus increased procoagulant synthesis.
2. Infections: Urinary immunoglobulin G (IgG) loss increased susceptibility to encapsulated bacteria (pneumococcus, Haemophilus influenzae), spontaneous bacterial peritonitis (SBP), and cellulitis.
3. Acute kidney injury: Usually reversible, arising from prerenal factors or interstitial oedema.
4. Steroid-related morbidity: Osteoporosis, glucose intolerance, cushingoid features and psychiatric disturbances, which are particularly burdensome for the

30-50% who experience frequent relapsing or steroid dependence.

Among these, PVT is exceedingly rare and diagnostically challenging, as abdominal symptoms are often subtle and misattributed to steroid side effects or nephrotic ascites. This case report describes a patient with relapsed MCD complicated by PVT successfully treated with corticosteroids and anticoagulant therapy.

### CASE PRESENTATION

A 28-year-old man presented in June 2024 with a one-week history of frothy urine, bilateral lower limb swelling, and shortness of breath. He had a history of MCD diagnosed in 2023 via renal biopsy and had achieved complete remission in May 2024. He denied fever, haematuria, or recent infections. No history of any prior thrombotic events, liver disease, malignancy, or use of prothrombotic medications. He was a non-smoker with no family history of coagulation disorder. He was haemodynamically stable with 3+ pitting oedema in the lower extremities. Laboratory results showed severe hypoalbuminemia (8 g/L), proteinuria (protein 4+ and urine protein creatinine ratio {UPCR} 1001mg/mmol), hyperlipidaemia (total cholesterol 11.8 mmol/L), and mild impairment of renal function (creatinine 108 µmol/L). Coagulation studies were unremarkable, with an international normalized ratio of 1.02. Liver function tests were normal (ALP 79 U/L, ALT 7 U/L). Prednisolone 50mg once daily (1mg/kg/day) was initiated, and he was discharged with a one-week clinic appointment.

During his clinic review in early July 2024, he complained of progressive bilateral lower limb oedema and frothy urine, associated with abdominal distension and shortness of breath. Physical examination revealed ascites and a tender right hypochondriac region. Laboratory evaluation revealed albumin of 9 g/L, UFEME protein 3+, blood negative, a UPCR of 663.88 mg/mmol, serum creatinine of 89 µmol/L, normal liver function tests, leucocytosis (white cell count 16.8 x 10<sup>9</sup>/L) and raised CRP of 107.3 mg/L. Diagnostic peritoneal tapping yielded a transudative ascites with a serum ascites albumin gradient (SAAG) of <1.1. Both peritoneal Gram stain and AFB were negative, and cytology was benign in findings. Given the elevated infective markers, empirical intravenous ceftriaxone and metronidazole were administered for 7 days to cover for possible spontaneous bacterial peritonitis.

This article was accepted: 22 January 2026

Corresponding Author: Anim Md Shah

Email: animshah@upm.edu.my

Table I

	June 2024	Early July 2024	End July 2024	Mid August 2024	End August 2024	Oct 2024	Nov 2024	Jan 2025
Haemoglobin (12-15 g/dL)			15.7					
White cell count (x10 <sup>9</sup> /L)		16.8	14.6					
Platelet (x 10 <sup>9</sup> /L)			248					
Creatinine (62-115 μmol)	108	89		75		85	76	76
Albumin (32-48 g/L)	8	9	13	24	32	36	41	43
AST (U/L)	7		154	113	161			
ALT (U/L)		8	311	333	131	64	31	23
ALP (U/L)	79	93	274	175	114	81	76	86
Total Cholesterol (<5.2 mmol/L)	11.8		11.2				5.62	4.6
Urine PCR (mg/mmol)	1001	663.88	1021.84	256.9				5.82
R factor			4.9					
D-dimer (< 0.5 μg/mL)			7.61					
Anti-B2GP1 IgM			positive					

Table II

Re	Age (yr)	Sex	Onset	Clinical Presentation	Thrombosis location	Serum albumin (g/L)	Proteinuria	Serum cholesterol (mmol/L)	Renal biopsy
Varghese J et al <sup>6</sup>	45	M	At diagnosis	Abdominal pain, distension	Portal vein	16	24hr UP: 5.5 g/day	12.7	MCD
Kim G et al <sup>7</sup>	26	M	At relapse	Abdominal pain, nausea, vomiting, ascites	Portal vein	17	24hr UP: 25.3g/day	12.21	MCD
Our patient	28	M	At relapse	Abdominal pain, distension	Portal vein	13	25.3g/day UPCR 1021.84 mg/mmol	11.22	MCD



Fig. 1: There echogenic thrombus seen at the portosplenic confluence causing partial thrombosis of the vein

Diuresis was achieved with furosemide. Following clinical improvement with resolution of ascites and lower limb oedema, he was subsequently discharged with prednisolone 50mg once a day.

Upon his next visit at the end of July 2024, his bilateral lower limb swelling and frothy urine persisted even though he was compliant with medications. Clinically, his vitals were stable,

no ascites, but gross pitting oedema in the lower extremities were noted. Laboratory investigations (Table I) now showed deranged liver profile with R factor of 4.9 (mixed pattern), hypoalbuminemia, hyperlipidaemia, proteinuria and normal renal profile. Full blood count and coagulation profile were unremarkable while D-dimer was elevated. Hepatitis screening and autoimmune hepatitis panel were both negative. Given the abrupt-onset hepatitis with ALT

predominance and raised D-dimer, abdominal ultrasound with Doppler was performed, revealing partial main portal vein thrombosis extending to the porto-splenic confluence (Fig.1). A limited thrombophilia screen showed positive anti- $\beta$ 2GP1 IgM with negative anticardiolipin IgM/IgG and lupus anticoagulant.

The patient was started on subcutaneous enoxaparin (1mg/kg twice daily) with warfarin. In addition, high-dose prednisolone 1mg/kg/day was slowly tapered down. Follow-up in the clinic showed a significant reduction in his urine protein creatinine index - 5.89mg/mmol, and LFT showed improvement with each follow-up. Warfarin was continued for 6 months until clinical stability was confirmed. He has remained in remission without recurrence of thrombosis.

## DISCUSSION

Thromboembolic complications are noted to affect up to 25% of patients with nephrotic syndrome (NS) as it is a well-established prothrombotic condition.<sup>1</sup> MCD results in severe proteinuria with concomitant hypoalbuminemia and urinary loss of proteins, including anticoagulants such as antithrombin III and protein S, thus disturbing the coagulation equilibrium and raising the risk of thrombosis formation. Additionally, overactivity of procoagulant factors, corresponding to fibrinogen, and increased platelet activation further propels thrombus formation. This constellation of factors gives rise to a prothrombotic state, making patients susceptible to venous thromboembolism, particularly PVT.<sup>1,4</sup> In PVT, thrombus forms in the portal vein with resultant obstruction of hepatic blood flow, which may cause portal hypertension, varices or ischaemic liver damage.

Isolated PVT as a complication of nephrotic syndrome is quite rare due to the unique haemodynamic and anatomic features of the portal venous system. The MCD hypercoagulable state might predispose to thrombosis more easily in high-flow venous systems such as the renal veins where stasis and endothelial damage are more marked. Furthermore, the low flow state of the portal vein is rare and needs additional stimuli for thrombosis (e.g., endothelial damage or stasis due to cirrhosis) that are less commonly present in MCD.<sup>2,5</sup>

Few case reports described PVT in patients with MCD, and out of the cases documented, there were only two cases involving isolated portal vein thrombosis (Table II).

Since PVT can manifest in a subtle manner, clinical vigilance is warranted among patients who exhibit new-onset abdominal symptoms, ascites, deranged liver profiles, or signs of intestinal ischemia. The deranged liver enzymes could be explained by either congestive hepatitis from the ascites or ischaemic hepatitis from the vein thrombosis itself. Ultrasound with Doppler is the primary imaging modality on account of its availability and sensitivity (80-100% for ruling out PVT).<sup>8</sup> Contrast-enhanced CT or magnetic resonance imaging is more specific to determine thrombus extent, but since the earlier performed ultrasound doppler done already showed partial main portal vein thrombosis extending to the porto-splenic confluence, this was not done. Thrombophilia

testing is indicated to exclude both inherited and acquired coagulation abnormalities in young patients with no apparent trigger.

Treatment of PVT in MCD requires control of the underlying nephrotic syndrome and of the thrombus itself. Immunosuppressive therapy, such as corticosteroids, is essential to minimize hypercoagulability by reducing proteinuria and normalizing the levels of anticoagulant proteins. The preferred class of choice at an initial stage is low-molecular-weight heparin (eg enoxaparin) because of its quick onset and reversibility, followed by warfarin for maintenance. While direct oral anticoagulants (DOACs) like apixaban or edoxaban have shown some benefit in nephrotic syndrome-associated thrombosis, data on PVT remain very limited.<sup>9</sup> There are no specific guidelines in terms of optimal duration of anticoagulation, and oftentimes it is to be continued until the remission of nephrotic syndrome or thrombus, typically 3–6 months.<sup>3</sup> For this patient, warfarin was continued for up to 6 months due to complete thrombus resolution as evidenced by normalisation of liver profile and remission of MCD.

The 2021 Kidney Disease: Improving Global Outcomes (KDIGO) guidelines<sup>10</sup> recommend prophylactic anticoagulation for patients with membranous nephropathy and NS who have:

- Serum albumin <20–25 g/L
- Additional risk factors for thrombosis include:
- Proteinuria >10 g/day
  - Body mass index (BMI) >35 kg/m<sup>2</sup>
  - Genetic predisposition to VTE (e.g., factor V Leiden)
  - Prolonged immobilization
  - Recent abdominal or orthopaedic surgery
  - New York Heart Association (NYHA) Class III–IV heart failure

For other glomerular diseases such as MCD and FSGS, the decision for prophylactic anticoagulant is less clear but may be considered in the presence of severe hypoalbuminemia (<20 g/L) and additional risk factors. Using tools like the HAS-BLED score, the KDIGO guidelines highlighted the need to balance thrombotic with bleeding risk. PVT outcomes in MCD are primarily dependent on prompt diagnosis, efficient anticoagulant treatment, and strict nephrotic syndrome management. Fatal outcomes can arise from complications like bowel ischaemia or portal hypertension if timely intervention is delayed. The favourable outcome of this case (complete remission in the form of normalization of liver profile and MCD remission) supports the combined therapy. Yet, the low incidence of PVT in MCD hampers large studies and makes management mainly based on case reports and expert opinion.

## CONCLUSION

Driven by a hypercoagulable state of nephrotic syndrome, portal vein thrombosis is a rare but major complication of minimal change disease. This case highlighted the need for a high index of suspicion for thrombotic events in patients with MCD presenting with abdominal pain and raised liver enzymes. Combining anticoagulation and

immunosuppressive treatment with prompt diagnosis using ultrasonography and/or CT will produce good results. Clinicians should remain alert for thromboembolic complications in MCD and modify treatment to target the underlying disease as well as the thrombus.

#### ACKNOWLEDGEMENT

The authors would like to thank the patient for his permission to publish this case report, and the staff of Hospital Kulim for their excellent support in the care and management of this patient.

#### CONFLICT OF INTEREST

The authors declared no potential conflict of interest with respect to the case report authorship, and publication of this article. The authors received no financial support for the publication of this article.

#### REFERENCES

1. Kerlin BA, Ayoob R, Smoyer WE. Epidemiology and pathophysiology of nephrotic syndrome-associated thromboembolic disease. *Clinical Journal of the American Society of Nephrology*, 2012; 7(3): 513-520.
2. Singhal R, Brimble KS. Thromboembolic complications in the nephrotic syndrome: Pathophysiology and clinical management. *Thrombosis Research*, 2006; 118(3): 397-407.
3. Glasscock RJ. Prophylactic anticoagulation in nephrotic syndrome: A clinical conundrum. *Journal of the American Society of Nephrology*, 2007; 18(8): 2221-5.
4. Mahmoodi BK, ten Kate MK, Waanders F, Veeger NJ, Brouwer JL, Vogt L, Navis G, van der Meer J. High absolute risks and predictors of venous and arterial thromboembolic events in patients with nephrotic syndrome: results from a large retrospective cohort study. *Circulation*. 2008; 117(2): 224-30.
5. Park BS, Park S, Jin K, Choi G, Park KM, Jo KM, Kim YW. Nephrotic syndrome complicated with portal, splenic, and superior mesenteric vein thrombosis. *Kidney Res Clin Pract*. 2014; 33(3): 161-4.
6. Varghese J, Mathew A, Seethalekshmy NV, Kurian G, Unni VN. Isolated portal vein thrombosis in nephrotic syndrome. *Indian J Nephrology* 2007; 17: 26-8.
7. Kim G, Lee JY, Heo SJ, Kee YK, Han SH. Portal Vein Thrombosis in Minimal Change Disease. *Ewha Med J*. 2014; 37(2): 131-5.
8. Margini C, Berzigotti A. Portal vein thrombosis: the role of imaging in the clinical setting. *Dig Liver Dis*. 2017; 49: 113-20.
9. Obata F, Abe H, Murakami T, Ueda S, Inagaki T, Minato M, et al. Direct oral anticoagulant successfully used to treat an adult nephrotic patient complicated with portal vein thrombosis. *CEN case reports*, 2019; 8(2): 134-8.
10. Kidney Disease: Improving Global Outcomes (KDIGO) Glomerular Diseases Work Group. KDIGO 2021 Clinical Practice Guideline for the Management of Glomerular Diseases. *Kidney Int*. 2021; 100(4S): S1-S276.

# Transmastoid repair of delayed traumatic cerebrospinal fluid (CSF) leak in a paediatric patient with skull base fracture

Yuanzhi Cheah, MD<sup>1,2</sup>, Asfa Najmi Mohamad Yusof, MMED ORL-HNS<sup>1</sup>, Noor Dina Hashim, MMED ORL-HNS<sup>2</sup>, Ing Ping Tang, FRCS<sup>1,3</sup>

<sup>1</sup>Otorhinolaryngology Head & Neck Department, Sarawak General Hospital, Kuching, Sarawak, Malaysia, <sup>2</sup>Department of Otorhinolaryngology-Head and Neck Surgery, Faculty of Medicine, Universiti Kebangsaan Malaysia, Kuala Lumpur, Malaysia, <sup>3</sup>Otorhinolaryngology Head & Neck Department, Faculty of Medicine & Health Sciences, Universiti Malaysia Sarawak, Sarawak, Malaysia

### SUMMARY

Cerebrospinal fluid (CSF) leakage is one of the complications of skull base fracture. This condition carries significant morbidity and mortality. We report a case of delayed onset traumatic CSF otorrhoea in a nine-year-old boy with a history of traumatic head injury sustained five years prior. He presented with a new onset of seizure associated with fever and was admitted with a diagnosis of meningoenzephalitis. Further history revealed right ear discharge noted a day prior to the admission. Imaging studies depicted a defect on the right tegmen tympani creating a communication between the middle ear, posterior cranial fossa and external ear canal. Following resolution of acute infection, right mastoid exploration and trans-mastoid approach for tegmen tympani repair were done. The child had no further seizure episodes and recovered well.

### INTRODUCTION

CSF otorrhoea occurs when there is a discontinuity in the tegmen tympani or mastoideum accompanied by breaching of the overlying mucosa, dura and arachnoid mater.<sup>1</sup> Post-traumatic CSF otorrhoea carries a mortality rate of 8.5%.<sup>2</sup> Additionally, 8% of petrous temporal bone fracture cases are complicated by CSF leak, while 19% result in persistent hearing loss.<sup>3</sup> Fatal complications of CSF otorrhoea include persistent CSF fistulae, meningitis and encephalitis.<sup>2</sup>

### CASE PRESENTATION

A nine-year-old boy with a history of traumatic brain injury at the age of five, who achieved full neurological recovery except for reduced hearing in the right ear, presented with a three-day history of fever along with headache and vomiting. He experienced an episode of generalised tonic clonic seizure which lasted for less than five minutes prior to admission. There was no prior history of seizures, ear or nasal discharge since the trauma. On examination, the patient was alert, fully conscious and obeying command. His vitals were stable with no new onset focal neurological deficit. The patient was admitted to the paediatric ward and further investigation including blood investigation, lumbar puncture and computed tomography scan of brain were done.

The blood investigation showed raised total white cell count of  $26.24 \times 10^3/\mu\text{L}$ , predominantly neutrophilic. A plain computed tomography (CT) scan of brain demonstrated soft tissue density within the right middle ear and mastoid air cells. Based on his clinical presentation, he was treated for meningoenzephalitis with broad spectrum antibiotics and anticonvulsant. However, subsequent CSF cytology and culture results were normal.

Following the CT scan findings, further questioning revealed an episode of copious clear right ear discharge. The patient was referred to Ear, Nose and Throat (ENT) team for an expert evaluation. Otoscopic examination revealed granulation tissue within the right external auditory canal (EAC). A high-resolution computed tomography (HRCT) scan of temporal revealed a 1cm defect in the right tegmen tympani, creating a communication with the middle ear, posterior cranial fossa and external ear canal (Fig. 1).

Right mastoid exploration was performed once the infective parameters had normalised. The postauricular skin incision was made 1cm posterior to the right post-auricular sulcus and extending inferiorly slightly beyond mastoid tip to harvest sternocleidomastoid muscle and cervical fat graft. Intra-operatively, a pseudomembrane in the lateral one third of the right EAC was observed, with cholesteatoma to it eroding the proximal part of posterior EAC wall. A gush of CSF from the middle ear was observed upon removing the granulation tissue and cholesteatoma while raising the TM flap. The tympanic membrane and middle ear structures were otherwise intact.

There was a 1 cm defect over the right tegmen tympani communicating with the middle cranial fossa noted (Fig. 2). The defect with its fistula tract and the mastoid cavity were filled up by granulation tissue. Tegmen tympani defect repair was performed in multilayers; using a layer of collagen-based dura patch, followed by a layer of crashed sternocleidomastoid muscle graft, and then a layer of bone dust followed by the superior base flap. Subsequently, fibrin glue was used to fix and stabilized the layers that were placed. The mastoid cavity and the aditus were obliterated with infra-auricular fat graft fixed with the fibrin glue as

This article was accepted: 22 January 2026

Corresponding Author: Ing Ping Tang

Email: [ingptang@yahoo.com](mailto:ingptang@yahoo.com)

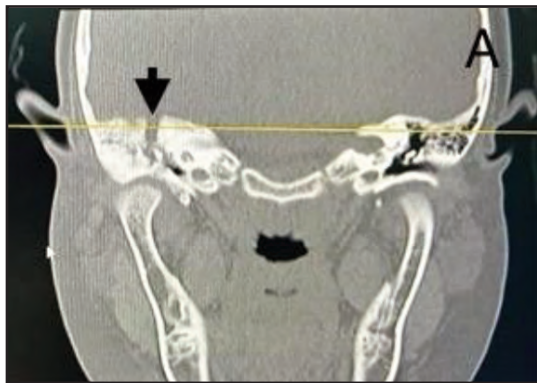


**Fig. 1:** Coronal view with the black arrow showing the defect in the right tegmen tympani creating a communication with the middle ear, posterior cranial fossa and external ear canal



**Fig. 2:** A microscopic view of cortical mastoidectomy showing at the defect of right tegmen tympani (black arrow)

mastoid obliteration. A small piece of muscle was plugged at the attic and the posterior canal defect. Tympanoplasty was performed using temporalis fascia graft as part of mastoid obliteration with middle ear reconstruction.

The middle ear and mastoid cavity were filled with the Gelfoam. Bismuth iodoform paraffin paste ribbon gauze was placed in the ear canal. Skin incision was closed interruptedly with non-absorbable suture and mastoid dressing was applied.

Post-operative recover was unremarkable. The surgical wound was clean during wound inspection on day three post-operation.

The patient was discharged on post-operative day six with a two-week course of oral antibiotics. At the next follow-up visit, the patient was remained well, with a fully healed postauricular incision and an intact tympanoplasty graft in place.

**DISCUSSION**

CSF is a clear, colourless and odourless fluid with different glucose and protein content as compared with plasma. Beta-2 transferrin assay has 100% sensitivity but it requires 2-5ml of CSF sample to achieve a higher sensitivity of 84%.<sup>4</sup> Besides, this assay is not widely available. Other laboratory test such as glucose oxidase test has poor diagnostic sensitivity and specificity and is not recommended as a diagnostic test.<sup>1,4</sup> A detail history taking is essential to alert physician the presence of CSF otorrhoea or otorhinorrhoea.<sup>1,5</sup> In this case, CSF otorrhoea was diagnosed clinically as laboratory test was not available.

The overall prevalence of petrous temporal bone fractures among the paediatric age group with skull fracture was 7%.<sup>3</sup> Petrous temporal bone fracture carries significant risk of acute and chronic complications including facial nerve palsy, hearing loss, CSF leak and neurological injuries.<sup>3</sup> The residual right ear hearing reduction is an alarming sign of high impact traumatic brain injury with petrous temporal bone fracture. A long-term follow-up for this case is essential for

early detection of the complication. Unfortunately, the patient had defaulted follow up after the trauma and represented with complicated CSF otorrhoea.

Imaging study such as HRCT aids in identifying the size and location of the osseous defect. This is an important guide for surgical planning.<sup>6</sup> In this case, HRCT temporal was done prior to the surgical planning to identify the location of the bony defect.

Majority of the traumatic CSF otorrhoea cases can be managed conservatively.<sup>1,6</sup> However, in the case of persistence CSF otorrhoea, iatrogenic, intermittent leaks, associated with skull base tumours or complicated case with meningitis, surgical intervention is the mainstay of treatment.<sup>1,6</sup> Surgical approach is based on the site and size of the osteodural defects, hearing status of the patient and the surgeon's experience.<sup>6,7,8</sup> Transmastoid approach using postauricular incision and mastoidectomy allows access to the tegmen. Study suggested less than 1cm tegmen defect without CSF leak could treat conservatively, 1-2cm tegmen defect with or without fistula or less than 1cm with CSF leak should repair through transmastoid approach, larger than 2cm defect or failed previous repair should repair through combined approach (transmastoid with minicraniotomy).<sup>6,9</sup> In this case, the tegmen mastoideum defect was 1cm with fistula and CSF leak, hence, transmastoid approach was chosen. A graft is placed through the tegmen defect in between dura and the superior edge of the tegmen. It can be reinforced with bone dust.<sup>7</sup> The choice of material for closure is based on the size of the defect and the presence of CSF leak.<sup>9</sup> Temporal fascia is used for defect less than 1cm; temporal fascia and auricular cartilage are used for defect 1 and 2cm; temporal fascia, auricular cartilage and bone from craniotomy are used for defect larger than 2cm. If CSF leak present, multilayer technique is indicated regardless the size of the defect. Fibrin glue is preferred for the adherence of the materials to the brain tissue.<sup>7,9</sup> In this case, in view of the tegmen defect was associated with CSF leak, multilayer technique was done using collagen-based dura patch, crashed sternocleidomastoid muscle graft, bone dust and superior base flap. Fibrin glue was used as the adherence material.

### CONCLUSION

Detail history and high index of suspicion are important to diagnose CSF otorrhoea in the paediatric age group. Long term follow-up for paediatric petrous bone fracture is important for early detection of the complication. HRCT is useful to demonstrate the bone anatomy and defects which facilitates in surgical planning. The approach of surgery for lateral skull base defect is based on the size of the defect and the association of CSF leak.

### ACKNOWLEDGEMENT

We would like to thank the parents of the parent for allowing us to publish this case. Our gratitude goes to Department of Otolaryngology Head and Neck Surgery, Paediatric and Radiology of Sarawak General Hospital for managing this case.

### DECLARATION

The authors declare that they are compliant with standards, no funding involved, no conflict of interest and ethical approval and informed consent are obtained.

### REFERENCES

1. Raine C. Diagnosis and management of otologic cerebrospinal fluid leak. *Otolaryngologic Clinics of North America*. 2005; 38(4): 583-95.
2. Liao KH, Wang JY, Lin HW, Lui TN, Chen KY, Yen DHT, et al. Risk of death in patients with post-traumatic cerebrospinal fluid leakage—analysis of 1773 cases. *Journal of the Chinese Medical Association*. 2016; 79(2): 58-64.
3. Leung J, Levi E. Paediatric petrous temporal bone fractures: a 5-year experience at an Australian paediatric trauma centre. *Australian Journal of Otolaryngology*. 2020; 3.
4. Mantur M, Łukaszewicz-Zajac M, Mroczko B, Kułakowska A, Ganslandt O, Kemona H, et al. Cerebrospinal fluid leakage—Reliable diagnostic methods. *Clinica Chimica Acta*. 2011; 412(11-12): 837-40.
5. Deng W, Liu J, Pang F, Zhang X. Diagnosis and management of pediatric cerebrospinal fluid leakage secondary to inner ear malformations: A report of 13 cases. *International Journal of Pediatric Otorhinolaryngology*. 2020; 135: 110049.
6. Hiremath S, Gautam A, Sasindran V, Therakathu J, Benjamin G. Cerebrospinal fluid rhinorrhea and otorrhea: A multimodality imaging approach. *Diagnostic and Interventional Imaging*. 2019; 100(1): 3-15.
7. Marchioni D, Bonali M, Alicandri-Ciufelli M, Rubini A, Pavesi G, Presutti L. Combined approach for tegmen defects repair in patients with cerebrospinal fluid otorrhea or herniations: our experience. *Journal of Neurological Surgery Part B: Skull Base*. 2014; 75(04): 279-87.
8. Sonmez S, Sahin B, Polat B, Comoglu S, Orhan KS. Repair of tegmen tympani defect presenting with spontaneous cerebrospinal fluid otorrhea using the middle cranial fossa approach. *J Int Adv Otol*. 2017; 13(3): 430-3.
9. Hernandez-Montero E, Caballero E, Garcia-Ibanez L. Surgical management of middle cranial fossa bone defects: meningoencephalic herniation and cerebrospinal fluid leaks. *Am J Otolaryngol*. 2020; 41(4): 102560.

# Rouleaux formation in acute myeloid leukemia: A morphological clue to COVID-19 co-infection

Kaveta Balasubramaniam, MBBS, Zainina Seman, MPath, Sabariah Md Noor, MPath

Department of Pathology, Faculty of Medicine and Health Sciences, Universiti Putra Malaysia, Serdang, Malaysia

## SUMMARY

**Introduction:** Acute myeloid leukaemia (AML) is a hematologic malignancy associated with significant immune dysfunction, predisposing patients to opportunistic infections, including SARS-CoV-2. While peripheral blood film evaluation mainly focuses on leukemic morphology, evolving red cell changes may provide important clues to concurrent inflammatory or infectious processes. Rouleaux formation typically reflects elevated plasma proteins or marked systemic inflammation and is rarely observed in AML patients. We describe a case of newly diagnosed AML with the unexpected emergence of rouleaux formation, later identified as a morphological marker of COVID-19 co-infection. **Materials & Methods:** Clinical, laboratory, and morphological data were collected from a 66-year-old man with newly diagnosed AML. Serial peripheral blood films, complete blood counts, inflammatory markers, and liver and renal biochemical parameters were reviewed. COVID-19 status was confirmed by RT-PCR. Morphological findings were correlated with clinical progression and laboratory indicators of systemic inflammation. **Results:** Initial blood films showed leukemic blasts without rouleaux formation. Two weeks later, the patient developed fever and tested positive for SARS-CoV-2. Repeat films demonstrated new moderate rouleaux formation (2+), coinciding with markedly elevated CRP, ESR, and ferritin levels. No alternative causes of rouleaux such as paraproteinemia or plasma cell dyscrasia were identified. The rouleaux formation appeared temporally related to the onset of COVID-19-associated inflammation. The patient's condition subsequently deteriorated with gastrointestinal bleeding and required transfer for tertiary care. **Conclusion:** The sudden appearance of rouleaux formation in AML should prompt evaluation for co-existing pathology, especially infectious or inflammatory triggers such as COVID-19. Peripheral blood film morphology remains a valuable, rapid, and accessible tool for detecting concurrent systemic processes in immunocompromised patients.

## INTRODUCTION

AML is a clonal hematopoietic malignancy characterized by the accumulation of immature myeloid blasts in the bone marrow and peripheral blood.<sup>1</sup> Due to both disease-related and therapy-induced immunosuppression, patients with AML are particularly vulnerable to opportunistic infections, including viral infections such as SARS-CoV-2.<sup>2</sup> Although peripheral blood film examination is primarily used to

evaluate leukemic morphology, it may also provide important clues to concurrent systemic infections or inflammatory states.

Rouleaux formation is a characteristic stacking of red blood cells resembling coins in a roll. It is commonly associated with elevated plasma protein levels in conditions such as multiple myeloma, chronic inflammatory diseases, autoimmune disorders, and hepatic dysfunction.<sup>3</sup> However, its appearance in AML patients, particularly in the context of acute viral infection, is unusual and may serve as a morphological indicator of co-infection or immune dysregulation. Although SARS-CoV-2 antigen and RT-PCR testing are widely available, immunocompromised patients such as those with acute myeloid leukemia may present with atypical or delayed clinical features of infection. In such settings, unexpected morphological changes on peripheral blood film may serve as an early adjunctive clue prompting further evaluation for intercurrent infection, rather than replacing standard virological testing.

## CASE PRESENTATION

A 66-year-old man with a medical history of type 2 diabetes mellitus presented with incidental findings of anemia and thrombocytopenia during routine laboratory evaluation. Initial complete blood count revealed hemoglobin 9.0 g/dL (13.5-17.5 g/dL), white blood cell counts of  $20.0 \times 10^9/L$  ( $4.0-10.0 \times 10^9/L$ ), and platelet count  $16 \times 10^9/L$  ( $150-450 \times 10^9/L$ ). Initial peripheral blood film showed 29% blasts with no obvious rouleaux formation (Figure 1). Bone marrow aspiration and biopsy demonstrated 29% myeloid blasts. Flow cytometric immunophenotyping revealed blast cells expressing myeloperoxidase (MPO), CD34, CD117, CD13, HLA-DR, CD36, CD33, and CD123, consistent with a diagnosis of AML according to WHO criteria.<sup>1</sup>

Two weeks following the initial diagnosis and prior to chemotherapy initiation, the patient developed fever (38.5°C) and progressive lethargy. A nasopharyngeal swab tested positive for SARS-CoV-2 RNA by reverse transcription polymerase chain reaction (RT-PCR). Blood cultures and a respiratory viral panel (excluding SARS-CoV-2) were negative, and there were no clinical or laboratory features suggestive of bacterial sepsis or other viral infections at the time rouleaux formation emerged. Repeat peripheral blood film (Figure 2) demonstrated an increased blast count of 68% and the new appearance of moderate rouleaux formation

This article was accepted: 25 January 2026

Corresponding Author: Sabariah Md Noor

Email: md\_sabariah@upm.edu.my

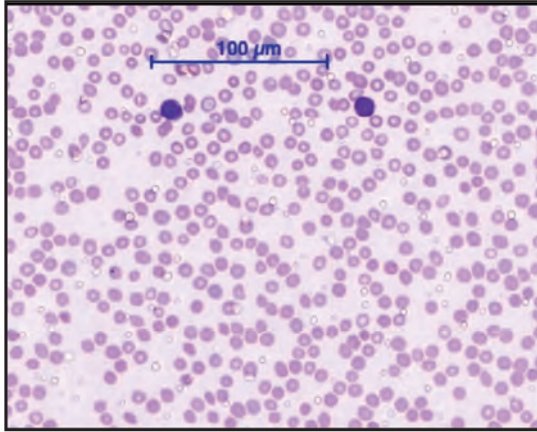


**Fig. 1:** Peripheral blood film (x40 magnification, Wright stain) at diagnosis, with two blast cells and no obvious rouleaux formation

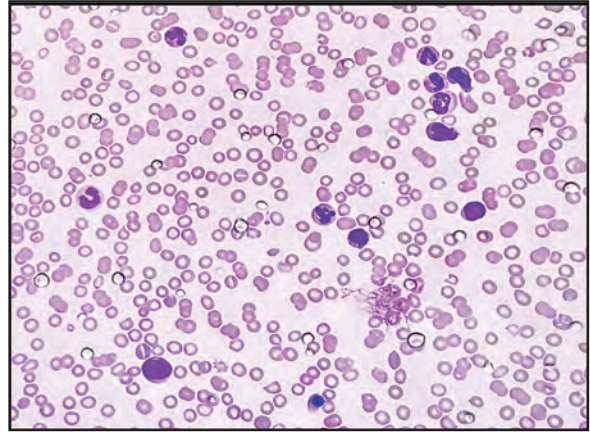


**Fig. 2:** Peripheral blood film (x40 magnification, Wright stain) after two weeks with prominent rouleaux formation (indicated by the blue arrows) and few blasts

(grade 2+), which was notably absent on initial blood films. Given that rouleaux formation is typically associated with elevated plasma protein concentrations or systemic inflammation, a comprehensive evaluation was undertaken. Inflammatory markers were significantly elevated, with C-reactive protein (CRP) at 62.5 mg/L (reference: <3.0 mg/L) and erythrocyte sedimentation rate (ESR) at 75 mm/hr (reference: <20 mm/hr), consistent with an acute phase response.

Liver function tests showed transient elevation of transaminases (ALT 89 U/L, AST 76 U/L; reference: <40 U/L) and mildly elevated bilirubin (total bilirubin 28 μmol/L; reference: <21 μmol/L). These parameters normalized over subsequent days, suggesting transient hepatic dysfunction secondary to systemic inflammatory response. Renal function, serum calcium, and urea levels remained within normal limits. Serum ferritin was markedly elevated at 569 μg/L (reference: 15-150 μg/L), reflecting both the underlying hematologic malignancy and acute inflammation.

Additional investigations excluded other causes of rouleaux formation. There was no clinical suspicion of monoclonal gammopathy, and serum protein electrophoresis was not performed given the clinical context. No recent administration of intravenous immunoglobulin or medications affecting plasma protein levels was documented. Additional microbiological investigations, including blood cultures and respiratory viral panel (excluding SARS-CoV-2), were negative.

The patient received supportive care for COVID-19 while chemotherapy was deferred pending clinical stabilization. Unfortunately, the patient's condition deteriorated rapidly, with development of hematemesis, abdominal distension, and rectal bleeding. Upper gastrointestinal endoscopy revealed portal hypertensive gastropathy with esophageal varices. The patient was transferred to a tertiary care facility for further management; however, follow-up data was not available due to transfer of care.

**DISCUSSION**

Rouleaux formation results from decreased erythrocyte surface charge (zeta potential), typically triggered by elevated fibrinogen or immunoglobulins that bridge adjacent red blood cells.<sup>3</sup> In our patient, rouleaux was absent on initial examination but appeared prominently during acute SARS-CoV-2 infection, suggesting an acquired inflammatory process.

COVID-19 is associated with intense systemic inflammation, characterized by marked increases in fibrinogen and other acute-phase proteins, endothelial activation, and cytokine release-conditions that create a biochemical environment conducive to rouleaux formation.<sup>4,5</sup> Alterations in red cell morphology, deformability, and aggregation have been well-documented in COVID-19 patients, particularly those with elevated inflammatory markers or severe disease.<sup>4</sup> In this case, the emergence of moderate rouleaux formation coincided temporally with confirmed SARS-CoV-2 infection and markedly elevated CRP, ESR, and ferritin levels, supporting an inflammatory etiology.

While rouleaux formation has been reported in rare AML-associated contexts such as reactive plasmacytosis, concurrent plasma cell disorders, or marked paraproteinemia, these conditions were not identified in our patient. Importantly, rouleaux was not observed on the initial peripheral blood film at diagnosis and only appeared following the onset of COVID-19 infection. This temporal relationship, together with the exclusion of alternative causes including paraproteinemia, immune-mediated hemolysis, and other documented infections, supports the interpretation that rouleaux formation in this case was more likely related to COVID-19-associated systemic inflammation rather than the underlying leukemia itself.

The management of AML patients with concurrent COVID-19 presents significant clinical challenges. Large registry studies, including data from the EPICOVIDEHA (European Hematology Association COVID-19 and Hematology) database, report high mortality rates among AML patients with concurrent COVID-19. Importantly, delaying chemotherapy during active COVID-19 infection, when

clinically feasible, has been associated with improved survival compared to continuing intensive treatment during active infection.<sup>6</sup> In this context, early recognition of intercurrent infection is critical for patient management.

Although rouleaux formation is a non-specific morphological finding, its sudden appearance in immunocompromised patients may serve as an adjunctive clue to underlying systemic inflammation. In the specific context of COVID-19-associated inflammation, elevated fibrinogen and acute-phase reactants may promote red blood cell aggregation; however, outside this setting, rouleaux formation and its semi-quantitative grading do not reliably correlate with fibrinogen levels or overall inflammatory severity. Therefore, interpretation of rouleaux formation should always be made in conjunction with clinical findings and laboratory markers rather than as a standalone indicator.

Reports describing rouleaux formation in AML patients remain scarce and are largely confined to settings of reactive plasmacytosis, plasma cell dyscrasia, or concurrent inflammatory or autoimmune conditions. Sharma et al. described a case of AML with marked reactive plasmacytosis and prominent rouleaux formation, attributed to elevated serum globulins rather than clonal plasma cell disease.<sup>7</sup> Other reports involving AML occurring alongside plasma cell disorders or therapy-related leukemias have similarly emphasized the importance of distinguishing reactive causes of rouleaux formation from primary hematologic pathology.<sup>8,9</sup> These limited reports reinforce the concept that rouleaux formation in AML typically reflects an accompanying systemic or inflammatory process.

This report is limited by its nature as a single case study, and a causal relationship between SARS-CoV-2 infection and rouleaux formation cannot be definitively established. Nevertheless, the clear temporal association, accompanying inflammatory markers, and exclusion of alternative etiologies support a probable link between COVID-19-associated inflammation and the observed morphological change. This case highlights the continued relevance of peripheral blood film examination as a rapid, accessible adjunct in the holistic assessment of immunocompromised patients.

## CONCLUSION

The unexpected appearance of rouleaux formation in patients with AML should prompt evaluation for co-existing pathology, particularly infectious complications. In the context of COVID-19-associated systemic inflammation, this morphological finding may reflect an acute inflammatory response rather than primary leukemia-related pathology. Serial blood film examination remains a valuable adjunctive tool that can provide insights beyond leukemic morphology, when interpreted alongside clinical findings and laboratory markers of inflammation.

## CONFLICT OF INTEREST

The authors declare no competing interests.

## FUNDING

No funding was received for this study.

## ETHICS

Verbal consent was obtained from this patient. The patient described in this manuscript is deceased. As per ethical and publication guidelines, written consent could not be obtained. Institutional ethics approval was not required for this case report.

## REFERENCES

1. Arber DA, Orazi A, Hasserjian R, et al. The 2016 revision to the World Health Organization classification of myeloid neoplasms and acute leukemia. *Blood*. 2016; 127(20): 2391-405.
2. Wood WA, Neuberger DS, Thompson JC, et al. Outcomes of patients with hematologic malignancies and COVID-19: a report from the ASH Research Collaborative Data Hub. *Blood Adv*. 2020; 4(23): 5966-75.
3. Bain BJ, Bates I, Laffan MA, Lewis SM. *Dacie and Lewis Practical Haematology*. 12th ed. Elsevier; 2017.
4. Lippi G, Plebani M. Laboratory abnormalities in patients with COVID-2019 infection. *Clin Chem Lab Med*. 2020; 58(7): 1131-4.
5. Terpos E, Ntanasis-Stathopoulos I, Elalamy I, et al. Hematological findings and complications of COVID-19. *Am J Hematol*. 2020; 95(7): 834-47.
6. García-Suárez J, de la Cruz J, Cedillo Á, Llamas P, Duarte R, Jiménez-Yuste V, et al. COVID-19 in adult patients with acute myeloid leukemia: a report from the EPICOVIDEHA registry. *Blood Adv*. 2022; 6(5): 1520-9.
7. Sharma S, Malhan P, Pujani M, Pujani M. Auer rod-like inclusions in reactive plasmacytosis seen with acute myeloid leukemia. *J Postgrad Med*. 2009; 55(3): 197.
8. Rangan A, Arora B, Rangan P, Dadu T. Florid plasmacytosis in a case of acute myeloid leukemia: A diagnostic dilemma. *Indian J Med Paediatr Oncol*. 2010; 31(1): 36-8.
9. Rosenthal NS, Farhi DC. Reactive plasmacytosis and lymphocytosis in acute myeloid leukemia. *Hematol Pathol*. 1994; 8(1-2): 43-51

# <sup>99m</sup>Tc-Sestamibi scintigraphy to differentiate benign and malignant renal masses: A case report

Muhammad Azizul Daud, MMed<sup>1</sup>, Khadijah Abdul Hamid, MMed<sup>2</sup>, Othman Puteh, MMed<sup>1,3</sup>, Khin Thuzar Pyone, MMed.Sc<sup>1,4</sup>, Wan Fatimah Wan Sohaimi, MMed<sup>1,4</sup>

<sup>1</sup>Hospital Pakar Universiti Sains Malaysia (HPUSM), Kubang Kerian, Kelantan, <sup>2</sup>Department of Biomedical Imaging, Advance Medical and Dental Institute (AMDI), Bertam, Kepala Batas, Pulau Pinang, <sup>3</sup>Department of Radiology, School of Medical Sciences, Health Campus, Universiti Sains Malaysia (USM), Kubang Kerian, Kelantan, <sup>4</sup>Department of Nuclear Medicine, Radiotherapy & Oncology, School of Medical Sciences, Health Campus, Universiti Sains Malaysia (USM), Kubang Kerian, Kelantan

### SUMMARY

The increasing use of cross-sectional imaging has led to a rise in the incidental detection of small renal masses. However, anatomical imaging techniques often lack the ability to effectively distinguish benign from malignant renal lesions. Renal biopsy has inherent limitations, including a high non-diagnostic rate, poor negative predictive value, and associated procedural risks and costs. As a result, many benign renal tumours undergo unnecessary surgical resection due to the presumed malignancy. Technetium-99m (<sup>99m</sup>Tc) sestamibi single photon emission computed tomography/computed tomography (SPECT/CT) is a molecular imaging modality that differentiates benign oncocytomas and hybrid oncocytic/chromophobe tumours from malignant renal cell carcinomas (RCCs). This differentiation is based on variations in mitochondrial density and multidrug resistance pump expression. We present a case of a 61-year-old male who underwent <sup>99m</sup>Tc-sestamibi SPECT/CT for renal mass evaluation, demonstrating its usefulness in differentiating benign from malignant renal lesions. The lesion showed absent sestamibi uptake, raising strong suspicion for malignant RCC and prompting further diagnostic assessment. A targeted renal biopsy was subsequently performed, revealing a papillary neoplasm with transitional and glandular (mucin-producing) differentiation.

### INTRODUCTION

The widespread use of abdominal cross-sectional imaging has led to an increasing detection rate of renal masses. However, distinguishing benign from malignant renal tumours remains a clinical challenge. Conventional modalities such as contrast-enhanced computed tomography (CT) and magnetic resonance imaging (MRI) often yield indeterminate lesions.<sup>1</sup>

Among benign renal tumours, oncocytoma is the most frequently diagnosed, accounting for approximately 10% of all solid renal masses.<sup>2</sup> In contrast, RCC is significantly more common, with clear cell RCC alone comprising approximately 70–75% of malignant renal tumours.<sup>3</sup> This striking difference in prevalence highlights a key clinical

dilemma: while accurate non-invasive identification of oncocytoma is important to prevent unnecessary surgery, the probability that a solid renal mass represents RCC remains much higher, reinforcing the need for cautious interpretation of imaging findings and, when necessary, histopathological confirmation.

Renal biopsy is an established diagnostic tool, but has notable limitations, including a non-diagnostic rate of 8–14%<sup>4</sup> and less effective for small renal masses.<sup>5</sup>

Non-invasive imaging modalities such as <sup>99m</sup>Tc-sestamibi SPECT/CT have gained prominence as promising tools and has been proposed as an alternative to renal mass biopsy for distinguishing renal oncocytomas from RCCs.<sup>6</sup> This technique exploits differences in mitochondrial content and multidrug resistance pump expression between benign and malignant renal tumors.<sup>7</sup>

### CASE PRESENTATION

A 61-year-old male presented to Hospital Raja Perempuan Zainab II, Malaysia, in 2022 with lower urinary tract symptoms, fatigue, and persistent vomiting over three months. Clinical examination was unremarkable.

Imaging with ultrasound of the kidney, urinary and bladder revealed bilateral gross hydronephrosis, bilateral renal calculi, and a right lower pole lesion. CT Urography confirmed the presence of an isodense lesion at the right lower pole with calcifications (1.6 × 3.3 × 3.4 cm), suggestive of a residual renal cortex with parenchymal calcification or renal lesion. A renal MAG3 scan demonstrated mildly reduced right renal function with evidence of urinary outflow obstruction and moderate-to-severe left renal dysfunction. A CT renal 4-phase scan identified a rounded, hypodense lesion in the right lower pole (2.2 × 2.9 × 3.2 cm), with progressive enhancement in the corticomedullary and nephrogenic phases, followed by washout in the excretory phase (Figure 1).

Due to the uncertain nature of the lesion, <sup>99m</sup>Tc-sestamibi renal SPECT/CT was performed. The scan showed absence of

This article was accepted: 26 January 2026

Corresponding Author: Wan Fatimah Wan Sohaimi

Email: fatihahkk@usm.my

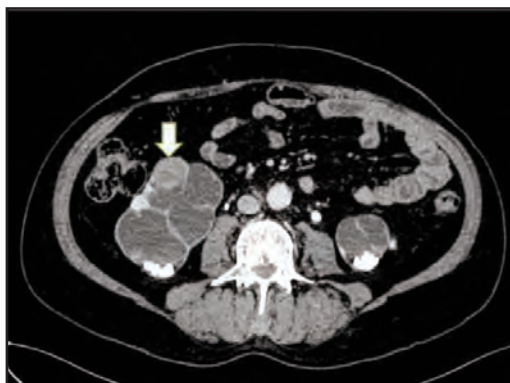


**Fig. 1:** Axial CT renal 4-phase scan showing a rounded, hypodense soft tissue lesion at right lower pole (arrow)

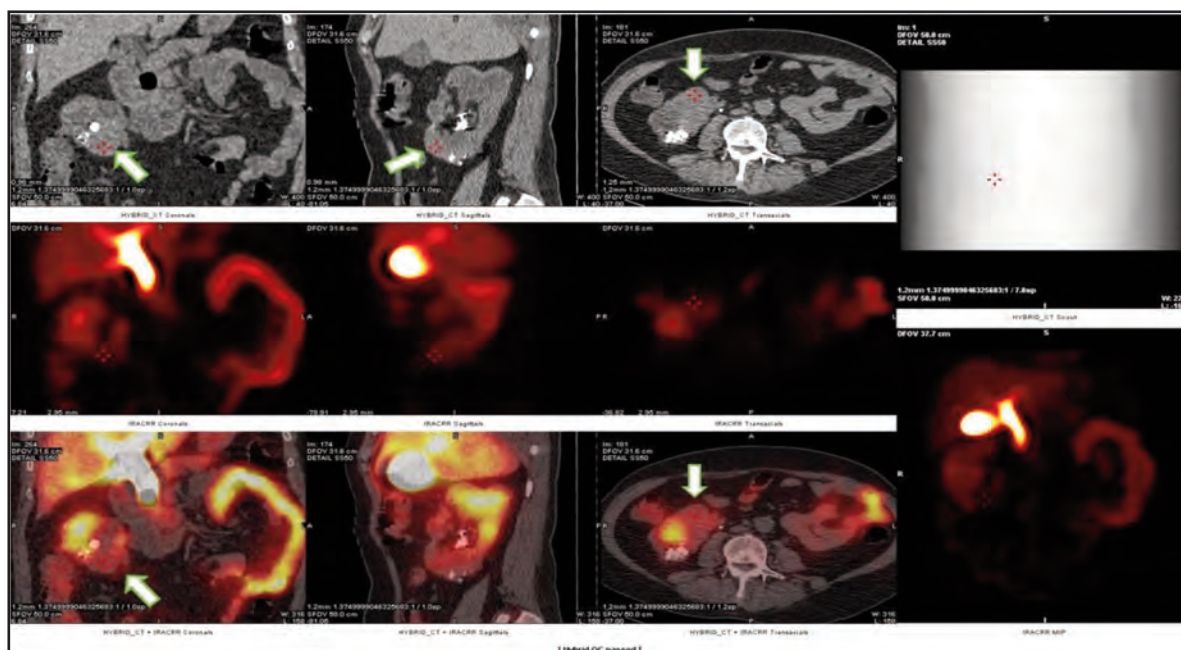


**Fig. 2:** First row: CT images; second row: SPECT images; third row: SPECT/CT fusion images. Absence of sestamibi tracer uptake is observed at the right lower pole corresponding to a soft tissue lesion

radiotracer uptake in the right lower pole, corresponding to the soft tissue lesion identified on CT, raising suspicion for RCC (Figure 2).

A repeat CT renal 4-phase scan in July 2024 demonstrated a slight increase in the size of the soft tissue lesion at the lower pole of the right kidney. Subsequently, a renal biopsy was performed in November 2024, revealing features consistent with a papillary neoplasm exhibiting transitional and glandular (mucin-producing) differentiation. However, the biopsy was superficial and inadequate for comprehensive assessment. The patient was advised to undergo surgery but declined the recommendation and default subsequent follow-up.

**DISCUSSION**

This case highlights the clinical utility of <sup>99m</sup>Tc-sestamibi SPECT/CT in renal mass characterization. Contrast-enhanced CT remains the first-line imaging modality for characterising

renal masses; however, its ability to differentiate benign oncocytomas from malignant RCC is limited. Published studies report only modest performance, with sensitivity ranging from 60–70%, specificity from 55–75%, and overall diagnostic accuracy of approximately 63–70%.<sup>8,9</sup> Although MRI offers superior soft-tissue contrast compared to CT, conventional MRI sequences still perform suboptimal in distinguishing benign oncocytomas from RCC. Reported diagnostic metrics remain modest, with sensitivity ranging from 65–80%, specificity from 60–85%, and overall diagnostic accuracy of approximately 70–78%.<sup>9,10</sup> Similarly, FDG PET/CT demonstrates limited sensitivity for differentiating benign oncocytic tumours from malignant RCC because both can show low or variable uptake, resulting in modest overall accuracy.<sup>11</sup>

In contrast, <sup>99m</sup>Tc-sestamibi SPECT/CT has emerged as a promising adjunctive modality due to the differential uptake of sestamibi between oncocytomas and RCCs is attributed to variations in mitochondrial density and multidrug-resistant

(MDR) pump expression. Oncocytomas are composed of cells with abundant mitochondria, leading to high  $^{99m}\text{Tc}$ -sestamibi retention. Conversely, RCCs exhibit reduced mitochondrial content and overexpression of MDR transporters, leading to low radiotracer uptake.<sup>7</sup> This phenomenon enables  $^{99m}\text{Tc}$ -sestamibi SPECT/CT to differentiate benign from malignant renal masses, offering a non-invasive alternative to renal biopsy in selected cases.

Systematic review and meta-analyses by Wilson et al.<sup>12,13</sup> and Rowe et al.<sup>13</sup> report that  $^{99m}\text{Tc}$ -sestamibi SPECT/CT offers high diagnostic performance, with sensitivity ranging from 92–95% and specificity from 88–91% in differentiating benign oncocytic tumors from malignant RCC. And study by Sistani et al.<sup>14</sup> suggested that this imaging technique could reduce unnecessary nephrectomies in patients with benign renal tumors.

While this approach holds promise, some limitations exist. False-positive uptake can be seen in chromophobe RCC and hybrid oncocytic/chromophobe tumors, which may share high mitochondrial density similar to oncocytomas.<sup>15</sup> Conversely, false-negative findings may arise in oncocytomas with central fibrosis or necrosis, small lesions affected by partial-volume effects or tumors with high multidrug-resistance expression which reduce sestamibi retention.<sup>13</sup> Technical factors such as motion artefacts and limited sensitivity for cystic or predominantly necrotic lesions can further compromise accuracy. Therefore, while sestamibi SPECT/CT is a valuable adjunct for renal mass characterization, results must be interpreted cautiously in the presence of these biological and technical pitfalls. Furthermore, the limited availability of  $^{99m}\text{Tc}$ -sestamibi SPECT/CT in routine clinical practice remains a barrier.

Despite these challenges,  $^{99m}\text{Tc}$ -sestamibi SPECT/CT represents a valuable diagnostic tool for risk stratification of renal masses, reducing the reliance on invasive biopsy procedures.

## CONCLUSION

$^{99m}\text{Tc}$ -sestamibi SPECT/CT has emerged as a valuable imaging tool for distinguishing benign oncocytomas from malignant RCC, helping to overcome the diagnostic limitations of conventional imaging and, in some cases, renal biopsy. This case highlights the potential of  $^{99m}\text{Tc}$ -sestamibi SPECT/CT to enhance diagnostic confidence and support more informed clinical decision-making, thereby reducing the likelihood of unnecessary surgical intervention. Its use is particularly advantageous in the further evaluation of renal masses that remain indeterminate on CT or MRI.

## REFERENCES

1. Aggarwal A, Das CJ, Sharma S. Recent advances in imaging techniques of renal masses. *World J Radiol.* 2022; 14(6): 137-50.
2. Meyer AR, Allaf ME, Rowe SP, Gorin MA. The role of molecular imaging in the characterization of renal masses. Vol. 28, *Current Opinion in Urology.* Lippincott Williams and Wilkins; 2018: 159-65.
3. Capitanio U, Montorsi F. Renal cancer. In: *The Lancet.* Lancet Publishing Group; 2016: 894-906.
4. Marconi L, Dabestani S, Lam TB, Hofmann F, Stewart F, Norrie J, et al. Systematic review and meta-analysis of diagnostic accuracy of percutaneous renal tumour biopsy. Vol. 69, *European Urology.* Elsevier BV; 2016: 660-73.
5. Richard PO, Jewett MAS, Bhatt JR, Kachura JR, Evans AJ, Zlotta AR, et al. Renal Tumor Biopsy for Small Renal Masses: A Single-center 13-year Experience. *Eur Urol.* 2015; 68(6): 1007-13.
6. Basile G, Fallara G, Verri P, Uleri A, Chiti A, Gianolli L, et al. The Role of  $^{99m}\text{Tc}$ -Sestamibi Single-photon Emission Computed Tomography/Computed Tomography in the Diagnostic Pathway for Renal Masses: A Systematic Review and Meta-analysis. Vol. 85, *European Urology.* Elsevier B.V.; 2024; 63-71.
7. Roussel E, Capitanio U, Kutikov A, Oosterwijk E, Pedrosa I, Rowe SP, et al. Novel Imaging Methods for Renal Mass Characterization: A Collaborative Review. Vol. 81, *European Urology.* Elsevier BV; 2022: 476-88.
8. Akin IB, Altay C, Güler E, Çamlıdağ İ, Harman M, Danacı M, et al. Discrimination of oncocytoma and chromophobe renal cell carcinoma using mri. *Diagnostic and Interventional Radiology.* 2019; 25(1): 5-13.
9. Baytok A, Ecer G, Balasar M, Koplay M. Computed tomography and magnetic resonance imaging characteristics of renal cell carcinoma: Differences between subtypes and clinical evaluation. Vol. 15, *Journal of Clinical Imaging Science.* Scientific Scholar; 2025.
10. Akinci O, Turkoglu F, Nalbant MO, Inci E. Differentiating renal cell carcinoma and oncocytoma with volumetric MRI histogram analysis. *North Clin Istanbul.* 2023; 10(5): 636-41.
11. Lindenberg L, Mena E, Choyke PL, Bouchelouche K. PET imaging in renal cancer. Vol. 31, *Current Opinion in Oncology.* Lippincott Williams and Wilkins; 2019: 216-21.
12. Wilson MP, Katlariwala P, Murad MH, Abele J, McInnes MDF, Low G. Diagnostic accuracy of  $^{99m}\text{Tc}$ -sestamibi SPECT/CT for detecting renal oncocytomas and other benign renal lesions: a systematic review and meta-analysis. *Abdominal Radiology.* 2020; 45(8): 2532-41.
13. Rowe SP, Gorin MA, Solnes LB, Ball MW, Choudhary A, Pierorazio PM, et al. Correlation of  $^{99m}\text{Tc}$ -sestamibi uptake in renal masses with mitochondrial content and multi-drug resistance pump expression. *EJNMMI Res.* 2017; 7.
14. Sistani G, Bjazevic J, Kassam Z, Romsa J, Pautler S. The value of  $^{99m}\text{Tc}$ -sestamibi single-photon emission computed tomography-computed tomography in the evaluation and risk stratification of renal masses. *Canadian Urological Association Journal.* 2020; 15(6).
15. Campbell SP, Tzortzakakis A, Javadi MS, Karlsson M, Solnes L, Axelsson R, et al. Pictorial review  $^{99m}\text{Tc}$ -sestamibi SPECT/CT for the characterization of renal masses: a pictorial guide [Internet]. 2018. Available from: <https://academic.oup.com/bjr/article/91/1084/20170526/7450848>

# When ulcers do not heal: Recognising behçet's disease from recurrent oral ulcers in primary care

Syed Mohd Taufiq Wan Obeng, MB BCh BAO<sup>1,2</sup>, Muhammad Naqib Ibrahim, MD<sup>1</sup>, Aznida Firzah Abdul Aziz, PhD<sup>1</sup>

<sup>1</sup>Department of Family Medicine, Faculty of Medicine, Universiti Kebangsaan Malaysia, Kuala Lumpur, <sup>2</sup>Ministry of Health, Malaysia

## SUMMARY

Oral ulcers are a common condition in primary care, usually benign and self-limiting. However, recurrent or persistent ulcers that do not respond to conventional symptomatic treatment should prompt a re-evaluation of the diagnosis and an investigation into underlying systemic disease. We present the case of a 35-year-old woman who repeatedly presented to primary care with painful, recurrent oral ulcers that substantially impaired her daily functioning. Initial investigations, including a biopsy, indicated a benign condition, so symptomatic management was pursued without achieving clinical resolution. Two years later, the development of genital ulcers prompted a diagnostic reassessment and the presence of cutaneous lesions resulting in a diagnosis of Behçet's disease. Although immunomodulatory treatment was initiated, symptom control was limited by suboptimal adherence. This case highlights the critical role of primary care in recognising mucocutaneous symptoms, maintaining diagnostic vigilance and ensuring longitudinal follow-up. Due to the multisystemic and clinically driven nature of Behçet's disease, it is essential to recognise it early and implement coordinated multidisciplinary management to reduce morbidity and optimise long-term outcomes.

## INTRODUCTION

Individuals with oral ulcers often first seek care from a general practitioner or dental practitioner. While most ulcers are benign and self-limiting, a minority may represent malignant disease. It is estimated that aphthous ulcers occur in as many as 25% of individuals worldwide.<sup>1</sup>

Recurrent aphthous stomatitis (RAS), also known as canker sores, is a common but complex oral disorder characterised by recurrent painful ulcers on non-keratinized oral mucosa. Its exact aetiology remains uncertain, presenting challenges for both patients and clinicians. Several contributing factors have been implicated, including local trauma, psychological stress, smoking cessation, anaemia, and hematinic deficiencies. Gastrointestinal disorders such as Crohn's disease, ulcerative colitis, and malabsorption syndromes (e.g., coeliac disease) have also been associated with oral aphthous ulceration and other systemic conditions such as Behçet's disease or HIV infection.<sup>2</sup>

Recurrent oral ulcers constitute one of the diagnostic criteria for Behçet's disease, first identified by the famous Turkish dermatologist Hulusi Behçet. It is a chronic inflammatory

disorder of uncertain aetiology that involves the oral mucosa, genitalia, eyes, skin, and joints. Mucocutaneous lesions are considered the hallmark feature and often represent the earliest manifestations. The occurrence of oral aphthous ulceration in conjunction with ulcerations at other anatomical sites should prompt consideration of Behçet's disease.<sup>2</sup> This case report discusses a patient with recurrent oral ulcers associated with Behçet's disease, highlighting the crucial role of multidisciplinary collaboration between primary and tertiary care in achieving optimal diagnosis and management.

## CASE PRESENTATION

A 35-year-old Malay woman, Para 2 with a known thalassemia carrier status, presented to our primary care clinic in March 2023 with a one-week history of fever, sore throat, and painful oral ulcers unresponsive to over-the-counter topical treatment. The severity of the ulcers markedly limited her oral intake, resulting in a 4-kg weight loss over several weeks, as she could only tolerate fluids and soft foods. She reported similar episodes of painful oral ulcers during her adolescence, although these had previously resolved completely within a few days. Otherwise, she had no family history of oral malignancy or autoimmune disease.

On examination, she had injected pharynx, exudative tonsillitis, and multiple aphthous ulcers over the bilateral buccal mucosa, anterior tongue, and floor of mouth. She was treated as tonsillopharyngitis with oral amoxicillin-clavulanate 625 mg twice daily for 5 days, in addition to symptomatic medications. At follow-up a week later, the ulcers showed no improvement. Given the persistence of oral ulcers beyond two weeks, she was referred to the oral and maxillofacial surgery (OMFS) team to exclude oral malignancy.

Further history by the OMFS team revealed the onset of ulcers shortly after a dental filling procedure, raising suspicion of traumatic ulcer. However, as the ulcers persisted, an incisional biopsy was performed. Histopathology demonstrated benign ulcer margins. Due to the laboratory investigations also revealed microcytic hypochromic anaemia with underlying thalassemia carrier status (normal iron study findings), the impression was revised to recurrent aphthous ulcer secondary to anaemia, and she was discharged from the OMFS service in June 2023 and to continue follow up in primary care.

This article was accepted: 6 February 2026

Corresponding Author: Aznida Firzah Abdul Aziz

Email: drznida@ppukm.ukm.edu.my



Fig. 1: Multiple aphthous ulcers over upper and lower lips and lateral tongue (Photo on 19.12.2024)

Manifestation	Definition
Recurrent oral ulceration	Observed by a physician or reported reliably by patient, recurring at least three times in one 12-month period
<b>Plus any two of the following findings:</b>	
Recurrent genital ulceration	Recurrent genital aphthous ulceration or scarring, observed by a physician or reported reliably by patient
Eye lesions	Anterior uveitis, posterior uveitis, or cells in vitreous on slit lamp examination; or retinal vasculitis observed by qualified physician (ophthalmologist)
Skin lesions	<ul style="list-style-type: none"> <li>• Erythema nodosum-like lesions, observed by a physician or reported reliably by patient;</li> <li>• Pseudofolliculitis or papulopustular lesions; or acneiform nodules observed by a physician in post adolescent patients not receiving glucocorticoids</li> </ul>
Positive pathergy test	Test interpreted as positive by a physician at 24–48 h, performed with oblique insertion of a 20-gauge needle or smaller under sterile conditions

Fig. 2: International Study Group criteria<sup>10</sup>

The patient re-presented in February 2024 with another episode of painful recurrent oral ulcers of two-week duration, again poorly responsive to topical treatment. She also reported fatigue, alopecia, and unquantified weight loss. Examination revealed multiple aphthous ulcers involving the lips, lateral tongue, and floor of mouth, ranging from 0.5 × 0.5 cm to 2 × 1 cm. Autoimmune screening was performed, showing ANA positivity (1:320) with elevated C3 and C4 (165 and 45.7mg/dL respectively). Anti-dsDNA, rheumatoid factor, and infectious disease screens were negative.

She was referred to rheumatology in March 2024, where detailed genital examination was also performed, revealing a solitary ulcer over the left labia majora (0.5 × 0.5 cm). A provisional diagnosis of Behçet’s disease was made, and she was commenced on oral colchicine 0.6 mg daily. At subsequent primary care visits over the following months, she reported recurrent painful oral ulcers interfering with eating, speaking, and her job as a teacher. Symptomatic medications were provided while awaiting rheumatology follow-up.

By July 2024, review by the rheumatology team noted clinical improvement with colchicine, but worsening upon discontinuation. Colchicine, prednisolone, and hydroxychloroquine were initiated, and further blood investigations were performed, including anti-dsDNA, anti-ENA panel, complement (C3/C4), and HLA-B51/B52. The results were negative except for anti-SSA positivity, with normal complement levels and elevated ESR and CRP (65mm/hr and 2.69mg/dl respectively).

Despite receiving treatment, her medication adherence was inconsistent, largely due to work-related constraints and concerns about the long-term side effects of the newly prescribed oral therapies. Between July and December 2024, she presented to primary care four times with recurrent ulcers and reported that her symptoms worsened during the premenstrual period. At her rheumatology review in December 2024, her ulcers were noted to improve with good adherence but recur during periods of non-compliance. A clinical diagnosis of Behçet’s disease was made with subsequent follow up also reveals presence of recurrent papulopustular lesions over left forehead, left axilla and recurrent erythema over lateral side of left ring finger nailbed.

In August 2025, at her consequent rheumatology follow-up, ongoing issues with non-adherence were noted. She had continued prednisolone but had not taken colchicine or hydroxychloroquine as prescribed. Azathioprine 50 mg daily was initiated, in addition to continuing hydroxychloroquine and prednisolone. She was referred for ophthalmology and gastroenterology assessments. Ophthalmological review, prompted by a past episode of right-eye redness (self-resolving within 4 days), showed no evidence of uveitis; meanwhile, her esophagogastroduodenoscopy and colonoscopy show no finding. At her latest rheumatology follow up in December 2025, patient has good compliance to the medication and this reflected on her marked reduction in both recurrence and the number of active oral lesions and skin lesions at any given time and better function in daily life

with marked reduction of CRP level more than 50% and normal ESR level.

## DISCUSSION

The assessment of chronic oral ulcers in primary care must begin with careful exclusion of malignancy. According to Paleri V et al. (2010), malignant oral ulcers are typically non-healing and painless, persisting for more than three weeks. They often exhibit induration with minimal surrounding inflammation and may have a rolled, thickened edge. Risk factors such as male, smoking, alcohol consumption, and older age further increase clinical suspicion. Additional red flags include a previous history of a premalignant lesion or oral squamous cell carcinoma, as well as the absence of local or systemic factors that could otherwise explain the ulceration.<sup>1</sup>

Conversely, features that reduce suspicion of malignancy include recurrent ulcers that heal between episodes, multiple or clustered ulcers, or lesions associated with systemic or autoimmune diseases. Following this, other benign or systemic conditions should be considered.<sup>1</sup>

For primary care physicians (PCPs), the decision to refer a patient with a chronic oral ulcer of more than 3 weeks of duration is guided by the lesion's clinical characteristics and the clinician's diagnostic certainty. Ulcers exhibiting features suspicious for malignancy should be referred urgently within two weeks. Whereas, cases involving isolated traumatic ulcers or recurrent aphthous ulceration can be managed within primary care, provided the diagnosis is secure. This stratified approach supports timely identification of potentially malignant disease while ensuring efficient use of specialist services.<sup>1</sup>

Behçet's disease remains a primarily clinical diagnosis as no specific laboratory test exists to confirm it. The diagnosis of Behçet's disease for this patient satisfies the International Study Group criteria (ISG) as shown in the figure below.<sup>10</sup> Investigations such as brain MRI or blood tests may aid in assessing systemic involvement or ruling out alternative diagnoses, but they are not diagnostic. While HLA-B51 positivity is linked to increased disease risk, it is not a prerequisite for diagnosis.<sup>3</sup>

The identification of genital ulcers on detailed examination during rheumatology follow-up, together with the history of ocular involvement and other skin lesions underscores the importance of thorough history taking and physical examination during earlier primary care visits. The hallmark manifestation of Behçet's disease is recurrent, painful oral ulceration, which occurs in more than 95% of patients. These ulcers are thought to arise from dysregulation of the immune system, leading to overproduction of pro-inflammatory cytokines such as tumor necrosis factor-alpha (TNF- $\alpha$ ) and interleukin-6 (IL-6). The resulting mucosal inflammation contributes to ulcer formation and persistence.<sup>3</sup>

Genital ulcers, though less common, are another characteristic feature. Their immunopathogenesis parallel that of oral ulcers, driven largely by T-cell-mediated immune

responses and cytokine-driven mucosal injury. Unlike oral ulcers, genital ulcers often heal with scarring, which can aid in clinical differentiation.<sup>3</sup> Skin lesions such as erythema nodosum-like lesions, acneiform nodules, and pseudofolliculitis may occur, driven by vasculitis and neutrophil-mediated inflammation.<sup>3</sup>

Although Behçet's disease is a chronic condition characterised by alternating periods of remission and flare, many patients can maintain a good quality of life with appropriate treatment and monitoring.<sup>7</sup> Symptomatic relief of pain and inflammation in Behçet's disease may be achieved with nonsteroidal anti-inflammatory drugs (NSAIDs).<sup>4</sup> Corticosteroids are frequently employed for their potent anti-inflammatory effects and can be administered topically, orally, or intravenously depending on the severity and site of involvement.<sup>5</sup> In more severe or treatment-resistant cases, immunosuppressive agents are indicated to control disease activity, reduce the frequency of flares, and prevent long-term complications.<sup>6</sup>

Disease activity is often pronounced in the early years following diagnosis, with a tendency to decrease in severity over time.<sup>3</sup> Adherence to therapy is crucial for disease control and quality of life in patients with Behçet's disease. Patient's role as a mother and teacher highlights the impact of recurrent flares on daily functioning and underscores the importance of consistent treatment compliance. The unpredictable nature of disease flares can contribute significantly to psychological distress, as patients often experience anxiety and uncertainty regarding the timing and severity of future exacerbations. This emotional burden may impact adherence to treatment and overall quality of life, highlighting the need for holistic management that addresses both physical and psychological aspects of care.<sup>8</sup> In addition, the chronic pain associated with Behçet's disease has been linked to an increased risk of depression.<sup>9</sup>

PCPs plays this pivotal role as the first point of contact during disease exacerbations, allowing timely symptom management, reinforcement of treatment adherence, providing psychosocial support and coordination with the rheumatology team. In this case, the patient's early non-adherence was partly due to fear of medication side effects. This emphasizes the need for clear counselling to address patient concerns and support treatment compliance; PCPs are well-positioned to provide patient education, address misconceptions about medications, and empower patients to take an active role in their long-term management. Regular follow-up and multidisciplinary care are essential to optimise symptom control and to monitor for systemic involvement and complications.<sup>3</sup>

## CONCLUSION

This case highlights the importance of maintaining a broad differential diagnosis when evaluating patients with persistent or recurrent oral ulcers in primary care. Early recognition of Behçet's disease requires detailed history taking and comprehensive examination. Long-term outcomes are influenced by treatment adherence, patient education, and effective communication to dispel

misconceptions about therapy. Ultimately, coordinated multidisciplinary care between primary care providers and specialists is essential to ensure optimal disease control and preserve the patient's quality of life.

#### ACKNOWLEDGEMENTS

The authors would like to thank the patient for her cooperation and consent.

#### DECLARATIONS

No conflicts of interest declared.

#### REFERENCES

1. Paleri V, Staines K, Sloan P, Douglas A, Wilson J. 2010. Evaluation of oral ulceration in primary care. *Bmj* 340: c2639.
2. Plewa MC, Chatterjee K. Recurrent Aphthous Stomatitis. [Updated 2023 Nov 13]. In: StatPearls [Internet]. Treasure Island (FL): StatPearls Publishing; 2025 Jan-. Available from: <https://www.ncbi.nlm.nih.gov/books/NBK431059/>{Lavalley, 2024 #54}
3. Lavalley S, Caruso S, Foti R, Gagliano C, Cocuzza S, La Via L, et al. Behçet's Disease, Pathogenesis, Clinical Features, and Treatment Approaches: A Comprehensive Review. *Medicina (Kaunas)*. 2024; 60(4).
4. Korkmaz FN, Ozen G, Unal AU, Kahraman Koytak P, Tuncer N, Direskeneli H. Severe neuro-Behçet's disease treated with a combination of immunosuppressives and a TNF-inhibitor. *Acta Reumatol. Port.* 2016; 41: 367-71.
5. Davatchi F, Champs-Davatchi C, Shams H, Shahram F, Nadji A, Akhlaghi M, et al. Behçet's disease: Epidemiology, clinical manifestations, and diagnosis. *Expert Rev. Clin. Immunol.* 2017; 13: 57-65.
6. Hatemi G, Christensen R, Bang D, Bodaghi B, Celik AF, Fortune F, et al. 2018 update of the EULAR recommendations for the management of Behçet's syndrome. *Ann. Rheum. Dis.* 2018; 77: 808-18.
7. Yazici Y, Yurdakul S, Yazici H. Behçet's syndrome. *Curr. Rheumatol. Rep.* 2010; 12: 429-35.
8. Khabbazi A, Ebrahimzadeh Attari V, Asghari Jafarabadi M, Malek Mahdavi A. Quality of Life in Patients With Behçet Disease and Its Relation With Clinical Symptoms and Disease Activity. *Reumatol. Clin.* 2021; 17: 1-6.
9. Pagnoux C, Mahendira D, Laskin CA. Fertility and pregnancy in vasculitis. *Best Pract. Res. Clin. Rheumatol.* 2013; 27: 79-94.
10. Alibaz-Oner F, Direskeneli H. Update on the Diagnosis of Behçet's Disease. *Diagnostics (Basel)*. 2022; 13(1).

# Tuberculosis and Bartonella co-infection in people living with human immunodeficiency virus (HIV)

Juwie Chuah, MD, Gan Wee Fu, FRCP

Infectious Disease Unit, Internal Medicine Department, Hospital Melaka, Melaka, Malaysia

## SUMMARY

Malaysia is classified by the World Health Organization (WHO) as a country with an upper moderate burden of tuberculosis (TB). While TB cases are commonly reported, there is currently limited data on the prevalence of *Bartonella* infections in Malaysia. Here, we present the case of a Malaysian woman living with human immunodeficiency virus (HIV), who initially presented with right cervical lymphadenopathy and was subsequently diagnosed with, and successfully treated for, a TB and *Bartonella* co-infection. This case highlights the diagnostic challenges involved and underscores the importance of maintaining a high index of suspicion for TB and *Bartonella* co-infection, particularly in endemic areas.

## INTRODUCTION

It was estimated that 85,283 people were living with HIV in Malaysia at the end of 2023.<sup>1</sup> People living with HIV are 20 times more likely to develop active TB disease than people without HIV.<sup>2</sup> Malaysia is classified by the WHO as a country with an upper moderate burden of tuberculosis, with a notification rate of TB between 50 to 99 per 100,000 populations. The prevalence of TB-HIV co-infection in Malaysia was 12.6% in 2010, and the latest data in 2019 was 5.9%.<sup>3</sup> On the other hand, the global burden of *Bartonella*-associated diseases, although significant, may be underestimated as they often result in undifferentiated febrile illnesses.<sup>4</sup> In people with HIV, bartonellosis is often a chronic illness, lasting for months to more than a year.<sup>5</sup> While TB cases are commonly reported, there is a paucity of data regarding the prevalence of *Bartonella* infections to date. Lina et al. (2010) reported the first suspected case of cat scratch disease in a 29-year-old Malaysian febrile patient with a painful left neck mass and lymphadenopathy. Here, we report a case of cervical lymphadenopathy with tuberculosis and *Bartonella* co-infection in people living with HIV in Malaysia.

## CASE PRESENTATION

We encountered a 34-year-old woman who is HIV-positive and on antiretroviral therapy (ART). She was first diagnosed with HIV in year 2010 during premarital screening and was then started on an ART regimen of oral lamivudine 300mg, zidovudine 600mg, and efavirenz 600mg daily. Her disease remained stable until she defaulted on her medications and follow-up in year 2020 due to marital issues. After 2 years of defaulting treatment, she presented to us in year 2022 with

progressively enlarging right neck swelling. There was otherwise no history of fever, neurological or ocular symptom. She also denied any constitutional and opportunistic infection symptoms. Upon further questioning, she revealed that she had eight cats at home. She frequently played with them and occasionally sustained scratches. However, she did not seek medical attention for these wounds. On examination, her Glasgow Coma Scale (GCS) was full, and she appeared neither septic nor cachexic. Two right supraclavicular lymph nodes were palpable, measuring 3x4cm and 2x2cm, respectively. No other lymph nodes were palpable. Her lungs were clear on auscultation. There was evidence of a cat scratch wound on her right hand.

Her full blood count, renal profile, and liver function tests were unremarkable, with a CD4 count of 75 and viral load of 521 copies. *Treponema pallidum* serology was non-reactive. Her neck ultrasonography demonstrated multiple enlarged right anterior cervical, right posterior cervical and right supraclavicular lymph nodes with loss of fatty hilum. The largest lymph node was at her right submandibular, measuring approximately 1.8 x 2.7 x 2.9cm. Fine-needle aspirate from the lymph node was sent for fungal culture and sensitivity and was negative. Blood fungal cultures were also negative. She subsequently underwent excisional lymph node biopsy.

Histopathological examination (HPE) of the lymph node sample revealed granulomas with extensive caseous necrosis, composed of epithelioid histiocytes, with surrounding small lymphocytes and few large Langerhans-type multinucleated giant cells. Ziehl-Neelsen staining for acid fast bacilli was positive, suggestive of tuberculous lymphadenitis. Culture of the lymph node confirmed the presence of *Mycobacterium tuberculosis* complex. The patient was initiated on anti-tuberculous therapy, which she completed over a 9-month course. The finding of granulomas on HPE prompted consideration of a range of differential diagnoses, as listed in Table I. In view of the patient's history of exposure to cat scratches, *Bartonella* infection remained high on our list of differentials. Unfortunately, further specific staining, such as *Bartonella* staining, could not be performed at our centre and therefore was not included in this case report. Consequently, we proceeded with alternative investigations to confirm *Bartonella* co-infection in this case.

*Bartonella henselae* DNA was detected in the same lymph node sample by Polymerase Chain Reaction (PCR). Serological testing for *Bartonella* was also performed, showing

This article was accepted: 11 February 2026

Corresponding Author: Juwie Chuah

Email: juwiechuah@live.com

Table I: Differential diagnosis for infectious granulomatous inflammation<sup>9</sup>

Necrotizing granulomatous inflammation	Non-necrotizing granulomatous inflammation
Tularemia	<i>Mycobacterium tuberculosis</i>
Cat scratch disease	Nontuberculous mycobacterium (including Hansen disease)
<i>Yersinia lymphadenitis</i>	<i>Salmonella typhi</i>
Lymphogranuloma venereum	<i>Rickettsia</i> spp.
Dematiaceous fungal infection	<i>Coxiella</i>
Brucellosis	<i>Candida albicans</i>
<i>Actinomyces</i>	<i>Candida immitis</i>
Syphilis	Viral (cytomegalovirus, herpes, hepatitis)
Fungal infection ( <i>Cryptococcus</i> , <i>Histoplasma</i> , <i>Coccidiomycosis</i> , <i>Pneumocystis</i> , <i>Aspergillus</i> , <i>Blastomyces</i> , <i>Mucorales</i> )	Parasitic (toxoplasmosis, schistosomiasis)
<i>Mycobacterium tuberculosis</i>	
Nontuberculous mycobacteria	
<i>Nocardia</i>	

Table II: Reported cases of Bartonella and TB co-infection

Author	Age, sex	CD4 count	Clinical features	Clinical features	Treatment	Outcome
Bernit E et al. (2003)	32, female	416	Supraclavicular inflammatory lymphadenitis	Cultures onto Columbia agar with sheep blood and onto human endothelial cells in shell vial: <i>B. quintana</i> and <i>M. tuberculosis</i> hominis	Anti-TB, doxycycline	Remains well, no relapse
Eleftheriotis et al. (2014)	23, male	67	Fever, malaise, worsening neck pain, painful swallowing, bilateral cervical lymphadenopathy, axillary and inguinal lymphadenopathy	FNAC of lymph node: positive Ziehl - Neelsen stain for acid fast bacilli  Aspirate for culture and PCR: pan-susceptible <i>Mycobacterium tuberculosis</i> strain  Positive <i>Bartonella henselae</i> and <i>Bartonella quintana</i> IgM antibodies on a titer of 1:24 and IgG antibodies on a titer of 1:256	Anti-TB, methylprednisolone, doxycycline	Lymph node tenderness resolved after one month of tuberculosis treatment and lymph node size decreased.  One month after ART initiation, he presented with fever and bilateral painful cervical lymphadenopathy. Symptoms resolved after treating with doxycycline and methylprednisolone
Our patient (Malaysia)	34, female	75	Cervical lymphadenopathy	HPE of lymph node: tuberculous lymphadenitis, positive Ziehl-Neelsen staining for acid fast bacilli Lymph node TB C+S: Mycobacterium tuberculosis complex  Lymph node for Bartonella PCR: Bartonella henselae DNA detected  Bartonella henselae Ig M positive, Ig G > 1:512  Bartonella quintana Ig M positive, Ig G > 1:512	Anti-TB, doxycycline	Lymphadenopathy resolved after completed treatment

positive IgM results for both *Bartonella henselae* and *Bartonella quintana*, with an IgG titre >1:512. The patient denied any skin rashes or lesions, and there were no signs or symptoms suggestive of central nervous system or endocardial involvement. Abdominal ultrasonography revealed no evidence of intra-abdominal involvement or disease dissemination.

She was commenced on oral doxycycline, in addition to the existing rifampicin-based anti-tuberculous therapy. A repeat *Bartonella* serology done six months later revealed a significant response to treatment, showing positive *Bartonella henselae* Ig M and negative Bartonella henselae Ig G, with both *Bartonella quintana* IgM and IgG remaining negative. By the end of treatment, there was no palpable lymph node, and she remained well under our care with no new complaints.

## DISCUSSION

We describe the case of a Malaysian woman living with HIV who initially presented with right cervical lymphadenopathy and was treated for both tuberculosis and *Bartonella* infection. Her lymphadenopathy resolved after completing treatment for both infections.

Several case reports and studies have discussed co-infections of *Mycobacterium tuberculosis* (MTB) and *Bartonella* species, particularly *Bartonella henselae* and *Bartonella quintana*, in individuals with HIV. These co-infections pose a diagnostic challenge due to overlapping clinical symptoms such as fever and lymphadenopathy, which are common in both diseases.

The clinical presentation of our patient is similar to that reported by Bernit E et al. (2003).<sup>6</sup> However, in that case, the serological tests were negative. Diagnosis was confirmed by isolation of *B. quintana* and *M. tuberculosis hominis* from cultures onto Columbia agar with sheep blood and onto human endothelial cells in a shell vial. This case emphasized the difficulty of diagnosing *Bartonella* in HIV-positive patients, as its symptoms often mimic other diseases, especially TB.

Eleftheriotis et al. (2014) discussed an HIV-infected patient who developed both TB lymphadenopathy and *Bartonella* lymphadenopathy, along with immune reconstitution inflammatory syndrome (IRIS).<sup>7</sup> The patient was treated with anti-TB therapy and doxycycline, leading to subsequent resolution of symptoms. This case illustrates the complexity of diagnosing and treating co-infections in HIV-infected individuals, especially in the presence of IRIS.

*Bartonella* infection is a major cause of unexplained fever in patients with advanced HIV and should be considered in the differential diagnosis of patients with CD4 counts <100 cells/mm<sup>3</sup> and fever. *Bartonella* species can cause infections that include cat scratch disease (CSD), retinitis, trench fever, relapsing bacteremia, culture-negative endocarditis, bacillary angiomatosis (BA), and bacillary peliosis hepatis. The latter two manifestations occur almost exclusively in individuals who are immunocompromised. BA most often occurs late in HIV infection in patients with median CD4 T lymphocyte (CD4) cell counts <50 cells/mm<sup>3</sup>. The development of BA lesions caused by *B. henselae* is statistically linked to cat exposure in people with HIV.<sup>5</sup> In contrast, BA caused by *B. quintana* is associated with body louse infestation and homelessness.<sup>5</sup>

Lymphadenopathy was one of the initial presentations of *Bartonella* and TB co-infection in most of case reports. In a review of 1200 patients with CSD by Carithers, all patients in the series had lymphadenopathy; 85% had single-node involvement and the remainder had regional lymph node involvement, usually with only two, occasionally three, and rarely four or more nodes enlarged. None of the patients in this series had generalized lymphadenopathy.<sup>8</sup>

Co-infection with TB and *Bartonella* can lead to a range of similar symptoms, such as fever, weight loss, fatigue, and lymphadenopathy, which can obscure the diagnosis. The overlapping clinical signs necessitate the use of multiple

diagnostic approaches (cultures, PCR, serological tests) to accurately identify both pathogens.

Serological testing is the most accessible, and when positive, is helpful both for diagnosis and subsequent monitoring of treatment response. However, as many as 25% of *Bartonella* culture-positive patients never develop antibodies in the setting of advanced HIV infection.<sup>5</sup> Monitoring of antibody levels can be useful for tracking treatment response, reflecting resolution or recrudescence.<sup>5</sup> Due to interlaboratory variability, longitudinal testing should be conducted at the same laboratory to enable direct comparison of titres over time.<sup>5</sup>

This case report highlights an important yet underrecognized issue. *Bartonella* infection should be considered in the differential diagnosis of lymphadenopathy in people living with HIV, alongside TB. *Bartonella* infection should be ruled out in patients with risk factors, even when a TB diagnosis is confirmed, as co-infection can occur, as shown in our case. Early recognition of TB and *Bartonella* co-infection is crucial for the initiation of prompt and effective treatment. A high index of suspicion should be maintained, with careful screening for risk factors for TB and *Bartonella* infection in patients presenting with lymphadenopathy, and investigations should be tailored accordingly. Routine *Bartonella* PCR testing may not be necessary in all cases and can be considered based on clinical context and individual risk assessment. This report advocates for increased awareness and further research into the immune interactions between these pathogens and the development of tailored treatment regimens for TB and *Bartonella* co-infection in HIV patients.

## CONCLUSION

Co-infection with TB and *Bartonella* in HIV-infected patients remains an important clinical consideration. Awareness of the possibility of both infections, especially in endemic areas, is crucial for timely diagnosis and effective treatment. While TB is a well-known complication in HIV, *Bartonella* should also be considered, particularly in patients with a history of exposure to cats or fleas. Further studies and case reports are needed to better understand the epidemiology and management of TB and *Bartonella* co-infection in HIV-positive individuals.

## ACKNOWLEDGEMENT

The authors wish to thank the patient for her cooperation and willingness to share her experience for educational purposes.

## DECLARATIONS

The authors declare no conflicts of interest related to this publication.

## REFERENCES

1. The global AIDS monitoring 2024 - country progress report Malaysia. Ministry of Health Malaysia; 2024.

## Case Report

2. Malaysian consensus guidelines on antiretroviral therapy 2022. Malaysian Society For HIV Medicine
3. World Health Organization. Global TB Report 2019. Geneva, Switzerland: WHO; 2019.
4. Blasdell KR, Perera D, Firth C. High Prevalence of Rodent-Borne Bartonella spp. in Urbanizing Environments in Sarawak, Malaysian Borneo. *The American Journal of Tropical Medicine and Hygiene*. 2019; 100(3): 506–9.
5. Panel on Guidelines for the Prevention and Treatment of Opportunistic Infections in Adults and Adolescents with HIV. Guidelines for the Prevention and Treatment of Opportunistic Infections in Adults and Adolescents with HIV. National Institutes of Health, Centers for Disease Control and Prevention, HIV Medicine Association, and Infectious Diseases Society of America. 2024.
6. E Bernit, Veit V, B La Scola, H Tissot-Dupont, J Gachon, D Raoult, et al. Bartonella quintana and Mycobacterium tuberculosis coinfection in an HIV-infected Patient with Lymphadenitis. *Journal of infection*. 2003; 46(4): 244–6.
7. Eleftheriotis G, Skopelitis E. Concurrence of cat-scratch disease and paradoxical tuberculosis-IRIS lymphadenopathy: a case report. *BMC Infectious Diseases*. 2022 Mar 3; 22(1).
8. Carithers HA. Cat-scratch Disease. *American Journal of Diseases of Children*. 1985; 139(11): 1124.
9. Granulomatous inflammation [Internet]. [www.pathologyoutlines.com](http://www.pathologyoutlines.com). Available from: <https://www.pathologyoutlines.com/topic/lymphnodesgranulomatous.html>. Date accessed: 26 January 2026

# Priapism in chronic myeloid leukemia: A rare case report

Ni Putu Merlynda Pusvita Dewi, MD<sup>1</sup>, Adiba Hasna Hanifah, MD<sup>2</sup>

<sup>1</sup>Hematology and Oncology Division, Department of Internal Medicine, Sentra Medika Hospital, Cibinong, Indonesia,

<sup>2</sup>Medical Doctor, Sentra Medika Hospital, Cibinong, Indonesia

## SUMMARY

**Chronic Myeloid Leukemia (CML) is a clonal myeloproliferative neoplasm characterized by the BCR::ABL1 fusion gene and accounts for about 15% of adult leukemia cases. Its global prevalence has increased due to improved survival with tyrosine kinase inhibitor (TKI) therapy. Priapism is a rare urological emergency in CML, usually associated with severe hyperleukocytosis. This report describes a 32-year-old man presenting with generalized body pain, spontaneous bruising, and a painless penile erection lasting more than four days without sexual stimulation. Examination revealed splenomegaly (Schuffner 4), while laboratory tests showed extreme leukocytosis ( $420 \times 10^9/L$ ), anemia, and thrombocytopenia. The BCR::ABL1 (b3a2) transcript was detected by RT-PCR, confirming CML. Treatment included leukapheresis, hydroxyurea, imatinib, and a Winter procedure due to persistent priapism. Bone marrow biopsy confirmed CML in the chronic phase. Although leukocytosis and spleen size decreased, the patient developed erectile dysfunction, likely due to irreversible ischemic injury. This case highlights priapism as a rare but serious initial manifestation of CML caused by leukostasis, emphasizing the need for prompt cytoreduction and early urologic intervention.**

## INTRODUCTION

Chronic myeloid leukemia (CML) is a myeloproliferative neoplasm with an annual incidence of two cases/100 000. It accounts for approximately 15% of newly diagnosed adult leukemia cases.<sup>1</sup> In 2024, an estimated 9280 new CML cases will be diagnosed in the United States (US), and about 1280 patients will die of CML (due to its high prevalence today). Since the introduction of imatinib in 2000, the annual mortality in CML has decreased from 10%–20% to 1%–2%.<sup>2</sup> The CML-specific mortality is 0.5%–1%. Consequently, the prevalence of CML in the US, estimated at about 30 000 cases in 2000, has increased by approximately 9000/year to an estimated 150 000+ cases in 2024. Early estimates indicated the CML prevalence to reach a plateau of about 180 000 cases by 2030–2040.<sup>3</sup>

Priapism is a urological emergency. Ischemic priapism is the most common type, with one of the causes being a hematologic disorder in the form of leukemia.<sup>4</sup> The incidence of priapism is 1.5 per 100,000 people. About 20% of cases of priapism are caused by hematological disorders. In patients with leukemia, 50% of cases of priapism are due to CML.<sup>5</sup>

However, based on the current incidence of near 9000 cases/year in the US (population expansion) and an estimated annual overall mortality of 1%–2%, the prevalence plateau (annual incidence equal to annual mortality of 9000 cases) is now estimated to be  $9000 \times 100/2 = 400\text{--}450\ 000$  cases in the US, which may not be reached until 2040–2050 with full TKI optimal treatment. Considering a world population of 8 billion and optimal CML management worldwide with the availability of affordable generic BCR::ABL1 tyrosine kinase inhibitors (TKIs), the world prevalence of CML (25 times that of the US) might reach above 10 million cases. These projections depend on difficult-to-estimate variables like the population growth in the US and worldwide, and the TKIs treatment penetration, optimization, and affordability.<sup>6</sup>

## CASE PRESENTATION

A 32-year-old man was referred from the regional hospital with chief complaints of body aches, spontaneous bruising, and lumps. These complaints were accompanied by significant weight loss, from over 100 kg to 77 kg in 4 months. The patient also complained of frequent, unexplained bruising. There was no history of previous illnesses or drug allergies. The patient's father had a family history of chronic kidney failure. 3 days before, the patient experienced prolonged erections without sexual stimulation—a condition that suggested priapism. Laboratory tests revealed a white blood cell (WBC) count of  $454,970/mm^3$ , hemoglobin of 7.3 g/dL, hematocrit of 22.5%, and a platelet count of  $178,000/mm^3$ . An abdominal ultrasound revealed splenomegaly with a spleen size of Schuffner 4. Based on the clinical and laboratory findings, the patient was referred to the internal medicine department for further evaluation.

Initial treatment began with hydroxyurea  $2 \times 1000$  mg per day, imatinib  $2 \times 400$  mg per day, and calcium carbonate. The treatment plan included a Winter procedure to treat priapism and leukapheresis to reduce the leukocyte count. As part of the initial chemotherapy regimen, the patient was also given cytarabine  $2 \times 20$  mg subcutaneous leukapheresis and a 600 ml packed red blood cell transfusion. A central double lumen (CDL) was inserted for leukapheresis.

After leukapheresis, the leukocyte count decreased from  $420$  to  $385 \times 10^9/L$ , and the spleen size also gradually decreased to Schuffner 2, then reached Schuffner 0 in 2 weeks. Furthermore, after Hb 10, a Winter procedure was finally

This article was accepted: 11 February 2026

Corresponding Author: Adiba Hasna Hanifah

Email: adibahasna@rocketmail.com



**Fig. 1:** Initial condition of the penis on presentation to the emergency department

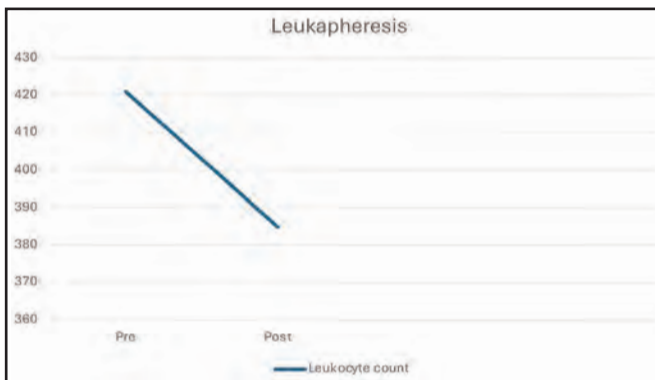


**Fig. 2a:** Leukocyte reduction with leukapheresis

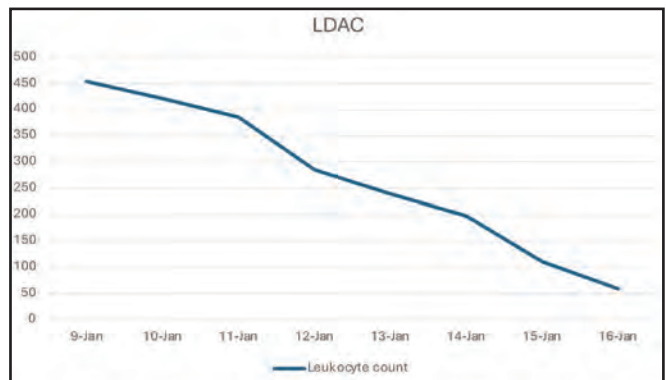


**Fig. 2b:** Leukocyte reduction with low-dose Cytarabine (LDAC)

performed and the hydroxyurea dose was increased to 3 x 1000 mg per day. In the following week, the patient entered the aplasia phase, with leukocytes decreasing to 1,650/ $\mu$ L, so imatinib and hydroxyurea therapy were temporarily discontinued.

A month later, imatinib therapy was resumed at a dose of 400 mg per day, and hydroxyurea was administered twice daily at 500 mg. Molecular testing revealed a positive BCR-ABL result with a b3a2 fusion, confirming the diagnosis of CML. Priapism persisted until the patient reported erectile dysfunction in the second month. At the end of the second month, a bone marrow puncture (BMP) was performed, the results of which supported the definitive diagnosis of CML. During follow-up, the patient's overall condition steadily improved as his underlying disease was brought under

control. The episodes of priapism resolved completely without recurrence, and no further urologic complications were observed. Despite the previous prolonged erections, erectile function was fully preserved, and the patient maintained normal sexual function. His clinical course remained stable, with continued improvement in hematologic parameters, and he experienced a significant enhancement in quality of life. Overall, the priapism was successfully managed, the condition resolved, and the patient's erectile function remained intact, reflecting a positive long-term outcome.

Bone marrow aspiration/biopsy (H&E stain) showing marked hypercellularity with predominant myeloid lineage proliferation, reduced fat spaces, relative suppression of erythroid precursors, and increased megakaryocytes — features consistent with Chronic Myeloid Leukemia (CML).



Fig. 3: Postoperative penile condition following the Winter procedure

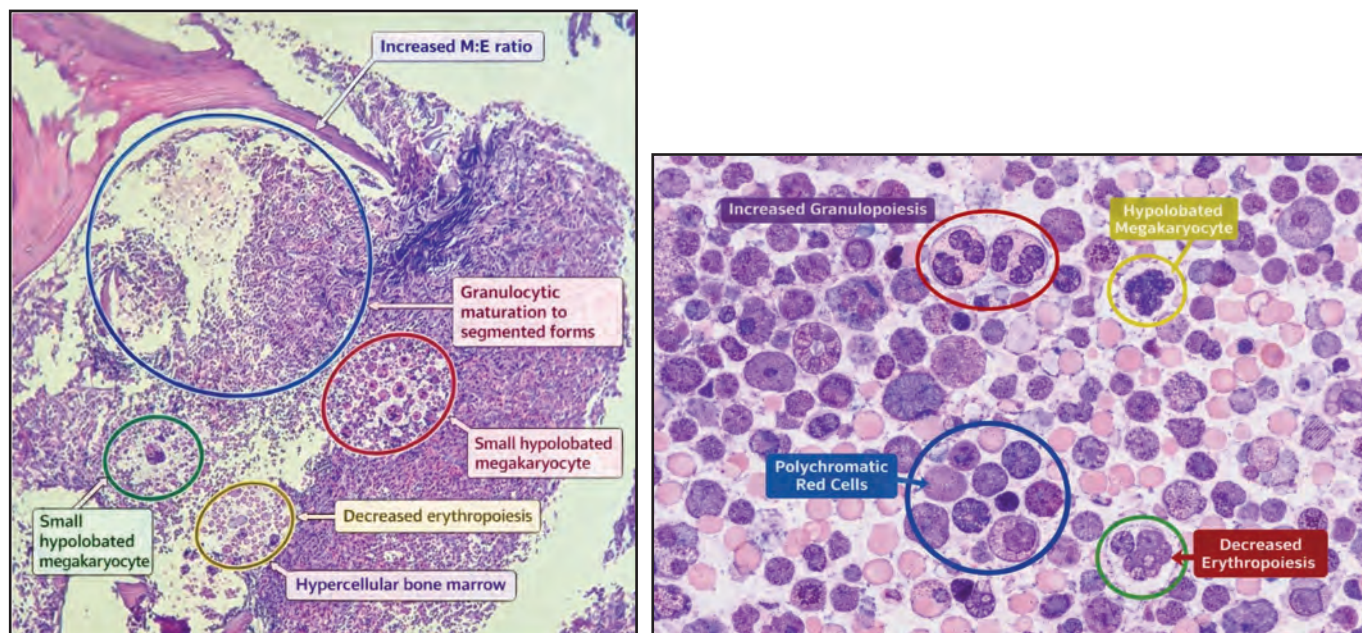


Fig. 4: BMP results

The bone marrow section demonstrates marked hypercellularity due to excessive proliferation of myeloid precursors, with cells present at all stages of granulocytic maturation (myelocytes, metamyelocytes, band forms). There is a myeloid predominance with a left shift, while erythroid elements are relatively decreased, resulting in an increased

myeloid-to-erythroid (M:E) ratio. Megakaryocytes may be increased and often appear small or hypolobated, a characteristic finding in CML. These marrow features correlate with CML, a myeloproliferative neoplasm driven by the BCR-ABL fusion gene (Philadelphia chromosome), leading to uncontrolled proliferation of the myeloid lineage.

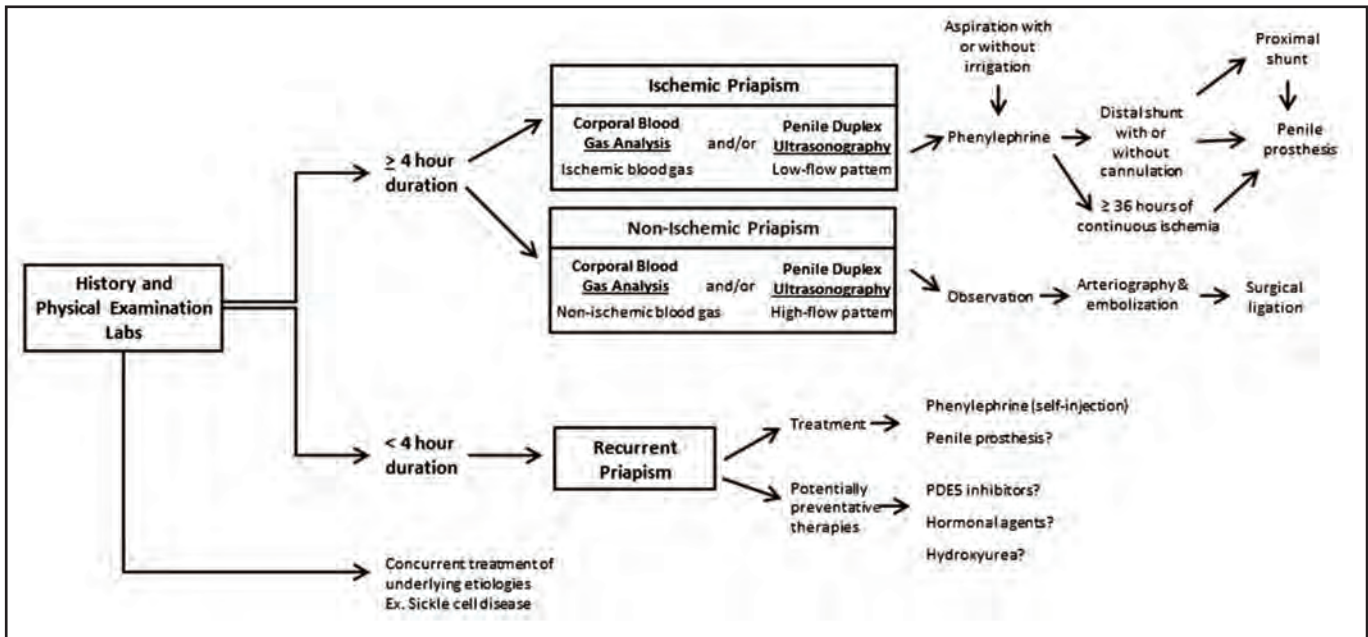


Fig. 5: Algorithm of priapism management<sup>11</sup>

**DISCUSSION**

CML characterized by the proliferation of abnormal and immature myeloid cells in the bone marrow, disrupting the production of normal blood cells. CML is a myeloproliferative neoplasm characterized by the presence of the Philadelphia chromosome (Ph+), resulting from a reciprocal translocation between chromosomes 9 and 22, resulting in the BCR::ABL1 fusion gene encoding a constitutively active tyrosine kinase, leading to uncontrolled cell proliferation and evading apoptosis.<sup>7</sup> Initial examination of the patient revealed hyperleukocytosis, anemia, and thrombocytopenia, as well as splenomegaly up to Schuffner 4. Extreme hyperleukocytosis in CML can lead to complications such as leukostasis, an emergency condition caused by the aggregation of leukemic cells in the circulation that disrupts blood flow to vital organs, including the penis, as occurred in this patient who experienced ischemic priapism without sexual stimulation. Priapism is a rare but characteristic complication of CML, occurring due to obstruction of the microcirculation by leukemic cells that causes ischemia of the penile cavernous tissue.<sup>5</sup> Severe splenomegaly, in this case reaching Schuffner 4, reflects the overwork of the spleen in destroying abnormal blood cells, as well as the extramedullary site of hematopoiesis due to bone marrow failure.<sup>3</sup>

Molecular testing identified the **BCR::ABL1** fusion gene with the **b3a2** transcript, producing the p210 protein and confirming the diagnosis of **CML**. CML is diagnosed based on morphological, cytogenetic, and molecular findings, with detection of the Philadelphia chromosome or **BCR::ABL1** by RT-PCR being essential and serving as a therapeutic target. Bone marrow examination showed myeloid hyperplasia, consistent with **chronic-phase CML**, characterized by <10% blasts and generally good treatment responsiveness.<sup>7</sup> Patient therapy begins with hydroxyurea to rapidly control the leukocyte count. Hydroxyurea is a cytotoxic agent that inhibits ribonucleotide reductase,

inhibiting DNA synthesis, and reducing the leukocyte count in emergencies such as leukostasis.<sup>3</sup> Leukapheresis is performed to mechanically reduce the extreme leukocyte count (420 x 10<sup>9</sup>/L), which is essential to reduce the risk of complications such as stroke, visual impairment, or subsequent priapism. Definitive therapy begins with imatinib mesylate, a first-generation tyrosine kinase inhibitor, which specifically inhibits BCR::ABL1 activity by occupying the ATP-binding site on the protein. Imatinib's effectiveness in altering the natural history of CML is significant, increasing 10-year survival from approximately 20% to 85–90%.<sup>6,8</sup>

After several weeks of therapy, the spleen size decreased significantly and priapism symptoms began to resolve, although by the end of February the patient was reported to have lost erections, indicating permanent cavernous tissue damage due to prolonged ischemia. Treatment of priapism involves urologic interventions such as the Winter procedure, which involves aspiration of blood from the corpus cavernosum to relieve pressure and restore circulation. Rapid intervention is crucial, as ischemic priapism lasting more than 4–6 hours can lead to tissue fibrosis and permanent erectile dysfunction.<sup>4</sup>

On January 23, the patient entered the aplasia phase, marked by a drastic decrease in leukocyte count to 1,650/μL, so imatinib and hydroxyurea therapy were temporarily discontinued. Aplasia can occur in response to cytotoxic therapy that severely suppresses the bone marrow, so close monitoring and transfusion support are necessary during this phase. After improvement, imatinib therapy was resumed at a dose of 400 mg/day, the standard first-line regimen for patients with chronic CML. Imatinib has a good safety profile and a low resistance rate of approximately 10% over 10 years, and its effectiveness in inducing major molecular remissions makes it a global mainstay therapy for chronic CML.<sup>9</sup>

CML is one of the hematological malignancies with the best prognosis since the advent of targeted therapy using tyrosine kinase inhibitors (TKIs). With adherence to therapy and regular molecular monitoring to ensure hematological, cytogenetic, and molecular response, most patients can live near-normal lives. However, long-term monitoring remains crucial, as some patients can progress to the accelerated or blastic phase, although the incidence is only around 5–6% within 10 years.<sup>8,10</sup> The key to successful therapy lies in early diagnosis, appropriate therapy selection, patient adherence to long-term treatment and regular monitoring. Until the end of the last century, drug therapy for CML was limited to nonspecific agents such as busulfan, hydroxyurea, and interferon- $\alpha$  (IFN- $\alpha$ ). IFN- $\alpha$  therapy resulted in suppression of the Ph-positive cells and improved survival but had modest efficacy and significant toxicities. Allogeneic hematopoietic stem cell transplantation (allo-HSCT) is curative but carries the risks of morbidities and mortality. Allo-HSCT is an option for younger patients with good performance status and organ functions, and who have an appropriate donor.

The CML therapeutic landscape changed dramatically with the development of the small molecule BCR::ABL1 TKIs that potently interfered with the interaction between the BCR::ABL1 oncoprotein and adenosine triphosphate (ATP), blocking cellular proliferation of the malignant clone.<sup>9</sup> This “targeted” approach altered the natural history of CML, improving the 10-year survival rate from approximately 20% to 80%–90% over 20 years of follow-up.<sup>10</sup> While the 10-year survival rate is about 85%, many patients now die from causes unrelated to CML (old age, second cancers, and others). With imatinib as frontline therapy, the 10-year CML-specific survival rate is 90%, the 10-year rate of CML resistance is only 10%, the CML-specific mortality rate is 10%, and the 10-year incidence of blastic transformation only is 5%–6%.<sup>8</sup>

Imatinib mesylate was the first TKI to receive approval by the United States Food and Drug Administration (FDA) for the treatment of patients with CML-CP. It acts via competitive inhibition at the ATP-binding site of the BCR::ABL1 oncoprotein, which results in the inhibition of phosphorylation of proteins involved in cell signal transduction. It efficiently inhibits the BCR::ABL1 kinase and also blocks the platelet-derived growth factor receptor and the C-KIT tyrosine kinase.<sup>7</sup>

## CONCLUSION

This case underscores that ischemic priapism, while uncommon, represents a potentially serious and urgent complication of chronic myeloid leukemia, typically arising from extreme hyperleukocytosis and leukostasis. The accumulation of leukemic cells can obstruct microcirculation, including within the penile cavernous tissue, leading to prolonged, painful erections without sexual stimulation. If not addressed promptly, this can result in tissue ischemia and permanent erectile dysfunction. Early recognition and rapid

intervention with cytoreductive measures, such as leukapheresis and hydroxyurea, are therefore critical to relieve obstruction, restore normal blood flow, and prevent irreversible damage. Furthermore, definitive urologic management, when indicated, can safely resolve the priapism once hematologic parameters are stabilized. Beyond the acute management, effective long-term control of CML through targeted therapy with tyrosine kinase inhibitors like imatinib is essential, as these agents specifically inhibit the BCR::ABL1 oncoprotein, induce hematologic and molecular remission, and reduce the risk of disease progression and mortality. Patient adherence, close monitoring of therapeutic response, and achievement of major molecular remission are key determinants of durable outcomes. Importantly, this case highlights the value of a multidisciplinary approach, involving hematology, urology, and emergency care teams, to optimize both functional and disease-related outcomes. Overall, it demonstrates that with timely recognition, coordinated care, and targeted therapy, even rare and potentially devastating complications like ischemic priapism can be successfully managed, with complete resolution and preservation of erectile function.

## CONFLICT OF INTEREST

The authors declared that they have no conflict of interest.

## REFERENCES

1. American Cancer Society. Cancer Facts & Figures 2024. Atlanta: American Cancer Society; 2024. Available from: <https://www.cancer.org/research/cancer-facts-statistics/all-cancer-facts-figures/cancer-facts-figures-2021.html>
2. Sasaki K, Haddad FG, Short NJ, et al. Outcome of Philadelphia chromosome-positive chronic myeloid leukemia in the United States since the introduction of imatinib therapy: The Surveillance, Epidemiology, and End Results Database, 2000–2019. *Cancer*. 2023; 129: 3805-381.
3. Jabbour E, Kantarjian H. Chronic myeloid leukemia: 2022 update on diagnosis, therapy, and monitoring. *Am J Hematol*. 2022; 97(9): 1236-56.
4. Salonia A, Eardley I, Giuliano F, et al. Guidelines on priapism. *European Association of Urology*. 2015: 5-13.
5. Farhan S, Khan F, Ahmed R, et al. Chronic myeloid leukemia presenting with priapism. *J Leukemia*. 2015; 3(1): 1-4.
6. Hehlmann R, Lauseker M, Sauße S, et al. Assessment of imatinib as first-line treatment of chronic myeloid leukemia: 10-year survival results of the randomized CML study IV and impact of non-CML determinants. *Leukemia*. 2017; 31(11): 2398-406.
7. Jabbour E, Kantarjian H. Chronic myeloid leukemia: 2025 update on diagnosis, therapy, and monitoring. *Am J Hematol*. 2024; 99(11): 2191-212.
8. Hochhaus A, Larson RA, Guilhot F, et al. Long-term outcomes of imatinib treatment for chronic myeloid leukemia. *N Engl J Med*. 2017; 376(10): 917-27.
9. Kantarjian HM, Welch MA, Jabbour E. Revisiting six established practices in the treatment of chronic myeloid leukemia. *Lancet Haematol*. 2023; 10(10): e860-e864.
10. Senapati J, Sasaki K, Issa GC, et al. Management of chronic myeloid leukemia in 2023 – common ground and common sense. *Blood Cancer J*. 2023; 13(1): 58.
11. Anele UA, Le BV, Resar LMS, Burnett AL. How I treat priapism. *Blood*. 2015; 125(23): 3551-8.

# The silent “Cheeky” mystery: A case of indolent yet invasive dermatofibrosarcoma protuberans

Ingrid Ting Pao Lin, AdvMDerm<sup>1</sup>, Azam Hilmi Mohd Zain, MPath<sup>2</sup>, Koh Siang Chai, MS<sup>3</sup>, Min Moon Tang, AdvMDerm<sup>1</sup>

<sup>1</sup>Department of Dermatology, Sarawak General Hospital, Sarawak, Malaysia, <sup>2</sup>Department of Pathology, Sarawak General Hospital, Sarawak, Malaysia, <sup>3</sup>Department of Plastic Surgery, Sarawak General Hospital, Sarawak, Malaysia

### INTRODUCTION

Dermatofibrosarcoma protuberans (DFSP) is a rare fibrohistiocytic tumor with low-to-intermediate malignant potential. Here we described a neglected, painless and slow-growing mass on the right cheek in a 46-year-old man.

### CASE PRESENTATION

A 46-year-old man, with chronic Hepatitis B infection, presented with a slow but progressively enlarging, painless mass over his right cheek for 3 years. There were no complaints of speech, chewing and pain. The patient reported no prior history of trauma or dental infection. On examination, a firm, erythematous-to-brown lobulated nodule measuring 8x5cm was noted on the right cheek, with prominent peripheral telangiectasia (Figure 1a). There were no palpable lymph nodes. Computed tomography revealed a subcutaneous mass extending from right cheek to the lower eyelid, with erosion of the right maxillary sinus. There was no regional lymphadenopathy. However, subsequent magnetic resonance imaging shows no infiltration to surrounding tissue.

Histopathological examination of the swelling demonstrated a poorly circumscribed, spindle cell proliferation arranged in a storiform pattern in the dermis, with presence of grenz zone. The spindle cells were uniform, with ovoid to elongated nuclei, fine chromatin, and scant cytoplasm. Immunohistochemical stains showed diffuse positivity for CD34, confirming the diagnosis of DFSP (Figure 2a, b).

The patient underwent wide local excision of the right cheek and partial maxillectomy, followed by reconstruction with titanium mesh, a left radial forearm free flap, and split-thickness skin graft (Figure 1b, c). Given the tumour's close proximity to the anterior maxillary wall, this structure was excised en bloc with the lesion to ensure adequate margins. A titanium mesh was placed to restore the contour of the right cheek. The orbital floor remained intact. Suspension of the lower eyelid was achieved with a palmaris longus tendon sling. In addition, a neck dissection was performed to expose suitable recipient vessels for microvascular free-flap reconstruction. Post operative histopathological study showed clear margin. Review at 18-month postoperatively showed that he was well without any clinical recurrence (Figure 1d).

### DISCUSSION

DFSP is a locally aggressive soft tissue neoplasm characterized by indolent growth with high tendency for local recurrence due to its infiltrative nature.<sup>1</sup> Population-based studies and national cancer registry data confirm that DFSP remains a rare cutaneous malignancy, with incidence rates consistently below 1 case per 100,000 person-years.<sup>2</sup> Epidemiologic data from Europe and North America demonstrate relatively stable incidence over time, although a modest increase has been observed in more recent analyses. For example, national registry studies from Denmark<sup>3</sup> and the United States<sup>4,5</sup> have reported incidence rates ranging from approximately 0.4 to 0.5 per 100,000 person-years, while a recent SEER database analysis indicated a slightly higher age-standardized incidence of 0.62 per 100,000 person-years.<sup>6</sup> Similarly, registry data from England showed a small, non-significant upward trend between 2013 and 2019.<sup>7</sup> Although population-based studies and national cancer registries from Europe and North America have provided valuable insights into the epidemiology of dermatofibrosarcoma protuberans, comparable data remain scarce in many regions, including our local setting. The absence of regional or national incidence statistics limits the ability to assess disease burden, demographic patterns, and temporal trends within the local population. This lack of data likely reflects the rarity of DFSP, under-recognition, and the absence of dedicated sarcoma or skin cancer registries, underscoring the importance of individual case reports and institutional series in contributing to the existing literature and improving clinical awareness.

DFSP generally shows no strong sex-related predilection, occurring in men and women at comparable rates, though one series by Asuquo et al.<sup>8</sup> observed a modest male majority. The tumour is most frequently diagnosed in adults in their 20s through 50s.<sup>9</sup> Previous literature has also described cases arising within areas of prior injury or surgical scarring.<sup>10</sup> In contrast, our patient did not report any history of trauma or operative intervention at the site.

DFSP frequently erupted on the trunk (50-60%) and proximal extremities (20-30%). Head and neck involvement is less commonly reported, occurring in approximately 10-15% of all DFSP.<sup>1</sup> DFSP on the cheeks such in our case are extremely rare and tends to have a higher recurrence rate at 30 to 50%, attributed to the complex anatomy and the tumor's propensity to invade deeper structures, such as periosteum, skeletal muscle, and, in rarely, bone.<sup>1</sup>



**Fig. 1:** a) Lobulated nodules on right cheek measuring 8x5cm; b) Wide local excision of right cheek, and right anterior wall maxillectomy followed by reconstruction with titanium mesh; c) Post left radial forearm free flap and split-thickness and skin graft; d) The outcome after 18 months

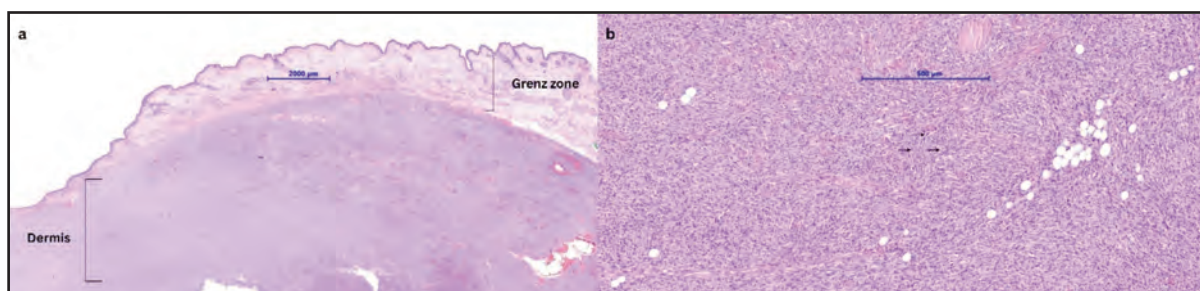


**Fig. 2:** a) (H&E) A circumscribed, dense spindle cell proliferation in the dermis, demonstrating a clear Grenz zone, demonstrating storiform growth pattern. b) Under high power, the spindle cells are large, with ovoid nucleus, mitoses are present with clear chromatin, and high N:C ratio (black arrows)

Clinically, in its early phase, it often presents as an indurated, skin-coloured to erythematous or brownish-yellow plaque with irregular borders, typically ranging from 2 to 5 cm in size. However, these lesions may be larger and display nodular or multilobulated surfaces.<sup>11</sup> With progressive growth, it infiltrates deeply into the dermis and subcutaneous layers, giving rise to multiple indurated nodules that become fixed to adjacent anatomical structures, including adipose tissue, fascia, muscle, periosteum, and, in advanced cases, bone.<sup>12</sup> Three non-protuberant variants have been described—morphea-like, atrophoderma-like and angioma-like forms.<sup>13</sup> The presentation in our patient, a large plaque with multiple nodules, represents the most clinical morphology in adults.

Diagnosis of early facial DFSPs often challenging as shown in our case. It may present as long-standing painless indurated plaques or nodules, frequently misdiagnosed as benign

lesions.<sup>11</sup> The average delay to diagnosis in such cases ranges from 2 months to 41 years, reflecting the tumor's indolent progression and clinical ambiguity.<sup>13</sup> The differential diagnoses include dermatofibroma, schwannoma, cutaneous neurofibroma, solitary fibrous tumor, intradermal spindle cell lipoma, spindle cell squamous cell carcinoma, and desmoplastic or spindle cell melanoma.<sup>14</sup>

Definitive diagnosis requires a multidisciplinary approach combining clinical, histopathological, immunohistochemistry, and radiological assessments. Histologically, DFSP is typified by a storiform proliferation of uniform spindle cells infiltrating the dermis and subcutis. Immunohistochemically, the tumor cells exhibit diffuse CD34 and vimentin positivity while lacking HMB45, desmin, smooth muscle actin (SMA), and S100.<sup>1,15</sup>

Once the diagnosis of DFSP has been histologically established, the next step is to evaluate the extent of local disease, exclude distant spread, and assess patient suitability for subsequent treatment. The priority of initial staging is determining involvement of deeper structures, such as the fascia or beyond, for which contrast-enhanced soft-tissue MRI remains the preferred modality.<sup>11</sup>

Currently, there is no universally accepted staging system for DFSP.

In 2020, a modified staging scheme was proposed in the United States, adapted from the 2015<sup>16</sup> guideline recommendations. This system stratifies DFSP into five stages: Stage I, comprising non-protuberant lesions such as atrophic, macular, or sclerotic plaques; Stage II, representing protuberant primary tumours and subdivided into Stage IIA, limited to superficial tissues without fascial invasion, and Stage IIB, in which the tumour infiltrates or extends beyond the underlying fascia; Stage III, defined by regional lymph node involvement; and Stage IV, reserved for cases with distant metastatic spread. This proposed classification was applied in the 2024 guideline as it corresponds logically with conventional TNM-style staging frameworks.<sup>11</sup> Nevertheless, it should be noted that external validation of this system has not yet been reported. According to the 2020 DFSP staging proposal, the tumour in our patient is best categorised as Stage IIB. This corresponds to a protuberant primary tumour with extension beneath and beyond the superficial fascia, evidenced by involvement of the anterior maxillary wall, with no clinical or pathological evidence of lymph node involvement or distant metastatic disease.

DFSP demonstrates marked local aggressiveness, and recurrence remains a significant concern depending on the therapeutic approach. Published recurrence rates vary considerably, ranging from 0% to 40%, although more contemporary series report lower figures. One cohort with a median follow-up of 59 months demonstrated recurrence-free survival rates of 86% at five years and 76% at ten years.<sup>14</sup> In another large study involving 200 DFSP cases and 34 patients with fibrosarcomatous transformation, none of the conventional DFSP patients developed distant metastases. In contrast, metastatic spread occurred in 23.6% of those with transformed DFSP, most frequently affecting the lungs, soft tissues, and skeletal system.<sup>17</sup> The fibrosarcomatous variant is the most aggressive variant, characterised histologically by high-grade transformation and clinically by significantly greater risks of recurrence and distant metastasis relative to classic DFSP.<sup>12</sup> This transformation is typically indistinguishable from conventional DFSP on clinical examination, making tissue diagnosis essential for detection. Recurrence risk in DFSP is influenced by several tumour-related characteristics, including histologic subtype, degree of cellularity, lesion size, anatomical location within the head and neck region, and an elevated mitotic index.<sup>18</sup>

Achieving adequate surgical margins on the face poses significant challenges due to aesthetic and functional constraints. Although wide local excision with margins 2-5 cm remains the mainstay of treatment, clear margins are often difficult to achieve in cosmetically sensitive areas. Reported recurrence rates are significantly higher when

excision margins are less than 3 cm (approximately 46%) compared to 7% when margins of 3-5 cm are achieved.<sup>13</sup> Micrographically controlled surgery has been shown to provide superior margin control and lower recurrence rates.<sup>11</sup> The cure rate reported ranges from 0.6-6.6%.<sup>13</sup> When Mohs micrographic surgery is unavailable, the recommended treatment approach is wide local excision with comprehensive histopathological assessment of all surgical margins to ensure complete tumor clearance.<sup>13</sup> The choice of reconstructive technique is influenced by multiple factors, including the location and size of the tumor. Complex or extensive defects such as our patient require distant or free flaps to achieve both functional restoration and satisfactory cosmetic outcomes and function while minimizing morbidity.<sup>19</sup>

Interestingly, more than 90% of DFSP demonstrated a translocation t(17;22)(q22;q13), resulting in COL1A1-PDGFB fusion gene. This leads to constitutive activation of the platelet-derived growth factor receptor beta (PDGFR $\beta$ ) signaling pathway, promoting autocrine-driven tumor proliferation.<sup>11</sup> The detection of this fusion through fluorescence in situ hybridization (FISH) or RT-PCR is diagnostic and has guided the introduction of targeted therapy with tyrosine kinase inhibitors such as imatinib. It is particularly useful for unresectable, recurrent, or metastatic cases.<sup>11</sup> Radiotherapy may be considered when additional surgery is not feasible or in cases involving fibrosarcomatous transformation.<sup>1</sup> DFSP on the face and scalp, especially those greater than 5cm, typically recur within 3 years of surgery, while distant metastasis remains rare (<5%).<sup>11</sup> Although our patient remains disease-free at 18-month post-surgery, long-term clinical surveillance is required.

The clinical course in our patient mirrors previously reported cases, with a prolonged period of indolent plaque development before nodular progression. Similar delays in diagnosis of approximately 3-5 years have been documented in the literature, underscoring the deceptively benign appearance of early DFSP. Notably, involvement of the cheek with extension to the anterior maxillary wall remains uncommon, and few published cases describe the need for maxillary resection and microsurgical reconstruction, highlighting the complexity of management in this anatomical region.

## CONCLUSION

This case highlights the importance of early recognition and prompt management of slow-growing facial masses. A timely management includes a crucial diagnostic biopsy may lead to an early yet less extensive surgery. This will greatly reduce the reconstructive complexity and thence minimize postoperative morbidity.

## AUTHOR CONTRIBUTIONS' STATEMENT

IPLT was responsible for the study design, data collection, manuscript writing, AHMZ and KSC participated in data collection. IPLT, AHMZ, KSC, and MMT was involved in the discussion, manuscript editing, and language proofreading. All authors read and approved the final manuscript.

## ACKNOWLEDGEMENT

We would like to thank the Director General of Health Malaysia for his permission to publish this article.

**Statement of financial or other relationships that might lead to a conflict of interest:** The authors hereby certify that, to the best of our knowledge, the work which is reported on in said manuscript has not received financial support from any pharmaceutical company or other commercial source and neither us nor any first degree relatives have any special financial interest in the subject matter discussed in said manuscript.

**Statement on Consent for publication:** The patient in this manuscript has given written informed consent to the publication of case details.

**Statement on Ethical approval and informed consent:** This article does contain studies with human participant and was registered via the National Medical Research Register, Ministry of Health Malaysia with ID NMRR ID-25-03335-9DN. The patient in this manuscript has given written informed consent for participation.

## REFERENCES

1. Kedous S, Amri A, Methnani A, et al. Head and neck dermatofibrosarcoma protuberans: Case series of extensive resections and reconstructions with literature review. *F1000Research*. 2025; 14: 294.
2. Kuzel P, Metelitsa AI, Dover DC, Salopek IG. Epidemiology of dermatofibrosarcoma protuberans in Alberta, Canada, from 1988 to 2007. *Dermatologic surgery*. 2012; 38(9): 1461-8.
3. Akram J, Wooler G, Lock-Andersen J. Dermatofibrosarcoma protuberans: clinical series, national Danish incidence data and suggested guidelines. *Journal of plastic surgery and hand surgery*. 2014; 48(1): 67-73.
4. Criscione VD, Weinstock MA. Descriptive epidemiology of dermatofibrosarcoma protuberans in the United States, 1973 to 2002. *Journal of the American Academy of Dermatology*. 2007; 56(6): 968-73.
5. Kreicher KL, Kurlander DE, Gittleman HR, Barnholtz-Sloan JS, Bordeaux JS. Incidence and survival of primary dermatofibrosarcoma protuberans in the United States. *Dermatologic Surgery*. 2016; 42: S24-S31.
6. Maghfour J, Genelín X, Olson J, Wang A, Schultz L, Blalock TW. The epidemiology of dermatofibrosarcoma protuberans incidence, metastasis, and death among various population groups: a surveillance, epidemiology, and end results database analysis. *Journal of the American Academy of Dermatology*. 2024; 91(5): 826-33.
7. Lim SX, Ramaiya A, Levell NJ, Venables ZC. Review of dermatofibrosarcoma protuberans. *Clinical and Experimental Dermatology*. 2023; 48(4): 297-302.
8. Asuquo M, Umoh M, Ebughe G. Dermatofibrosarcoma protuberance. *Annals of African medicine*. 2007; 6(2): 80-3.
9. Dragoumis DM, Katsohi L-AK, Amplianitis IK, Tsiftoglou AP. Late local recurrence of dermatofibrosarcoma protuberans in the skin of female breast. *World Journal of surgical oncology*. 2010; 8(1): 48.
10. McKee PH. Pathology of the skin with clinical correlations. *Plastic and Reconstructive Surgery*. 1991; 87(2): 378.
11. Saiag P, Lebbe C, Brochez L, et al. Diagnosis and treatment of dermatofibrosarcoma protuberans. European interdisciplinary guideline—update 2024. *European Journal of Cancer*. 2025: 115265.
12. Stivala A, Lombardo GA, Pompili G, Tarico MS, Fraggetta F, Perrotta RE. Dermatofibrosarcoma protuberans: Our experience of 59 cases. *Oncology letters*. 2012; 4(5): 1047-55.
13. Monnier D, Vidal C, Martin L, et al. Dermatofibrosarcoma protuberans: a population-based cancer registry descriptive study of 66 consecutive cases diagnosed between 1982 and 2002. *Journal of the European Academy of Dermatology and Venereology*. 2006; 20(10): 1237-42.
14. Hao X, Billings SD, Wu F, et al. Dermatofibrosarcoma protuberans: update on the diagnosis and treatment. *Journal of clinical medicine*. 2020; 9(6): 1752.
15. Chan IL, Carneiro S, Menezes M, et al. Dermatofibrosarcoma protuberans: a case report. *Case Reports in Dermatology*. 2014; 6(2): 134-9.
16. Saiag P, Grob J-J, Lebbe C, et al. Diagnosis and treatment of dermatofibrosarcoma protuberans. European consensus-based interdisciplinary guideline. *European journal of cancer*. 2015; 51(17): 2604-8.
17. Alshaygy I, Mattei J-C, Basile G, et al. Outcome after surgical treatment of dermatofibrosarcoma protuberans (DFSP): does it require extensive follow-up and what is an adequate resection margin? *Annals of Surgical Oncology*. 2023; 30(5): 3106-13.
18. DuBay D, Cimmino V, Lowe L, Johnson TM, Sondak VK. Low recurrence rate after surgery for dermatofibrosarcoma protuberans: a multidisciplinary approach from a single institution. *Cancer*. 2004; 100(5): 1008-16.
19. Besharah BO, Ghazzawi RA, Al-Kaff HH, Abdelmonim SK, Al-Essa MA. Reconstruction of facial dermatofibrosarcoma protuberans using an anterolateral thigh flap: a case report and literature review. *Journal of Surgical Case Reports*. 2020; 2020(9)

# Primary nasal tuberculosis complicated by mrsa co-colonization and septal perforation: A rare case report

Sonny Soebjanto, MD, ORLHNS, Shod Abdurrachman Dzulkarnain, MD, M.Biomed

Faculty of Medicine, Universitas Negeri Surabaya, Surabaya, East Java, Indonesia

### SUMMARY

Primary nasal tuberculosis is an exceptionally rare extrapulmonary manifestation, usually arising after trauma or direct inoculation and presenting with chronic nasal obstruction, rhinorrhea, epistaxis, anosmia, or intranasal masses, frequently complicated by septal perforation. This report describes a 58-year-old woman with bilateral obstruction, anosmia, and rhinorrhea, in whom endoscopy revealed a friable nasal mass with anterior septal perforation. Pulmonary tuberculosis was excluded by negative sputum AFB, GeneXpert, and chest radiography. Nasal biopsy demonstrated caseating granulomas with Langhans giant cells, confirming primary nasal tuberculosis without pulmonary involvement. Concurrent MRSA colonization was identified. Management consisted of standard first-line anti-tuberculosis therapy with conservative septal care and targeted MRSA eradication. Follow-up showed improvement and clearance.

### INTRODUCTION

Primary nasal tuberculosis (TB) is exceedingly rare, with fewer than a few dozen cases reported in the modern literature. The septum, particularly the cartilaginous portion, is a common site for TB involvement because of its vulnerability to trauma and infection. Caseous necrosis associated with TB granulomas can destroy cartilage and mucosa, leading to anterior septal perforation.<sup>1</sup> Primary nasal TB mimics fungal or malignant sinonasal disease but is distinguished by caseating granulomas and response to anti-TB therapy.<sup>2</sup> Nasal TB involving nasal septum perforation requires anti-TB treatment followed by surgical intervention, such as debridement or endoscopic sinus surgery.<sup>3</sup>

A further challenge in patients with nasal TB is the risk of secondary bacterial infections with multidrug-resistant bacteria. Resistant bacteria, such as methicillin-resistant *Staphylococcus aureus* (MRSA), have emerged as major global pathogens. MRSA infections are associated with higher morbidity and require targeted eradication therapy combining systemic and topical antimicrobials.<sup>4</sup>

### CASE PRESENTATION

A 58-year-old woman presented with bilateral nasal obstruction for one month, accompanied by complete anosmia. She reported thick rhinorrhea that was initially

white, occasionally turning green, and sometimes mixed with blood, along with a nasal voice and post-nasal drip. She denied recurrent epistaxis, foul nasal odor, facial pain, or headaches. Systemic symptoms such as cough, hemoptysis, fever, night sweats, weight loss, and anorexia were absent. No auditory or vestibular symptoms were noted, including otalgia, hearing loss, tinnitus, or otorrhea. There were no throat-related complaints such as dysphagia, odynophagia, foreign body sensation, or hoarseness. She had no history of diabetes, hypertension, or prior pulmonary TB. Family history was notable for malignancies (mother with a uterine tumor, sibling with a lymph node tumor). Social history revealed a neighbor with a chronic cough and a husband who smoked 2-3 packs of cigarettes daily. She reported no allergies.

On examination, her general condition was fair, and she was alert. Vital signs were within normal limits: blood pressure 130/80 mmHg, pulse 80/min, respiratory rate 20/min, and body temperature 36.8 °C. There were no signs of respiratory distress such as stridor or chest retractions. Cardiopulmonary and abdominal examinations were unremarkable. No systemic lymphadenopathy was initially detected; however, during the course of illness, a firm, mobile, non-tender 2 cm mass was palpated in the left supraclavicular region, later interpreted as lipofibroma versus chronic lymphadenitis on fine needle aspiration biopsy (FNAB).

Ear, nose, and throat (ENT) evaluation revealed normal ears, with intact tympanic membranes and preserved light reflexes. Rhinoscopy and subsequent endoscopic assessments consistently showed a friable mass covered with greenish crusts and an anterior septal perforation. Post-nasal drip was observed. The tonsils were small (T1-T1) without erythema, crypt debris, or detritus. The pharynx was not hyperemic and showed no granulations. Endoscopy confirmed persistent septal perforation without active bleeding or new mass formation.

The diagnosis of primary nasal TB was supported by the presence of bilateral nasal obstruction with a mass covered by greenish crusts, anterior septal perforation, and post-nasal drip on physical examination, all of which suggested a destructive granulomatous process localized to the nasal cavity. Laboratory evaluation showed mild anemia, neutrophilia, and monocytosis, with negative ANCA, HIV, and sputum AFB results, excluding systemic granulomatous diseases and pulmonary TB. Imaging revealed iso-dense

---

This article was accepted: 20 February 2026

Corresponding Author: Sonny Soebjanto

Email: sonnysoebjanto@unesa.ac.id

**Table I: Evidence supporting diagnosis of primary nasal TB with MRSA co-colonization (no pulmonary involvement)**

Category	Findings	Interpretation/Support
Physical Examination	<ul style="list-style-type: none"> <li>- Nasal mass with greenish crusts</li> <li>- Anterior septal perforation</li> <li>- Post-nasal drip (+)</li> <li>- Later supraclavicular 2 cm mass (lipofibroma/lymphadenitis)</li> </ul>	Suggests destructive granulomatous disease of the nasal cavity → consistent with nasal TB; perforation also seen in granulomatous diseases. <sup>5</sup>
Laboratory	<ul style="list-style-type: none"> <li>- Hb 11.1 g/dL (mild anemia) → later normalized</li> <li>- Neutrophilia, monocytosis</li> <li>- ANCA negative (rules out Wegener's)</li> <li>- HIV negative</li> <li>- TB ICT, GeneXpert, AFB negative</li> <li>- MRSA swab positive initially, later eradicated</li> </ul>	Histopathology confirmed TB despite negative sputum; consistent with localized nasal TB. <sup>5</sup> MRSA confirmed as secondary infection. <sup>6</sup>
Imaging	<ul style="list-style-type: none"> <li>- CT: Iso-dense bilateral nasal lesions, septal deviation, suspected granuloma</li> <li>- Endoscopy: perforated nasal septum.</li> <li>- Chest radiograph: Normal repeatedly</li> </ul>	Supports localized granulomatous nasal disease without pulmonary involvement. <sup>5</sup>
Histopathology	<ul style="list-style-type: none"> <li>- Caseating granulomas with epithelioid cells and Langhans giant cells</li> <li>- Chronic granulomatous inflammation due to TB</li> </ul>	Diagnostic hallmark of TB <sup>1</sup> ; excludes malignancy.
Microbiology	<ul style="list-style-type: none"> <li>- MRSA swab positive initially, later eradicated</li> </ul>	Confirms secondary MRSA infection complicating TB. <sup>6</sup>

**Table II: Diagnostic & therapeutic plan with objectives and reasoning**

Objective/Condition	Plan	Reasoning
Confirm the etiology of the nasal lesion	Multiple biopsies (nasal cavity, septum) with histopathology	Gold standard for nasal TB <sup>5</sup> ; rules out malignancy, midline granuloma, Wegener's, sarcoidosis.
Exclude systemic TB or mimics	Chest radiograph, sputum AFB, GeneXpert, ANCA, HIV test	Differentiate nasal TB from pulmonary TB or systemic granulomatous diseases. <sup>5</sup>
Assess the extent of the lesion	CT scan head & neck	Defines nasal/para-nasal involvement <sup>5</sup> , excludes sinus extension, and guides surgical biopsy.
Evaluate lymph node mass	FNAB supraclavicular node, planned neck ultrasound	Rule out malignant spread or TB lymphadenitis <sup>5</sup> ; FNAB showed a benign lesion.
Treat primary nasal TB	Anti-TB therapy Category I: 2HRZE/4HR; extended 9-12 months if persistent	Standard regimen for extrapulmonary TB <sup>7</sup> ; extended duration in bone/cartilage involvement.
Manage septal perforation	Conservative (nasal irrigation, sprays)	Relieves symptoms, reduces crusts <sup>5</sup> , and prevents secondary infection.
Eradicate MRSA coinfection	Oral cotrimoxazole, mupirocin nasal ointment, and chlorhexidine baths	Evidence-based eradication <sup>4</sup> ; eradication confirmed.
Supportive therapy	Vitamin B6 with OAT, analgesics, and ciprofloxacin if needed	Prevents neuropathy, relieves symptoms, and treats superinfections.
Monitor treatment response	ENT & pulmonary follow-up, repeat swabs, imaging, blood monitoring	Ensure TB resolution, MRSA eradication, and detect complications early.

lesions in the nasal cavity with septal deviation but normal paranasal sinuses and chest radiographs, consistent with a localized extrapulmonary process. The initial lesion was not documented as the patient never noticed the perforation. Histopathology confirmed TB by demonstrating caseating granulomas with epithelioid cells and Langhans giant cells, ruling out malignancy. Additionally, microbiology identified MRSA colonization in the nasal cavity and throat, which was treated and eradicated, confirming a secondary infection complicating the underlying nasal TB.

The diagnostic and therapeutic approach in this case was aimed at confirming the etiology, excluding systemic involvement, and providing targeted management. Multiple biopsies of the nasal cavity and septum were performed to establish a definitive diagnosis. At the same time, chest radiographs, sputum AFB, GeneXpert, ANCA, and HIV testing ruled out pulmonary TB and systemic granulomatous diseases. CT scan defined the local extent of the disease, and

FNAB of the supraclavicular lymph node excluded malignancy.

Once nasal TB was confirmed histologically, the patient was started on standard anti-TB therapy (Category I, 2HRZE/4HR), with possible extension to 9-12 months if granulomatous lesions persisted. Septal perforation was managed conservatively with saline irrigation and sprays to relieve symptoms, while secondary MRSA infection was eradicated with cotrimoxazole, mupirocin ointment, and chlorhexidine baths. Supportive treatment with vitamin B6, analgesics, and antibiotics for superinfections was added, and the patient was monitored closely with regular ENT and pulmonary follow-ups, repeat cultures, imaging, and laboratory tests to ensure resolution and prevent recurrence.

On follow-up, the patient continued anti-TB therapy (Category I, extended up to 9-12 months) with gradual clinical improvement. Repeated chest radiographs and

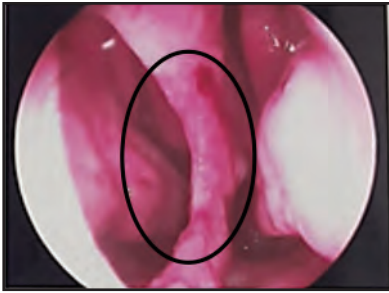


**Fig. 1:** An endoscopic image, presenting a perforated nasal septum due to necrosis

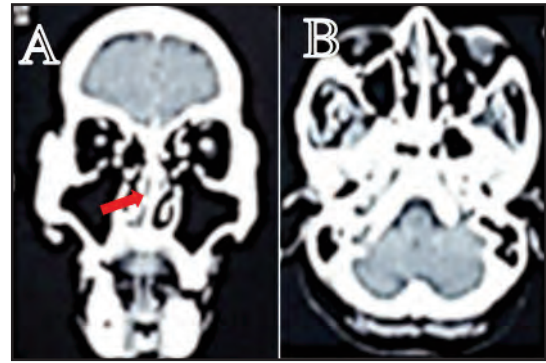


**Fig. 2:** A head CT-scan results, presenting a coronal(A)-axial(B) section, the red arrows highlight the rupture in the nasal septum

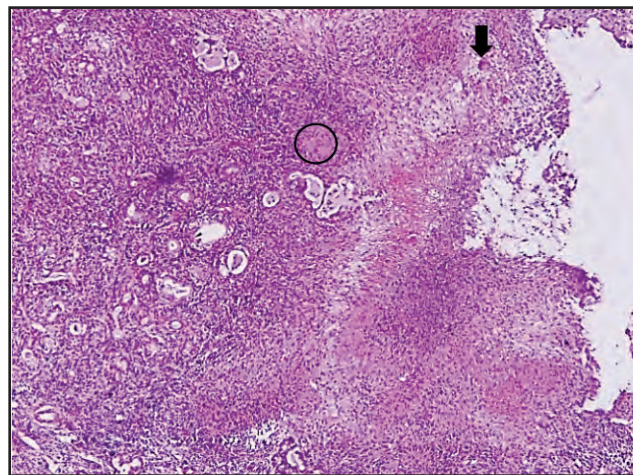


**Fig. 3:** In a histopathology evaluation, the circle indicates caseous necrosis, while the arrow indicates Langhans cells

sputum AFB remained normal, confirming no pulmonary involvement. MRSA colonization detected earlier was eradicated after cotrimoxazole, mupirocin, and chlorhexidine, with subsequent swabs turning negative. A supraclavicular lymph node mass was later found, but FNAB showed a benign process. The patient remained under regular ENT and pulmonary monitoring with stable progress.

**DISCUSSION**

Primary nasal TB is an extremely rare form of extrapulmonary TB. Since the first case was described in the 18th century, only a limited number of cases have been documented in the medical literature, with most reports highlighting its rarity and diagnostic difficulty. The disease can present either as a secondary manifestation of pulmonary TB or, more rarely, as a primary infection localized to the nasal cavity without pulmonary involvement.<sup>5</sup> Primary nasal TB is strongly associated with immunocompromised states, with sinonasal involvement typically arising from hematogenous or lymphatic spread.<sup>8</sup>

Reported cases span across all adult age groups, but several studies suggest a predominance in women, consistent with the present case. Although the nasal mucosa is generally

resistant to *Mycobacterium tuberculosis* due to protective mechanisms such as mucociliary clearance and bactericidal nasal secretions, trauma or direct inoculation allows bacilli to penetrate the nasal mucosa and cause infection. Common presenting symptoms include chronic nasal obstruction, rhinorrhea, anosmia, and epistaxis, with anterior septal involvement being the most frequent site of pathology.<sup>5,8</sup>

In this patient, the combination of nasal obstruction, anosmia, a friable intranasal mass, and anterior septal perforation closely matched the typical features described in the literature. Nasal septal perforation is a complication of TB, as caseous necrosis associated with granulomatous inflammation destroys cartilage and mucosa of the upper respiratory tract.<sup>9</sup> The clinical significance of septal perforation extends beyond structural damage: it alters the intranasal environment, leading to recurrent crusting and creating a niche for bacterial colonization.<sup>3</sup> In this case, the perforation was further complicated by MRSA colonization, which underscores the importance of considering secondary infections in TB-affected nasal mucosa.<sup>6</sup>

The diagnostic process remains a challenge. Established modalities, chest radiography, sputum AFB smear, and GeneXpert, were consistently negative in this patient,

consistent with isolated nasal TB without pulmonary disease.<sup>1</sup> This diagnostic limitation necessitates reliance on histopathological examination of nasal tissue, which in this case revealed caseating granulomas with epithelioid cells and Langhans giant cells, confirming the diagnosis.<sup>1,5</sup> The granulomatous-hyperplastic cells are clinically important because their mass-forming and chronic inflammatory nature may mimic or predispose to malignant transformation, necessitating careful long-term surveillance.<sup>5</sup> However, histopathology has limitations due to sampling errors or low bacillary load; hence, repeat biopsies are required. These challenges highlight the need for innovative yet accessible diagnostic approaches for extrapulmonary TB. Treatment of nasal TB follows the same principle as pulmonary TB, employing the standard two-phase anti-TB regimen. In this case, the patient received Category I therapy consisting of an intensive phase with four drugs (isoniazid, rifampicin, pyrazinamide, ethambutol) followed by a continuation phase with two drugs (isoniazid, rifampicin). This regimen remains effective in eradicating bacilli and preventing relapse, although therapy may be extended to 9-12 months in cases with persistent granulomatous lesions or bony involvement.<sup>7</sup> Supportive local therapy, such as nasal saline irrigation, was beneficial for reducing crusting and improving hygiene.

Management of the secondary MRSA infection was essential for the patient's recovery. MRSA colonization of the nasal cavity was likely facilitated by mucosal disruption and environmental changes resulting from septal perforation. The eradication protocol, oral cotrimoxazole, topical mupirocin ointment, and chlorhexidine baths, proved effective, with subsequent swabs confirming clearance.<sup>4</sup>

## CONCLUSION

This case illustrates the diagnostic complexity of primary nasal TB, particularly in the presence of negative conventional tests, and the value of histopathological confirmation. It also highlights the clinical importance of recognizing complications such as nasal septal perforation and secondary MRSA infection, both of which can significantly alter disease course and management. A comprehensive approach combining systemic anti-TB therapy, targeted eradication of resistant bacterial coinfection, and supportive nasal care allowed favorable clinical outcomes in this rare presentation.

## ACKNOWLEDGEMENT

We appreciate the assistance of all staff from the Medical Record Installation of dr. Saiful Anwar Hospital, Malang.

## CONFLICT OF INTEREST

The authors have no conflicts of interest to declare.

## FUNDING

The authors declared that this study has received no financial support.

## REFERENCES

1. Elbehiry A, Marzouk E, Edrees HM. Advancing the fight against tuberculosis : integrating innovation and public health in diagnosis, treatment, vaccine development, and implementation science. *Front Med.* 2025; 12: 1596579.
2. Bahethi R, Talmor G, Choudhry H, Lemdani M, Singh P, Patel R, et al. Chronic invasive fungal rhinosinusitis and granulomatous invasive fungal sinusitis: A systematic review of symptomatology and outcomes. *Am J Otolaryngol - Head Neck Med Surg.* 2024; 45(1): 104064.
3. Zhang Z, Ma Z, Li Y, Wang J, Hou L. Primary nasal tuberculosis: A rare case report. *Ear, Nose Throat J.* 2025; 104(2\_suppl): 1S-6S.
4. Santosaningsih D, Erikawati D, Hakim IA, Santoso S, Hidayat M, Suwenda AH, et al. Reducing transmission of methicillin-resistant *Staphylococcus aureus* in a surgical ward of a resource-limited hospital in Indonesia: an intervention study. *Infect Prev Pract.* 2019; 1(3-4): 100028.
5. Bouatay R, Bouaziz N, Harrathi K, Koubaa J. Primary sinonasal tuberculosis: A diagnostic challenge. *Otolaryngol Case Reports.* 2024; 31: 100611.
6. Sherry NL, Gorrie CL, Kwong JC, Higgs C, Stuart RL, Marshall C, et al. Multi-site implementation of whole genome sequencing for hospital infection control: A prospective genomic epidemiological analysis. *Lancet Reg Heal - West Pacific.* 2022; 23: 100446.
7. Zhang M, Wang M, He JQ. Intensified antituberculosis therapy regimen containing higher dose rifampin for tuberculous meningitis: A systematic review and meta-analysis. *Front Med.* 2022; 9: 822201.
8. Swain SK, Behera IC, Sahu MC. Primary sinonasal tuberculosis: Our experiences in a tertiary care hospital of eastern India. *Egypt J Ear, Nose, Throat Allied Sci.* 2017; 18(3): 237-40.
9. Shu C, You T, Huang M, Xu M, Zhang J, Peng Z. Case Report: A rare case of tuberculous otitis media mimicking chronic suppurative otitis media — an ongoing challenge. *Front Med.* 2025; 12: 1521011.

# Unravelling the Frozen Gaze: A rare occurrence of superior orbital fissure syndrome (SOFS) post craniofacial trauma

Hui Wen Tay, Sherrie Mei Yee Chong, BDS, MClinDent, Juliana binti Khairi, BDS, MClinDent (OMFS), Szu Ching Khoo, BDS, MClinDent (OMFS), Marzuki Zainal Abidin, BDS, MClinDent (OMFS)

Department of Oral and Maxillofacial Surgery, Hospital Tengku Ampuan Rahimah, Klang, Selangor, Malaysia

### SUMMARY

Superior Orbital Fissure Syndrome (SOFS), part of the orbital apex disorders, is characterized by ophthalmoplegia, ptosis, mydriasis and neurosensory disturbance over the ophthalmic branch of trigeminal nerve. We describe an uncommon case of SOFS in a 27-year-old fit and healthy Malay gentleman involved in an industrial injury with severe blunt trauma to his face. He sustained mild traumatic brain injury which was treated conservatively; and multiple facial bone fractures including i) displaced right zygomaticomaxillary complex (ZMC), ii) right frontal bone and superior orbital rim, iii) Lefort I, iv) nasal bone fractures and v) comminuted right orbital walls fracture; with compressed SOF by a displaced lateral wall fracture segment. The patient presented with all the classical features of SOFS with preserved optic nerve (CN II) function. There were restriction of extraocular muscle movements and binocular diplopia in all gazes. Reverse relative afferent pupillary defect (RAPD) was negative. Open reduction internal fixation (ORIF) via bicoronal flap, subciliary and intraoral upper vestibular approach was done. SOFS symptoms of diplopia and ophthalmoplegia showed improvement starting sixth week post-operatively. SOFS may prove challenging to manage due to variable and unpredictable outcomes. With timely surgical decompression and reduction of displaced fracture segments, the prognosis for SOFS may prove favourable.

### INTRODUCTION

Superior Orbital Fissure Syndrome (SOFS), also known as Rochon-Duvigneaud syndrome, is part of a larger group of disorders known as orbital apex disorders. It is rather rare with a reported incidence of 0.3-0.8%.<sup>1,2</sup> SOFS is caused by compression of contents within the superior orbital fissure causing impairment of cranial nerve (CN) III, IV, V, VI. It consists of a constellation of classical symptoms including i) ptosis, ii) numbness over the forehead and upper eyelid, and iii) ophthalmoplegia. SOFS does not involve the optic nerve (CN II) and vision is usually preserved, differentiating it from orbital apex syndrome. The etiologies vary and include trauma, most commonly in zygomaticomaxillary complex (ZMC) and orbital wall fractures<sup>3,4</sup>; tumours; infection such as herpes zoster; and vascular diseases for example, carotico-cavernous fistula or carotid aneurys.<sup>5</sup> It may also occur as a complication of open reduction internal fixation of midface

fracture.<sup>6</sup> Trauma-related SOFS usually presents within 48 hours of a craniofacial injury<sup>2</sup>, but delayed presentation has also been reported.<sup>7</sup>

To better understand the pathophysiology and mechanism of SOFS, it is crucial to be cognizant of the anatomy. The superior orbital fissure (SOF) is bound laterally by the greater wing of the sphenoid, medially by the lesser wing of the sphenoid, and superiorly by the frontal bone. It serves as a pathway between the orbit and the middle cranial fossa. According to Raymond et al. (2008)<sup>8</sup>, the size of the SOF in an adult is approximately 2–3 mm in width at the apex, 7–8 mm at the base and 22 mm in length. The tendons of the lateral rectus muscle divide the fissure into two parts: the superior part containing the trochlear, frontal and lacrimal nerves (branches of CN V), and the superior ophthalmic vein; and the inferior part containing the superior and inferior branches of the oculomotor, abducens, nasociliary branch of ophthalmic nerve, and the inferior ophthalmic vein. Compression of structures that course through the SOF can be attributed to osseous fragment or mass effect from hematoma or oedema in the retrobulbar space or orbital muscle cone. Signs and symptoms of the syndrome may be either complete or partial depending upon the degree of compression of its related anatomical structure. Partial SOFS has been reported where involvement is strictly confined to the central sector, associated with isolated oculomotor, abducens and nasociliary dysfunction<sup>9</sup>; or without complete involvement of the ophthalmic division of the trigeminal nerve and without ptosis.

This report aims to describe an uncommon case of traumatic SOFS and its mechanism; discuss our experience in the management and treatment considerations and outcomes; and review existing literature.

### CASE PRESENTATION

A 27-year-old fit and healthy Malay gentleman sustained severe blunt injury to his face caused by an industrial machinery. He was brought to the Emergency Department conscious and alert with a Glasgow Coma Scale of 15. He sustained traumatic brain injury with left frontal contusional bleed which was treated conservatively with close monitoring under the neurosurgical team. He was found to have multiple facial bone fractures including i) right zygomaticomaxillary

*This article was accepted: 08 February 2026*

*Corresponding Author: Hui Wen Tay*

*Email: tayhw91@gmail.com*

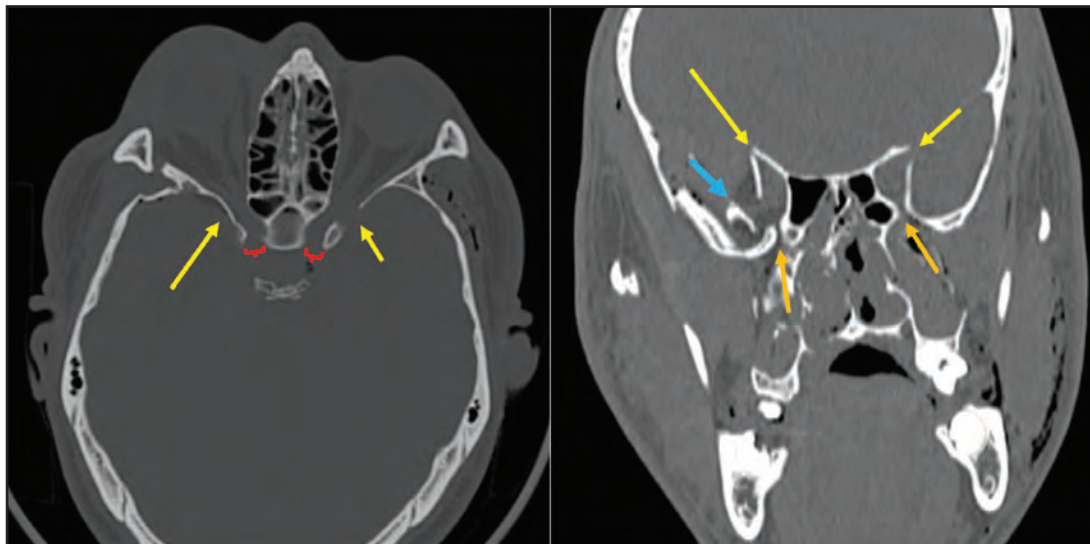


**Fig. 1:** Axial view of computed tomography showing compressed right superior orbital fissure (long yellow arrow) when compared with normal left superior orbital fissure (short yellow arrow). Optic canals appeared intact (in red). Coronal view showing displaced greater wing of sphenoid bone (blue arrow), compressed right superior orbital fissure (long yellow arrow) while inferior orbital fissures (orange arrows) appeared intact

complex with displaced right zygomatic arch, ii) right orbital walls, iii) Lefort I and II with palatal split, iv) nasal bone and septum, v) right frontal bone and right supraorbital rim fractures.

On examination, the right zygoma, cheek and superior orbital rim regions were depressed with palpable step deformity. Complete anaesthesia was present over the right forehead with an impairment of two-point discrimination. There was hypoesthesia over the right cheek, likely attributed to the Lefort fractures with right infraorbital nerve involvement. Mouth opening was satisfactory at 35mm. Occlusion was deranged with a mobile maxilla but firm mandible.

Comprehensive assessment of the right eye revealed periorbital haematoma, ptosis, mild proptosis, subconjunctival hemorrhage, ophthalmoplegia with complete absence of eye movements in all gazes and a positive forced duction test. Dystopia present was likely due to downward displacement of zygomaticomaxillary complex with right orbital floor blowout fracture and herniation of orbital contents. He also complained of binocular diplopia in all gazes. The right pupil was fixed and dilated at 7mm but with intact vision. Further ophthalmic examination showed loss of corneal reflex and relative afferent pupillary defect was negative. Fundoscopic examination by ophthalmology team was unremarkable and there was no raise in intraocular pressure.

Computed tomography revealed fractures of all walls of the right orbit with constriction of the right superior orbital fissure by displaced osseous fragment of the lateral wall. Bilateral optic canals were patent and intact. There was also evidence of impingement of the medial and inferior rectus muscles by fractured bony fragments. Both globes were intact and no intraconal or extraconal hematoma was noted. A diagnosis of multiple facial bone fractures complicated with superior orbital fissure syndrome (SOFS) was made.

One-week post trauma, open reduction internal fixation (ORIF) was performed for the right superior orbital rim and right zygomatic arch via bicoronal approach; right inferior orbital rim and right orbital floor reconstruction via subciliary approach; maxillary buttress and pyriform rims via intraoral upper vestibular approach. Post-operative forced duction test was negative. Dystopia was corrected and the depressed right malar and supraorbital rim projection were restored. A postoperative occipitontal view radiograph was done to evaluate the reduction.

At the sixth week post-surgery, there was an improvement of ptosis and ophthalmoplegia. Six months after surgery, there was almost complete recovery. Based on literature, a recovery period of up to 12 weeks has been reported and reaches its plateau by the end of 6 months. The patient is still being monitored closely for progression and recovery under the oral maxillofacial surgery and ophthalmology department.

## DISCUSSION

The optimal management of traumatic SOFS remains poorly defined and is usually related to treating the cause. Management reported includes conservative treatment with close observation alone, medical management involving steroid administration with or without surgical intervention. In cases of obvious constriction of the SOF by displaced bone fragment, usually as evidenced on computed tomography, decompression surgery is warranted. Variable outcomes have been reported after surgery, including no improvement of SOFS symptoms and gradual recovery up to 12 weeks post-operatively.<sup>2</sup>

ORIF was performed one-week post-trauma to allow resolution of soft tissue oedema. The aims of surgery were to i) anatomically reduce and fix the fractures and restore the malar and superior orbital rim projection, ii) restore the orbital volume and correct the dystopia via orbital floor reconstruction, iii) mechanical decompression and release of



**Fig. 2:** (a) Post-trauma, right eye ptosis and ophthalmoplegia with complete absence of movement in all gazes showed significant improvement at (b) six months post-ORIF

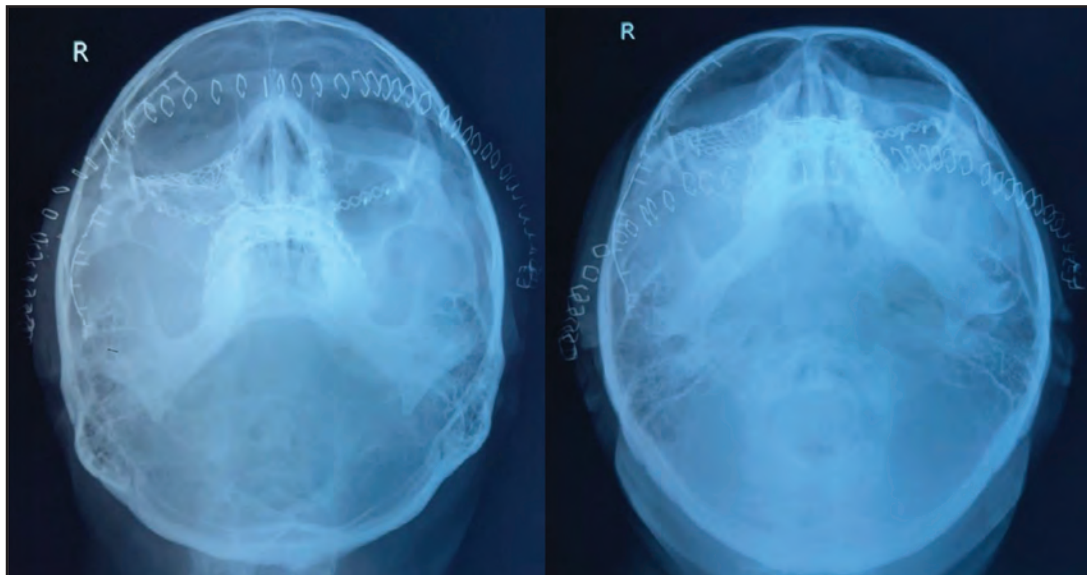


**Fig. 3:** Occipitontal 30 degrees view and Water’s view of skull radiograph showing satisfactory reduction and fixation of facial bone fractures

neuronal contents of superior orbital fissure. According to literature, an initial observation period of 10–14 days before any surgical intervention was carried out is generally advocated due to concerns of raised ocular pressure and swelling.<sup>9</sup> Oedema developed immediately post-trauma may directly compress on the nerve or push the nerve against the bony margin of the fissure, which may attribute to nerve palsy and its subsequent transient dysfunction. Naturally narrower superior orbital fissure has been reported as a risk factor for SOFS.<sup>10</sup>

The pathophysiology or mechanism of injury can be broadly divided into neurological and/or muscular injury. Any entrapped extraocular muscles should be mechanically released and can be confirmed with a negative forced duction test. If decompressive surgery is delayed, the muscles may undergo compressive ischaemic injury and become irreversibly damaged from fibrosis. Studies have shown that early intervention in cases of muscle entrapment resulted in less postoperative diplopia.<sup>11</sup>

If ophthalmoplegia persists despite release of entrapped muscles, the cause is likely neurological in origin due to cranial nerve palsies. Neurological damage may be due to direct blunt trauma to cranial nerves III,IV,VI or indirect compression of nerves by osseous fragment or hematoma or oedema within the limited intraconal space.<sup>12,13</sup> Transmitted traumatic forces on the cranial nerves along its course through the superior orbital fissure may lead to axonal injury of varying severities, either neuropraxia, axonotmesis or neurotmesis. Tolerance of the nerve to injury and its reversibility depend on the type, diameter, location and direction of nerve course. Spontaneous improvement with just conservative management and careful observation has been documented in cases of ophthalmoplegia due to oedema without evidence of displaced bony fragment and compressed SOF.<sup>2</sup>

Varying doses of systemic corticosteroids have been advocated as treatment alone, or in conjunction with surgical decompression of facial bone fractures. Initial steroid therapy post-trauma has been shown to have variable results, generally with a favourable prognosis.<sup>2,9,14</sup> Different regimes of steroid administration, usually involving ‘megadose’, have been reported.<sup>5,14</sup> The mechanism appears to be from the ability of high doses steroid in rapidly reducing oedema in the limited intraconal space of the orbit and subsequent ischemia of delicate neuronal structures. Specific to this case, a routine peri-operative dose of IV Dexamethasone 8mg 8 hourly was administered intraoperatively and up to 3 days post-operatively in addition to eye drops of 0.1% dexamethasone 6 hourly. Corticosteroid, associated with morbidity in patients with traumatic brain injury, as reported by the Corticosteroid Randomisation After Significant Head injury (CRASH) trial protocol; was not administered in the acute setting pre-operatively in this case.<sup>15</sup>

In conclusion, superior orbital fissure syndrome may prove challenging to manage due to variable and unpredictable outcomes. With timely surgical decompression and reduction of displaced fracture segments, the prognosis for SOFS is generally favourable. Randomized clinical trial is recommended to further evaluate the efficacy of high dose steroids for SOFS in the acute setting . This case report may add value to the existing literature, owing to its scarcity.

**CONFLICT OF INTEREST**

None.

**FUNDING**

None.

**ETHICAL APPROVAL**

None.

### PATIENT CONSENT

Written consent was obtained from the patient including the use of anonymized medical data and images for the publication of this case report, ensuring compliance with ethical standards.

### STATEMENT TO CONFIRM

All authors have viewed and agreed to the submission.

### ACKNOWLEDGEMENTS

The authors would like to gratefully acknowledge the support and contributions of everyone who made this case report possible.

We would like to thank the Director General of Health Malaysia for his permission to publish this article.

### REFERENCES

1. Zachariades N, Vairaktaris E, Papavassiliou D, Papademetriou I, Mezitis M, Triantafyllou D. The superior orbital fissure syndrome. Vol. 13, *J. max.-fac. Surg.* 1985.
2. Chen CT, Wang TY, Tsay PK, Huang F, Lai JP, Chen YR. Traumatic superior orbital fissure syndrome: Assessment of cranial nerve recovery in 33 cases. *Plast Reconstr Surg.* 2010; 126(1): 205-12.
3. Shokri T, Zacharia BE, Lighthall JG. Traumatic Orbital Apex Syndrome: An uncommon sequela of facial trauma. *Ear Nose Throat J.* 2019; 98(10): 609-12.
4. Taniguchi H, Nishioka H, Kuriyama E, Inoue Y, Okumoto T. Craniofacial fracture with superior orbital fissure syndrome resulting in pupil-sparing oculomotor nerve palsy. *Plast Reconstr Surg Glob Open.* 2024; 12(5): E5828.
5. Postma MP, Seldomridge GW, Vines FS. Superior orbital fissure syndrome and bilateral internal carotid pseudoaneurysms. *J Oral Maxillofac Surg.* 1990; 48(5): 503-8.
6. Fujiwara T, Matsuda K, Kubo T, Tomita K, Yano K, Hosokawa K. superior orbital fissure syndrome after repair of maxillary and naso-orbito-ethmoid fractures: A Case Study. *Journal of Plastic, Reconstructive and Aesthetic Surgery.* 2009; 62(12).
7. Kim YJ, Choi WK. Delayed superior orbital fissure syndrome after reconstruction of blowout fracture. Vol. 27, *Journal of Craniofacial Surgery.* Lippincott Williams and Wilkins; 2016; e8-10.
8. Reymond J, Kwiatkowski J, Wysocki J. Clinical anatomy of the superior orbital fissure and the orbital apex. *Journal of Cranio-Maxillofacial Surgery.* 2008; 36(6): 346-53.
9. Chen CT, Chen YR. Traumatic Superior orbital fissure syndrome: current management. *Cranio-maxillofac Trauma Reconstr.* 2010; 3(1): 9-16.
10. Park Y, Kim Y. A Statistical analysis of superior orbital fissure width in korean adults using computed tomography scans. *Arch Craniofac Surg.* 2017; 18(2): 89-91.
11. Boyette JR, Pemberton JD, Bonilla-Velez J. Management of orbital fractures: challenges and solutions. Vol. 9, *Clinical Ophthalmology.* Dove Medical Press Ltd; 2015; 2127-37.
12. Warburton RE, Brookes CCD, Golden BA, Turvey TA. Orbital apex disorders: a case series. *Int J Oral Maxillofac Surg.* 2016; 45(4) :497-506.
13. Cui V, Kouliev T. Isolated oculomotor nerve palsy resulting from acute traumatic tentorial subdural hematoma. *Open Access Emergency Medicine.* 2016 Oct; Volume 8: 97-101.
14. Acartürk S, Seküçoğlu T, Kesiktäs E. Mega dose corticosteroid treatment for traumatic superior orbital fissure and orbital apex syndromes. *Ann Plast Surg.* 2004; 53(1): 60-4.
15. Alderson P, Roberts I. Corticosteroids for acute traumatic brain injury. *Cochrane Database of Systematic Reviews.* 2005; 2009(3).